CARNEGIE MELLON UNIVERSITY

School of Architecture

College of Fine Arts

Thesis

Submitted in Partial Fulfillment of the requirements for the degree of

Doctor of Philosophy in Building Performance & Diagnostics

TITLE:

Surface Urban Heat Island: A Comparative Study Between India and the United States

AUTHOR:

Surekha Tetali

ACCEPTED BY ADVISORY COMMITTEE:

Professor NAME	Principal Advisor	4/27/23 DATE
Professor NAME	Advisor	DATE
Professor NAME	Advisor	27 April 2023 DATE
Professor NAME	Advisor	DATE

Surface Urban Heat Island: A Comparative Study Between India and the United States

Surekha Tetali

2023

Doctoral Dissertation

School of Architecture
Carnegie Mellon University
Pittsburgh, PA

Doctoral Committee

Professor Nina Baird
Professor Emeritus Volker Hartkopf
Dr. Kelly Klima

A Dissertation submitted in Partial Fulfillment of the requirements of the Degree of Doctor of Philosophy in Building Performance and Diagnostics in the School of Architecture, Carnegie Mellon University.

ABSTRACT

Global temperatures have risen by 0.18^0C per decade and could rise further due to increasing anthropogenic activity in urban areas, which may host 68% of the world's population by 2050. Urban Heat Island (UHI), the higher urban temperatures compared to the rural surroundings, is one of the most widely researched phenomena to study the impact of urbanization on climate. Yet, limited research exists across rapidly urbanizing countries, like India, which could be the biggest contributor to urban population growth in the following decades.

This research is a comparative examination of UHI and its association with the urban built environment in India and the US. It conducts a quantitative analysis of the Land Surface Temperatures (LST) and the Surface Urban Heat Island (SUHI) magnitude (ΔT) across 42 cities in India and 32 cities in the US using remote sensing data. Such large-scale multi-city analysis facilitated statistical analysis of the observed LST and ΔT.

The daytime analysis of LST and ΔT showed SUHI in the US but the reverse in India, where urban areas are cooler than rural surroundings. Rural LSTs in India were higher than urban LSTs, which are already 10-12^0C higher than in the US. The dry or non-green vegetation land cover is linked to higher daytime rural LSTs in India. Further investigations showed that the popular remote sensing indices used to quantify built-up areas cannot differentiate between built-up areas, cropland, and other sparse vegetative land covers that are dominant in India. Literature on the thermal characteristics, especially the thermal admittance of non-green vegetation, dry soil, and barren land covers, indicates rapid warming of such land covers during the daytime and cooling after sunset. Consistent with this, the subsequent nighttime SUHI analysis showed warmer urban areas than rural areas in India. This nighttime SUHI magnitude is higher in India than in the US, and this difference is statistically significant. Together these findings highlight the shortcomings of conventional SUHI research methods in global analysis.

Since the conventional SUHI analysis methods and indices did not show an association between urban LSTs or ΔT with built-up areas and vegetation in India, this study used impervious surface area (ISA) data to evaluate the temporal changes in diurnal and seasonal ΔT over 15 years and the summer daytime spatio-temporal variation in urban built-up LSTs. The temporal analysis of ΔT showed that urbanization, quantified using ISA data, and ΔT increased in both countries over 15

years. This increase in ΔT over time is higher in India than in the US during nighttime and is statistically significant. However, the daytime ΔT change between the two countries is not statistically significant. The summer daytime urban built-up LST analysis showed that the recent (2007-2016) built-up areas in India were warmer than those older (before 2007). However, the reverse pattern occurs in the US over the same periods. Further, cluster analysis of urban built-up LSTs showed that green vegetation, with a Normalized Difference Vegetation Index (NDVI) greater than 0.3, reduces the LST of the neighboring built-up areas. This reduction in built-up area LST with a green neighbor is higher in the US than in India.

This study indicates that rural areas are not consistently cooler than urban areas in India, although that assumption is implicit in the definition of UHI. Additionally, the current global SUHI research methods need revisions for locations where drought or other factors may result in non-green vegetation. This study's methodological approach showed the variation in urban LSTs with built-up areas and vegetation, which was not apparent through conventional methods. Such an approach can also be relevant for other countries with similar characteristics. The study's quantitative findings show the need and scope to improve urban surfaces and buildings to reduce urban LSTs. Although the results indicate green vegetation as a potential UHI mitigation strategy, its effectiveness needs evaluation in conjunction with limitations on water availability and overall urban densities. The study also emphasized the need for more localized SUHI research methods and measures that can specifically analyze the impact of the urban built environment on urban LSTs.

Keywords: Land Surface Temperature, Surface Urban Heat Islands, Land Use Land Cover, Spectral Indices, Urban Built Environment, Built-up Areas, Vegetation

To my friend, philosopher, and guide- my husband

Dr. Sivom Manchiraju

ACKNOWLEDGMENTS

During my long graduate life, I am grateful to many people who have helped me directly and indirectly complete this dissertation. I am incredibly thankful for the support from all these people through this journey.

I sincerely thank my doctoral advisory committee, Prof. Volker Hartkopf, Prof. Nina Baird, and Dr. Kelly Klima, for their guidance and support. I thank Prof. Volker Hartkopf for giving me the opportunity and freedom to work in my area of interest and for funding and supporting me throughout my time at CMU. I cannot thank Prof. Nina Baird enough for her intensive support and advice at every stage of my work. I thank her for the patience and time she put into reading several drafts of my work and for all her questions that made me think deeply about my work and challenged me to improve. This dissertation wouldn't have been complete without her guidance and encouragement. I am grateful for Dr. Kelly Klima's advice and guidance, especially in the preliminary stages of my research. Our weekly meetings through the first phase of my work provided some insightful assistance and, more importantly, molded me to think like a researcher. I also want to thank Prof. Kristen Kurland. Her courses in graduate school inspired me and introduced me to the potential of GIS and remote sensing analysis and tools.

I thank all my friends and colleagues at the IW who helped me have a wonderful time during this phase of life. I thank my best friend Hemu for being a phone call away any day, whenever I want.

I am incredibly grateful for all support from my family, especially while navigating through my high-risk pregnancy while at graduate school. I thank my in-laws for saying I should and can work things through. I thank my parents, who always encouraged and wished me the best. Thank you, Dad, for making my goal into your dream and constantly reminding me to focus on achieving it. You are my inspiration to pursue a Ph.D. A heartfelt thank you to all the rest of the family. You all are the best support system I have.

Throughout this time, my biggest strength has been my husband, Sivom. Thank you, Sivom, for giving up a comfortable job and your hometown in the US to move to Pittsburgh for me to pursue my Ph.D. Thank you for brainstorming with me, for the countless discussions on my work, for teaching me coding, and for guiding me with your 15+ years of experience in research and

development. Thank you for critically reviewing my work at every stage and supporting me even when I took things slow.

Lastly, I thank my twin boys, Vidvas and Vedhas. I learned a lot because of them and from them. I learned patience, determination, and above all, to embrace positivity. Thank you, boys, for adjusting at times and just being there for me no matter what.

ABBREVIATIONS

AOI	Area of Interest
ASHRAE	The American Society of Heating, Refrigerating, and Air-Conditioning Engineers
AWiFS	Advanced Wide Field Sensor
EBBI	Enhance Built-up Bareness Index
ECBC	Energy Conservation Building Code
GAIA	Global Artificial Impervious Area
GRIHA	Green Rating for Integrated Habitat Assessment
IBI	Index-Based Built-Up Index
IECC	International Energy Conservation Code
IRS	Indian Remote Sensing
ISA	Impervious Surface Area
ISRO	Indian Space Research Organization
LEED	Leadership in Energy and Environmental Design
LST	Land Surface Temperature
LULC	Land Use Land Cover
MODIS	Moderate Resolution Imaging Spectroradiometer
NASA	National Aeronautics and Space Administration
NDVI	Normalized Difference Vegetation Index
NDBI	Normalized Difference Built-Up Index
NPV	Non-Photosynthetic Vegetation
SUCI	Surface Urban Cool Island
SUHI	Surface Urban Heat Island
UHI	Urban Heat Island
US	United States of America
USGS	United States Geological Survey

TABLE OF CONTENTS

LIST OF FIGURES

LIST OF TABLES

1 INTRODUCTION

1.1 RESEARCH CONTEXT

Earth's temperatures increased by 0.7^0C between 1986-2016, compared to 1901-1960 (Wuebbles et al., 2017), and the hottest year on record was 2016, tied with 2020. It is now a fact that human activities are driving climate change. Rising global land surface temperatures, warming oceans, shrinking ice sheets, increasing frequency of extreme weather events, and rising sea levels are all evidence of climate change. Increased greenhouse gas emissions and changes in land use due to increased urbanization relate to climate change. As seen in Figure 1, increasing temperatures increase the probability of extreme weather events, and such climate events could impact the world's urban areas the most. The projected rapid urbanization, especially across developing nations, increasing 55% of the global population in urban areas to 68% in the next three decades(United Nations, Department of Economic and Social Affairs, 2019), is further expected to drive climate change.

Urban areas of the world are at both the causing and receiving end of climate change, forming a vicious cycle. A recent study(Wei, Wu, & Chen, 2021) showed that out of the 167 cities studied, 25 megacities result in 52% of total greenhouse gas emissions through stationary energy uses (buildings) and transportation. Urbanization, together with changing climate such as the frequent heatwave events (Arias, P.A., N. Bellouin, E. Coppola, R.G. Jones, G. Krinner, J. Marotzke, V. Naik, M.D. Palmer, G.-K. Plattner et al., 2021; Mandal et al., 2019) exacerbate the impacts of increasing temperatures. The summer heatwave events, especially across hot urban areas, impact human health and well-being (Bradford, Abrahams, Hegglin, & Klima, 2015; Prosdocimi &

Klima, 2020) and are increasing the heat-related mortality rate(Mazdiyasni et al., 2017). For example, in India, heat-related mortality exceeded 2,000 in 2015 (Kumar & Singh, 2021), the highest in the last 15 years. Therefore, understanding the interplay between urbanization and urban climate is more relevant now than ever.

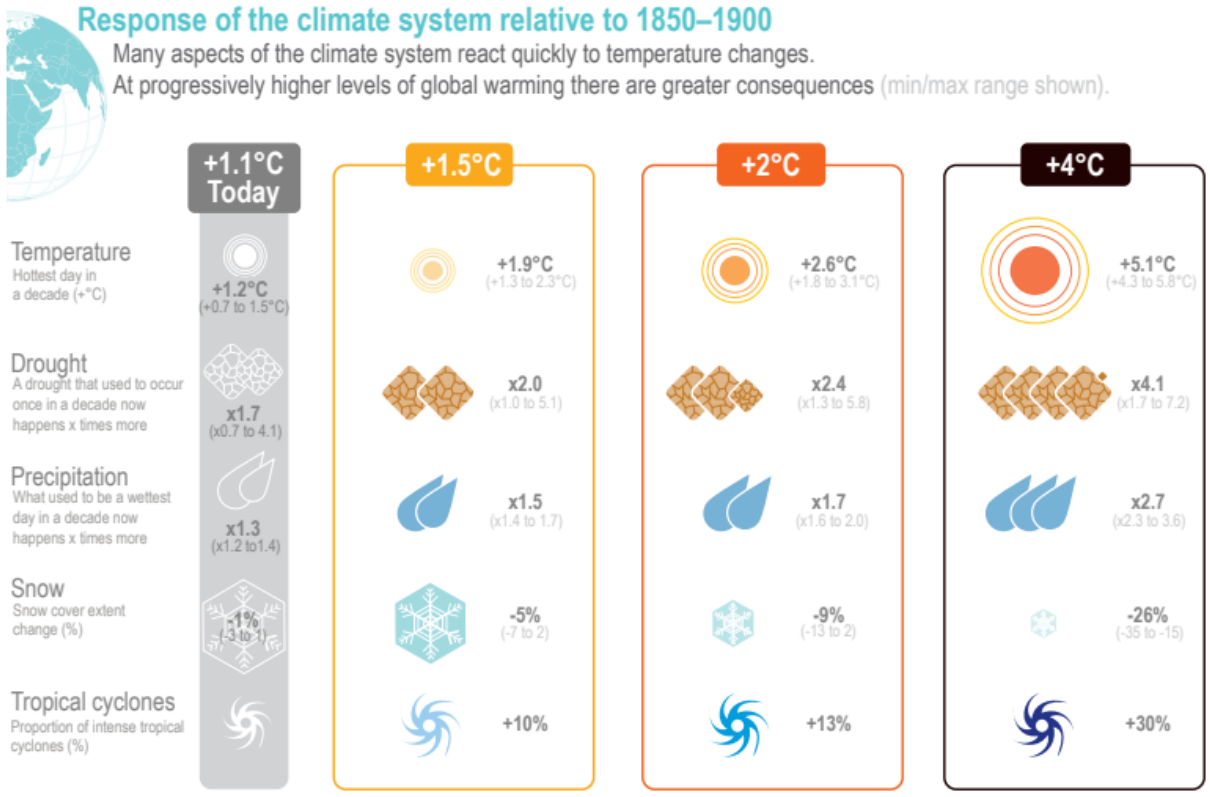

Figure 1: Changes in the climate with rising temperatures compared to the average global temperature between 1850-1900. This figure shows the increase in impact with increasing temperatures. Picture credit: Technical Summary. In Climate Change 2021: The Physical Science Basis. Contribution of Working Group I to the Sixth Assessment Report of the Intergovernmental Panel on Climate Change (Arias, P.A., N. Bellouin, E. Coppola, R.G. Jones, G. Krinner, J. Marotzke, V. Naik, M.D. Palmer, G.-K. Plattner et al., 2021)

1.2 URBANIZATION AND UHI

The Urban Heat Island phenomenon – defined as higher urban temperatures compared to rural surroundings, is the most researched impact of urbanization on temperatures. With rapid urbanization across the world's developing and already hot regions, like India, there is an impending need to conduct UHI research across such locations. Between 2018-2050 India is

projected to be the most significant contributor to urban population growth, adding 416 million to the current 460 million urban population. To put this in perspective, the current urban population estimate in the US is 268 million, which is close to half of that in India. There will be 235 urban settlements in India with > 300,000 urban dwellers by 2030, compared to 181 in 2018 and 94 in 1990. Detail on the past, current, and future urban population and the number of cities in India compared to the US is shown in Figure 2.

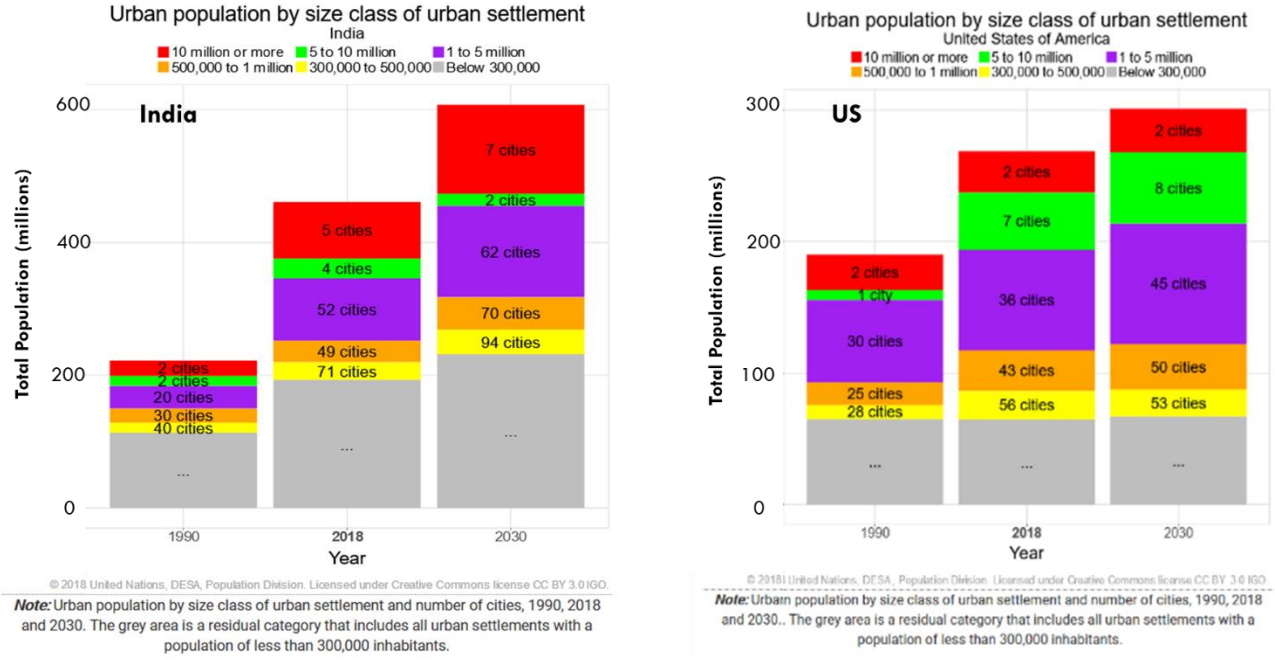

Figure 2: Urban population and the number of cities in India and the US: the past, present, and future. Note that the predicted urban population by 2030 in the US is half that in India. (Image ref:(United Nations, 2018)*)*

Suppose UHI increases with urbanization, as shown in some prior studies. In that case, there could be an intense UHI phenomenon noticed across countries like India, and in turn, such a UHI phenomenon could impact a larger population. A recent study(Hari, Dharmasthala, Koppa, Karmakar, & Kumar, 2021) from India identified that the migrant population across Indian megacities would be most affected by climate hazards. With this intense urbanization phenomenon, existing cities and those yet to be built face several impending environmental and

social issues. The UHI phenomenon could further increase energy demand, exacerbate poor air quality, reduce health and well-being, increase urban poverty, and reduce overall quality of life.

1.3 RESEARCH MOTIVATION

Urban areas, especially urban buildings, contribute to UHI formation and get impacted due to UHI. On the latter front, some dominant impacts of UHI on buildings are increased cooling energy consumption and decreased thermal comfort(T. Xu, Sathaye, Akbari, Garg, & Tetali, 2012) (Santamouris, 2014a). A meta-analysis(Santamouris, 2014b) conducted across studies that evaluate the impact of UHI on building energy showed that the cooling load in the urban building is 13% higher compared to a similar building in a rural area. Another study that analyzed 15 studies(Santamouris, Cartalis, Synnefa, & Kolokotsa, 2015) reported that the increase in electricity demand could vary from 0.5% to 8.5% per degree of temperature increase.

With increasing whole building energy modeling capabilities and expertise among building scientists, incorporating the impact of increased urban temperatures in predicting building energy performance is becoming a norm. However, it is still essential to understand how buildings and the built environment contribute to UHI. Such research is still in its infancy, primarily due to the interdisciplinary approach needed for using current analysis tools and methods. Traditionally, while building and urban designers focus on improving a space's indoor and spatial performance, urban climatologists and meteorologists study atmospheric phenomena like UHI. There was little interaction between these two groups. However, this is changing. Now in 2023, approximately 200 years after the first observation of UHI, when more than half the world’s population is urban, and when the eight warmest years on record are from the last 8 years, understanding UHI dynamics and how to mitigate the UHI effect have become essential even for building scientists.

1.4 PURPOSE STATEMENT

This mixed-method research aims to estimate the association between the built environment and the surface UHI (SUHI) phenomenon across highly populated cities in India compared to the United States (US). The such comparative analysis could help understand the relevance and efficacy of global SUHI research methods and SUHI drivers in the context of a less researched and rapidly urbanizing country, India.

This study analyzed the land surface temperatures (LST) and SUHI during one of the warmest years to date, 2016. This research studied SUHI and used remote sensing data to overcome the limitations and inconsistencies that could exist in air temperature data availability and measurement methods across multi-city, multi-nation studies like this. Remote sensing satellites provide data gathered and processed using consistent methods across different spatial (local to multiple global locations) and temporal(diurnal, seasonal, and inter-annual) scales- the majority available free of cost. This study quantifies SUHI magnitude (ΔT) as the difference between urban and rural mean LST. The built-up areas were quantified using spectral indices and the impervious surface area data. Remote sensing spectral index – the Normalized Difference Vegetation Index (NDVI) represents vegetation. The study used qualitative and quantitative analysis methods to estimate the variation in LST and ΔT with built-up land use and vegetation in India compared to the US.

1.5 RESEARCH GOAL AND HYPOTHESES

The primary goal of this dissertation is to understand the differences, if any, in the Surface Urban Heat Island phenomenon and its association with the urban built environment across highly populated cities in India compared to the US.

Some current research directions relevant to SUHI are 1.) Contributors to SUHI – natural and human-made factors, 2.) Standardization of urban-rural definitions and delineation methods, 3.) Intra-urban differences in LST 4.) Multi-location and multi-year studies of SUHI, 5.) Interactions between SUHI and canopy UHI, and 6.) Understanding remote sensing data, viewing angles, and method. Based on existing gaps in the literature in the first four categories, the hypotheses of this study are:

- **Hypothesis #1:** The surface urban heat island magnitude (ΔT), measured as the difference between urban and rural mean land surface temperatures, is higher in India compared to the United States.
- **Hypothesis #2:** Urbanization increases SUHI. This increase is higher in India compared to the US.
- **Hypothesis #3:** With the advent of building energy efficiency standards, green building ratings, and construction materials and technology improvement, recent urban built-up areas have lower land surface temperatures than the older ones.
- **Hypothesis #4:** Green vegetated areas reduce land surface temperatures and SUHI.

1.6 RESEARCH OBJECTIVES

This research aims to assemble the explanatory observations of SUHI in India compared to the US, specifically focusing on its association with built-up areas and vegetation. Some of the specific objectives of this research therefore are:

1. Quantify and compare diurnal and seasonal SUHI in India and the US.
2. Analyze and compare the variation of LST and ΔT with built-up areas and vegetation in India and the US.
3. Assess the impact of the increase in built-up with urbanization on SUHI in a rapidly urbanizing country, India, compared to a developed nation, the US.
4. Verify the relevance of global SUHI methods and metrics in the Indian context.

1.7 DISSERTATION STRUCTURE

The core of this dissertation is in three parts and four chapters. The first part compares and discusses the existing SUHI and its association with built-up areas and vegetation in India and the US during daytime and nighttime. The second part discusses the temporal changes in SUHI to estimate the impact of urbanization on SUHI. The third part quantifies the thermal performance of urban built-up areas. The third part of this work is in two parts – one that understands built-up area LST in two different scenarios based on the construction period and the second that quantifies built-up area LST based on the neighboring land use.

The first chapter of this dissertation explains the need and motivation for this research. It lists the hypotheses and objectives of the research.

The second chapter discusses a few relevant concepts and the background. This chapter also includes a literature review from the area of focus of this research and identifies the knowledge

gaps in the existing literature. While there isn't any literature specific to SUHI comparative analysis between India and the US, several studies assisted in developing this study's research questions and methodology. Such studies are critically reviewed and presented.

The third chapter presents the data and methodology used in this research. It details the study locations, the remote sensing data used in this research, the urban-rural delineation methodology, the LST calculation methodology, and the analysis metrics used. This chapter presents examples from various cities to explain the data and the maps generated for analysis.

This dissertation's fourth and fifth chapters discuss the first part of this research work, which focuses on analyzing LST, SUHI, and their variation with built-up areas and vegetation. The third chapter presents a daytime analysis of LST and SUHI. Correlations between vegetation, built-up areas, and LST or ΔT show the association between these variables. An analysis of each country's Land Use Land Cover (LULC) characteristics show its role in the observed SUHI/SUCI trends.

The fifth chapter extends the daytime analysis to nighttime and diurnal and seasonal comparisons of SUHI. This chapter primarily focuses on comparative analysis – satellite data Landsat 8 vs. MYD11A2, day vs. night, seasonal, and India vs. the US. The diurnal variation in SUHI/SUCI is quantified and explained using the LULC data.

The sixth chapter provides a temporal analysis of SUHI. It discusses the SUHI change with urbanization. The impervious surface area (ISA) changes in each city represented urbanization, which relates to the ΔT change.

The seventh chapter focuses on the analysis of the built-up area LSTs. This study analyzes built-up area LSTs in different scenarios, 1.)based on the construction period and 2.)based on the spatial neighbors' land use. The first part of the chapter discusses the variation in urban built-up land use

LSTs in the new (2007-2016) and old (prior 2007) areas to understand how the 'newly' built-up land use compares the old in terms of their thermal performance. The second part of the chapter analyzes the variation in built-up land use LST with its spatial neighbors.

The eighth or final chapter summarizes the findings and provides conclusions. This chapter also outlines the limitations of this work and the prospects of future work.

2 BACKGROUND AND LITERATURE

2.1 OVERVIEW

The synergistic effects of intense urbanization and climate change already have a marked effect on human health and quality of life and demand closer scrutiny on many fronts. Consequently, understanding the interaction of building design, land use, energy use, anthropogenic heat release, and local air temperature is critical within building science and urban design disciplines. This chapter discusses the overall urban energy balance and introduces UHI and its types, presenting a broader explanation of the phenomenon in a generic scenario. This chapter also details specific literature relevant to the goal of this research.

2.2 CONCEPTS: URBAN CLIMATE AND THE URBAN HEAT ISLAND PHENOMENON

2.2.1 Urban Climate and Energy Balance

Several natural and human-modified changes impact the urban boundary layer (an imaginary atmospheric layer above the urban area) climate across the temporal and spatial scales. From small-scale turbulences at the micro-scale to the macro-scale jet streams and hurricanes, the climatic system is altered by the natural and human-modified earth's surface characteristics, as seen in Figure 3.

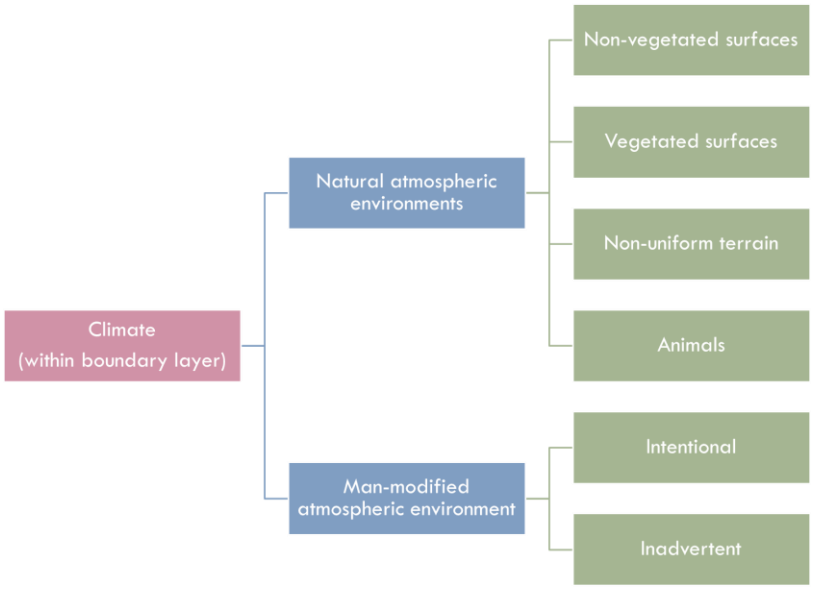

Figure 3: Factors altering urban boundary layer climate(Oke, 1987)

While natural impacts of the earth's surface on climate may or may not be interfered with, it is crucial to understand and limit the negative impact of the human-modified environment on climate. Urban areas are the best examples of human-modified environments. From Figure 4, the factors that most impact UHI can be related to human-made modifications of urban areas.

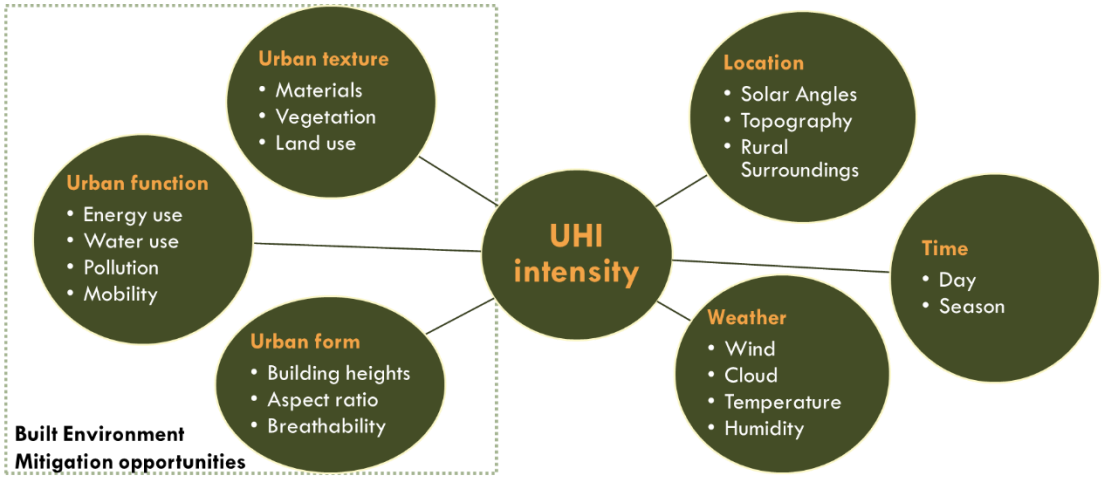

Figure 4: Natural and human-modified factors that contribute to UHI formation

Understanding the energy exchanges within the urban areas could provide insight into the contributors and mitigation measures related to UHI. The energetic basis behind an arbitrary urban area can be explained using Equation 1(Oke, 1987). Any given system tends to be in equilibrium by balancing energy, and therefore for any given system:

Energy Input - Energy Output ± Change in Stored energy = 0

Based on this, Equation 1 represents the net change in energy in any controlled volume. Figure 5 shows these energy exchanges within a hypothetical urban area.

$$Q^* + Q_F = Q_H + Q_E + \Delta Q_S + \Delta Q_A \qquad \text{……Equation 1}$$

Where;

Q^*	Net radiation (shortwave + longwave) entering the control volume
Q_F	Anthropogenic heat, added to the control volume by human-made factors such as buildings, transportation, humans
Q_H	Sensible heat leaving the control volume
Q_E	Latent heat leaving the control volume
ΔQ_S	Net storage heat within the control volume
ΔQ_A	Net advection heat happening horizontally from the sides of the control volume

All units in W/m^2

As shown in Equation 1, each energy exchange changes with space and time. For example, in a rural area, Q_F – the anthropogenic heat flux would be minimal compared to a dense urban area. Q^* predominantly comprises shortwave radiation during the day, while only longwave radiation at night. Using this energy balance as the basis, comparing human-modified urban environments with natural or near-natural rural areas could provide information on the association between urban areas and urban climate. Different types of UHI at different spatial scales can also be explained using the terms in Equation 1, as seen in Section 2.2.2 and Table 1.

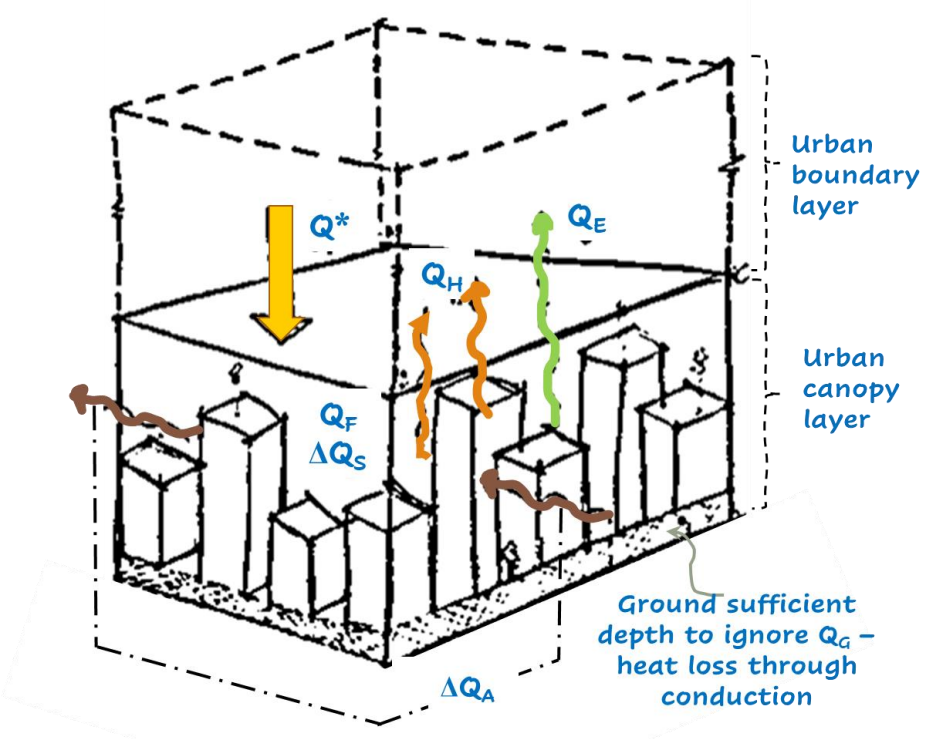

Figure 5: Energy Balance in Building-Air Volume (Reference: Oke, 1987)

2.2.2 The Urban Heat Island Phenomenon

The first UHI studies date back to the 1800s when Luke Howard compared temperatures in London to those outside the city(Howard, 2012). This study contemplated that the higher London temperatures represented an "artificial warmth induced by the city's structure, by a crowded population, and by the consumption of great quantities of fuels in fires" (Howard, 2012). Since then, UHI has been defined as the higher temperatures recorded in urban areas compared to their rural surroundings and quantified as the difference between urban and rural temperatures (ΔT). The annual average ambient temperature can be 1-3^{0}C higher than surrounding rural areas in a city with at least one million people. In addition, exposed surfaces of the built environment in peak summers can be 30^{0}C to 40^{0}C hotter than the urban ambient air dry bulb temperature(H Akbari,

Pomerantz, & Taha, 2001). Figure 6 shows an example of a grey roof's surface temperature compared to a shaded roof in Ho Chi Minh City, Vietnam.

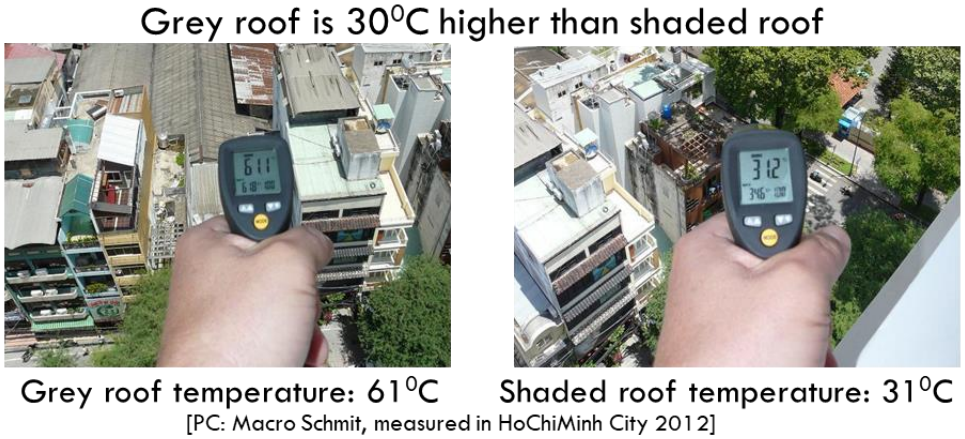

Figure 6: Grey roof temperature compared to the shaded roof temperature in HoChiMinh City, Vietnam. (PC: Prof. Marco Schmit, TU-Berlin)

As demonstrated in Figure 7, the differences in the energy exchanges between urban and rural relate to the UHI formation(Oke, 1987, 1988). The characteristics of urban areas that could impact UHI formation(Oke, 1987, 1988; Haider Taha, 1997) are:

- increased absorption of radiation ($+\Delta Q_S$),
- increased intensity of longwave radiation ($+Q^*$),
- increased sensible heat storage capacity (due to impervious surfaces) ($+Q_H$),
- increased anthropogenic heat (from buildings, humans, vehicles) ($+Q_F$),
- reduction in the latent heat fraction ($-Q_E$) (due to decreased vegetation and evapotranspiration), and
- the reduction in heat transfer due to decreased wind speeds ($-\Delta Q_A$).

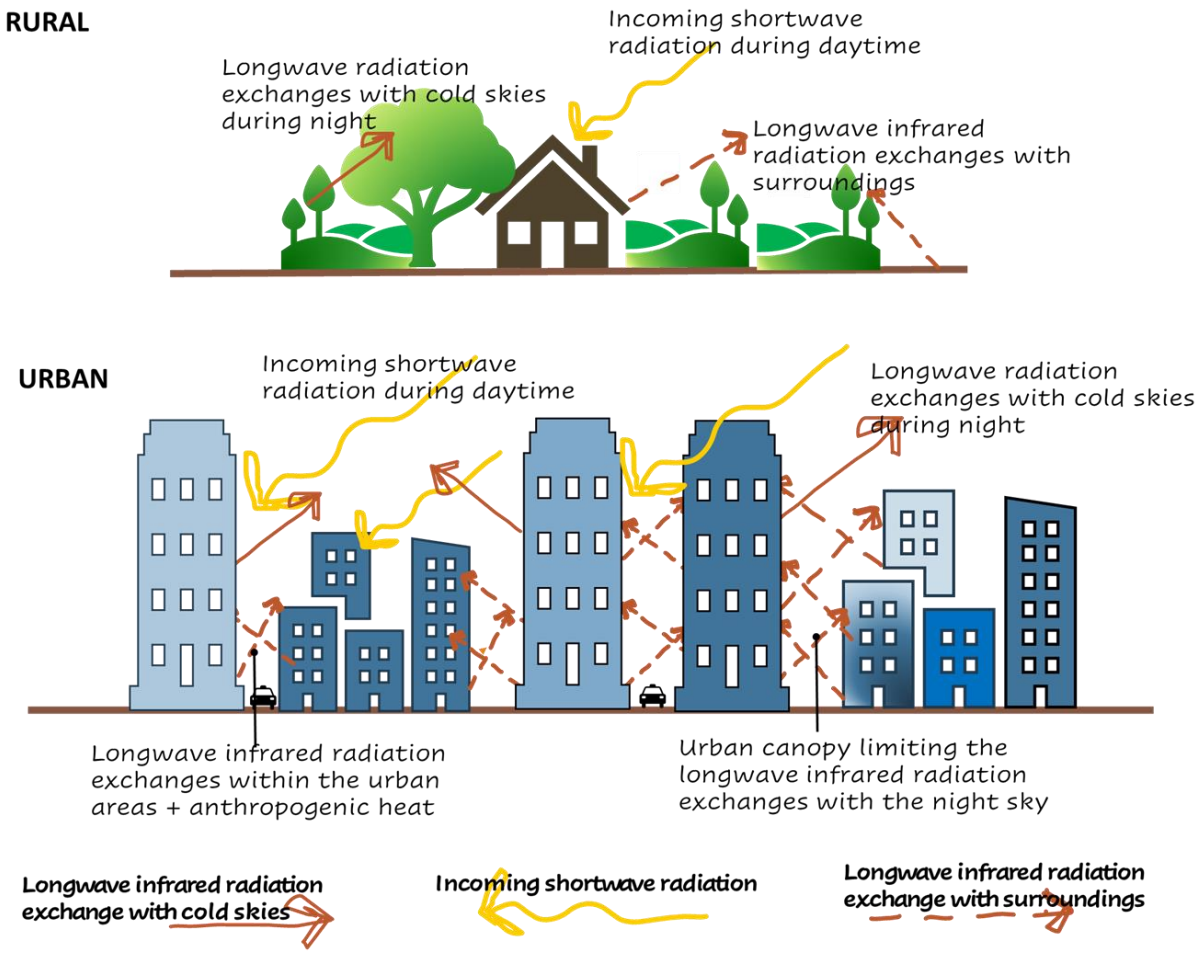

Figure 7: Differences in energy exchanges between urban and rural areas attributed to the UHI formation.

2.3 TYPES OF URBAN HEAT ISLANDS

To advance the scientific understanding of this complex phenomenon, researchers branched the phenomenon into three different types, as seen in Figure 8, based on the location of the temperature measurement - addressing different spatial scales. The UHI phenomenon in three categories is A.) Surface UHI (SUHI), B.) Canopy UHI (CUHI), and C.) Boundary Layer UHI. Figure 8 shows a typical temperature profile across the cross-section of urban-rural areas and the different types of UHI.

As seen in the figure, in simple terms, the type of UHI can be identified based on the location of the temperature measurement. SUHI represents the land surface temperatures (LST) commonly measured using remote sensing methods. CUHI and boundary layer UHI are air temperature measurements. CUHI is measured in the urban canopy (≈2m from ground level), and boundary layer UHI is air temperatures measured in the urban boundary layer, as shown in Figure 8C. All three UHI types can vary in magnitude and intensity of impact on the environment and human well-being for a given location and time. For example, SUHI and CUHI are more relevant when studying the impact of the urban built environment on human well-being and energy consumption. However, boundary layer UHI is important in studying the variation in macro-scale weather conditions due to urban areas. Table 1 lists the UHI types, study methods, energetic processes, and relevant impacts. Though not extensive, Table 1 lists the most common characteristics of each type of UHI. Equation 1 on the energetic basis of urban climate can explain the urban and rural energy processes contributing to UHI formation. As seen in the table, radiation (both longwave (LS)and shortwave (SW)), heat fluxes (sensible, latent, and storage), and anthropogenic heat (addition of heat due to human-modified environments) are all altered by the urban built environments-contributing to UHI formation. In the case of SUHI, the increased absorption of radiation by urban material and reduced latent heat flux due to no or minimal vegetation are expected to be the crucial factors influencing SUHI formation. For CUHI, urban buildings and human and vehicular populations contribute to reduced radiation loss, increased storage, and anthropogenic heat. Boundary layer UHI, which is more impacted by atmospheric changes, is also an indirect impact of the urban built environment but at a larger horizontal scale and higher in the vertical atmospheric scale. As seen in the table, each type of UHI could provide different information related to the built environment and mitigation measures.

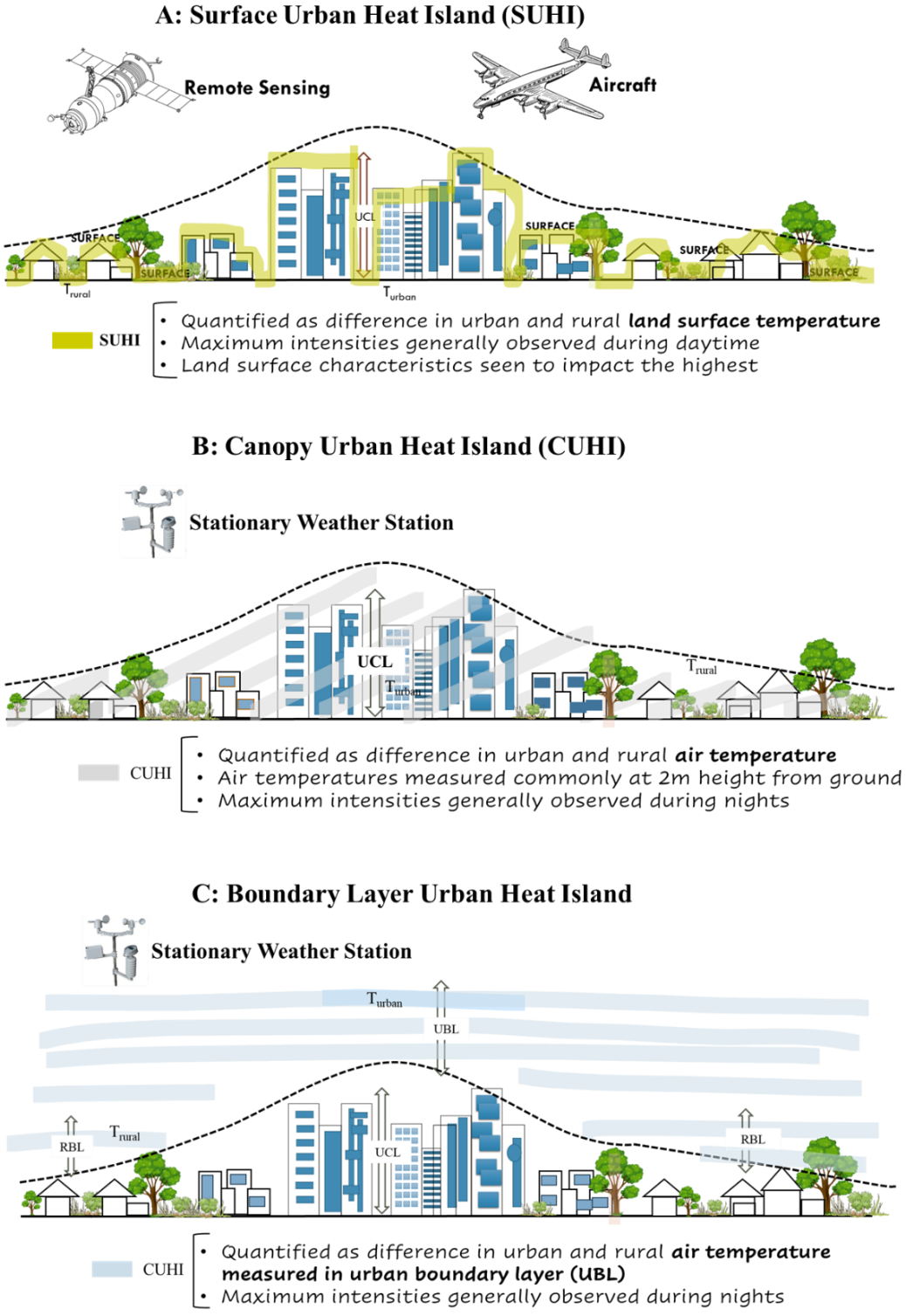

Figure 8: Typical temperature profile of the UHI phenomenon across a location and the three different types of UHI. A.) Surface, B.) Canopy, and C.) Boundary Layer UHI with the temperature measurement locations shown.

Table 1: Urban Heat Island types- their study methods, energy processes, urban/rural features, and possible impacts

UHI Type	Data & Study Method	Process – Energy exchanges	Examples of Urban/Rural Feature	Possible Impact
Surface UHI	• Remote Sensing – satellites and other airborne instruments.	• Increased net SW radiation • Increased storage heat flux • Decreased latent heat flux	• Absorption by materials with low emissivity and reflectance • Increased thermal admittance of construction material and barren land • Increased impervious surfaces and reduced vegetation in urban areas	• Urban planning • Outdoor thermal comfort • Stormwater runoff
Canopy UHI	• Fixed weather station • Traverse measurements using land transportation • Urban canopy models	• Decreased LW radiation loss • Increased anthropogenic heat • Increased net SW radiation • Increased storage heat flux • Decreased latent heat flux	• Increased surface area and multiple reflections in urban areas • Reduced sky view factor in urban areas • Humans, buildings, and automobiles reject heat into the street canyons • Increased waterproofing of building material	• Thermal comfort • Building energy consumption • Wind speeds • Air quality • Urban ecology • Stormwater runoff
Boundary layer UHI	• Fixed weather stations • Traverse measurements using aircraft • Meso-scale models	• Increased incoming LW radiation • Decreased LW radiation loss	• Air pollution increases heat gain from urban areas into the upper atmosphere	• Air mixing and circulation • Air quality • Atmospheric cloud formation • Atmospheric winds

As seen in Table 1, SUHI and CUHI analysis could provide critical feedback needed for the planning of urban areas. In the case of SUHI, the increased absorption of radiation by urban impervious material and reduced latent heat flux due to no or minimal vegetation might relate to SUHI formation. For CUHI, urban building design and mechanical conditioning, human population, and vehicular population contribute to reduced radiation loss, increased heat storage, and anthropogenic heat. SUHI analysis is more relevant for local scale (a neighborhood) analysis, especially across multiple locations. In contrast, CUHI analysis can provide detail on the interaction between buildings and outside air temperatures at a micro-scale (an urban street canyon). The in-situ measured air temperatures for CUHI analysis lack the spatial scale offered by remote sensing-based SUHI analysis (Voogt & Oke, 2003; Weng, 2009). Also, remote sensing-based SUHI analysis provides consistency in data extraction and analysis methods for multi-city or multi-study comparisons (Deilami, Kamruzzaman, & Liu, 2018; D. Zhou et al., 2018). Land surface temperatures from SUHI studies are also helpful in estimating the surface energy and water balance across different spatial scales (Z. L. Li et al., 2013). The applicability and validity of satellite-derived LSTs are also apparent from studies that estimated air temperatures using LST (Bechtel, Zakšek, Oßenbrügge, Kaveckis, & Böhner, 2017; Hooker, Duveiller, & Cescatti, 2018). A few studies (Good, Ghent, Bulgin, & Remedios, 2017) also showed a strong correlation between LST and air temperatures. Therefore, both SUHI and CUHI research are essential to estimate the impact of the urban built environment on urban climate, precisely urban temperatures. Factors contributing to all these types of UHI include various bio-physical characteristics that can be specific to a location and a given time, making UHI a dynamic phenomenon that changes with space and time. Despite this, most of the current UHI research is still from countries of North America, Europe, and China, and the available research for a rapidly urbanizing and highly

populated country like India is still scant and is in its infancy (Deilami et al., 2018; D. Zhou et al., 2018).

2.3.1 Urban Cool Islands

Urban cool islands (UCI), as the name suggests, are urban areas that are cooler than the surrounding suburban and rural areas. This phenomenon is a relatively newer observation by the research community, and its causes and impacts are still under scrutiny (X. Yang, Li, Luo, & Chan, 2017). Prior studies(Oke, 1988; Theeuwes, Steeneveld, Ronda, Rotach, & Holtslag, 2015) discussed an early morning UCI observed in cities and attributed it to the slow heating of urban fabric compared to the rural areas. UCI is most reported across some tropical and dry locations of the world and is more predominant when studying land surface temperatures (Surface UCI or SUCI). However, few prior studies showed the occurrence of urban cool islands in some parts of the US (Imhoff, Zhang, Wolfe, & Bounoua, 2010; Theeuwes et al., 2015; L. Zhao et al., 2014). Based on research to date, the UCI formation is due to the difference in urban and rural land use and the amount of solar radiation each of these areas receives based on the time of the day. However, a more detailed understanding of the formation of UCI and its mitigation measures is still missing in the literature.

2.4 BACKGROUND ON SUHI: REMOTE-SENSING DATA AND VARIABLES

Remote sensing is the process in which sensors mounted on aircraft, other airborne instruments, or, most commonly, satellites record data from the earth's surface to provide information on the characteristics of the earth's surface in the form of geographically referenced digital images with data. Some typical remote sensing applications are environmental studies, climate change, and meteorology. Urban climates, especially UHI, are widely studied using this method and are referred to as SUHI(Deilami et al., 2018; D. Zhou et al., 2018). Land Surface Temperature (LST) is almost always the most useful metric to characterize, map, and quantify SUHI. Studies show that Land Use Land Cover (LULC), the Impervious Surface Area (ISA), and vegetation have a vital role to play in SUHI formation.

2.4.1 Remote Sensing SUHI

Thermal remote sensing is the name given to remote sensing data used to calculate temperatures. A 2003 study(Voogt & Oke, 2003) on thermal remote sensing shows its relevance in urban climate studies, especially in understanding the correlation between surface and air temperatures and extracting information that would serve as inputs into other urban climate models. The study pointed out that while there are some advancements in this field, there are still several limitations, especially in studying the urban surface and air temperatures to solve the urban surface energy balance. Another meta-analysis(Weng, 2009) reviews thermal remote sensing data's methods, techniques, and applications in understanding UHI. This study shows that while UHIs are most studied by correlating LSTs with vegetation and other urban biophysical parameters, deriving UHI parameters from this data to solve surface energy balance is still limited. This study seconded the previously mentioned study regarding the importance of defining an "urban surface" at different scales and how remote sensing could resolve this. While these studies show the critical applications

of remote sensing in urban climate analysis, a more recent study(Deilami et al., 2018) reviewed 75 peer-reviewed articles to identify the standard methods used in studying SUHI and the spatio-temporal factors influencing SUHIs. This study showed LST as a standard metric to explain SUHI, and most studies agree with % ISA and LULC as the most critical factors impacting SUHI. According to this study, the most reported factors influencing SUHI were vegetation cover, season, built-up area, diurnal changes, population densities, and water bodies. All three of these meta-analyses conducted over the last 15 years show that quantifying SUHI and its contributing factors are crucial standalone and in coordination with other types of UHI.

2.4.2 Satellite Data

Figure 9 shows the data transfer process of remote sensing. As seen in the figure, in remote sensing, the airborne sensors on the satellite capture the reflected light from the earth's surface in the form of pictures and data. These images and data collected need to be further processed by the researchers to convert and interpret them in the necessary analysis metrics. The advantages of remote sensing methods for UHI analysis are apparent in multiple-city studies like this. Consistency in the data collection methods and how the data is processed reduces or eliminates bias and allows for better comparison across multiple cities.

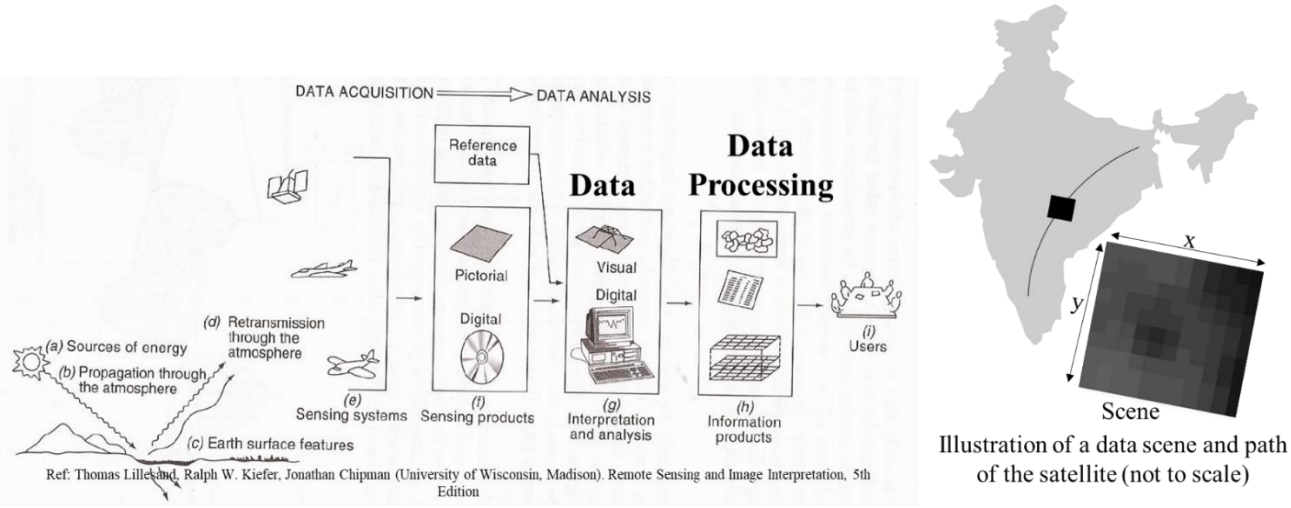

Figure 9: Overview of the remote sensing satellite data collection and processing and a data scene.

Remote sensing data are most commonly available in different wavelengths. Sensors mounted on satellites read the reflected light from the earth's surface in different wavelength ranges, each referred to as a Band (#). The band numbers and wavelengths of data may vary with sensors. Figure 10 and Table 2 show an example of the data collected in different bands using Landsat 7 and 8 satellites. Each wavelength range could provide different information on the surface conditions. For example, the vegetation on the earth's surface absorbs light in the visible range and reflects light in the near-infrared (NIR) range. Hence, vegetation on the earth's surface can be studied using data from these two wavelengths. Depending on the data satellite type, each data band or the processed data is provided to the user in the form of data scenes (rectangles measuring X by Y that vary with the sensor) constituted of several pixels (squares with a size that vary with sensors).

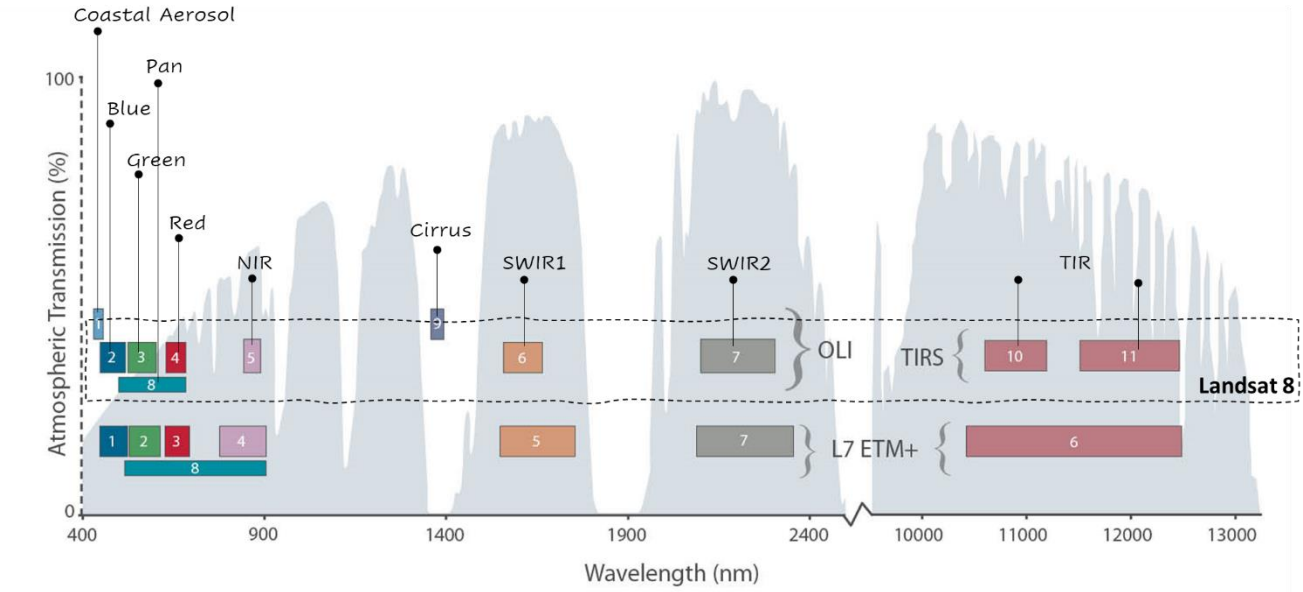

Figure 10: The wavelengths in which Landsat 7 and 8 satellites collect data and their corresponding band numbers. Image source: (US Geological Survey, 2019)

Table 2: The spectral bands, wavelengths, and spatial resolution of data from Landsat 7 and 8 satellites (Table source: (US Geological Survey, 2019)

Landsat-7 ETM+ Bands (µm)			Landsat-8 OLI and *TIRS* Bands (µm)		
			30 m Coastal/Aerosol	0.435 - 0.451	Band 1
Band 1	30 m Blue	0.441 - 0.514	30 m Blue	0.452 - 0.512	Band 2
Band 2	30 m Green	0.519 - 0.601	30 m Green	0.533 - 0.590	Band 3
Band 3	30 m Red	0.631 - 0.692	30 m Red	0.636 - 0.673	Band 4
Band 4	30 m NIR	0.772 - 0.898	30 m NIR	0.851 - 0.879	Band 5
Band 5	30 m SWIR-1	1.547 - 1.749	30 m SWIR-1	1.566 - 1.651	Band 6
Band 6	60 m TIR	10.31 - 12.36	*100 m TIR-1*	*10.60 – 11.19*	Band 10
			100 m TIR-2	*11.50 – 12.51*	Band 11
Band 7	30 m SWIR-2	2.064 - 2.345	30 m SWIR-2	2.107 - 2.294	Band 7
Band 8	15 m Pan	0.515 - 0.896	15 m Pan	0.503 - 0.676	Band 8
			30 m Cirrus	1.363 - 1.384	Band 9

SWIR: Shortwave Infrared, NIR: near-infrared, TIR: thermal infrared.

Some of the most common sensors and related satellites used in thermal remote sensing applications are 1.) ETM+ and TIRS are on board NASA's Landsat 7 and 8 satellites, respectively,

2). MODIS sensor on NASA's Terra and Aqua satellites, 3). ASTER on board an American Japanese ASTER satellite, and 4). AVHRR – Advanced Very High-Resolution Radiometer on board an NOAA satellite. While there are several others, these four are some of the most common sensors, and Landsat and MODIS are most commonly used in global studies(Deilami et al., 2018; D. Zhou et al., 2018). The advantage of these two satellites is cost-free data availability for global locations. However, since each of these satellites' spatial and temporal resolution varies, their applicability in SUHI studies would depend on the study's goal.

2.4.3 Remote sensing analysis variables – Spectral Indices

The remote sensing analysis variables in the main categories are the LST and SUHI magnitude (ΔT) - the dependent variables, and the various factors that impact them (independent variables). Based on the satellite type, the user calculates LST, or it is directly available as a data product for download. On the other hand, SUHI magnitude quantification is done by the researchers using various methods. Section 1.4.1 discusses the SUHI quantification methods more.

When it comes to the factors contributing to SUHI, there are several. Some prevalent factors impacting SUHI are LULC, built-up or impervious surface areas, vegetation, population, anthropogenic heat release, and other climatic factors (air temperature, wind, precipitation). Different data sources and methods are used across studies to quantify these factors and their association with SUHI. Among those, spectral indices are one of the most common ways of quantifying the LULC using remote sensing data.

Remote sensing spectral indices explain the land surfaces characteristics such as vegetation, soil, water, snow, built-up area, barren areas, and other geological features on the earth's surface. Table 3 presents the most used spectral indices on the built environment across SUHI studies. A review of these indices showed that while the Normalized Difference Built-up Index(NDBI)(Zha, Gao, &

Ni, 2003) is an extensively used index to explain built-up, separating barren lands from urban built-up could be a limitation. The Enhanced Built-up Bareness Index (EBBI)(As-syakur, Adnyana, Arthana, & Nuarsa, 2012) tried to address this; however, the application of this index is still minimal. Other indices, such as Urban Index(UI)(Kawamura, Jyamanna, & Tsujiko, 1996), Built-up Index (BUI)(Lee, Lee, & Chi, 2010), and New Built-up Index (NBI)(Kaimaris & Patias, 2016), are also reported to have issues in identifying barren lands from built-up. The number of researchers using these metrics is minimal. Based on the literature, the Index Based Index (IBI) showed the potential of differentiating barren from built-up land and could provide more appropriate information on urban built-up areas.

Along with these built-up indices, the other most common spectral indices used in SUHI studies fall in the categories of vegetation and water. While this study doesn't detail water indices, the vegetation index used in the analysis is the Normalized Difference Vegetation Index (NDVI)(The Earth Observatory, 2000). NDVI ranges between -1 and +1, with 1 being the highest density, and < 0.1 is mainly observed in areas other than vegetation (such as built-up, sand, snow, and barren). Sparse vegetation results in moderate NDVI (0.2 - 0.5), and the NDVI of dense green forests is highest (0.6 - 0.9). NDVI calculation in Table 3 uses data from visible and near-infrared wavelengths. The leaves of vegetation absorb the visible band of sunlight for photosynthesis. While doing this, leaves strongly reflect the near-infrared light. Therefore, the light reflected in these wavelengths predicts the density and greenness of vegetation, as demonstrated in Figure 11. As seen in Figure 11, the NDVI value of healthy green vegetation is higher than the NDVI of non-green vegetation.

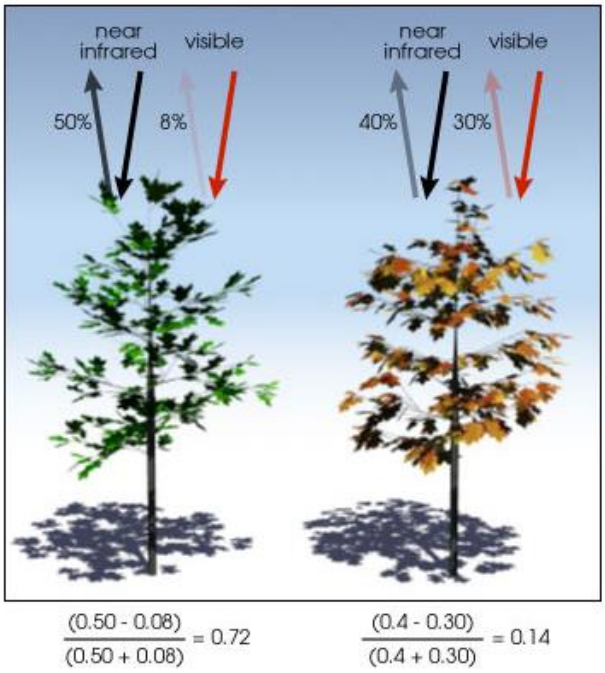

NDVI is calculated from the visible and near-infrared light reflected by vegetation. Healthy vegetation (left) absorbs most of the visible light that hits it, and reflects a large portion of the near-infrared light. Unhealthy or sparse vegetation (right) reflects more visible light and less near-infrared light. The numbers on the figure above are representative of actual values, but real vegetation is much more varied. (Illustration by Robert Simmon).

Figure 11: An illustration showing NDVI of green vegetation vs. NDVI of non-green vegetation. Image source: (The Earth Observatory, 2000)

Table 3: Details on the most commonly used spectral indices across SUHI studies

Spectral Index		Represents	Calculation
NDVI	Normalized Difference Vegetation Index	**Determines live greenery** NDVI quantifies the green vegetation and explains the vegetation density	$\frac{NIR - Red}{NIR + Red}$
NDBI	Normalized Difference Built-Up Index	**Identifies the urban areas** Map urban built-up areas with an accuracy of 92.6%, as reported by the author. Extensively used across prior studies	$\frac{SWIR1 - NIR}{SWIR1 + NIR}$
EBBI	Enhanced Built-Up and Bareness Index (EBBI)	**Identifies built-up areas** EBBI targets to differentiate the built-up and barren lands in urban areas more accurately than IBI, NDBI, and UI.	$\frac{SWIR1 - NIR}{\sqrt[10]{SWIR1 + NIR}}$
UI.	Urban Index (UI.)	**Identifies the urban areas** It was developed and verified for a tropical climate – Colombo, Sri Lanka	$\frac{SWIR2 - NIR}{SWIR2 + NIR} +$
IBI	Index-Based Built-Up Index (IBI)	**Show the built-up areas based on other indices such as NDBI, SAVI[1], MNDWI[2]** Computed based on other indices, including built-up areas, vegetation, and water features.	Refer to Equations 6 and 7 in this dissertation $\frac{\frac{2 * SWIR1}{SWIR1 + NIR} - \left[\frac{NIR}{NIR + Red} + \frac{Green}{Green + MIR}\right]}{\frac{2 * SWIR1}{SWIR1 + NIR} + \left[\frac{NIR}{NIR + Red} + \frac{Green}{Green + MIR}\right]}$ $= \frac{\frac{2Band6}{Band6 + Band5} - \left[\frac{Band5}{Band5 + Band4} + \frac{Band3}{Band3 + Band6}\right]}{\frac{2Band6}{Band6 + Band5} + \left[\frac{Band5}{Band5 + Band4} + \frac{Band3}{Band3 + Band6}\right]}$

[1] Soil Adjusted Vegetation Index
[2] Modified Normalized Difference Water Index

2.5 LITERATURE REVIEW

2.5.1 SUHI Quantification Methods

SUHI magnitude (ΔT) is commonly calculated or defined as the difference between urban and rural mean LSTs. Most prior research broadly uses two different ways of defining urban and rural areas, as shown in Figure 12. In the first type, urban areas are geographically delineated based on different datasets or information representing urban areas. In the second type, urban and rural parcels of land are identified based on the LULC data. However, this urban-rural delineation methodology has always been a topic of interest for UHI researchers, and there are several other differences across methods that make each of them unique.

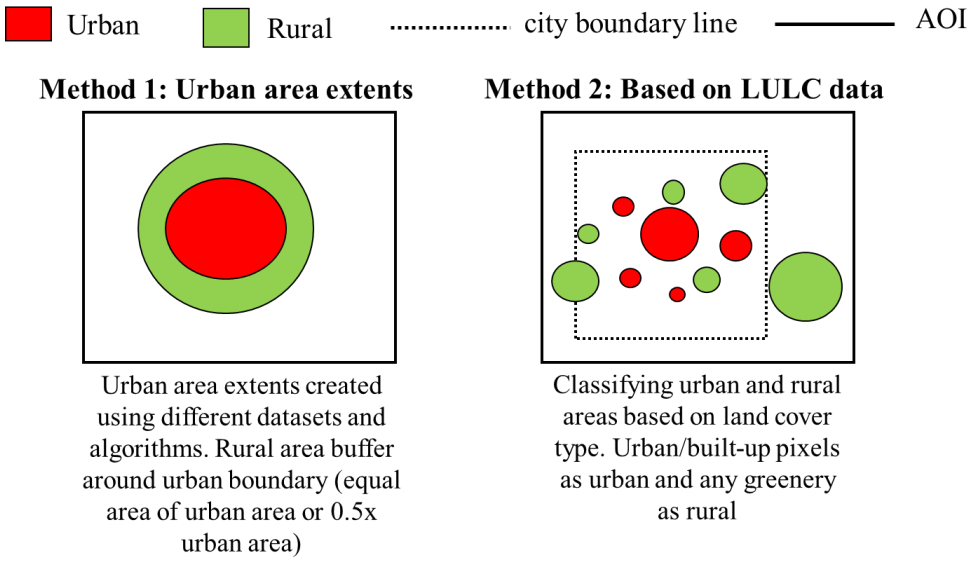

Figure 12: Most typical ways SUHI studies define urban and rural areas to quantify SUHI.

For this reason, this study reviews 47 peer-reviewed journal articles from the last 10+ years (2010-2022) to identify the most common ways of quantifying ΔT and defining urban and rural areas. The three main questions this review aims to answer are:

1.) Does the urban-rural delineation method vary with the geographical location of the study?

2.) Does the urban-rural delineation method vary with the satellite data?

3.) Does the urban-rural delineation method impact the ΔT?

Figure 13 summarizes the reviewed literature about the study location, the satellite used, and the ΔT results. The figure shows that the most recent literature (especially between 2005-2020) is from Asia and other non-European and non-North American countries, unlike the UHI research from the initial years. MODIS and Landsat thermal data are most widely used across these studies, with Landsat being more predominant in the US and Europe. This analysis also showed that the occurrence of Surface Urban Cool Islands (rural LST > urban LST) is not specific to a location or the satellite data.

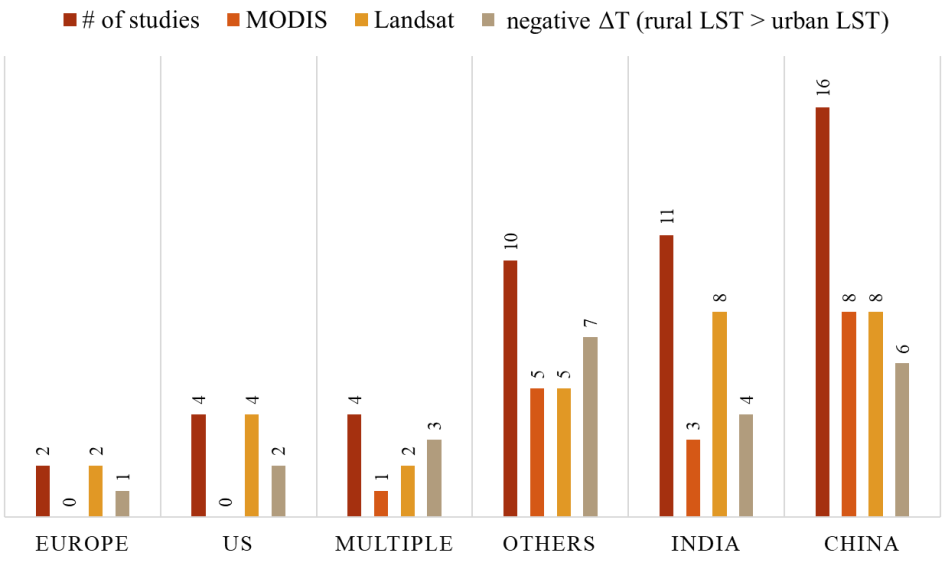

Figure 13: Summary of the literature review on urban-rural delineation methods across 47 studies from the past 10 years

Figure 14 summarizes the urban-rural delineation literature reviewed, the type of SUHI quantification method used, the location of the study, the data type, and the observation. Based on this literature review from the last 10+ years, the urban-rural delineation methodology can be categorized into four primary categories and several sub-categories, as shown in Figure 14 and Table 5. The urban-rural delineation methods categorized based on the review are:

1. Administrative Boundaries: In this category, the city's administrative boundaries or the traffic rings/ring road/ circumferential highways separate the urban from the rural.

    1A. Most (11/47) of the studies fall under this category: an urban area is a city or the metropolitan area extent, and the area beyond this urban boundary is rural.(Alves, 2016; Borbora, Das, Sah, & Hazarika, 2018; Cheval & Dumitrescu, 2015; Cui, Xu, Dong, & Qin, 2016; Haashemi, Weng, Darvishi, & Alavipanah, 2016; Rasul, Balzter, & Smith, 2015, 2016; Schwarz, Lautenbach, & Seppelt, 2011; C. Wang, Myint, Wang, & Song, 2016; C. Yang et al., 2017)

    1B. The administrative division of the city or areas based on traffic rings is defined as urban, while the areas beyond the outer traffic circle are rural. (Y. Cai, Zhang, Zheng, & Pan, 2016; K. Liu et al., 2015; H. Wang, Zhang, Tsou, & Li, 2017)

    1C. The urban area is the city or the metropolitan area extent, as defined in 1A. However, the rural areas are specific districts beyond this boundary based on the rural land cover type (Taheri Shahraiyni et al., 2016).

    1D. The LST of individual pixels within the city boundary and rural is a sub-urban buffer beyond the city boundary (Clinton & Gong, 2013).

2. Urban Area Maps: The urban areas are delineated using the urban area maps generated by various algorithms (e.g., city clustering algorithm) and datasets (e.g., impervious surface area and nightlight data). The sub-categories in this method are:

    2A. The urban area is defined using urban area extents developed by prior researchers using various datasets and methods. The rural area is an equal area buffer around the urban area. Ten of 47 studies review fall into this category (Fu & Weng, 2018; Kumar et al., 2017; X. Li, Zhou, Asrar, Imhoff, & Li, 2017; Peng et al., 2012;

Schwarz et al., 2011; Shastri, Barik, Ghosh, Venkataraman, & Sadavarte, 2017; J. Wang, Huang, Fu, & Atkinson, 2015; S. Zhao, Zhou, & Liu, 2016; B. Zhou, Rybski, & Kropp, 2013)

2B. In this category, cities are divided into zones based on urban development intensity (UDI), built-up intensity, or the % impervious surface areas. The least UDI areas or buffers around the urban areas represent the rural areas (Imhoff et al., 2010; D. Zhou et al., 2016; D. Zhou, Zhao, Liu, Zhang, & Zhu, 2014; D. Zhou, Zhao, Zhang, Sun, & Liu, 2015).

3. Land Use Land Cover: In this third category, the LULC of a location is used to identify urban and rural areas.

   3A. Few studies used a pixel-based selection of built-up areas to represent urban areas, and the vegetative pixels from the data represent rural areas(Choi, Suh, & Park, 2014; Schwarz et al., 2011; L. Zhao et al., 2014).

   3B. Urban maps are developed based on built-up area land use, and rural areas are buffers around the built-up extent(Gupta, Mathew, & Khandelwal, 2019; Mathew, Khandelwal, & Kaul, 2016; Mathew, Sreekumar, Khandelwal, & Kumar, 2019; Q. Yang, Huang, & Li, 2017).

   3C. Urban areas are parcels of built-up land use, and rural areas are vegetative land cover parcels(Dobrovolný, 2013; Heinl, Hammerle, Tappeiner, & Leitinger, 2015; Mohanta & Sharma, 2017; Schwarz et al., 2011).

4. Statistical approaches: The researchers defined SUHI magnitude using various statistical indexes or variables. Though this SUHI quantification method isn't the focus of this study, some of the statistical ways in which SUHI is quantified are:

4A. In two studies(L. Liu & Zhang, 2011; Singh, Kikon, & Verma, 2017), researchers used the Urban Thermal Field Variance Index (UTFVI) quantified using the equation below.

$$UTFVI = \frac{T_s}{T_s - T_{mean}}$$

Where T_s = LST of a particular pixel and T_{mean} = mean LST of the study area.

4B. In a few other studies, hot spots based on the ΔT thresholds represent SUHI(Taheri Shahraiyni et al., 2016)

4C. The city is diving into multiple SUHI zones using the mean and standard deviation of the LST(L. Chen, Jiang, & Xiang, 2016; W. Chen, Zhang, Pengwang, & Gao, 2017; Ma, Kuang, & Huang, 2010).

4D. Few studies identified SUHI using the LST anomaly-based approaches(Sharma & Joshi, 2014)

Some of the relevant observations from this review are:

- Studies from India mainly used LULC in urban-rural delineation. Six of 11 studies from India fall in category #3B (urban areas map based on LULC), and 2/11 studies used LULC-based pixel representation of urban and rural (category #3C).
- Two studies from the US used the urban area extents (category #2) developed using relevant data and algorithms.
- Administrative boundaries or traffic rings (category #1)define urban-rural areas in countries like Iraq, Iran, Romania, Brazil, and some in China.
- Most multi-city studies defined urban areas using the urban area maps (category #2) or the definition of urban areas based on LULC (category #3).

- Studies that used statistical approaches for quantifying ΔT did not report negative ΔT (SUCI).

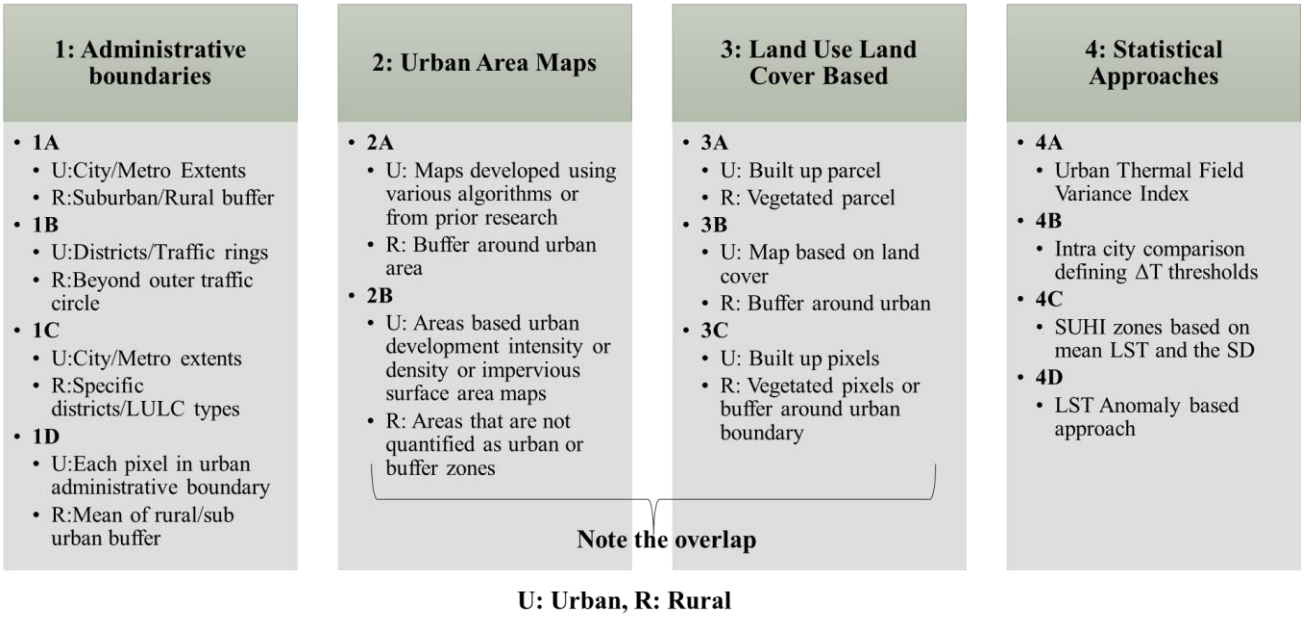

Figure 14: The categories and sub-categories of the urban-rural delineation and SUHI quantification method literature

The analysis discussed in this section showed some patterns in terms of the urban-rural delineation method and the location of the study. However, the urban-rural delineation method did not vary based on the satellite. The urban-rural delineation method did show an impact on the observed ΔT. Studies that used statistical approaches to quantify ΔT always showed positive ΔT. Another relevant observation from this review is that several studies use outdated LULC compared to the date of LST analysis. Prior research(Deilami et al., 2018; S. Zhao et al., 2016; D. Zhou et al., 2018) showed a mismatch in the date of LULC or other data used, and the date of LST analysis could impact the results. Such findings could be especially relevant for rapidly developing countries like India.

.

Table 4: A literature review of 47 peer-reviewed journals to analyze the urban-rural delineation and ΔT calculation methodology and its relevance to satellite data used, location, and the observations (SUHI vs. SUCI)

STUDY	METHOD													SATELLITE			LOCATION						Observation	
	Adminstrative				Urban Area		LULC			Statistical														
	1A	*1B*	*1C*	*1D*	*2A*	*2B*	*3A*	*3B*	*3C*	*4A*	*4B*	*4C*	*4D*	Landsat	MODIS	Other	India	US	China	Europe	Multiple	Other	SUHI	SUCI
Yang et al, 2017	●													●					●				●	
Wang et al, 2017		●												●					●				●	
Li et al, 2017					●										●			●					●	
Chen et al, 2017												●		●		●			●				●	
Zhou et al, 2016						●								●	●				●				●	
Wang et al, 2016	●													●	●			●					●	
Shahraiyni et al,2016			●								●			●								●	●	●
Cui et al,2016					●										●						●		●	●
Alves, 2016	●													●								●	●	●
Wang et al., 2015					●										●				●				●	●
Liu et al., 2015	●													●					●				●	
Heinl et al, 2015									●					●								●	●	
Cheval et al, 2015	●														●							●	●	
Choi et al, 2014							●									●					●		●	
Schwarz et al, 2011	●				●		●		●						●					●			●	
Ma et al, 2010												●		●					●				●	
Zhao et al, 2014							●								●			●				●	●	●
Kumar et al., 2017					●				●						●		●						●	●
Zhou et al,2015						●									●				●				●	●
Peng et al, 2012					●										●						●		●	●
Zhou et al, 2014						●									●				●				●	●
Imhoff et al, 2010						●									●			●					●	●
Cai et al, 2016		●												●					●				●	
Chen et al, 2016												●		●					●				●	
Dobrovolny, 2013									●					●								●	●	
Gupta et al, 2019								●						●			●						●	
Mathew et al, 2018								●						●			●						●	●
Mathew et al,2016								●							●		●						●	
Mathew et al, 2017								●							●		●						●	
Mathew et al, 2019								●							●		●						●	
Mathew et al, 2018								●							●		●						●	●
Mohanta and Sharma, 2017									●						●		●						●	
Shastri et al, 2017					●										●		●						●	●
Borbora et al, 2018	●														●		●						●	
Liu and Zhang, 2011										●				●					●				●	
Singh et al, 2017										●				●			●						●	
Sharma and Joshi, 2014													●										●	●
Rasul et al, 2016	●														●							●	●	●
Haashemi et al, 2016	●								●						●							●	●	●
Rasul et al, 2015	●													●								●	●	●
Clinton and Gong,2013				●											●						●		●	●
Zhou et al, 2013					●										●					●			●	●
Zhao et al, 2016	●				●										●				●				●	
Miles and Esau, 2017		●													●							●	●	●
Yang et al, 2017								●							●				●				●	●
Zhou et al, 2016						●									●				●				●	●
Peng et al, 2018					●										●				●				●	●

2.5.1.1 The local climate zone classification (LCZ) system

To address this issue of standardization of UHI quantification and the urban-rural delineation methods, UHI research in the past decade has moved towards adopting the Local Climate Zone (LCZ) classification system. LCZs are "regions of uniform surface cover, structure, material, and human activity that span hundreds of meters to several kilometers in horizontal scale" (Stewart & Oke, 2012). The LCZs intend to serve as universal LULC or landscape descriptions at a local scale. It aims to provide consistency and comparability of UHI or any urban temperature studies across the globe. The use of LCZs in UHI studies gained pace in the recent past. However, its application in SUHI research in India is still limited and needs a more comprehensive analysis(Xue, You, Liu, Chen, & Lai, 2020). Following the overall UHI research trend, most of the existing SUHI studies using the LCZ classification system are also from China(Shi, Xiang, & Zhang, 2019; R. Wang et al., 2019; Xia et al., 2022; J. Yang et al., 2020; Z. Zhao, Sharifi, Dong, Shen, & He, 2021), Europe(Dian, Pongrácz, Dezső, & Bartholy, 2020; Geletič, Lehnert, & Dobrovolný, 2016; Lehnert, Savić, Milošević, Dunjić, & Geletič, 2021), and the US (C. Wang et al., 2018; C. Zhao, Jensen, Weng, Currit, & Weaver, 2020). Many of the studies mentioned above are focused across 1-3 cities at a time and used Landsat 8(M. Cai, Ren, Xu, Lau, & Wang, 2018; Shi et al., 2019; J. Yang et al., 2020); MODIS (Dian et al., 2020; R. Wang et al., 2019) or ASTER(Geletič et al., 2016; C. Wang et al., 2018) dataset to extract LSTs. Irrespective of location and satellite data used, all studies except from arid regions(Eldesoky, Gil, & Pont, 2021; C. Wang et al., 2018) showed that LSTs vary significantly across the LCZs. Most studies generally observed higher LSTs in the built and industrial zones and lowest in vegetation and water zones. A few global(Bechtel, Demuzere, et al., 2019; Eldesoky et al., 2021) and national(N. Li et al., 2021) studies analyze LST and SUHI using LCZs. The first study(Bechtel et al., 2019) evaluated the applicability of LCZs in SUHI studies by

analyzing the diurnal LST and SUHI for 50 cities across the globe. The second (Eldesoky et al., 2021) discusses the suitability and limitations of LCZ use in LST analysis for the world's tropical, temperate, cold, and arid climate zones. In another(N. Li et al., 2021), 63 cities from China were used to show midrise and compactly built LCZ zones warmer compared to high-rise, low-rise areas, or open built-type, especially during summers. Two studies (Budhiraja, Pathak, & Agrawal, 2017; Das & Das, 2020) from India showed higher LSTs in compactly built zones compared to cooler vegetated and water areas. Both studies use the WUDAPT framework ((Bechtel et al., 2015)) to create LCZ maps and Landsat data for LST calculations. Extending such studies to multiple locations and improving the temporal scale could provide more information on existing SUHIs trends and possible mitigation measures.

2.5.2 LST and SUHI variation with different factors

This section introduces the variation and association of LST and SUHI with various factors. Built-up areas (all related variables such as built-up indices, ISA, albedo, and city size) and vegetation are the two main SUHI contributors of interest in this study. While the focus was on multi-city studies from peer-reviewed journals, a few relevant non-multi-city studies were also analyzed.

2.5.2.1 LST and SUHI variation with location and time of day

Prior studies indicate diurnal and spatial differences in LST and SUHI. In a multi-city study conducted across 32 major cities in China(D. Zhou et al., 2014), the daytime SUHI intensities varied between 0.01 -1.87^{0}C during daytime and 0.35-1.95^{0}C during nighttime. The study showed that while natural land cover and climate played a crucial role in daytime SUHI formation, human-made factors such as built-up density, albedo, and anthropogenic heat influence the nighttime SUHI formation. In another multi-city study from China(J. Wang et al., 2015), using the correlations and SUHI from 67 cities, scores were assigned to evaluate the role of various factors

on spatio-temporal variation in SUHI. The study showed that population density and the number of public buses were ranked important in impacting daytime SUHI in southern China compared to NDVI and albedo for northern China. During the nighttime, too, the impact of the studied factors varied. In southern China, NDVI and annual electricity consumption impacted SUHI the most, vs. albedo and the number of taxis for northern China.

In a study across 65 cities in North America(L. Zhao et al., 2014), the authors extracted LSTs to solve the surface energy balance and understand the relation between SUHI intensity and various natural (precipitation, climate, radiation)and human-modified(population, anthropogenic heat) factors impacting it. The study correlated MODIS-derived annual mean UHI magnitude with annual mean precipitation and population. The results showed that precipitation correlates ($r=0.74, p<0.001$) to daytime SUHI, and the population explains more of the nighttime SUHI ($r=0.54, p<0.001$) formation. Further, the cities were classified based on the Koppen-Geiger climate classification to quantify the differences between SUHI based on climates. The study showed that the daytime annual mean SUHI average for 24 cities in the humid southeast US is 3.3 K higher than that of the 15 dry regions. In another study from the US (Imhoff et al., 2010), SUHI across different biomes varied between -1- 9^0C. In this study, the least and maximum SUHI occurred when urban areas replaced the desert-xeric shrublands and temperate broadleaf-mixed forests, respectively.

In India, a study(Kumar et al., 2017) that analyzed diurnal urban-rural temperature differences showed that across most cities in India, the rural temperatures are higher than urban during daytime (SUCI). During the nighttime, however, around 90% of the study locations in India show SUHI. The study concludes that vegetation – agriculture, and irrigation are the two main factors influencing the urban-rural temperature gradients in India. In another study(Shastri et al., 2017),

diurnal and seasonal SUHI analysis also showed negative ΔT (urban LST < rural LST) during daytime. The study showed poorly vegetated non-urban regions and low evapotranspiration impact ΔT, especially during summers. Another two-city study(Mathew, Khandelwal, & Kaul, 2018) draws a similar conclusion on SUCI during daytime.

Also, a global multi-city study(Peng et al., 2012) across 419 big cities showed diurnal differences in SUHI. Daytime SUHI intensities reached 7^0C, while the nighttime maximum was 3.4^0C. This study also reported that 5% of the cities, such as Jeddah in Saudi Arabia and Mosul in Iraq, recorded negative SUHI intensities. Based on the results, albedo and vegetation seemed to have played an essential role in SUHI formation.

This review indicates that SUHI changes with space and time. Cities within the same country vary in terms of SUHI magnitude. While most temperate locations exhibit higher daytime SUHI, many tropical locations show daytime SUCI. Therefore, understanding the urban-rural temperature difference (ΔT) for different locations during different times of the day could provide a comprehensive insight into SUHI formation and influencing factors.

2.5.2.2 LST and SUHI variation with Vegetation

Of all the factors influencing LST and SUHI, the location's Land Use Land Cover (LULC), especially the vegetation and built-up land use types, is most frequently used to explain SUHI(Deilami et al., 2018; D. Zhou et al., 2018). In remote sensing studies like this - vegetation is commonly quantified using the Normalized Difference Vegetation Index (NDVI). The built-up areas are quantified using indices such as the Normalized Difference Built-up Index (NDBI) (Zha et al., 2003), Index Based Built-Up Index (IBI) (H. Xu, 2008), and Enhanced Built-up and Bareness Index (EBBI) (As-syakur et al., 2012). Photosynthetic vegetation (green vegetation) decreases LST and SUHI in most cases (W. Chen et al., 2017; Grover & Singh, 2015; Heinl et al.,

2015; Kikon, Singh, Singh, & Vyas, 2016; J. Li et al., 2011; Peng et al., 2012; Sharma, Chakraborty, & Joshi, 2014). However, the impact of vegetation (NDVI) on LST and SUHI varies with seasons (J. Li et al., 2011; Zhang, Odeh, & Han, 2009) and the background soil surface conditions (X.-L. Chen, Zhao, Li, & Yin, 2006; Yuan & Bauer, 2007). There is a non-linear correlation between NDVI and LST (Guo et al., 2015; Weng, Lu, & Schubring, 2004), and it depends on the season, soil conditions, and amount of vegetation. Such complex correlation between NDVI and LST led the prior researchers to propose the use of alternative metrics such as percentage impervious surface area (%ISA) (Yuan & Bauer, 2007) or vegetation fraction (Weng, Lu, & Schubring, 2004) to quantify the impact of vegetation and built-up areas on LST. Despite these possible limitations associated with using NDVI, it is still one of the most used indexes to quantify vegetation (Deilami et al., 2018; D. Zhou et al., 2018).

2.5.2.3 LST and SUHI variation with Built-up areas

Prior research shows that the correlation between built-up indices and LST is more straightforward than between NDVI and LST. Most prior research (X.-L. Chen et al., 2006; H. Xu, 2008; Zhang et al., 2009) shows a strong positive correlation between built-up surface density (predominantly quantified using NDBI) and LST, irrespective of seasons. As with built-up indices, a strong positive correlation exists between %ISA and LST. A US study(Imhoff et al., 2010) conducted across 38 urban regions from 8 different biomes showed that %ISA explains 70% of the variance in LST for all cities combined. Similar findings also exist from the Indian city Jaipur(Mathew, Khandelwal, & Kaul, 2017), for which the authors reported a season-independent strong linear (R^2 > 60%) positive correlation between %ISA and mean LST. In another study(Ali, Marsh, & Smith, 2017), LSTs from two different (climates and morphologies) cities – London and Baghdad showed a moderate positive correlation with built-up indices and a weak negative correlation with NDVI

in both cities. Based on the LULC data, correlations, and the LST maps, the study concluded that developing barren lands would reduce LSTs in Baghdad and increase LSTs in London. Like the positive correlations observed between %ISA and LST, an increase in urban area size increased SUHI non-linearly. As the urban areas doubled, SUHI increased to 0.7^0C in the US (X. Li et al., 2017).

2.5.2.4 Impact of urbanization on SUHI

Prior studies showed urbanization by quantifying the LULC changes over time. Most of such temporal SUHI studies explaining the impact of urbanization are from China and a few from the rest of the world. A 2018 study from Nanjing, China(S. Wang, Ma, Ding, & Liang, 2018), using Landsat data from 1985, 1991, 1996, and 2009 showed increased LSTs and decreased vegetation. Another study from Beijing, China(W. Chen et al., 2017) reported similar findings when studying LSTs from 1995 and 2009. These studies, however, do not quantify the change in SUHI over time.

Two studies from India show the impact of urbanization on SUHI and LST in Bengaluru(Sussman, Raghavendra, & Zhou, 2019) and Lucknow(Singh et al., 2017), respectively. The study from Bengaluru, India, reported an increase in SUHI from 2003 to 2018 during both daytime and nighttime of the wet season (August, September, October) and only during the nighttime of the dry season (December, January, February). The Lucknow study showed changes in LST and LULC from 2002 to 2014. Similarly, a study from the US(Jiang, Fu, & Weng, 2015) showed a change in LULC and LST between 2001 and 2006 in Marion county, Indiana. However, all these studies are single-city studies, and two studies use single-day(Jiang et al., 2015; Singh et al., 2017) Landsat data to compare LST from two different years. Another single-city study from the Metropolitan area of Rio de Janeiro (MARJ), Brazil (Peres, Lucena, Rotunno Filho, & França, 2018) analyzed the LST trend over 30 years using multiple Landsat data images. This study used

data from two 15-year periods (1984-1999 and 2000-2015) 30 years apart to show the impact of urbanization on LST and SUHI. The study showed that the LST increase is highest in urban areas compared to the rural (low-density urban) areas.

A multi-city study (Fan et al., 2017) analyzed the SUCI effect in five desert climate cities worldwide. The study showed that the magnitude of SUCI decreased over time due to an increase in urban LSTs. A few recent multi-city studies from India(Mohammad & Goswami, 2021; Raj, Paul, Chakraborty, & Kuttippurath, 2020) and globally(Z. Liu et al., 2022) also analyzed the impact of urbanization on LST and SUHI. Two studies from India analyzed the temporal trend of SUHI across 44 cities(Raj et al., 2020) and 150 cities(Mohammad & Goswami, 2021). Both studies showed a nighttime increase in SUHI over time. These studies showed that the daytime SUHI temporal change varies with the climate zone(Mohammad & Goswami, 2021) and the season(Raj et al., 2020). Another recent global study(Z. Liu et al., 2022) showed that the impact of urbanization on LSTs is more evident in urban areas than rural areas. The study used MODIS LST data between 2002 to 2021 to calculate the change in LST and the factors influencing it across 2000-plus urban clusters worldwide.

Very recent literature from multi-city temporal analysis of SUHI shows the relevance and need to understand the impact of urbanization on SUHI. However, the number of temporal or inter-annual studies of SUHI is still limited, especially in countries like India and the US. Further, the existing studies do not verify whether the observed SUHI change is statistically significant or compare the findings with less urbanizing or developed world locations.

2.6 LITERATURE REVIEW SUMMARY AND EXISTING GAPS

Table 5 lists some of the key studies reviewed in this chapter and their scope of work. A review of popular peer-reviewed journals showed that SUHI research has recently (after 2000) gained prominence. As of 2022, the challenge limiting SUHI comparisons from local and regional studies is a lack of a standard SUHI quantification method. The literature review shows that the SUHI quantification method could impact the magnitude of SUHI. The use of non-concurrent data for quantification of SUHI - as seen in the multi-city studies from India, is another factor that skews the magnitude of SUHI. While these are the methodological characteristics of SUHI literature, existing studies also helped understand the factors that impact LST and contribute to SUHI formation.

Multi-city studies showed that SUHI and its drivers varied with space and time. Overall, the daytime SUHI was higher across most studies than the nighttime. Studies indicate higher daytime SUHI in temperate and humid climates compared to dry or desert conditions. While most studies did a diurnal and seasonal analysis of SUHI, the studies on the inter-annual variability of SUHI are still limited, indicating a prospect for future research.

Regarding influencing factors, vegetation was the most studied driver of SUHI, followed by built-up land use and other climatic and social factors. The literature shows the predominant role of built-up areas and vegetation in SUHI formation, using quantification metrics such as spectral indices and percentage impervious surface area. Interestingly most studies either analyze LST or SUHI. Very few studies show the variation in both LST and SUHI with vegetation and built-up areas.

While SUHI research is gaining popularity, it is still limited to a rapidly developing tropical country, India. Researchers show India is one of the least studied places and should be one of the most-studied locations (Deilami et al., 2018; D. Zhou et al., 2018) for UHI research. Much of the literature on quantifying SUHI and the factors influencing them is still from China and the United States. While there are a few global studies, they are limited to summarizing SUHI across big global cities. Studies focusing on just two countries or regions and quantitatively comparing them are close to none. However, the SUHI research community is now moving towards multi-city studies that could assist in understanding global and regional trends of UHI and its drivers. Using remote sensing data for such multi-cities studies provides a unique opportunity to use consistent data, unlike air temperature measurements which could be subject to human errors and instrument differences.

Therefore, a summary of existing gaps based on this literature review are:

1. Very few multi-city studies from India and none that quantitatively analyze and compare LST and SUHI from India with the rest of the well-researched locations, such as the US or China.
2. The lack of consistent SUHI quantification and urban-rural delineation methods limits the comparisons of SUHI across locations and studies.
3. No multi-city studies from India explain how LST varies with vegetation and built-up areas.
4. Very few studies focus on the temporal change in SUHI, and none compare India's temporal SUHI with the US. Such a comparison could show how a rapidly urbanizing country performs compared to a developed nation.
5. No studies from India or US statistically quantify ΔT or its change over time.

Therefore, for a country like India, the sparsity in UHI research and the lack of consistent observations across the existing studies restrict the development of localized UHI mitigation policies by basing them on research from the rest of the world(Lall, Talwar, Shetty, & Singh, 2014). To address such inconsistencies, a multi-city study comparing SUHI in India with a well-researched location like the US could help put the observations from India into a global perspective. A comparative study could also assist in highlighting the differences and similarities in the SUHI trends and its contributors and provide information on the relevance of popular UHI mitigation measures, such as increasing urban greenery and other built-up area measures (e.g., cool roofs, green roofs, green walls).

Table 5: A list of relevant studies reviewed and details on the study locations and scope of work.

Study	Location of Study			Number of cities		Temporal SUHI	Contributors				LST analysis
	India	US	Other	Multi-City	Single-City		Vegetation	Built-up areas	Urbanization	Other	
(Ali et al., 2017)			●	●							●
(D. Zhou et al., 2014)			●	●			●	●		●	
(Fan et al., 2017)	●	●	●	●		●			●		
(Guo et al., 2015)			●		●						●
(Heinl et al., 2015)			●		●		●				●
(Imhoff et al., 2010)		●		●			●	●			
(J. Li et al., 2011)			●		●						●
(J. Wang et al., 2015)			●	●		●	●	●		●	●
(Jiang et al., 2015)		●			●				●		●
(Kumar et al., 2017)	●			●							
(L. Zhao et al., 2014)		●		●		●	●			●	
(Mathew et al., 2017)	●				●						●
(Mathew, Khandelwal, Kaul, & Chauhan, 2018)	●			●			●	●			●
(Mohammad & Goswami, 2021)	●			●		●	●	●	●		
(Peng et al., 2012)	●	●	●	●			●	●		●	
(Peres et al., 2018)			●		●	●			●		
(Raj et al., 2020)	●			●		●	●		●	●	
(S. Wang et al., 2018)			●		●				●		●
(Shastri et al., 2017)	●			●			●				
(Singh et al., 2017)	●				●				●		●
(Sussman et al., 2019)	●				●	●			●		
(W. Chen et al., 2017)			●		●	●	●			●	●
(W. Chen et al., 2017)			●		●				●		●
(X. Li et al., 2017)		●		●				●			
(Z. Liu et al., 2022)	●	●	●	●		●			●		
(Zhang et al., 2009)			●		●						●
This study	●	●		●		●	●	●	●		●

3 DATA AND METHODS

3.1 OVERVIEW

This chapter describes the study's data, land surface temperature, and ΔT calculation methodology. The overall study methodology is in three main stages 1.) Data collection, 2.) Spatial Processing of the Data, and 3.) Post-processing analysis. The data collection includes the selection of the location of the study, the selection of a satellite for LST data, selecting the time and date of data, identifying other relevant data, and the data download. In the second stage of remote sensing data processing, -a crucial step is identifying each selected location's urban and rural areas. An urban-rural delineation methodology customized based on existing methodologies is applied to identify all the urban and rural areas of the study locations, as discussed in Section 3.5. Depending on the LST dataset, several steps are involved in quantifying ΔT. The chapter lists a step-by-step methodology of LST calculation using Landsat 8 data and the ΔT quantification. This study compares LST and ΔT between India and the US and discusses the impact of vegetation and built-up areas on them. Therefore, quantifying vegetation and built-up areas is another essential step in this stage. In the third or final stage of post-processing data analysis, statistical analysis, such as regressions, Spearman's rank correlation, and t-tests, were used to address the research questions.

3.2 STUDY LOCATIONS

All the urban agglomerations with a greater than one million population in India and US were shortlisted and reviewed for data availability. Demographia (Demographia, 2016) world urban area dataset that follows a consistent urban land area calculation method for urban areas with > 5000,000 population across the globe was referenced for the population data. Cloud-free data from

Landsat 8 satellite (NASA Landsat Science, 2020) was reviewed for the summer (April-June in India, June-September in the US) and winter (November-February) days of 2016 - one of the warmest years to date. For locations with multiple cloud-free days, the highest and lowest daily maximum air temperature days were chosen for summers and winters, respectively. Based on these criteria, this study analyzed 42 Indian cities and 32 US cities. Appendix A provides a list of all the cities, and Section 3.3 of this chapter discusses the satellite data used in this study.

3.2.1 Comparison of the 10 populous cities of India and the US

This section provides an overview of the population and climatic differences between the two countries using the example of the 10 most populous cities in India and the US. Table 6 quantitatively compares the 10 most populous urban agglomerations from India and the US. Population data shows that 9 out of the 10 most populous urban areas in India and the US have greater than 5 million people. While the population across some megacities in India and the US are comparable, the population densities differ. The highest population density in the US – in Los Angeles is 2400 people/km^2 (includes Riverside-San Bernardino and Mission Viejo), which is 13x lower than the highest in India (Vijayawada: 31,200 people/km^2) and 1.7x lower than the lowest density found in an urban area (> 500,000 people) (Thoothukkudi: 4000 people/ km^2) of India. Table 6 also compares the heating degree day (HDD) and cooling degree day (CDD) of these 10 locations from India (Bhatnagar, Mathur, & Garg, 2018)and the US(NOAA, 2016). Information on the HDD and CDD is relevant in showing how hot or cold the temperatures could be and indicates the need for mechanical cooling and heating. From Table 6, most cities in India have no heating requirement, while only one city, Miami (out of the 10 populous) in the US, has a negligible heating requirement. On the other hand, in India, there is a need for mechanical cooling in most of the cities, with only a few comparable (≈ 3000 CDD or more) US cities from the

southern states like Texas and Florida (Miami). Therefore, this information on population, CDD, and HDD provides an overview of the cities in India compared to the US cities. While there are considerable differences in population densities, there are some commonalities – in population- New York City, US, Mumbai, India, and in CDD - Houston, Dallas, and Miami comparable to cities in India, across a few cities in India and US.

Table 6: Population, Population Density, Heating Degree Days, and Cooling Degree Days across the 10 most populous cities in India and the United States

City	Population (thousands)	Population Density (people/km^2)	HDD (base temp: 18^{0}C)	CDD (base temp: 18^{0}C)
10 most populous Urban Agglomerations in India				
Delhi	25,735	11,900	248	2926
Mumbai	22,885	26,000	0	3457
Kolkata	14,810	12,300	6	3232
Bengaluru	10,165	8,700	0	2342
Chennai	9,985	10,300	0	3992
Hyderabad	7,750	6,300	0	3154
Ahmedabad	7,410	21,200	6	3587
Pune	5,785	12,100	9	2290
Surat	5,685	24,400	0	3471
Jaipur	3,485	8,400	109	3046
10 most populous Urban Agglomerations of the United States				
New York	20,685	1,800	3978	1732
Los Angeles	15,135	2,400	889	966
Chicago	9,185	1,300	5690	1162
Dallas	6,280	1,200	1602	3227
Houston	6,005	1,200	997	3452
San Francisco	5,995	2,100	1983	146
Miami	5,820	1,700	71	4931
Philadelphia	5,595	1,100	4074	1711
Atlanta	5,120	700	2168	2550
Washington DC	4,950	1,300	3594	1982

3.2.2 Climate

3.2.2.1 The climate and seasons in India and the US

According to the Indian Meteorological Department(Attri & Tyagi, 2010; Indian Meteorological Department, 2019), India has four seasons, as shown in Table 7. Monsoon timings could vary across the country based on the location. However, the onset of south-westerly monsoons would

happen no later than July 15 across the country. Rains could also happen during the post-monsoon season in the eastern and southeastern states due to the northeastern monsoon. For the development of regional building codes and standards, the National Building Code (NBC) and the Energy Conservation Building Code (ECBC) of India divide the country into five climatic zones: Hot and Dry, Composite, Temperate, Warm and Humid, and Cold, as shown in

Figure 15. The figure shows that summer temperatures in most areas, except India's very few cold locations, can range between 30-45^{0}C. There are very few cold regions in the country- the extreme northern part and other few hill stations across the country, where the winter temperatures go below 0^{0}C.

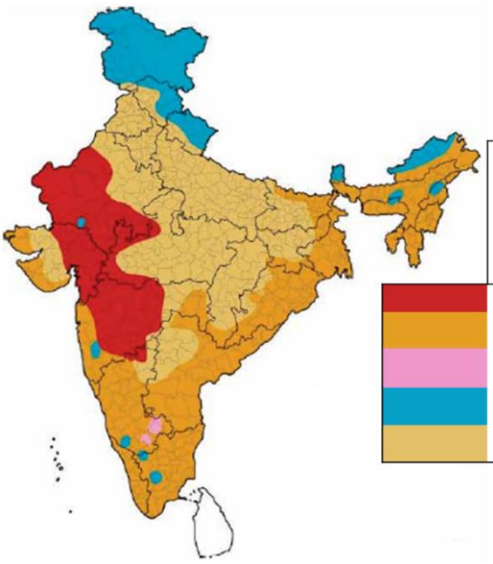

Climate Zone	Mean Temperature (^{0}C)		Mean Relative Humidity	Cloud cover
	Summer midday (High)	Winter midday (Low)		
HOT & DRY	40-45	0-10	25-40%	Cloudless
WARM & HUMID	30-35	20-25	70-90%	Overcast (40-80%)
TEMPERATE	30-34	16-18	60-85%	Clear, occasionally overcast in summer
COLD	17-30	-14-4	0-100% (Variable)	Overcast most of the year
COMPOSITE	32-43	4-10	Wet period 50-95%	Variable

Figure 15: Climate zones in India as shown in the Energy Conservation Building Code of India

In the US, however, seasons and their timings vary compared to India, as seen in Table 7. The US has four meteorological seasons (NOAA, 2021), as shown in Table 7. The temperatures and precipitations vary by season across the US. Unlike India, there isn't a monsoon season in the US. Rainfall happens at different times of the year based on the location. For example, the Midwest

and the eastern states experience maximum rainfall during late spring and early summer, while on the west coast, rainfall occurs during winter.

In the US, for building design and HVAC equipment load design purposes, the climate zone classification provided by ASHRAE 169 is followed by the country's commercial and residential building codes. ASHRAE Standard169 (ASHRAE, 2020) divides the country into 8 thermal zones, 0. Extremely hot, 1. Very hot, 2. Hot, 3. Warm, 4. Mixed, 5. Cool, 6. Cold, 7. Very cold, and 8. Subarctic/arctic, and 3 moisture zones, A. Humid, B. Dry, and C. Marine. The temperatures, precipitation, cooling degree days (CDD), and heating degree days (CDD) vary across all the zones.

Table 7: Meteorological seasons of India and the US

India		**United States**	
Season	**Calendar Months**	**Season**	**Calendar Months**
Winter	January, February	**Winter**	December, January, and February
Pre-monsoon or **Summer**	March, April, and May	**Summer**	June, July, and August
Monsoon	June, July, August, and September	Spring	March, April, and May
Post-monsoon	October, November, and December	Fall	September, October, and November.

3.2.2.2 Climate classification using Koppen Gieger Climate

This section details the cities' climate classification using the Koppen Geiger system to compare the climate across cities in India and the US using the same weather classification system, unlike previously discussed ECBC and ASHRAE climate zones. At the time of processing of these results, ASHRAE 169 climate classification system classified the whole of India into one climate zone, zone 1A; this, however, was changed in the 2021 revision of the ASHRAE standard.

Koppen-Gieger climate(Kottek, Grieser, Beck, Rudolf, & Rubel, 2006) classifies the world into 5 climates (A to E) and several sub-classes based on temperature and precipitation of the location. India constitutes several climate classes, most under the A: equatorial and B: arid categories, with

a few northeastern locations under C: warm temperate. However, most US is C: warm temperate and D: snow climates, with a few southwestern locations under B: arid category. While few overlaps exist in the Koppen classification across India and the US, the countries vary widely in temperatures and seasons.

Figure 16 shows the study locations and their Koppen climate classification. As seen on the map, the maximum (18/42)of the study locations in India are Equatorial climates with dry winters (Aw), followed by arid- hot steppe (BSh) (10/42). In India, 9/42 cities belong to the warm temperate climate class, compared to the majority (27/32) in the US. More than half (21/32) of US cities' studied belong to the warm temperate and humid with hot summers (Cfa) climate class. Only 2 of the 11 classes observed across both countries have cities in common. One city in each of the country (US: Phoenix, India: Jodhpur) fall in BWh (Arid-Desert-Hot Arid temperatures) climate class, and 2 cities from the US and 4 cities from India are under Csa (Warm Temperate with warm and dry summers). The air temperature and precipitation differences can be high between equatorial (Tmin $\geq 18^0$C) and warm temperate climates (Tann $\geq 22^0$C), the two primary climate classes in India and the US, respectively. Therefore, this climate classification indicates that India and the US have cities with different climates; hence, quantifying SUHI across these climate classes might show the impact of climate on SUHI. Understanding the SUHI based on Koppen Geiger Classification is relevant, not only because it is a widely used climate classification system but also because of its basis on vegetation, air temperature, and precipitation that impact SUHI(Imhoff et al., 2010; Kumar et al., 2017; L. Zhao et al., 2014).

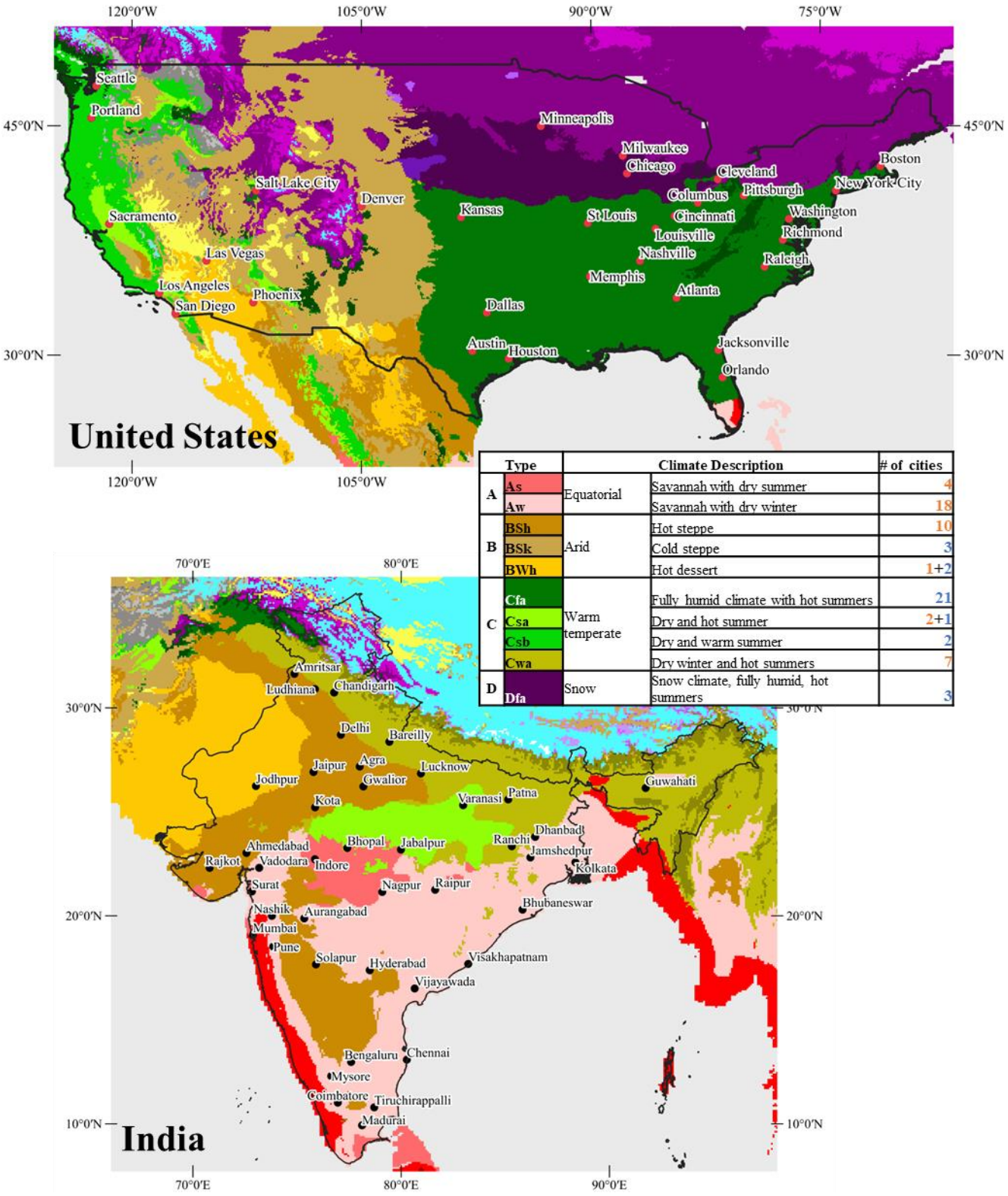

	Type		Climate Description	# of cities
A	As	Equatorial	Savannah with dry summer	4
	Aw		Savannah with dry winter	18
B	BSh	Arid	Hot steppe	10
	BSk		Cold steppe	3
	BWh		Hot dessert	1+2
C	Cfa	Warm temperate	Fully humid climate with hot summers	21
	Csa		Dry and hot summer	2+1
	Csb		Dry and warm summer	2
	Cwa		Dry winter and hot summers	7
D	Dfa	Snow	Snow climate, fully humid, hot summers	3

Figure 16: Study locations from the US and India on the Koppen-Geiger Climate Classification Map

3.3 LAND SURFACE TEMPERATURES: SATELLITE DATA

This dissertation uses LST data from two different satellites 1.) Landsat, and 2.) MODIS Aqua. While Chapter 2 Section 2.4.2 discussed the Landsat and MODIS as the most common satellite data used across SUHI studies, this section discusses the specific data used in this work. This section details the data characteristics, and the collection date and time

3.3.1 Landsat 8 Data

Landsat 8 satellite(NASA Landsat Science, 2020), launched in the year 2013, uses two sensors – the Operational Land Imager (OLI) and the Thermal Infrared Sensor (TIRS) to provide data across 11 bands (wavelengths). This satellite captures data images (in digital numbers) called scenes that are typically sized 170m (north-south) by 182 m (east-west) once every 16 days during mornings (9 am-12 noon). The equatorial crossing time of this satellite is around 10 am. The Landsat 8 data is available in 9 spectral bands and two thermal bands. The two thermal bands (bands 10 and 11) collect data at 100m spatial resolution and are resampled to 30 m spatial resolution to match the spectral band(1-9) resolutions of 15-30m.

In this study, cloud-free (<5% cloud cover) Landsat 8 data (all the bands) was downloaded for 42 cities from India and 32 cities from the US. Landsat 8 data from 2016, one of the warmest years to date, was used in this analysis. Cloud-free data for the highest maximum daily air temperatures days during summers in India (April-June) and the US (June-September) were selected. The cloud-free data with the lowest daily maximum air temperature was downloaded for analysis during winter (November-Febrauary)—Appendix A lists all the cities and the date of Landsat 8 data. Non-summer month data was used in the case of Houston, TX (5/5/16) and Orlando, FL (5/6/16) due to high cloud cover on the days when data were available in summer. Chennai, India, was not included in the winter analysis due to a lack of cloud-free data in this location, resulting in 41

Indian cities for winter compared to 42 during summer. The USGC EarthExplorer (USGS, 2019)site was used for the Landsat 8 data download.

Section 3.6 of this chapter details the LST calculation using the Landsat 8 thermal band 10. Other spectral band data were also used in the spectral indices calculations, as discussed in Section 3.7. In this dissertation, Chapter 4- the daytime-specific analysis of LST and ΔT, which also studied the correlations with built-up areas and vegetation, used Landsat 8 data. Chapter 7 also uses Landsat 8 data to study the variation in built-up area LSTs with construction period and neighboring land use. In both these chapters, higher resolution LST data is more appropriate to understand the correlations and the variation in LST with land use.

3.3.2 MODIS Landsat Surface Temperature Data

MODIS, or the Moderate Resolution Imaging Spectroradiometer, is the sensor on the Terra and Aqua satellites(MODIS, n.d.). These satellites orbit the earth every 1-2 days during the daytime and the nighttime. The availability of daily data for both day and nighttime is one of the most significant advantages of MODIS. The main difference between MODIS Terra (MOD) and MODIS Aqua (MYD) is the time of data collection. MODIS Terra collects data in the morning (≈10.30 am) and early at night (≈10.30 pm), whereas MODIS Aqua's data collection times are approximately 1.30 pm and 1.30 am. This study used MODIS Aqua data (1.30 pm and 1.30 am) for the diurnal and nighttime analysis of ΔT. Since Landsat 8 daytime data was from the mornings, MODIS Aqua data from the afternoon helps understand if any differences in ΔT pattern exist when calculated at a different time of the day. Unlike Landsat 8 - data available in different bands and needs further processing for LST conversion, the MODIS data provides Land Surface Temperature data as a direct download for its users. This work uses the MYD11A2 v6.1(Wan, Hook, & Hulley, 2015) product that provides an average 8-day per-pixel (calculated from the daily data) LST and

Emissivity. The spatial resolution of this LST is 1km, and each scene is 1200 km x 1200km in size.

The MYD11A2 data available at an 8-day interval for 2016 was downloaded for all 42 Indian and 32 US cities, listed in Appendix A. The monthly average LST for all the Indian and the US seasons (see Table 7) was calculated by averaging the 8-day average MYD11A2 (≈ 4 scenes from each month) data. Chapter 5 of this dissertation uses these average monthly LSTs in the diurnal and seasonal analysis of ΔT. Chapter 6 of this dissertation also used MYD11A2 data for the seasonal, temporal analysis of ΔT. In Chapter 6, the MYD11A2 LST from April and May were averaged to represent Indian summers and from July and August to represent US summers. LSTs from January and February were averaged to represent the winter LSTs in both countries. MYD11A2 LST data is available from 2002 and was downloaded for several years ranging between 2003-2022 in this dissertation for the temporal analysis, in Chapter 6. This dissertation used the AppEEARS(AppEEARS Team, 2023) web tool for the MODIS LST data downloads.

3.4 LAND USE LAND COVER DATA

The LULC data is crucial for determining the urban-rural boundaries and analyzing the LST and ΔT results. This study used two LULC datasets 1.) LULC for India from IRA AWiFS sensors at 56m resolution(Bhuvan/ISRO, n.d.), and 2.) the global Copernicus LULC data (Buchhorn et al., 2020), which only became available in the year 2020. The first LULC dataset from India defines the urban boundaries for the 42 locations in India, and Section 3.6 further discusses this urban-rural delineation methodology. The Copernicus global LULC data from 2016 shows the LULC across all the study locations -using the same classification for both countries. Figure 17 shows all the cities from the US and India marked on the Copernicus LULC map from 2016. This LULC

data helps explain the similarities and differences in ΔT between India and the US, as seen in Chapter 4 and Chapter 5 of this dissertation. As seen in Figure 17, India's LULC is significantly different from the US. While most of India is cropland, the US is a mixture of herbaceous vegetation, cropland, and forests.

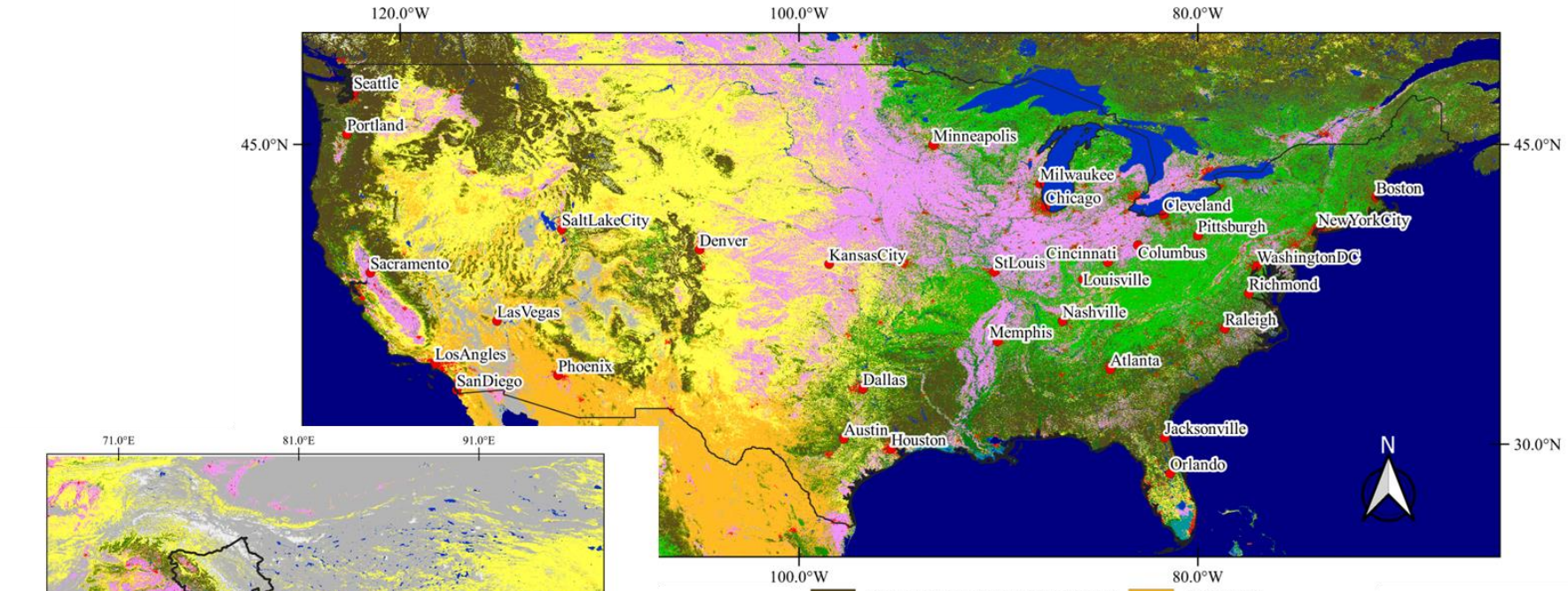

LULC Type	% of land area in India	% of land area the US
Cropland	**63%**	15%
Built-up	**2.3%**	1.5%
Forests	23.8%	39.1%
Shrubland	4.3%	9.2%
Herbaceous vegetation	3.7%	28.4%

Figure 17: The study locations marked on the 2016 Copernicus Land Use Land Cover map of the United States and India

3.5 AREA OF INTEREST (AOI) – THE URBAN-RURAL DELINEATION

Landsat 8 data scenes and the MYD11A2 LST data need the cropping to this study's area of interest (AOI) – rural area boundary. This study customized the existing methodology of defining urban boundaries based on urban area maps and LULC. Including the surrounding urban sprawl areas and using concurrent LULC or urban extent data based on the year of analysis are the main differences between the urban-rural delineation methodology proposed in this study and the existing urban-rural delineation methodologies in the literature. To date, there is no standardized definition of "urban" and "rural" across the SUHI studies (Giridharan & Emmanuel, 2018; Weng, 2009), and the use of non-concurrent data sets could affect the ΔT(D. Zhou et al., 2018). A detail on this is in Section 2.5.1 of Chapter 2.

In India, the urban built-up areas often extend beyond the city's administrative boundaries and sometimes the district (see Figure 18). Therefore, it is essential to use concurrent LULC data to identify the urban areas in India. To address this, based on the year of analysis, concurrent LULC data from IRS AWiFS sensors (available from 2005 onwards) at 56 m resolution (Bhuvan/ISRO, n.d.)was used to create urban boundaries. Urban built-up area land use for each city was polygonized, and then a bounding box was created around these polygons to include the spillovers that exist in urban built-up land use, as shown in Figure 18. In the US, due to the lack of up-to-date LULC data when this data were processed, urban area extents data (US Census Bureau, 2019) from the concurrent year, based year of analysis, were used to define the urban boundaries similar to those done for Indian cities. In both countries, the rural boundary was an equal area buffer zone around the urban area.

The Landsat 8 bands and the MYD11A2 LST data scenes were extracted into urban and rural areas for each of the 42+32 study locations with these urban-rural boundary polygons developed using this methodology. In the methodology used here, the urban boundary includes the spill-offs and urban sprawl – all the areas that might have a direct impact from the main urban built-up areas, as seen in Figure 15.

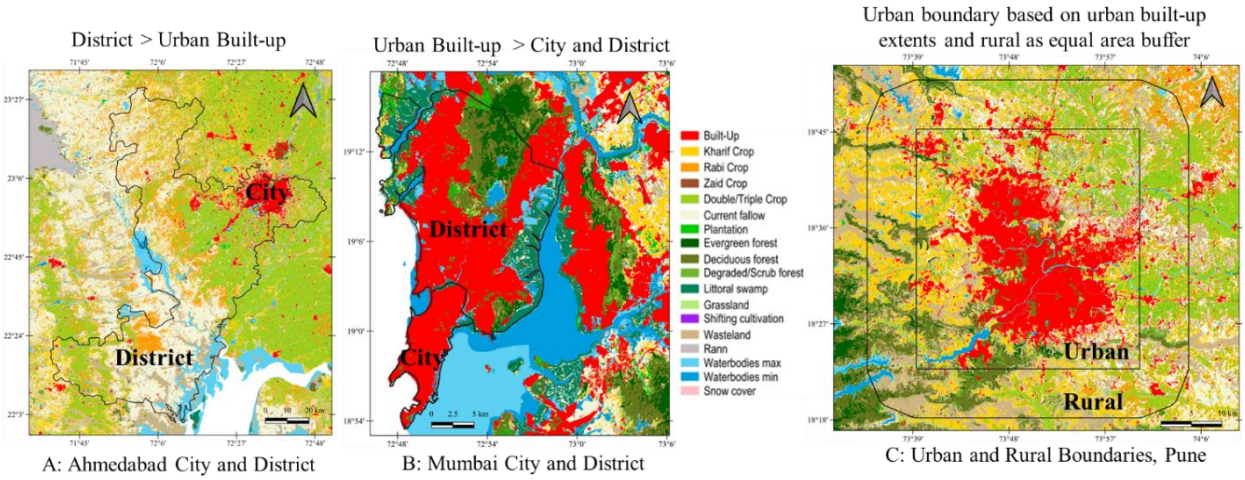

Figure 18: Administrative city and district boundaries marked on the Land Use Land Cover map (2016-17) (Bhuvan/ISRO, n.d.) *for A: Ahmedabad and B: Mumbai. Examples show that neither the district nor city boundaries accurately represent built-up across Indian cities. C. Example of Pune showing urban-rural boundaries in the current study.*

3.6 Land Surface Temperatures and ΔT Calculation

While MYD11A2 data are directly an LST product and need no further processing, the Landsat 8 data, which are digital number format in various bands, must be processed to extract the LSTs. This section details the process of extracting LSTs from the AOI-cropped Landsat 8 bands.

3.6.1 LST from Landsat 8 data

Figure 19 provides an overview of the LST calculation methodology used in this study. The LST calculation in this study uses the method specified in (Barsi, Schott, Palluconi, & Hook, 2005). This method uses a radiative transfer equation to calculate the atmospheric correction variables that are, in turn, used to calculate LST. A step-by-step process of the LST calculation is as follows:

1. Landsat 8 thermal band (Band 10) data was used to calculate the top of the atmosphere spectral radiance (L_{TOA}) using equation 1 and Landsat 8 thermal band (Band 10) data. In equation 1, M_L and A_L are band-specific multiplicative and additive rescaling factors, respectively, available in Band 10 metadata. Qcal is the Band 10 data in digital numbers.

$$L_{TOA} = M_L Q_{cal} + A_L \qquad \textit{Equation 2}$$

2. In the second step, the NDVI maps for each AOI were developed by inputting Landsat 8 Band 5 and Band 4 data into equation 2.

$$NDVI = \frac{NIR-Red}{NIR+Red} = \frac{Band\ 5-Band\ 4}{Band\ 5+Band\ 4} \qquad \textit{Equation 3}$$

3. Next, the emissivity values across AOI are calculated based on the NDVI range developed by (Valor & Caselles, 1996). These NDVI-based emissivities were also used for LST calculations across similar prior studies (Kikon, Singh, Singh, & Vyas, 2016; R. Sharma & Joshi, 2014).

Table 8: Emissivity values used based on NDVI ranges

NDVI	Emissivity (ε)
NDVI < -0.18	0.985
0.157>NDVI<0.727	1.0094+0.0047ln (NDVI)
-0.18>NDVI<0.157	0.955
NDVI >0.727	0.99

4. The atmospheric correction variables- atmospheric transmission (τ), upwelling radiance (L_u), and downwelling radiance (L_d) were calculated using the NASA Atmospheric Correction parameter calculator (NASA, 2019). This web-based calculator requires latitude, longitude, date, and time of data collection as inputs (see Appendix A).

5. To calculate the surface-leaving radiance (L_T), L_{TOA}, emissivity(ε), and the atmospheric correction variables (τ, L_u, and L_d) that were calculated in the previous steps are input into equation 3.

$$L_{TOA} = \tau\varepsilon L_T + L_u + \tau(1-\varepsilon)L_d \qquad \textit{Equation 4}$$

6. Planck's law was then applied to L_T to calculate LST (in Kelvin), as shown in equation 4, and are subtracted by 273.15 to convert to Celcius. In equation 4, k1 and k2 are the thermal conversion constants for Band 10 of Landsat 8 data available in the metadata file.

$$T = \frac{k_2}{ln\left(\frac{k_1}{L_T}+1\right)} \qquad \textit{Equation 5}$$

Figure 20 and Figure 21 show examples of the LST maps generated using Landsat 8 data during summer daytime. In Figure 20, the LST map of Delhi and Guwahati from India shows possible LST patterns across Indian cities. Similarly, the LST maps from Chicago and Phoenix show the possible LST differences across these cities.

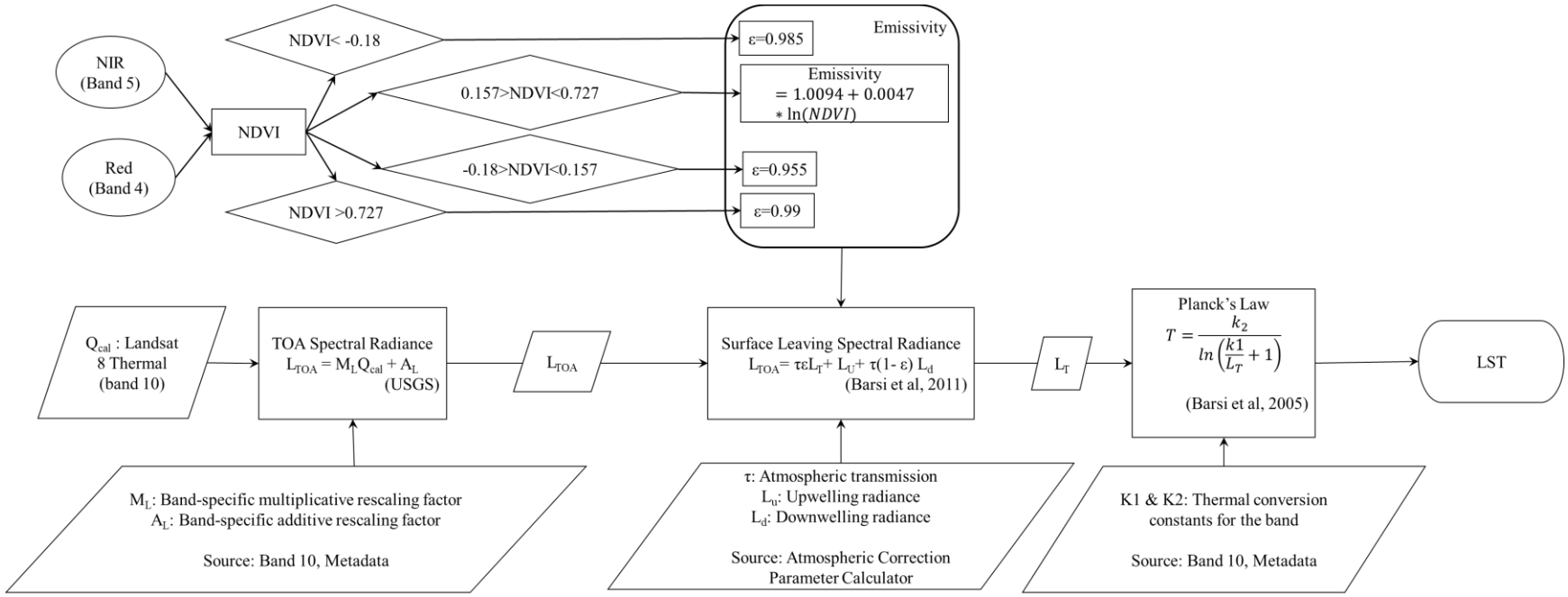

Figure 19: Overview of Land Surface Temperature Extraction Methodology

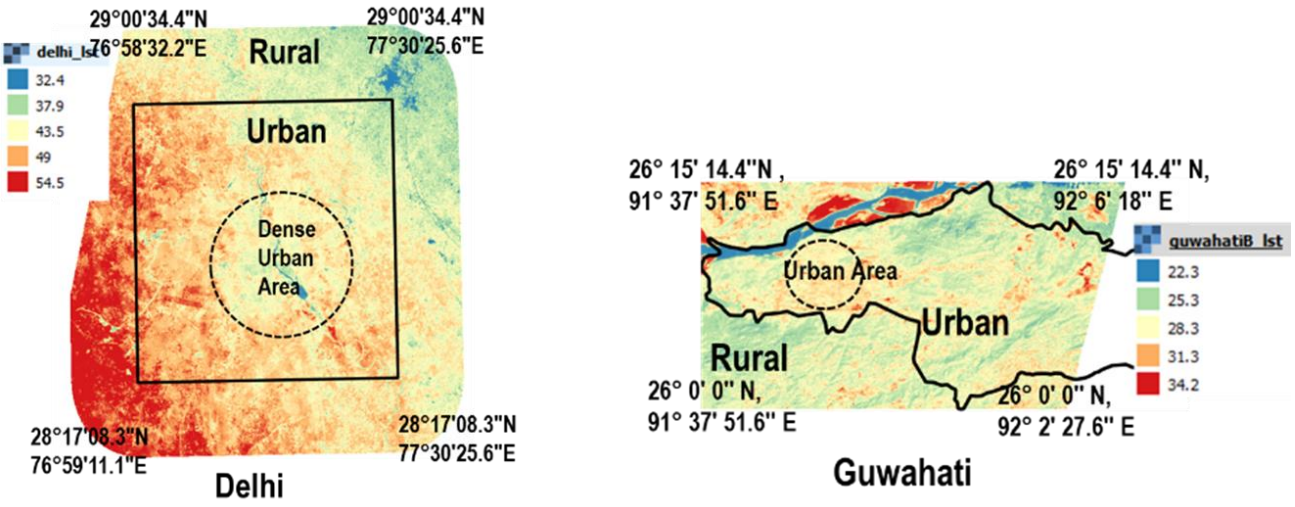

Figure 20: LST maps of Delhi and Guwahati showing urban and the surrounding rural areas. Delhi shows higher LSTs in rural areas compared to urban areas, and Guwahati shows higher LSTs in urban areas compared to surrounding rural areas

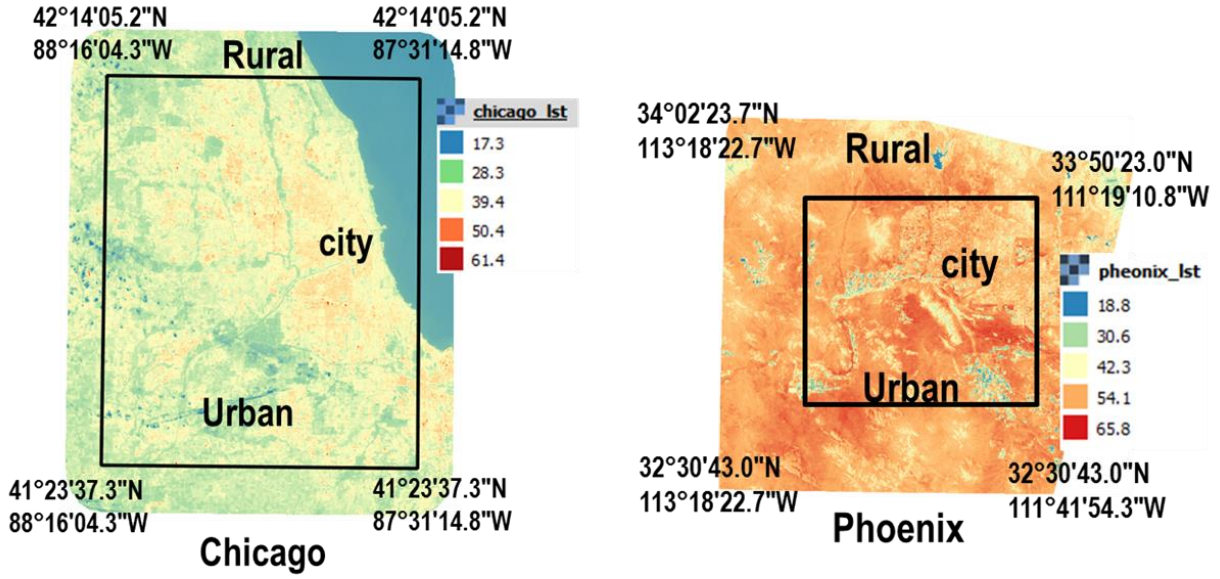

Figure 21: LST maps of Chicago and Phoenix showing urban and the surrounding rural areas. Chicago shows higher LSTs in urban areas than rural areas, and Phoenix has higher LSTs across the area, with slightly lower LSTs in urban areas.

3.6.2 ΔT Calculation

In this study, ΔT represents the SUHI magnitude in each city. The ΔT calculation method remains the same for Landsat 8 and MYD11A2 datasets. In both cases, ΔT is the difference between the

urban and rural mean LST from the LST maps generated in the previous step. As shown in Equation 6, ΔT of each city is the difference between urban and rural LST means.

$$\Delta T_S = \overline{LST_{urban}} - \overline{LST_{rural}} \quad \textit{Equation 6}$$

3.7 Quantification of Vegetation and Built-up Areas

The common ways of quantifying vegetation and built-up areas in remote sensing studies are through spectral indices or variables such as impervious surface area. Spectral indices are ratios calculated for each pixel (representing a 30m x 30m parcel of land in Landsat 8) using digital number (a representation of spectral reflectance) data from two or more wavelengths. This study reports two spectral indices, NDVI (Normalized Difference Vegetation Index) and IBI (Index Based Built-Up Index), to quantify the vegetation and built-up surface densities, respectively. Landsat 8 data were used to calculate NDVI and IBI for all the study locations. Further, a global artificial impervious area (Gong et al., 2020) dataset was used to quantify and represent built-up areas across the study locations, as discussed in the following sections.

3.7.1 Normalized Difference Vegetation Index (NDVI)

NDVI is one of the most used vegetation indices across remote sensing studies and is calculated by inputting Landsat 8 band data into Equation 2 (The Earth Observatory, 2000). NDVI represents the ratio of green vegetation in each pixel calculated using data from near-infrared (Band 5) and red (Band 4) wavelengths, as seen in Equation 2. Chlorophyll in green vegetation strongly reflects light in near-infrared (NIR) wavelengths and absorbs visible light (in red wavelength). The presence of chlorophyll corresponds to green vegetation and results in higher NDVI values (a more considerable difference between Band 5 and Band 4 in the numerator of Equation 2). However, dry, diseased, or deciduous non-green vegetation, referred to as non-photosynthetic vegetation

(NPV), has different reflectance properties than green vegetation. As a result, NPV has lower NDVI values (a more negligible difference between Band 5 and Band 4 lowers the value in the numerator of Equation 2) compared to green vegetation.

NDVI values range between -1 to +1. Negative NDVI values represent land covers such as water and snow, and values close to zero are observed for rock and barren soil. While lower NDVI values (0.2-0.3) are commonly observed across sparsely vegetated shrubs or grasslands, higher values (>0.6) represent green forests. In SUHI studies, NDVI is therefore valuable for identifying cooler (low LST) green vegetation (with high NDVI values) compared to hotter (high LST) sparsely vegetated or impervious built-up areas (with close to zero NDVI value). Figure 22B and Figure 23B show the example maps of NDVI from India (Delhi) and the US (Pittsburgh), respectively. In both countries, the LST is high for low NDVI values, as seen in Figure 22A and Figure 23A.

3.7.2 Index Based Built-Up Index (IBI)

The Index Based Built-Up Index (IBI) was developed (H. Xu, 2008)to estimate the amount of built-up land while eliminating the impact of vegetation and water; and is calculated by inputting Landsat 8 band data into Equation 6 (written as Equation 7 using Landsat 8 bands). In equation 6, NDBI stands for Normalized Difference Built-Up Index, NDVI is Normalized Difference Vegetation Index, and MNDWI stands for Modified Normalized Difference Water Index corresponding to the built-up surface, vegetation, and water densities, respectively. Built-up surfaces have high reflectance in the Short-Wave Infrared (SWIR) wavelength and absorb in NIR wavelength (Zha et al., 2003), unlike green vegetation that reflects in NIR wavelengths. Band 6 (SWIR1) and Band 5 (NIR) data are essential in identifying built-up land, as seen in the NDBI calculation in Equations 7 and 8.

$$IBI = \frac{NDBI-[(NDVI+MNDWI)/2]}{NDBI+[(NDVI+MNDWI)/2]} \quad \textit{Equation 7}$$

$$IBI = \frac{\frac{2*SWIR1}{SWIR1+NIR}-\left[\frac{NIR}{NIR+Red}+\frac{Green}{Green+MIR}\right]}{\frac{2*SWIR1}{SWIR1+NIR}+\left[\frac{NIR}{NIR+Red}+\frac{Green}{Green+MIR}\right]} = \frac{\frac{2Band6}{Band6+Band5}-\left[\frac{Band5}{Band5+Band4}+\frac{Band3}{Band3+Band6}\right]}{\frac{2Band6}{Band6+Band5}+\left[\frac{Band5}{Band5+Band4}+\frac{Band3}{Band3+Band6}\right]} \quad \textit{Equation 8}$$

This study uses IBI to quantify the built-up areas. Compared to existing built-up indices (see Section 2.4.3 of Chapter 2), IBI is expected to limit the impact of vegetation and water on the built-up index calculations. IBI ratios range between -1 to +1, and higher positive values represent dense built-up land within the pixel. Zero or negative values, which mean higher values in the numerator of Equation 2, occur in the presence of other LULC types, such as green vegetation (high NDVI value) and water (high MNDWI value). Figure 22A and Figure 23A show that the LST is high for high IBI values. Figure 22C and Figure 23C show the example maps of IBI from India (Delhi) and the US (Pittsburgh), respectively.

3.7.3 Impervious Surface Area (ISA)

Across SUHI literature, impervious surface areas primarily represent built-up areas such as buildings, roads, pavements, driveways, and other non-pervious surfaces. They are commonly quantified to study the impact of built-up land use on LSTs and ΔT. While there are different ways of quantifying ISA using different data, this study used the global artificial impervious areas (GAIA) dataset (Gong et al., 2020) to represent the artificial ISA or the built-up land use. Here, 'artificial' represents the human-made ISA, not the naturally occurring impervious surface areas such as barren rock or termite mounds. In this dissertation, the ISA and built-up area terms are used interchangeably, and both are quantified using the GAIA data unless otherwise specified. GAIA data's primary advantage is its spatial and temporal resolution. These data have been made available at a 30m spatial resolution (similar to Landsat 8) for over 30 years (1985-2018) and were shown to have more than 90% accuracy in identifying artificial impervious areas. A random visual

analysis was conducted across multiple cities in India and the US by comparing GAIA data with Google Earth imagery and the LULC data. This visual analysis showed that the GAIA data appropriately indicates the built-up areas and shows only the artificial (human-made) impervious surfaces, not natural ones. This accuracy of GAIA in Indian cities is also evident in the example in Figure 22. This visual comparative analysis of GAIA is only for cross-checking the data, and its accuracy testing isn't in the scope of this work. Chapter 6 of this dissertation further discusses the ISA maps and the relevant statistics from the GAIA data. Here, it is essential to mention that GAIA data were included in this research based on the finding related to the built-up spectral indices in the daytime LST and SUHI analysis in Chapter 4. Therefore, it has been used in this research's latter stages that quantify the temporal changes in ΔT (Chapter 6) and urban built-up LST (Chapter 7).

Examples of the daytime summer LST maps, along with the NDVI, IBI, and ISA from India and the US, are shown in Figure 22 and Figure 23, respectively. Figure 22 is the LST, NDVI, IBI, and ISA maps of Delhi, India, cropped to its administrative boundaries. Similarly, Figure 23 is the LST, NDVI, IBI, and ISA maps of Pittsburgh, US, cropped to its administrative boundaries. These figures show when the data are cropped to administrative boundaries and do not represent urban boundaries considered in this study. As discussed in Section 3.5, the study areas in this work are the urban and rural areas created using LULC data, as seen in Figure 18. Hence, Figure 22 and Figure 23 are only visual examples of the LST, NDVI, IBI, and ISA data generated in this work.

As seen in Figure 22, in India, the LST increases with a decrease in NDVI and an increase in IBI. However, this visual correlation isn't obvious between LST and ISA. The LSTs are high even in places where non-ISA exist (southwest corner of the city). There is also a difference between the IBI and ISA. In the southwest corner of Delhi, IBI represents built-up however the GAIA data

shows non-impervious surface areas. A visual cross-check using Google Earth imagery, and the LULC data showed that the southwest corner of Delhi is primarily a non-built-up area, indicating higher accuracy of the GAIA data, as seen in Figure 22. Unlike Delhi, Pittsburgh shows more definitive visual trends, and the IBI and ISA maps look more comparable than those of Delhi. Chapter 4 of this dissertation discusses these indices and their correlations with LSTs.

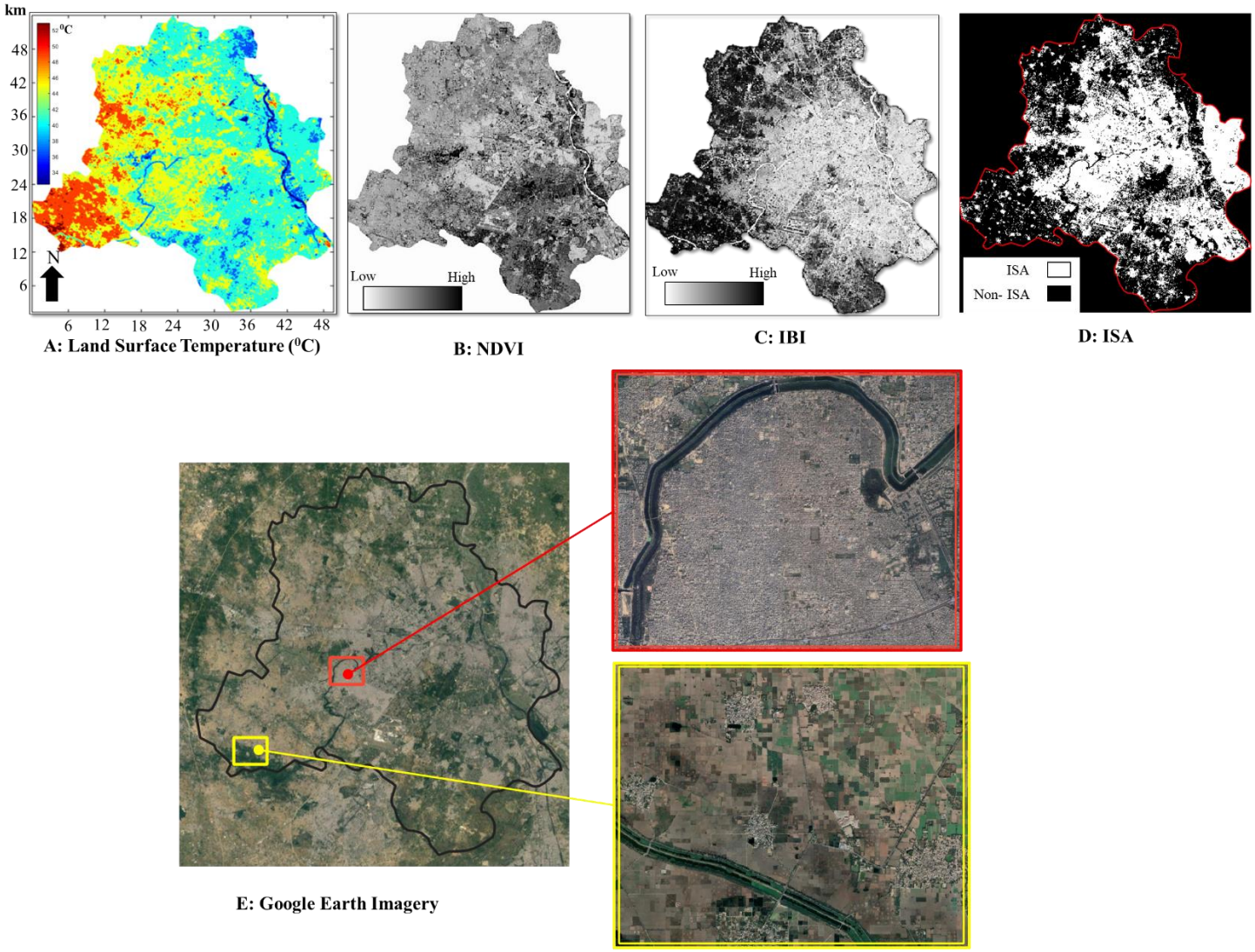

Figure 22: The A. Summer daytime LST, B. NDVI, C.IBI, D.ISA, D: Google Earth maps, and F: Three locations zoomed in to show the built-up and non-built-up land uses of Delhi, India, cropped to its city administrative boundary

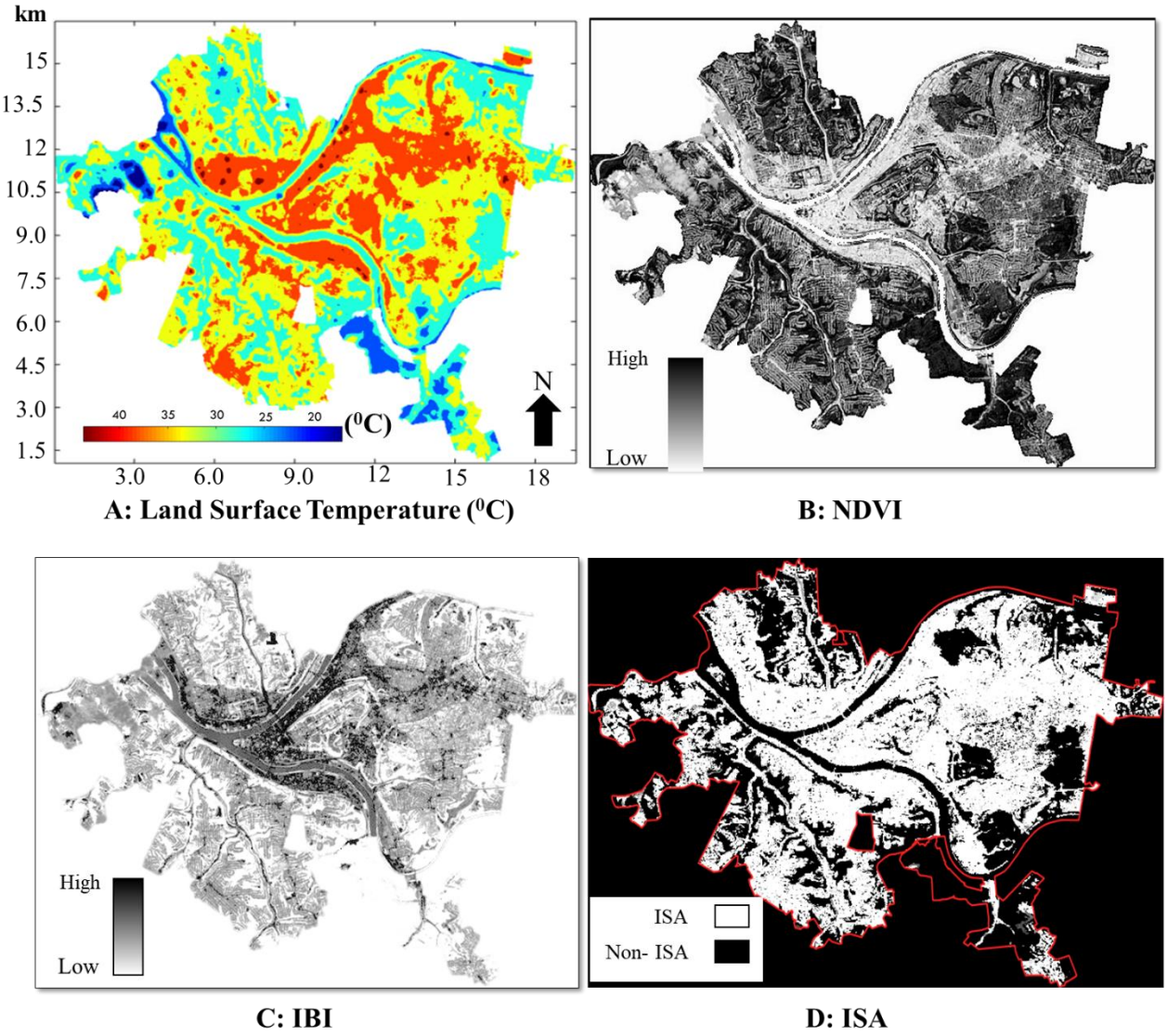

Figure 23: The A. Summer daytime LST, B. NDVI, C.IBI, and D.ISA maps of Pittsburgh, US, cropped to its city administrative boundary.

4 DAYTIME LAND SURFACE TEMPERATURES AND THE SURFACE URBAN HEAT ISLAND PHENOMENON

4.1 OVERVIEW

This chapter analyzes the daytime surface urban heat island (SUHI) magnitude and its association with vegetation and built-up areas across 42 cities in India and 32 cities in the US. A comparative analysis between urban-rural mean land surface temperature (LST) differences (ΔT) in India and the US showed how the daytime ΔT trends in India differ from the conventional SUHI observed in the US. A correlation analysis discusses the variation in LST and ΔT with vegetation and built-up areas in India and the US. Analyzing the observed ΔT trends and correlations involved utilizing the spectral reflectance properties of the Land Use Land Cover (LULC) in India and the US. In this chapter, the Normalized Difference Vegetation Index (NDVI) and Index Based Built-Up Index (IBI) (refer to Section 3.7 of Chapter 3) quantify vegetation and built-up areas, respectively. This section used the Landsat 8 data (refer to Section 3.3.1 of Chapter 3) LSTs calculated using the methodology discussed in Section 3.6.1 of Chapter 3. Section 3.5 of Chapter 3 discussed the urban and rural delineation and ΔT calculation methodology used in this chapter.

4.2 DAYTIME LST AND URBAN-RURAL LST DIFFERENCE (ΔT)

The daytime LST maps show that a conventional SUHI pattern with warm central urban areas surrounded by cooler rural areas exists in the US. In India, however, central densely built urban areas have lower LSTs than rural surroundings. Figure 24 and Figure 25 present the LST maps of typical cities in India and the US during summers and winters, respectively. Unlike in the US,

during the summers and winters, the LST increased from city centers to rural areas in India, as seen in Figure 24 and Figure 25. However, the cities in India are warmer compared to the US. In this example, shown in Figure 24, LST in Ahmedabad, India [35^{0}C, 61^{0}C] is higher compared to Minneapolis, US [15^{0}C, 41^{0}C]. During winters in India, there is a slight decrease in LST in the rural areas, making the LSTs more even across the urban-rural areas, as seen in Figure 25 in Surat, India. Also, in the US, the LST distribution across urban-rural areas is more homogenous during winters, as seen in Figure 25.

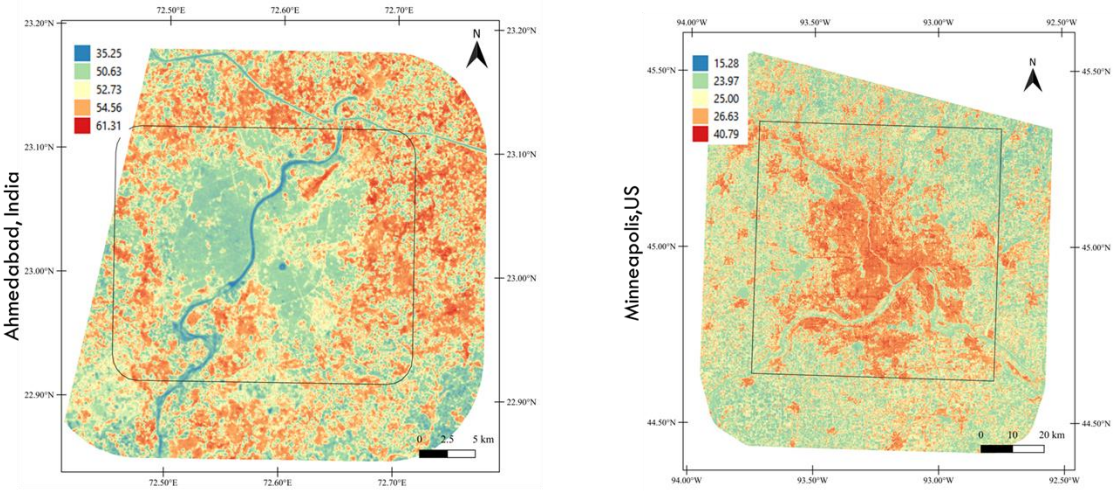

Figure 24: Daytime summer LST maps of Ahmedabad (ΔT = -0.9), India, and Minneapolis (ΔT = 1.6), US, show lower LST in central urban areas of India, higher LSTs in the central urban areas of the US.

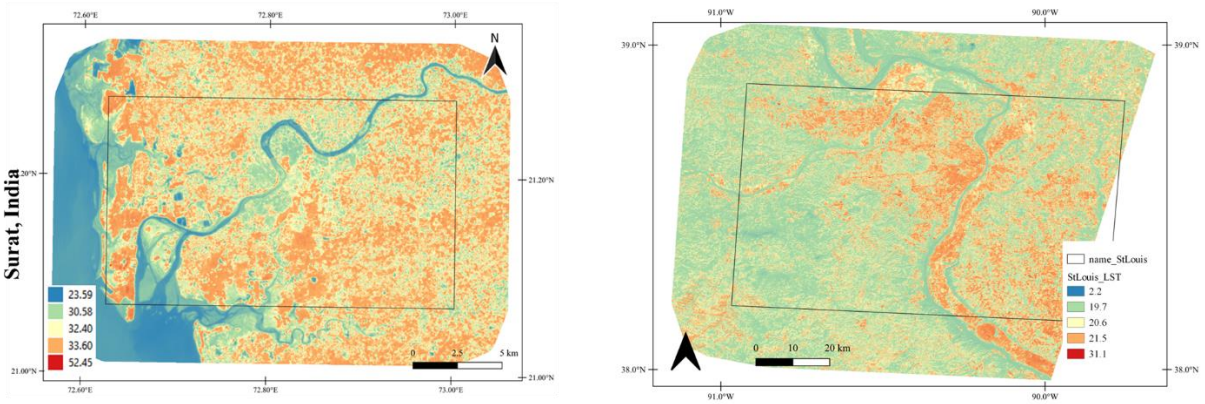

Figure 25: Daytime winter LST maps of Surat (ΔT = -0.3), India, and St. Louis (ΔT = 0.4), US, show low variation in LST across urban-rural areas

Summer and winter daytime ΔT show surface urban cool island (SUCI) pattern in India compared to surface urban heat island (SUHI) in the US, as seen in Figure 26. During summers, 34/42 cities showed SUCI with ΔT as large as -4.5^{0}C (Tiruchirappalli); during winter, 25/41 locations showed SUCI with the maximum ΔT of -1.7^{0}C (Tiruchirappalli). The mean ΔT ($\overline{\Delta T}$) across Indian locations were negative both during summers (-0.9 ± 1.2^{0}C, n=42) and winters (-0.3 ± 0.8^{0}C, n =41). However, conventional SUHI exits across the US cities with warmer urban surfaces compared to the rural ones. Unlike in India, in the US $\overline{\Delta T}$ values were positive for both summer (1.7 ± 1.6^{0}C) and winter (0.7±1.2^{0}C, n= 32). In the US, only 4/32 cities show SUCI and the magnitude of ΔT was much smaller (average of -0.6^{0}C) than that observed in India. In the US, the maximum ΔT is 5.3^{0}C (Houston) during summers and 4.9^{0}C during winters (Portland). The maximum noted ΔT in India is 1.6^{0}C during summer (Coimbatore) and 1.1^{0}C during winter (Lucknow). For both India and US, the magnitudes of SUHI/SUCI are lower during winters than in summers.

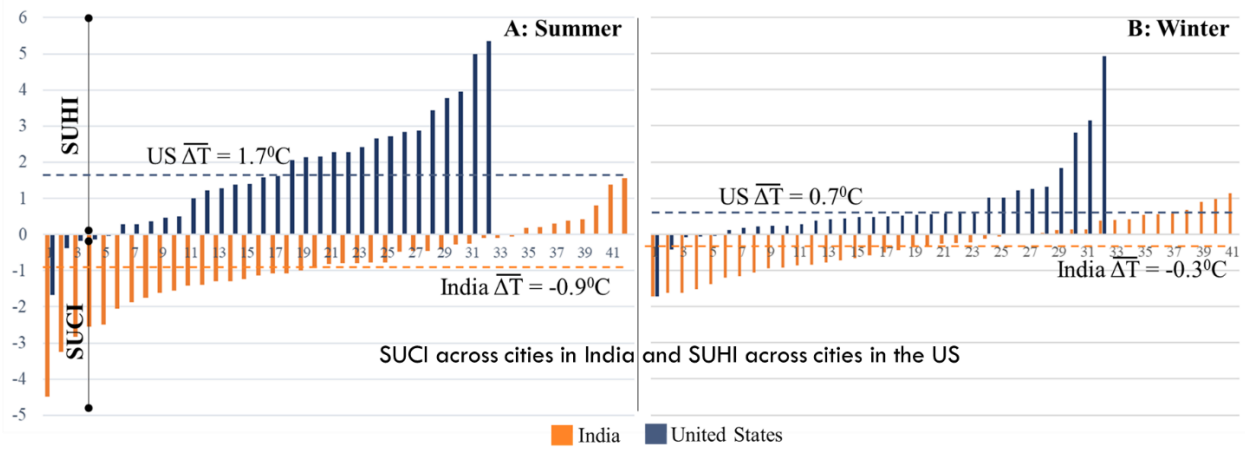

Figure 26: Daytime ΔT across all the Indian and US cities during A: Summer, and B: Winter, showing SUCI phenomenon predominantly across the Indian cities (>60% of studied locations) and SUHI across the majority of the US (>85% of studied locations) cities.

4.3 VARIATION IN LST WITH VEGETATION AND BUILT-UP AREAS

The two most important factors contributing to UHI formation are the decreased latent heat due to low vegetation and increased sensible heat due to high built-up surface densities (Oke, 1988, 1987). Using NDVI and IBI as spectral representations of existing vegetation and built-up areas, correlations show the association of LST with vegetation and built-up areas.

4.3.1 Correlation between NDVI and LST

Overall, Spearman's rank correlation coefficients (r_s) show vegetation's impact on LST was higher across the US than in India, especially during summers. A negative correlation was observed between NDVI and LST during summers, suggesting that as NDVI increases, LST decreases across all the cities in India and US, as seen in Figure 27. In India, 3/42 cities show a moderately strong negative correlation ($r_s > 0.5$, p-value <0.05), while this was in 26/32 cities in the US. In the winter, while the number of cities with this moderately strong negative correlation increased in India (7/41), it was substantially reduced among the US cities (3/32). In winter, in India, 12/41, and in the US, 14/32 cities showed weak ($r_s \leq 0.4$, p-value <0.05) positive correlation. There were four cities in the US with low urban mean LST (8-14^{0}C < overall urban mean of 17^{0}C) that showed moderate to strong positive correlation (r_s >0.4, p-value <0.05). These winter results from the US indicate that further investigation is needed to understand the variation in LST with vegetation, specifically in winters of cold climates.

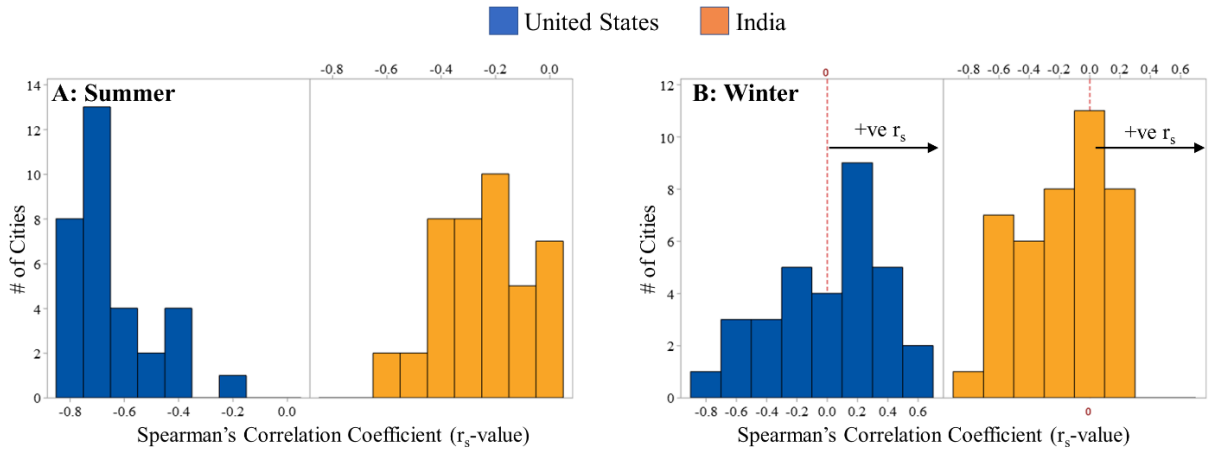

Figure 27: Spearman's rank correlation coefficient (r_s) between LST and NDVI across the urban areas of all the studied locations in India and the US. During summers, a strong correlation (r_s> 0.5) was observed across most of the US cities, while this is weak (r_s< 0.4) in the majority of the Indian cities. During winter, however, the correlation got stronger in India and weaker in the US.

4.3.2 Correlation between IBI and LST

The r_s (IBI, LST) values in Figure 28 show that a stronger correlation ($r_s \geq 0.5$, $p<0.001$) exists between IBI and LST across most of the cities in this study compared to the correlation between NDVI and LST (see Figure 27). As seen in Figure 28, during summers, most cities in India (30/42) and in the US (29/32) show a strong positive correlation ($r_s \geq 0.5$, $p<0.001$) between urban IBI and LST. However, during winters, while 29/41 Indian cities show a strong positive correlation, this falls to 4/32 in the US. A negative correlation between IBI and LST was also noticed in the US (10/32) during winters, showing some season dependency. Interestingly, most of these are the same cities that showed a positive correlation between NDVI and LST. Therefore, this could be because of the lack of vegetation during winters in the US, resulting in low NDVI values that alter the IBI values (see Equation 6 in Chapter 3). The results from the winters across US locations show that the LULC types and their performance vary and need further investigation and analysis beyond this study's scope.

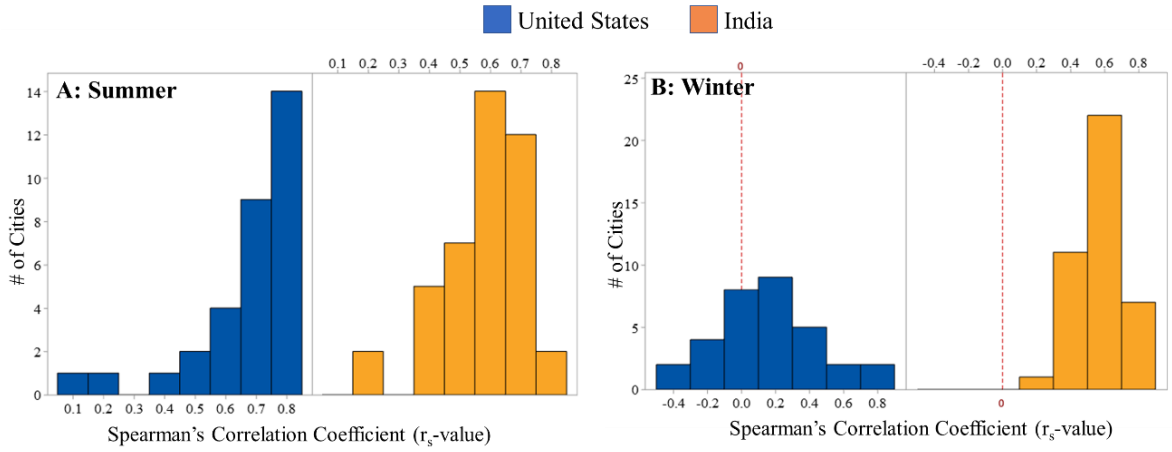

Figure 28: Spearman's rank correlation coefficient (r_s) between LST and IBI across the urban areas of all the studied locations in India and the US. A strong positive correlation (r_s> 0.5) was observed across most locations in US and India during summers. The number of cities showing a strong correlation is lower in winter than in summer, especially in the US. Some US cities also show a negative correlation between urban LST and IBI during winters.

4.4 VARIATION IN ΔT WITH VEGETATION AND BUILT-UP AREAS

Linear regression analysis showed how the urban-rural differences in vegetation and built-up areas impact ΔT. In Figure 29, the independent variables on the x-axis are ΔNDVI -the difference between urban and rural mean NDVI and ΔIBI – the difference between urban and rural mean IBI and are correlated with ΔT. Across Indian cities, the linear correlation between ΔNDVI and ΔT was negative and weak during summers (R^2 = 29.6%) and winters (R^2 = 36.5%). In the US cities, however, in summer, there was a stronger (R^2=54.3%) negative correlation (ΔT = 0.7547 – 42.27 (ΔNDVI)) that got weaker (10.3%) in winter. The negative correlation between ΔNDVI and ΔT shows that as urban greenery increases, the ΔT decreases. These results are consistent with prior studies conducted across locations from North America and China (J. Wang et al., 2015; D. Zhou et al., 2014) and one from 419 big global cities (Peng et al., 2012). A positive correlation between ΔIBI and ΔT shows that as the built-up area increased, the ΔT increased. Table 9 shows the R^2 values and the linear regression fit equations between ΔIBI and ΔT. The strongest (R^2 = 70.5%) and weakest (R^2 =15.2%) correlations are observed for the US in summer and winter, respectively.

In India, the correlation between ΔIBI and ΔT was moderately strong both in summer (R^2 = 41.2%) and winter (R^2 = 55.8%) and was stronger than the correlation between ΔNDVI and ΔT (see Figure 29).

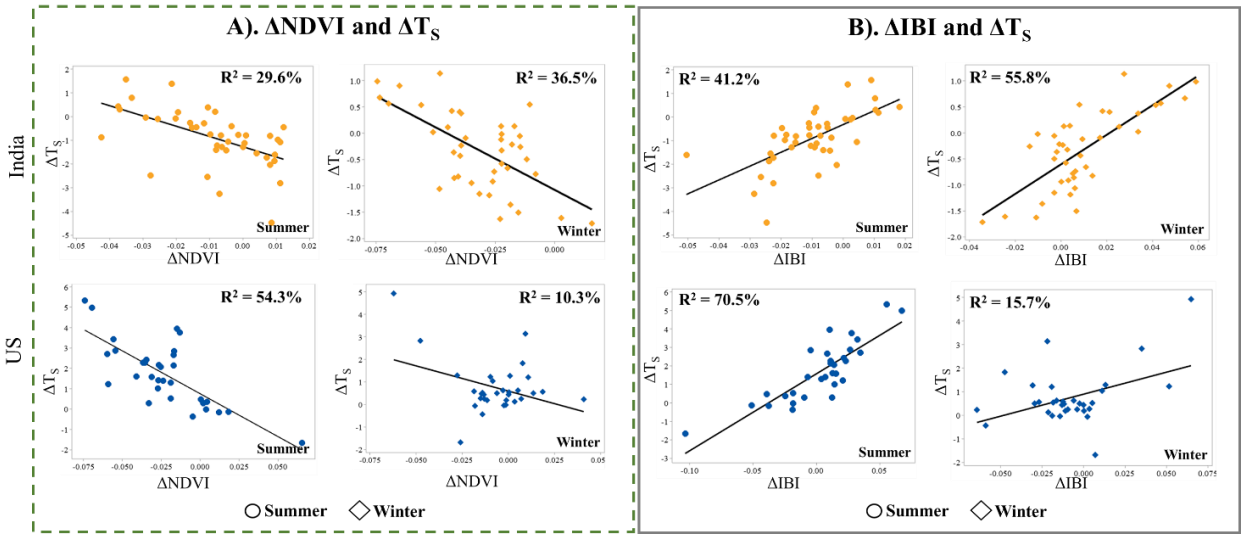

Figure 29: Linear regression line fitted between A.) ΔNDVI (urban-rural mean NDVI) and ΔT (urban-rural mean LST) for all the cities in India (top) and the US (bottom) during summers and winters. The negative slope shows that as the difference between urban and rural vegetation increases, the corresponding temperature difference decreases, reducing the SUHI/SUCI magnitude. B.) ΔIBI (urban-rural mean IBI) and ΔT. The positive slope shows that as the difference between urban to rural built-up surface densities increases, the corresponding temperature difference increases, increasing the SUHI/SUCI magnitude.

Table 9: ΔT and ΔIBI linear regression line fit R^2 values and equations for India and US during summers and winters

Country	Season	R^2	Equation
US	Summer	70.5%	ΔT = -1.571+41.79 ΔIBI
	Winter	15.7%	ΔT = 0.8889+18.70 ΔIBI
India	Summer	41.2%	ΔT = -0.3208+58.80 ΔIBI
	Winter	55.8%	ΔT = -0.6052+28.48 ΔIBI

4.5 VARIATION IN ΔT, LST, AND THE CORRELATIONS WITH THE LAND USE LAND COVER

The results of this study showed some conventional and expected observations in the case of the US. These include 1.) SUHI phenomenon across the US cities, 2.) Strong inverse correlation between vegetation (NDVI) and LST or ΔT during summers, and 3.) During summers, a strong

positive correlation exists between the built-up areas and LST or ΔT. However, in the case of India, 1.) The rural areas appear hotter than urban surfaces (SUCI), 2.) The correlation of vegetated (NDVI) and built-up (IBI) areas with LST and ΔT was moderate to weak in both seasons. These results are counterintuitive to the general understanding of UHI, which increases with urbanization. Therefore, this prompts an exploration of the factors contributing to such observations.

SUCI studies across some of the tropical and dry locations of the world (Ali et al., 2017; Faqe Ibrahim, 2017; Kumar et al., 2017; Mathew et al., 2018; Rasul et al., 2015; Zareie, Khosravi, Nasiri, & Dastorani, 2016) attributed its occurrence to the land surface characteristics. Prior literature showed how LST and ΔT varied with land use land cover (LULC) classification and spectral indices (especially NDVI) (see Section 2.4.3 of Chapter 2). However, a discussion of the spectral properties of the LULC types and how they impact LST, spectral indices values, and correlations are limited. This section discusses the vegetation and other LULCs of India and the US, their thermal and spectral characteristics, and how they contribute to the observed ΔT trends and correlations.

4.5.1 NDVI values linked to ΔT and Correlations.

An increase in vegetation mitigates SUHI. Though this broad trend existed across the cities in the US, in India, vegetation seems to have a lower impact on LST and ΔT due to its poor quality (less greenness). Figure 30 shows the average NDVI values across urban areas of India and the US during summers and winters. As seen in Figure 30, the average NDVI values across urban areas of India are lower than in the US during summers. In the winter in India, NDVI values increased in some northern and eastern states. The summer and winter NDVI values from India are still low compared to those observed in the urban US during summers. They are, however, comparable with

the NDVI values in winters in the US, when vegetation across many cold locations of the country sheds its leaves.

In India, across the cities with SUHI, the average NDVI ($\overline{NDVI}$) in rural areas is higher than in urban areas both in summers (by 14%) and winters (by 27%). However, in cities with SUCI, ΔNDVI is positive ($NDVI_{urban} > NDVI_{rural}$) or close to zero (e.g., ΔNDVI = 0.01 in Tiruchirappalli, the city with maximum -ΔT). Also, increasing greener vegetation (NDVI >0.3) lowers the LSTs. For example, in Coimbatore in summer (ΔT = $+1.7^0$C), 32% of the rural area ($\overline{NDVI}$=0.26) has NDVI > 0.3 compared to the 18% of urban areas ($\overline{NDVI}$= 0.22). In some cities (16/34 in summer and 23/25 in winter) in which urban areas are cooler (-ΔT), the rural $\overline{NDVI}$ is slightly (-0.01 - -0.04) higher compared to the urban. In this case, it can be hypothesized that the impact of surrounding non-green rural areas is higher on ΔT and might not mean that the urban areas are 'cooler.'

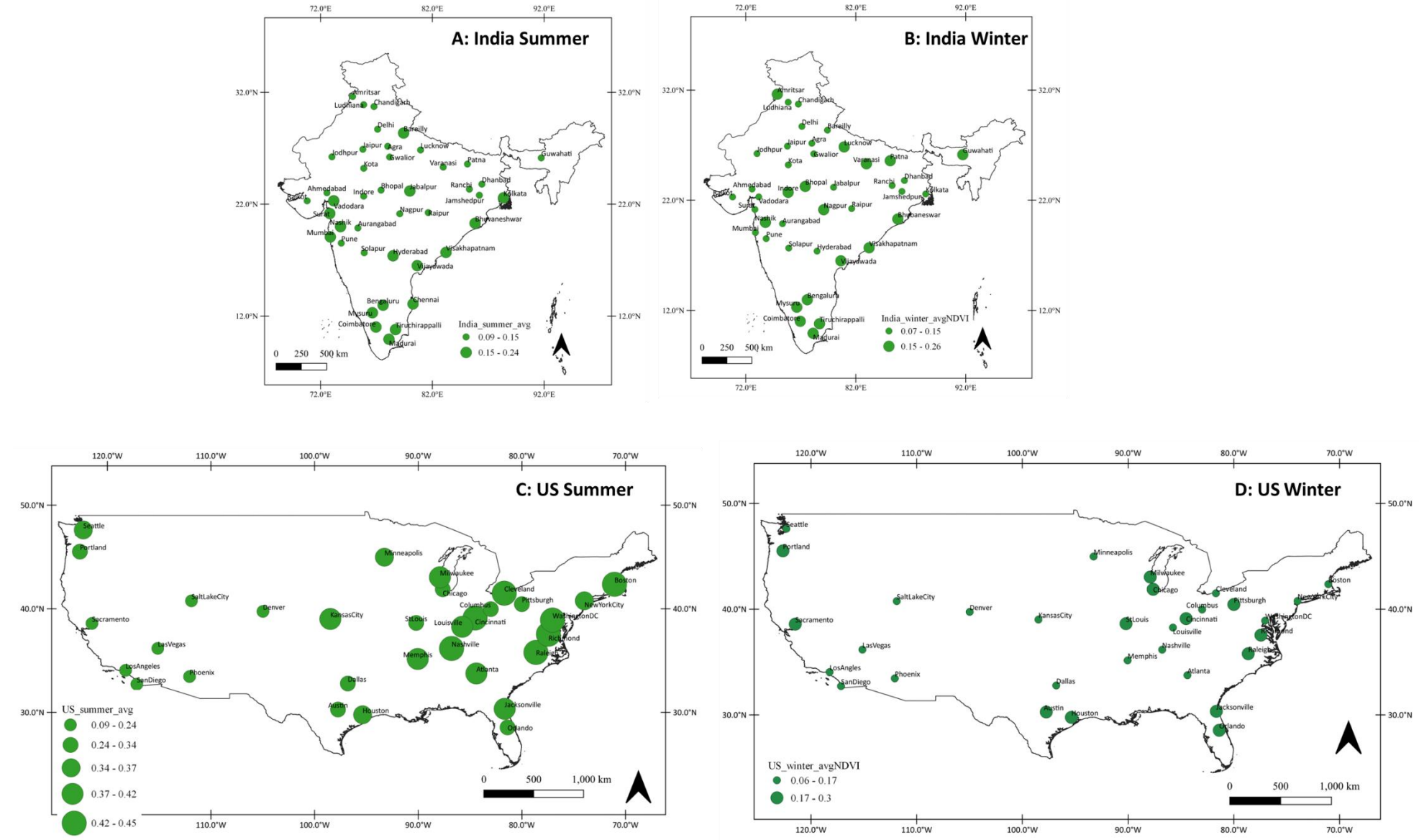

Figure 30: Average NDVI across urban areas of A: India in summer, B: India in winter, C: US in summer, and D: US in winter

Vegetation greenness and quantity also impact the correlations studied. Figure 31 shows vegetation quantity (area) under four categories based on greenness - the average NDVI value across the urban and rural areas of typical cities in India and the US. The cities presented here are based on each country's min, max, and mean ΔT. Figure 31 also mentions Spearman's correlation coefficient r_s between (NDVI, LST) and (IBI, LST) for each case. From the figure,

- The NDVI values are higher in the US compared to India.
- In urban and rural regions of India, the NDVI value increases during winters (e.g., Tiruchirappalli and Lucknow). In contrast, the NDVI value in the US decreases in winters compared to summers (e.g., Austin and Portland).
- In both the US and in India, for locations with high positive ΔT (>1σ), rural areas are greener (NDVI > 0.3 in India, and NDVI > 0.4 in the US), e.g., Lucknow, India, and Portland, US.
- The correlations strengthen with an increase in NDVI. For example, the correlations were weak in summers (r_s (LST, NDVI) = -0.27, r_s (LST, IBI) = 0.46) when Tiruchirappalli AOI (urban + rural) has only 6% of the land with NDVI >0.3. The correlations became stronger (r_s (LST, NDVI) = -0.67, r_s (LST, IBI) = 0.85) in winter when 22% of the land area has NDVI > 0.3.
- Similarly, in Lucknow, India, correlations became stronger from summers (r_s (LST, NDVI) = 0.0, r_s (LST, IBI) = 0.42) to winters (r_s (LST, NDVI) = -0.63, r_s (LST, IBI) = 0.73) when the land area with NDVI>0.3 increased from 2% to 25%.
- Also, correlations weaken in the US as vegetation greenness decreases in winter. For example, in Austin, the correlations get weaker as the land area with NDVI> 0.3 decreased

from 55% in summers (r_s (LST, NDVI) = -0.68, r_s (LST, IBI) = 0.62) to 4% in winters (r_s (LST, NDVI) = -0.10, r_s (LST, IBI) = 0.44).

The NDVI variable in IBI calculation (see Equation 6 in Chapter 3) alters the correlations between IBI and LST or ΔT. With the increase in NDVI, the correlations between (NDVI, LST) and (IBI, LST) are strengthening. In India, the correlations strengthened when an NDVI of 0.3 or greater existed in higher quantities across the urban or rural areas. The prevalence of non-green vegetation in high quantities across cities in India impacts the NDVI and the IBI values, hence the correlations. Comparing the vegetation and other LULC in India and the US and understanding its thermal and spectral performance provide more insights into the spectral indices values and the results observed.

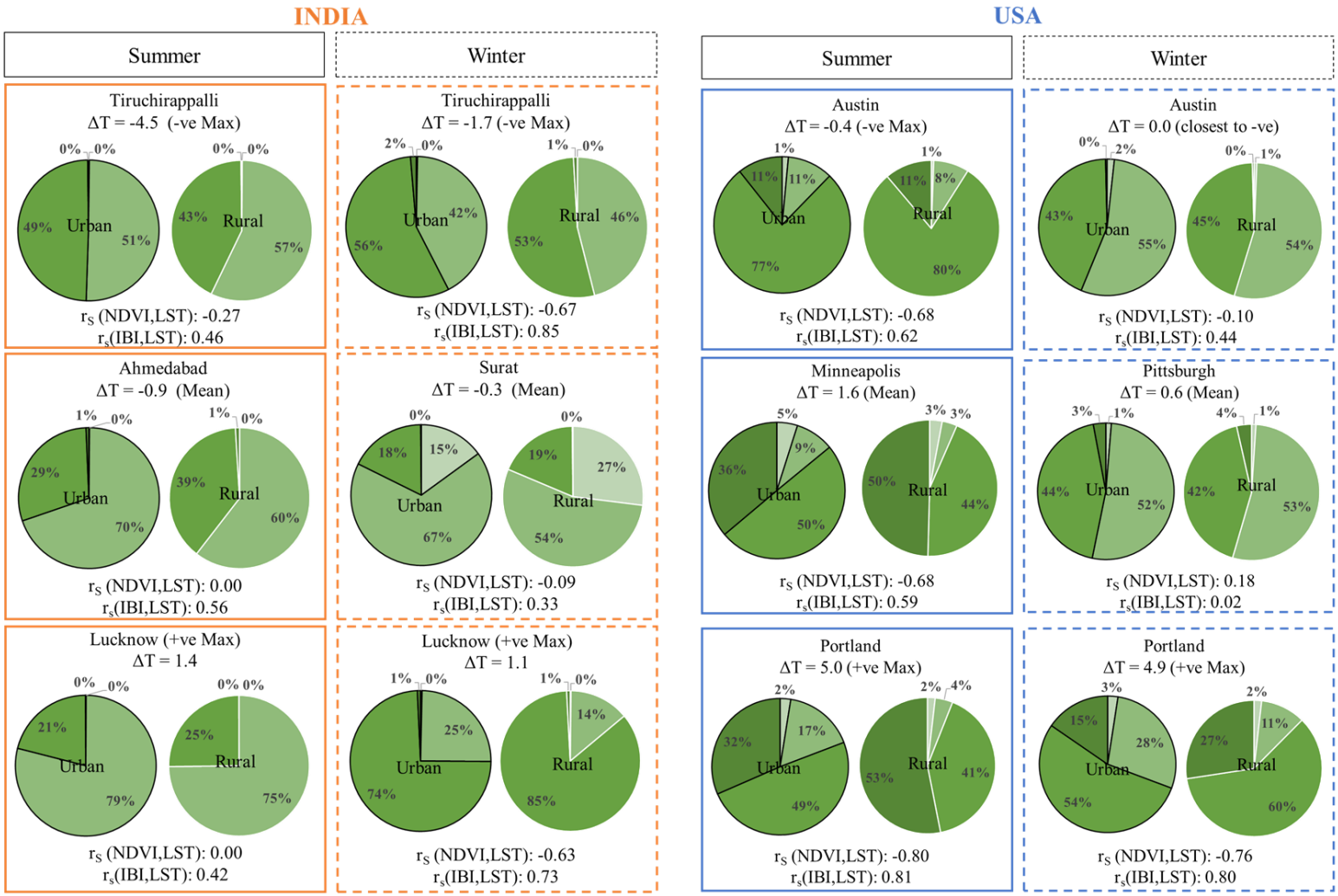

Figure 31: NDVI ranges and land area in each NDVI range in urban and rural areas of typical cities in India and the US during summers and winters. The darker the 'green' higher the NDVI and greenness of the vegetation. The US has higher quantities of green vegetation than India, and the quantities of green vegetation increase in winters in India and decrease in winters in the US.

4.5.2 LULC in India and the US

In both countries, most of the land cover is vegetation, however different kinds of vegetation. Over 60% of the land area in India is croplands. In contrast, in the US, it is forest (39%), herbaceous[3] vegetation (28%), and shrublands (9%), as seen in Figure 17. In India, 2.3% of its land area is built-up compared to 1.5% in the US.

4.5.2.1 Vegetation-NDVI in rural India and the US

The greenness and quantity of vegetation and the NDVI value vary with seasons. In India, there are two main crop-growing seasons, Rabi and Kharif. The rabi season is from November to March, and the Kharif is between June -October. Prior studies (de Jong, de Bruin, de Wit, Schaepman, & Dent, 2011) showed that NDVI varies with the vegetation development stages. The studies show that NDVI peak occurs mid-season, and the lowest values are during the start and end of the growing season. A recent study(Kashyap, Pandey, & Kuttippurath, 2022) shows that the photosynthetic activity in India peaks during post-monsoon months (September, October, November) and is the lowest during summers (March, April, and May). Another study (Revadekar, Tiwari, & Kumar, 2012) from India found that NDVI in India peaked in October. This study showed that temperatures and rainfall impact NDVI. The amount of rainfall from a year also impacted the NDVI of the following year. Depending on the temperatures and amount of rainfall, different regions of the country could have different levels of greenery. NDVI values in this study align with the observations from the literature indicating the high quantity of non-green vegetation during the summer and winter months in India (see Figure 30). Based on the literature, most months except a few monsoon and post-monsoon months between August-November would have

[3] "Plants without persistent stem or shoots above ground and lacking definite firm structure. Tree and shrub cover is less than 10 %." (Buchhorn et al., 2020)

non-green or low-green vegetation in India. In the US, while the evergreen forests remain green throughout the year, the deciduous forests and the shrublands show seasonal variation, with peak greening during the summers. All except the desert and xeric shrubland biome (e.g., Phoenix, AZ, Las Vegas, NV) of the US showed higher NDVI (>0.3) values during summer(Imhoff et al., 2010). The growing season of croplands in the US (most locations except the southwest) also coincides with summers being the mid-season for most crops harvested in the fall. Therefore, in the US, vegetation is greener in summers than in winters(Chun & Guldmann, 2018), resulting in higher NDVI values during summers, as noted in this study. Across all these vegetative land cover types, brown or dry non-photosynthetic vegetation (NPV) and leaf litter could also exist. Brown or dry NPV and leaf litter are prevalent in the croplands during non-cropping/non-growing seasons (summers) in India and the deciduous forests of the US during fall and winter. Therefore, low NDVI values and NPV across urban and rural areas of India potentially increase LSTs compared to US ones.

4.5.2.2 Soil moisture in India and the US

Non-growing seasons (summers) or the non-monsoon seasons (such as winters) in India also mean low soil moisture levels. Prior studies (Jiang et al., 2015; Mohammad & Goswami, 2021) showed the impact of soil moisture on LSTs and ΔT. A decrease in soil moisture increased LSTs. The soil moisture also affects evapotranspiration(Sebastian, Murtugudde, & Ghosh, 2023). Evapotranspiration - the evaporation of water through plants into the atmosphere, is a widely documented phenomenon that impacts UHI formation(Besir & Cuce, 2018; Shastri et al., 2017; Haider Taha, 1997). A decrease in soil moisture decreases evapotranspiration which in turn increases the temperatures.

Figure 32 shows an example of soil moisture levels in India and the US. The figure visually compares India and the US soil water index (SWI[4] – an indicator of soil moisture) during the summer and winter of 2016. The SWI data(Copernicus Global Land Service, 2018) used here is only for visual comparison, and this study doesn't analyze it quantitatively, nor is it used in any other analysis presented. As seen in the figure, during summers (May in India and July in the US), the soil moisture in the US is higher than in India. In this figure, during winters, though the data is missing some US locations (3/32 studied locations), the northeastern, northwestern, and midwestern US show slightly higher SWI compared to India. Compared to India, the soil moisture in the US is higher across most locations (except some southwestern and western locations) during all the months except the monsoon months of India (August – October)(Climate Prediction Center Internet Team, 2020). In India, the soil moisture peaks in the monsoon season (June-Septermber) when most (about 80%) of the rainfall occurs and then declines after a short lag (Pangaluru et al., 2019; Sebastian et al., 2023). Changing rainfall patterns are shown to increase drought conditions in India(Mishra & Liu, 2014), which in turn is leading to groundwater depletion, and around 42% of India's cultivable cropland lies in these drought-prone regions. Growing urban areas in already drought-prone regions of the country, and the high demand (90% of total water needs) for groundwater for the irrigation of crops, are creating water stress and scarcity in India(Dhawan, 2017). Water scarcity and groundwater depletion could add to the already low soil moisture levels during the non-monsoon season in India. A recent global study(W. Li et al., 2022) also showed a decreasing trend in vegetation (quantified using leaf area index) with decreasing soil moisture. The sensitivity of vegetation to soil moisture was more evident across dry locations like India and the southwestern US, and other drought-prone regions of the world, facing reduced precipitation levels

[4] SWI "describes the relation between surface soil moisture and profile soil moisture as a function of time." (Copernicus, 2018)

and relying on groundwater resources. Though there is a difference in the soil types between India and the US(NASA LDAS, 2022), the soil moisture levels seem to have a more significant impact on the LSTs(Sandholt, Rasmussen, & Andersen, 2002; Weng et al., 2004).

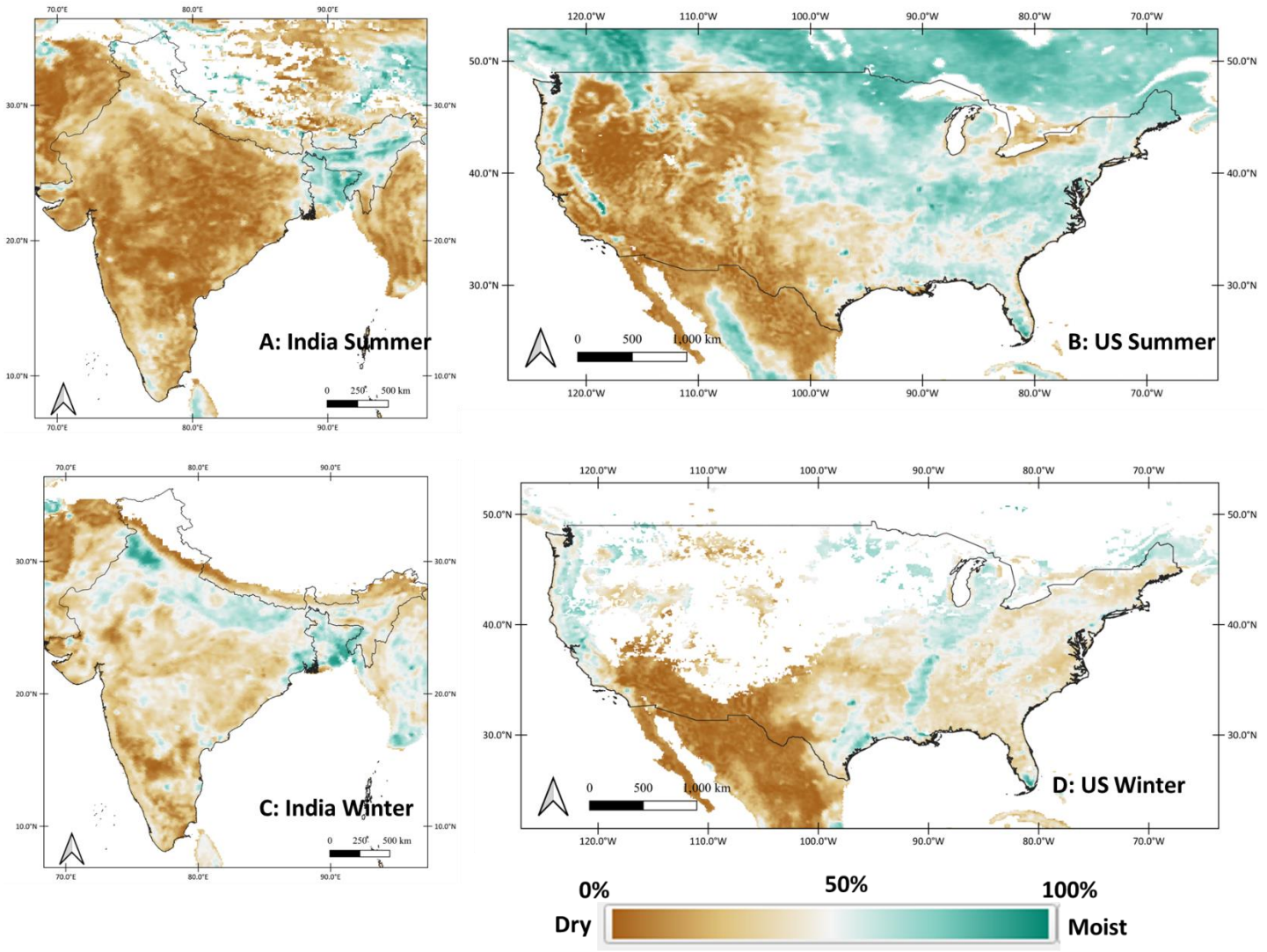

Figure 32: The visual comparison of soil moisture using the soil water index in A. India during summer(May), B. US during summer (July), C: India during winter(December), and D: US during winter (December)of 2016.

4.5.2.3 Thermal characteristics of rural and urban LULC in India and the US

Some thermal properties of surfaces that explain the heat transfer to and from a surface are 1. Thermal admittance (the ability of the surface to accept or release heat), 2. Thermal diffusivity (the ability of the surface to diffuse heat), 3. Heat capacity (amount of heat required to change temp. by 1 K), and 4. Thermal conductivity (the ability of a surface to conduct heat). For most soil types, the soil moisture and its thermal properties are positively correlated (see Figure 2.5 of (Oke, 1987)). Broadly, moist soils take time to accept heat (high admittance), diffuse the heat faster (high diffusivity), need a higher amount of heat to change temperatures (high heat capacity), and transfer more heat (high conductivity). Appendix B of this dissertation details the thermal properties of the conventional building and natural materials found in urban and rural LULC types in India and the US.

Therefore, most rural areas in India with NPV and unsaturated soils during summers and winters gain heat faster during daytime with solar radiation, showing higher LSTs. Urban areas in India predominantly have concrete and brick, which have a higher capability to transfer heat and require more heat to change temperature than dry soil (see Appendix B). Due to this, the urban areas heat up slowly compared to the rural areas in India, resulting in lower urban LSTs than rural LSTs (see Table 10) during the daytime. A remote sensing and in-situ measurement-based study for two cities in India (Mathew et al., 2018) also showed such LST patterns. In that study, SUCI in Jaipur and weak SUHI in Ahmedabad, India, was noted during the daytime. The prevalence of barren land in rural/suburban areas of Jaipur that tend to heat up quickly during daytime resulted in SUCI. In-situ surface temperature measurements of different LULC types: road, vegetation, soil, concrete block, and concrete showed higher temperatures of soil compared to other urban land covers- road

or concrete during the daytime. These findings align with the LST observations from this study (see LST from Table 10).

In the US, however, the higher soil moisture and greener vegetation in the rural areas keep the rural area LSTs lower than urban areas. Urban buildings are in concrete, wood, and glass. Urban roofs of commercial buildings are in concrete or metal and finished using single-ply membranes, modified bitumen, or asphalt surface coating. Sloped residential roof finishes include fiberglass asphalt shingles, wood shakes, clay, or concrete tiles(Hashem Akbari & Kolokotsa, 2016). These urban materials in the US have lower thermal admittance- heating up faster (see Appendix B), compared to the green and moist rural areas, and thus have higher LSTs than rural areas (see Table 10). Though less common, there are few locations in the US with mean rural LSTs higher or equal to urban LSTs. Such a trend existed in locations where rural areas are less forested and more shrublands or croplands (e.g., San Diego, CA, Las Vegas, NV). Prior studies also showed similar observations for locations in dry regions (L. Zhao et al., 2014) or desert and xeric shrublands (Imhoff et al., 2010). In winter, though, SUHI in many US cities could be impacted by other LULC types, such as snow and ice. More analysis is needed to understand SUHI during winters in the US and its variation with LULC, which is not the focus of this study.

Daytime heating up of non-green and low saturated rural areas in India could result in negative ΔT. In contrast, in the US, forested and moist rural areas with lower daytime LSTs than urban areas result in higher ΔT values.

4.5.3 Spectral Reflectance of common LULC, Spectral Indices, and the Correlations

To further understand the impact of LULC on ΔT and the spectral indices, the spectral properties of common LULC types, including vegetation and built-up surfaces in India and the US, were analyzed. This knowledge is instrumental in understanding how the spectral indices perform.

The spectral reflectance properties (Baldridge, Hook, Grove, & Rivera, 2009; Meerdink, Hook, Roberts, & Abbott, 2019) of the common LULC types are plotted in Figure 33 to understand how different LULC types reflect and absorb the different wavelengths (horizontal axis of Figure 33). For instance, NDVI (Equation 2 in Chapter 3) uses Band 4 and Band 5 data, and this is because green vegetation with chlorophyll absorbs most of the radiation in Band 4 and reflects most in Band 5, as seen in Figure 33. So, when vegetation is greener, the NDVI value is higher. However, as seen in Figure 33, NPV, soil, and concrete absorb in Band 4 wavelengths and reflect highly in Band 5, which could result in equal or close to equal NDVI values for these land covers. Likewise, for IBI (Equation 6 in Chapter 3) or NDBI (Section 2.4.3), Band 6 wavelengths are typically considered to represent concrete, which reflects highly in this band. However, the spectral reflectance curves of concrete, soil, and NPV in Band 6 are similar and could interfere with accurately representing built-up areas using IBI values. This interference would be higher for locations where barren soils or sparse vegetations are more prevalent, like in the case of India. Therefore, the prevalence of croplands in rural India alters the ΔT, spectral indices, and correlations compared to the US.

To support these theories of the impact of LULC and vegetation on the observed ΔT trends, indices, and correlations, the spectral indices (NDVI, IBI, and NDBI) values and LSTs in summer across the LULC types in Ahmedabad (India) and Minneapolis (the US) were quantified. Summer ΔT in Ahmedabad and Minneapolis is approximately equal to the mean across all cities studied in India and US, respectively. The global land cover data of 2016 from Copernicus Global Land Service (Buchhorn et al., 2020) was used to classify the LULC types in Ahmedabad and Minneapolis AOI (urban+rural). Table 10 shows the average NDVI, IBI, NDBI values, and the average LST for different LULC classes in Ahmedabad and Minneapolis during summers, along with the

percentage land area (of AOI) of each class. As seen in Table 10, the difference between average NDVI, IBI, and NDBI for each LULC type is lower in the case of India compared to the US. Also, the average IBI and NDBI values remain the same for built-up, cropland, and herbaceous vegetation classes in Ahmedabad, India. In Minneapolis, though, the difference in average IBI between croplands (greener, NDVI= 0.42 compared to NDVI = 0.20 in Ahmedabad) and built-up areas is higher. Therefore, India's lack of green vegetation seems to be confounding the correlations between LST and IBI and ΔT and ΔIBI- making them invalid. Further, as seen in Table 10, in India, the mean LST in croplands (53.06^0C) is higher compared to the mean LST in urban built-up areas (51.21^0C), unlike in the US, where urban-built-up areas have the highest mean LST (29.78^0C). It is therefore hypothesized that the negative ΔT in Indian cities is due to the prevalence of such high LST rural croplands - for instance, in the case of Ahmedabad, 90% of the rural area is cropland compared to 43% in Minneapolis.

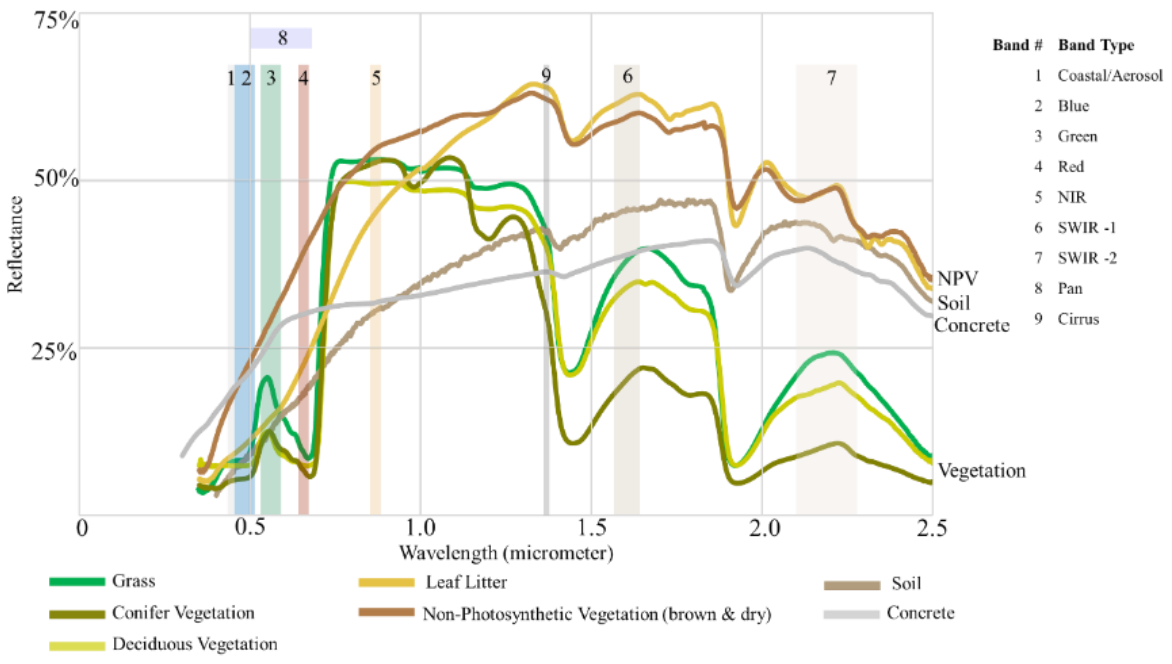

Figure 33: Spectral reflectance curves showing the total energy (%) reflected in each wavelength (band 1-9 of Landsat 8) by the common LULC types. Notice the similar curve trend for NPV, soil, and concrete compared to green vegetation.

The LST, NDVI, and IBI patterns were also visually and spatially analyzed, as shown in Figure 34. The LST maps show that the SUCI and SUHI patterns of Ahmedabad and Minneapolis are distinct. Visually NDVI in urban areas is lower, as expected, in both cities. However, the quantity of green vegetation (NDVI > 0.3) is deficient (4% of AOI) in Ahmedabad compared to Minneapolis (71% of AOI). Higher IBI values in the rural areas of Ahmedabad in Figure 34A show the limitation of IBI in differentiating fallow croplands from built-up areas. These maps visually support the observed results and the unconventional patterns of LST and IBI in Ahmedabad and show the conventional spatial pattern of SUHI (LST decreasing from the city core towards the rural) in Minneapolis. As seen in the LST maps of Figure 34 and the mean LSTs in Table 10, though Indian cities seem cooler compared to their rural counterparts, the absolute LSTs were high. The average LST in Indian urban areas was 10-12^{0}C higher than in the US.

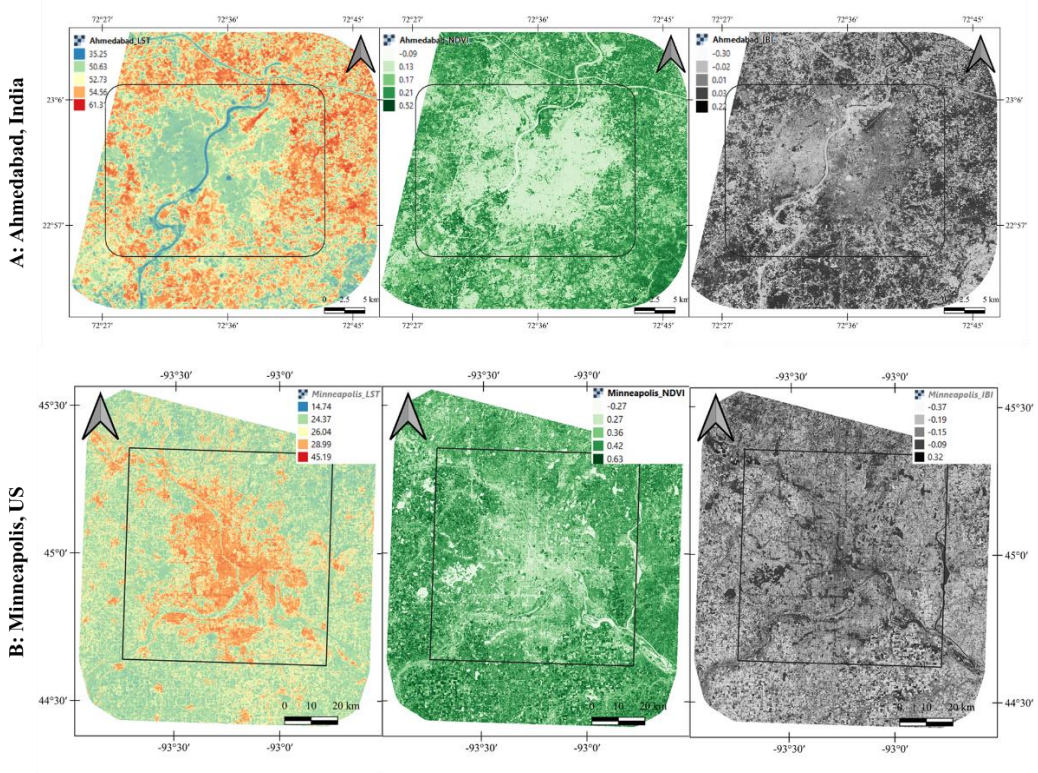

Figure 34: Summertime LST, NDVI, and IBI maps of A: Ahmedabad, India, and B: Minneapolis, US.

*Table 10: Average NDVI, IBI, NDBI, and daytime summer LST across the predominant LULC classes in Ahmedabad and Minneapolis in summer. Equal or close to equal indices values (in bold) across built-up, cropland, and herbaceous vegetation classes, especially in India, resulting in ambiguity in the representation of the LULC type using spectral indices. *LULC definition from* (Martins, Trigo, & Freitas, 2020)*

LULC Type	**Ahmedabad**					**Minneapolis**					**LULC definition***
	% AOI	NDVI	IBI	NDBI	LST(^{0}C)	% AOI	NDVI	IBI	NDBI	LST (^{0}C)	
Urban/Built-Up	25%	**0.13**	**0.00**	**-0.01**	51.21	10%	0.27	**-0.11**	**-0.14**	29.78	Land covered by buildings and other man-made structures
Cropland	72%	0.20	**0.00**	**-0.01**	53.06	32%	0.42	-0.18	-0.21	24.85	Lands covered with temporary crops followed by harvest and a bare soil period
Herbaceous vegetation	1%	**0.13**	**0.00**	**-0.01**	50.43	14%	0.36	**-0.13**	**-0.15**	26.62	Plants without persistent stems or shoots above ground and lacking definite firm structure. Tree and shrub cover is less than 10 %.
Closed forest, deciduous broad leaf	0%	-	-	-	-	10%	0.40	-0.18	-0.21	23.54	Tree canopy >70 % consists of seasonal broadleaf tree communities with an annual cycle of leaf-on and leaf-off periods.
Open forest, unknown	1%	0.24	0.04	-0.06	49.83	22%	0.36	-0.14	-0.17	25.67	Open forest not matching any of the other definitions

This analysis, therefore, suggests that the impact of the urban built-up environment (human-made) on LST across Indian cities cannot be analyzed using the conventional ΔT calculation method and the built-up spectral indices. Instead, these measures and methods shift the focus towards rural areas and their impact on LST.

4.6 CONCLUSION

The main findings of this study are 1.) SUCI exists in India both during summers ($\overline{\Delta T}$= -0.9) and winters ($\overline{\Delta T}$= -0.3) compared to conventional SUHI in the summers ($\overline{\Delta T}$= 1.7^{0}C) and winters ($\overline{\Delta T}$= 0.7^{0}C) of the US. Primarily, 60% of the land area in India is cropland which might stay dry or sparsely vegetated during non-growing seasons. This cropland can have higher LSTs compared to the built-up areas. However, rural areas in the US are more likely to be greener (NDVI >0.3) and moist forested or croplands, resulting in lower LSTs than built-up areas. 2.) In India and the US, the negative correlation between NDVI and LST strengthens as NDVI increases. In India, cities with r_s (LST, NDVI) > -0.5 increased from 3 in summer to 7 in winter. However, in the US, as the vegetation greenness decreased in winter, cities with r_s (LST, NDVI) >-0.5 decreased from 26 in summer to 3 in winter. Further, the negative correlation between ΔNDVI ($NDVI_{urban} - NDVI_{rural}$) and ΔT is strongest in the US during summers than in India. Therefore, the greenness and quantity of green vegetation change the correlation strength. 3.) In India, the average built-up indices (IBI and NDBI) values were similar across the built-up areas, croplands, and sparse vegetative land covers during summers and winters. Similar concrete, NPV, and soil spectral reflectance curves could result in similar built-up indices values. Therefore, India's non-built-up land use characteristics (low vegetation and soil moisture) during summers and winters are confounding correlations between IBI and LST, making them invalid. Since rural areas in India aren't like those

of North America or Europe from where the UHI research originated, customizing the definition of 'rural' is needed to estimate the impact of urbanization on UHI. Studies that showed urban areas are cooler in India could all be using methods that mask the impact of urban built-up areas on the UHI. There is, therefore, a need to develop localized ΔT calculation methods and spectral indices for Indian and similar type LULC types to appropriately estimate the impact of urban built-environment on the temperatures. Prior studies(Deilami et al., 2018; D. Zhou et al., 2018) emphasize the importance of studying UHI during daytime summers when the impact could be maximum. In India, understanding the variation of LST, ΔT, and LULC characteristics during monsoon and post-monsoon months could provide a wholesome understanding of SUHI/SUCI trends. With greener and more moist rural areas during monsoon seasons in India, most cities across India could show SUHI similar to the summers in the US. However, the limited availability of cloud-free satellite data during the monsoon months could impact such analysis. Using measures such as percentage impervious surface area instead of built-up indices and extending the temporal scale (day and night, seasonal, annual) of this daytime analysis could provide more insights into this comparative analysis of the Surface Urban Heat Island phenomenon. This daytime analysis of LST and ΔT led to two peer-reviewed journal articles (Tetali, Baird, & Klima, 2019, 2022) and a conference paper.

5 NIGHTTIME AND DIURNAL ANALYSIS OF THE SURFACE URBAN HEAT ISLAND PHENOMENON

5.1 OVERVIEW

This chapter extends the daytime SUHI analysis to the night and other seasons of the year. Since the daytime analysis from Chapter 4 of the dissertation indicated the shortcomings of the built-up indices in differentiating Indian LULC, this analysis quantified the total built-up area from the Copernicus LULC data from 2016 to show the variation in ΔT with the area of built-up land use. Statistical t-tests discussed the significance of diurnal and seasonal ΔT variation in both countries. They showed if a populous and highly urbanizing country like India would behave differently than the US. This chapter also attempts to explain the diurnal variation in ΔT using India and the US's land use land cover (LULC) characteristics. In this chapter, the ΔT is the mean LST difference between urban and rural areas (refer to Section 3.6.2 of Chapter 3) calculated using LST data from MODIS (MYD11A2) data from 2016. The urban and rural boundaries were defined using the urban and rural delineation methodology discussed in Section 3.5 of Chapter 3. Analysis metrics, such as the percentage area of cropland in rural areas, the percentage area of built-up areas in urban, and the normalized difference vegetation index (NDVI), were used in this chapter to correlate land use land cover properties with ΔT.

5.2 COMPARISON OF DAYTIME ΔT CALCULATED USING LANDSAT AND MODIS

MODIS data are available daily for both day and night at a 1km resolution (refer to Section 2.3.2 for more on MODIS data). Landsat 8 data are available only for daytime with a temporal resolution

of once every 16 days (refer to Section 2.3.1 for more on Landsat 8 data). Chapter 4 of this dissertation presented the daytime ΔT using Landsat 8, 30m resolution data. This section provides a statistical comparison of the daytime ΔT from Landsat 8 and MODIS- MYD11A2 data to check the fidelity of this 1km resolution data in calculating the daytime ΔT trends. The MODIS daytime ΔT was calculated from the monthly average LST using MYD11A2 data using the exact urban and rural delineation and ΔT calculation methodology shown in Section 3.5 of Chapter 3. Based on a particular city's date of the Landsat 8 data (as seen in Appendix A), the month for MODIS ΔT for each city was chosen. For example, Landsat 8 LST data for Ahmedabad, India, is from 05/19/2016, so the MODIS ΔT for Ahmedabad uses the LST average for May. MODIS monthly LST for ΔT calculations also helps understand if the Landsat 8 LST from a single day and time represents the month. A normality check of the data using the Ryan-Joiner (similar to Shapiro-Wilk) normality test showed that all the data – ΔT from Landsat8 and MYD11A2 dataset in India and the US during both summers and winters followed a normal distribution (RJ value > 0.97, and p-value > 0.05). A two-sample t-test then compared the ΔT from Landsat 8 and MYD11A2 datasets.

Table 11 shows the results from the two-sample t-test. From these results, with 95% confidence, there is not enough evidence to reject the null hypothesis of $\mu_1 - \mu_2 = 0$, where μ_1 = mean ΔT calculated using Landsat 8 and μ_2 = mean ΔT calculated using MYD11A2. Therefore it is safe to assume that there is no statistically significant difference between Landsat 8 and MYD11A2 calculated daytime ΔT means in India and the US.

Table 11: T value, degrees of freedom, p-values, and the ΔT mean from the two-sample t-test comparing ΔT from Landsat 8 and MYD11A2 datasets.

	T value	P value	μ_1 (^{0}C)	μ_2 (^{0}C)
	India			
Summer	1.0	0.31	-0.9	-0.6
Winter	1.9	0.06	-0.3	0.1
	US			
Summer	1.1	0.27	1.7	1.4
Winter	0.9	0.35	0.7	0.7

5.3 NIGHTTIME URBAN-RURAL LST DIFFERENCE (ΔT)

Nighttime ΔT calculated using MYD11A2 data from 2016, and the urban-rural delineation methodology discussed in Section 3.5 of Chapter 3 showed the SUHI phenomenon in India and the US, as shown in Figure 35. The ΔT calculated using monthly average LST from April and July represent summer in India and the US, respectively. The winter ΔT uses the monthly average LST from January for India and the US. Cloudfree data availability was the highest during these chosen summers and winter months across locations in India and the US. During summers and winters, urban LSTs in India and US were higher than rural LSTs, resulting in SUHI. In India, during both seasons, the ΔT was ≥ 0.0 ^{0}C. However, in the US, 3/32 cities showed negative ΔT (< 0.0^{0}C) during winters.

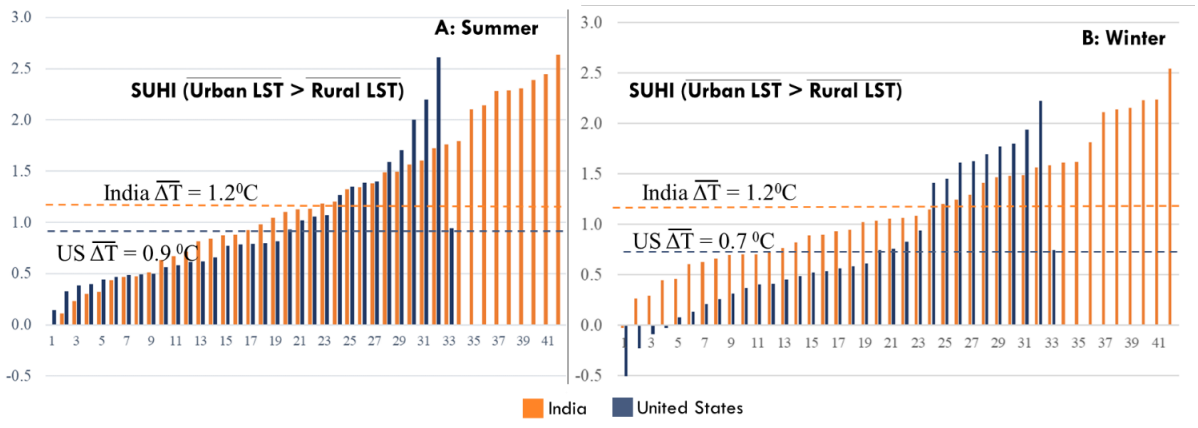

Figure 35: Nighttime ΔT across all India and the US cities during A: Summer and B: winter, showing the SUHI magnitude across the cities.

The $\overline{\Delta T}$ in India, during summer (1.2^0C $\pm0.7^0$C) and winter nights (1.2^0C $\pm0.6^0$C) was greater than the $\overline{\Delta T}$ in the US. The minimum ΔT (0^0C) across Indian cities was in Tiruchirapalli and Coimbatore in summers and winters, respectively. The maximum ΔT of 2.6^0C and 2.5^0C in summers and winters occurred in Jaipur, India. In the US, the $\overline{\Delta T}$ was 1.0^0C $\pm0.6^0$C and 0.7^0C $\pm0.7^0$C during summers and winters, respectively. Minimum ΔT occurred in San Diego (0.1^0C) in the summer and St.Louis (-0.6^0C) in the winter, while the maximum ΔT occurred in Las Vegas(2.6^0C) in the summer and Los Angeles(2.2^0C) in the winter. Overall, while both in India and US clear SUHI exist, the nighttime ΔT seems higher in India compared to the US.

5.4 DIURNAL AND SEASONAL ΔT IN INDIA AND THE US

The summer and winter ΔT analysis was extended to other seasons to understand and compare the day and night variation in ΔT across seasons. Until now, the daytime ΔT analysis used Landsat 8 data discussed in Chapter 3 of this dissertation. The nighttime ΔT analysis shown in Section 5.3 used the MYD11A2 dataset. In this section, the diurnal and seasonal ΔT calculations all use MYD11A2 data (from 2016) to improve the ease of comparison. The ΔT calculation uses the exact urban-rural boundaries and ΔT calculation method from Section 3.6.2. Due to the LST data limitation in India's monsoon season, this analysis does not include the monsoon season. This analysis, therefore, discusses the ΔT calculated for India's summers, winters, and post-monsoon, and the US's spring, summer, autumn, and winter. Table 12 shows the month of analysis and the season it represents in India and the US. The day and night ΔT uses the monthly average LST from the months specified in Table 12.

Table 12: Seasons in India and the US and each season's corresponding months. ΔT is from the average monthly LST of each month specified (MYD11A2 data from 2016)

Season	India	US
Summer	April	July
Winter	January	January
Post-monsoon	November	-
Spring	-	April
Autumn	-	October

Figure 36 shows the diurnal and seasonal ΔT values across cities in India and the US. As seen in the figure, the ΔT values show that during daytime in India, there are several cities with higher rural LSTs compared to urban LSTs (- ΔT values). The mean ΔT of 42 cities in India is close to zero or negative (in summers), indicating the occurrence of daytime surface urban cool islands (SUCI). However, this occurrence of negative ΔT is not common in the US. In the US, the conventional SUHI phenomenon with warmer urban areas compared to rural surroundings exist during both day and night across all the seasons. The $\overline{\Delta T}$ values also show that diurnal differences are higher for cities in India than in the US. The following sections in this dissertation detail these seasonal and diurnal differences in ΔT and provide a statistical discussion of the variations.

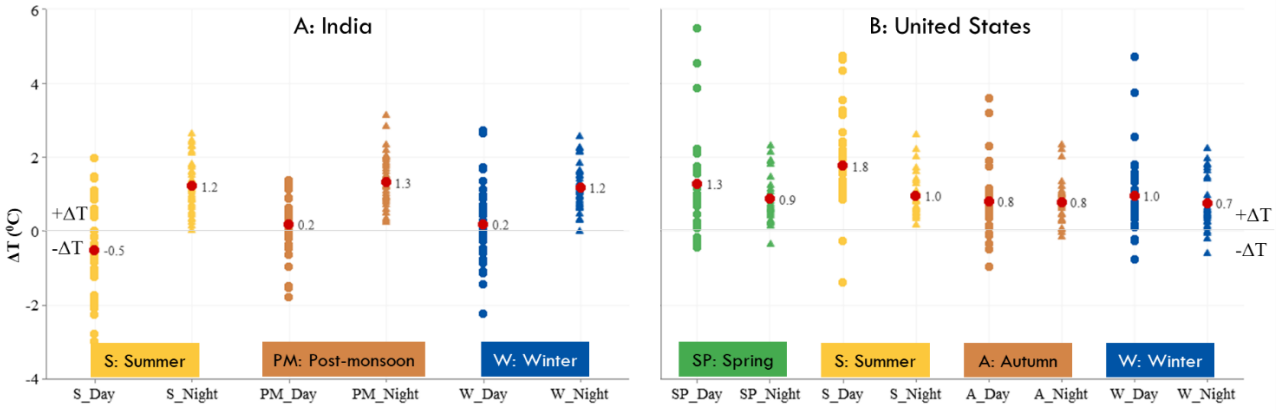

Figure 36: Compares the diurnal and seasonal urban-rural LST difference (ΔT) across cities in A: India and B: United States. In India, daytime ΔT is negative across most cities (urban LST < rural LST). Nighttime ΔT in India is positive (urban LST > rural LST) in all seasons showing SUHI. In the US, irrespective of the time of day, most cities show SUHI. Daytime ΔT is higher in the US; however, nighttime ΔT is higher in India. The diurnal differences in ΔT are higher across Indian cities compared to the US.

5.4.1 Diurnal variation in ΔT

Figure 36 shows seasonal daytime and nighttime ΔT values and the mean ΔT ($\overline{\Delta T}$) across all the cities in India and the US. Table 13 and Table 14 present the descriptive statistics of the day and night ΔT across the different seasons in India and the US, respectively. During the daytime, several cities (35-66% of the cities) in India show negative ΔT values across seasons, indicating warmer rural areas than their respective urban areas, resulting in the SUCI phenomenon. However, at night time in India, the conventional SUHI phenomenon exists. During nights in India the $\overline{\Delta T_{Night}}$ values increased, showing higher urban LSTs compared to rural LSTs, with maximum $\overline{\Delta T_{Night}}$ of 1.3^{0}C during post-monsoon nights, as shown in Table 13. One factor influencing these diurnal ΔT variations could be the LULC characteristics of the rural areas. As seen in Section 4.5.2 of Chapter 4, rural areas in India have non-green croplands, which could heat faster in the daytime with solar radiation and cool faster with the sunset. Section 5.6.2 of this chapter discusses this in more detail. Similarly, in the US, though a few cities (3-4 cities out of 32 cities) show negative ΔT during daytime in all seasons (see Figure 36), this number of cities with negative ΔT is meager (≈12% of the cities) compared to that of India. Therefore, in the US the $\overline{\Delta T_{Day}}$ show SUHI phenomenon across all the seasons, and the nighttime ΔT values were also primarily positive or close to zero showing nighttime SUHI. These results show a more predominant and consistent SUHI phenomenon in the US during daytime and nighttime. In India, though, nighttime SUHI magnitude seems higher than in the US. The nighttime ΔT was higher in Indian cities [0,4] compared to the US cities [0,2.5], which could be indicating differences in urban and rural LULC between India and the US or the higher nighttime anthropogenic effect of urban areas on LSTs in India compared to the US, or both.

Table 13: The mean, minimum, maximum day and night ΔT (in ^{0}C) across different seasons in India.

India						
	Summer		Winter		Post-monsoon	
	Day	Night	Day	Night	Day	Night
# of cities (N)	42	42	42	42	42	42
Mean	-0.5	1.2	0.2	1.2	0.2	1.3
St Dev	1.3	0.7	1.0	0.6	0.8	0.7
Min	-3.0	0.0	-2.2	0.0	-1.8	0.2
Max	2.0	2.6	2.7	2.5	1.4	3.1

Table 14: The mean, minimum, maximum day and night ΔT (in ^{0}C) across different seasons in the US

US								
	Spring		Summer		Fall		Winter	
	Day	Night	Day	Night	Day	Night	Day	Night
# of cities (N)	32	32	32	32	32	32	32	32
Mean	1.3	0.9	1.8	0.9	0.8	0.8	1.0	0.7
St Dev	1.3	0.6	1.6	0.6	1.0	0.6	1.1	0.7
Min	-0.5	-0.4	-3.4	0.1	-1.0	-0.2	-0.8	-0.6
Max	5.5	2.3	4.7	2.6	3.6	2.3	4.7	2.2

This diurnal data was further statistically analyzed. After checking the data for normality, t-tests showed that the diurnal ΔT variation is statistically significant. Figure 37 and Figure 38 show the distribution of ΔT data in India and the US, respectively. For India, a Ryan-Joiner normality test resulted in an RJ value > 0.98 and p-value >0.05 showing that the ΔT data follows a normal distribution in all six scenarios (Summer: day and night, winter: day and day and night, post-monsoon: day and night). Similarly, the ΔT data from the US followed a normal distribution (RJ > 0.96 and p-value>0.05), as shown in Figure 38. The paired t-test showed that, in India, the day-to-night mean ΔT difference is not equal to zero (p value<0.05) in all three seasons. In the US, however, the day-to-night mean ΔT difference is statistically significant (p value<0.05) only during summers. Table 15 presents the results from the t-test.

*Table 15: Results from paired t-test with a null hypothesis (μ_difference = 0): the difference between day and Night ΔT equals zero. The T-value and p-value in cases where the null hypothesis is rejected with 95% confidence are in **bold**.*

	India			US		
	T-value	*P value*	*μ_difference (day-night) in ^0C*	*T value*	*P value*	*μ_difference (day-night) in ^0C*
Summer	**8.34**	**0.00**	**0.7**	**6.02**	**0.00**	**0.9**
Winter	**5.16**	**0.00**	**1.0**	0.1	0.92	0.3
Post-monsoon	**6.33**	**0.00**	**1.1**	-	-	-
Spring	-	-	-	1.8	0.09	0.4
Fall	-	-	-	0.32	0.75	0.0

With 95% confidence, the null hypothesis (μ_difference = 0, where μ_difference is the difference between $\overline{\Delta T_{Day}}$ and $\overline{\Delta T_{Night}}$) was rejected in India during all seasons showing statistically significant variation in day and night ΔT. In the US, with 95% confidence, the null hypothesis (μ_difference = 0, where μ_difference is the difference between $\overline{\Delta T_{Day}}$ and $\overline{\Delta T_{Night}}$) was rejected only during summers. The differences in LULC characteristics between India and the US could lead to differences in diurnal ΔT variations between India and the US. Therefore, day and night variations in ΔT are more significant in India compared to the US.

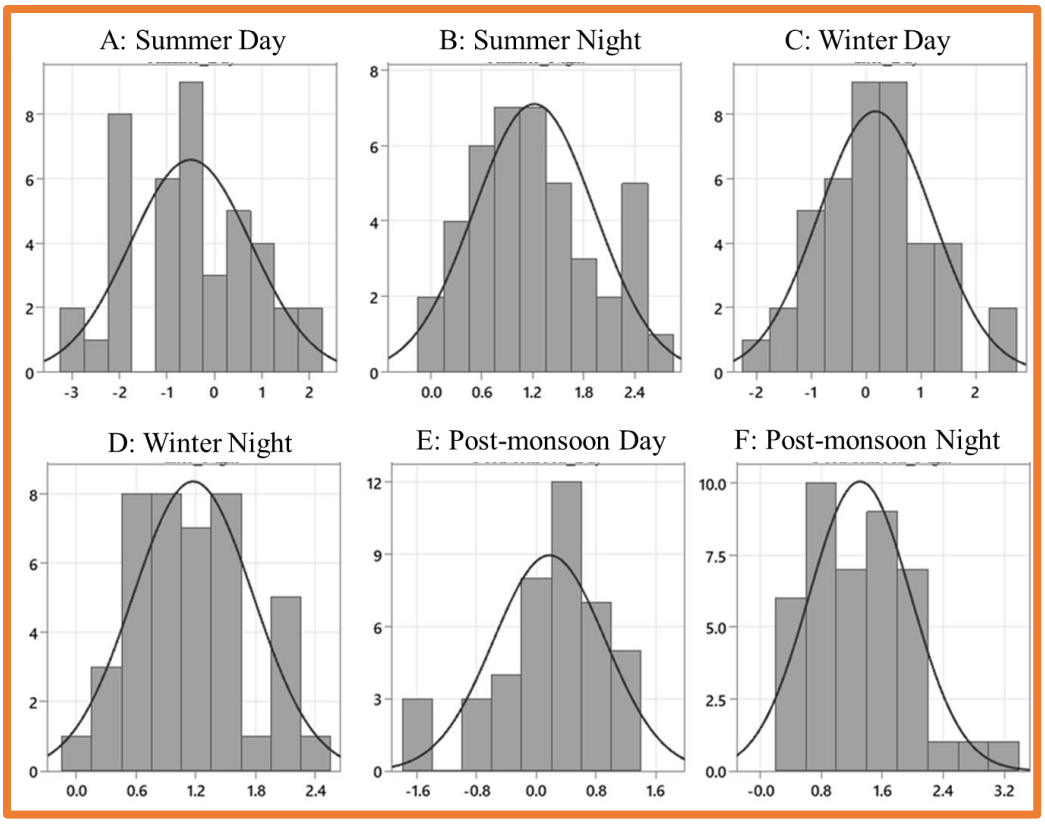

Figure 37: ΔT data distribution during A. Summer day, B.Summer night, C: Winter day, D: Winter night, E: Post-monsoon day, and F: Post-monsoon Night in India

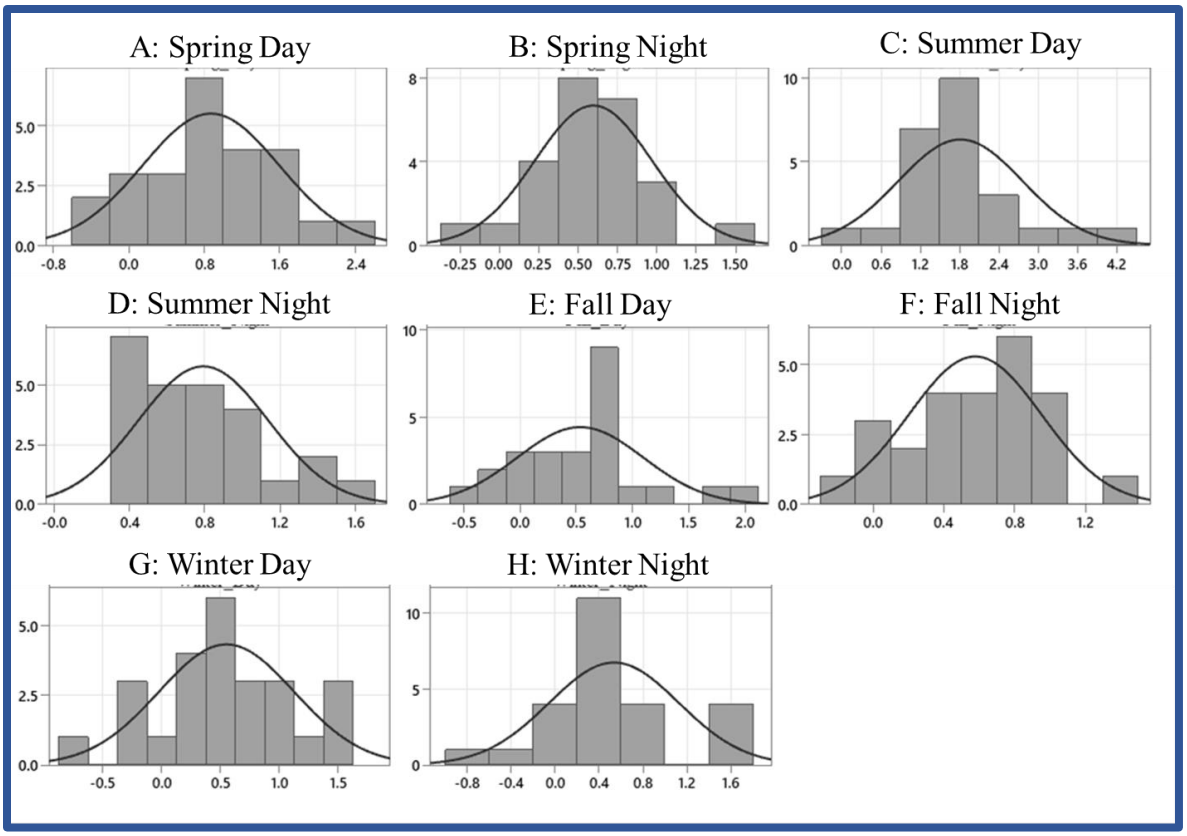

Figure 38: ΔT data distribution during A: Spring Day, B: Spring Night, C: Summer Day, D: Summer Night, E: Fall Day, F: Fall Night, G: Winter Day, and H: Winter Night in the US.

5.4.2 Seasonal variation in ΔT

In India, the mean daytime ΔT ($\overline{\Delta T_{Day}}$) values and range [-0.5, 0.2] are small (see Figure 36) across the seasons, indicating lesser differences between urban and rural LSTs. The daytime ΔT values are positive and higher during post-monsoon ($\overline{\Delta T_{Day}} = 0.2^0C$) and winters ($\overline{\Delta T_{Day}} = 0.2^0C$) compared to the summers ($\overline{\Delta T_{Day}} = -0.5^0C$), as seen in Table 13. Also, the number of cities showing daytime SUCI phenomena is lowest in post-monsoon (15/42), followed by winters (17/42) and summers (28/42). Cities with SUCI in both post-monsoon and winters are a subset of the 28 cities with SUCI during summers. In the US, the seasonal variation in daytime ΔT is more

prominent. The ΔT is highest during summer ($\overline{\Delta T_{Day}} = 1.8^0C$), followed by spring ($\overline{\Delta T_{Day}} = 1.3^0C$), winters ($\overline{\Delta T_{Day}} = 1.0^0C$), and autumn ($\overline{\Delta T_{Day}} = 0.8^0C$), as shown in Table 13. The cities showing negative ΔT (refer to Figure 36) are more in autumn (5/32) compared to the rest of the seasons (3 or 4/32), though the magnitude of SUCI is low (< -1.0^{0}C). As seen in the case of India, the non-green vegetation and low soil moisture could impact ΔT during autumn in the US. Nighttime ΔT ranges were consistent across seasons in India [0,3.0] and the US [0,2.6]. Nighttime mean ΔT were also similar across the seasons in both India (summer, winter $\overline{\Delta T_{Day}} = 1.2^0C$, and post-monsoon $\overline{\Delta T_{Day}} = 1.3^0C$) and the US [0.7,1.0].

A one-way ANOVA test showed the effect of season on mean ΔT. Figure 37 and Figure 38 from Section 5.4.1 show the normal distribution of the data. Results, as seen in Table 16, show statistically significant (p-value < 0.05) variation in seasonal daytime ΔT means (refer to Table 13 and Table 14) in both India and the US. However, there is no statistically significant difference in nighttime ΔT means across seasons in India and the US. Table 16 shows the results from the ANOVA test for the daytime. These seasonal differences in ΔT only in the daytime might indicate that the thermal characteristics of different LULC types vary with seasons only in the presence of solar radiation. With 95% confidence, the null hypothesis (all means are equal) is rejected during the daytime but not at nighttime.

Table 16: Results from the ANOVA test show that the difference in mean daytime ΔT across seasons is statistically significant in India and the US.

	F value	P value
India	6.07	0.003
US	17.58	0.000

Furthermore, a paired t-test comparing daytime ΔT from two seasons shows no statistically significant (p-value <0.05) difference between winter and post-monsoon daytime ΔT in India and between winter and fall daytime ΔT means in the US. With 95% confidence, the null hypothesis of μ_difference = 0, where μ_difference: population means of (Winter Daytime – PostMonsoon Daytime) in India cannot be rejected. Similarly, with 95% confidence, the null hypothesis of μ_difference = 0, where μ_difference: population means of (Fall Daytime – Winter Daytime) in the US, cannot be rejected. These t-tests, therefore, show the similarity in the daytime ΔT means between winters and post-monsoon in India and fall and winters in the US.

The diurnal and seasonal variations in ΔT show the dynamic nature of this phenomenon and how the factors influencing it can vary with the time of the day and season. Though seasonal understanding of ΔT and the factor influencing it is helpful, for India-US comparisons, summers and winters are the focus of this dissertation.

5.5 THE DIFFERENCE IN ΔT BETWEEN INDIA AND THE US

Figure 36 shows that ΔT and its mean differ in India compared to the US. A two-sample t-test confirmed this statistically significant difference in mean ΔT between India and the US. All the data follows a normal distribution, as shown in Figure 37 and Figure 38 and discussed in Section 5.4.1. With 95% confidence, the null hypothesis ($\mu_1 - \mu_2 = 0$) is rejected during daytime and nighttime, both in summer and winter. Table 17 and Table 18 show the results from the two-sample t-tests from daytime and nighttime, respectively.

Table 17: Results from two-sample t-tests showing statistically significant difference in daytime ΔT means from India and the US

	T value	P value	$\overline{\Delta T}$_India (μ_1) in ^{0}C	$\overline{\Delta T}$_US (μ_2) in ^{0}C
Summer	6.64	0.000	-0.5	1.8
Winter	3.09	0.003	0.2	1.0

Table 18: Results from two-sample t-tests showing statistically significant difference in nighttime ΔT means from India and the US

	T value	P value	$\overline{\Delta T}$_India (μ_1) in ^{0}C	$\overline{\Delta T}$_US (μ_2) in ^{0}C
Summer	2.3	0.025	1.2	0.9
Winter	2.78	0.007	1.2	0.8

From these results, it is safe to conclude that the ΔT means of India and the US are not the same and that the mean nighttime ΔT in India is higher than in the US. India and US have different ΔT trends that may be associated with the differences in LULC and urbanization trends.

5.6 THE LULC AND THE DAY-NIGHT VARIATION IN ΔT

5.6.1 Overview

Chapter 4 of this dissertation discussed how ΔT, LST, and the spectral indices values changed with LULC (see Table 10). The prevalence of non-green and unsaturated croplands in rural areas of India seems to result in negative ΔT – SUCI phenomenon during daytime (refer to Section 4.2). The LULC of India and the US are revisited in this chapter to understand how they impact the day and night variation in ΔT. The thermal performance analysis of different Land Use Land Cover (LULC) types in India, and the US explains the diurnal variation in ΔT. Further, correlations discuss the association between the LULC areas and ΔT.

5.6.2 LULC characteristics

As in the case of canopy-level air temperatures, the time of measurement of LST might make a difference in ΔT, and it is essential to understand how surfaces perform at a given time. SUCI is most common across some of the tropical and dry locations of the world (Rasul, Balzter, and Smith 2015, Ibrahim 2017, Ali, Marsh, and Smitha 2017, Kumar et al. 2017, Zareie et al. 2016). A few prior studies showed its occurrences even in some parts of the US (Imhoff et al. 2010, Zhao et al. 2014, Li et al. 2019, Chow and Svoma 2011). Results from this work align with prior research (Kumar et al., 2017) in observing daytime SUCI and nighttime SUHI in India.

The LULC of India is different compared to the LULC of the US (see Figure 17 in Section 3.4 in Chapter 3). Rural areas in India are croplands, whereas, in the US, the rural areas include dense forest vegetation across many locations. Figure 39 shows the urban and rural boundaries overlayed on the LULC map of a typical Indian (Hyderabad) and a US (Houston) city. Figure 40 shows the percentage of croplands in rural areas across cities in India and the US. Figure 39 and Figure 40 show that US rural areas have fewer croplands than Indian rural areas. In this study, on average, rural areas of India are 77% of cropland, whereas, in the US, 19% of the rural area is cropland.

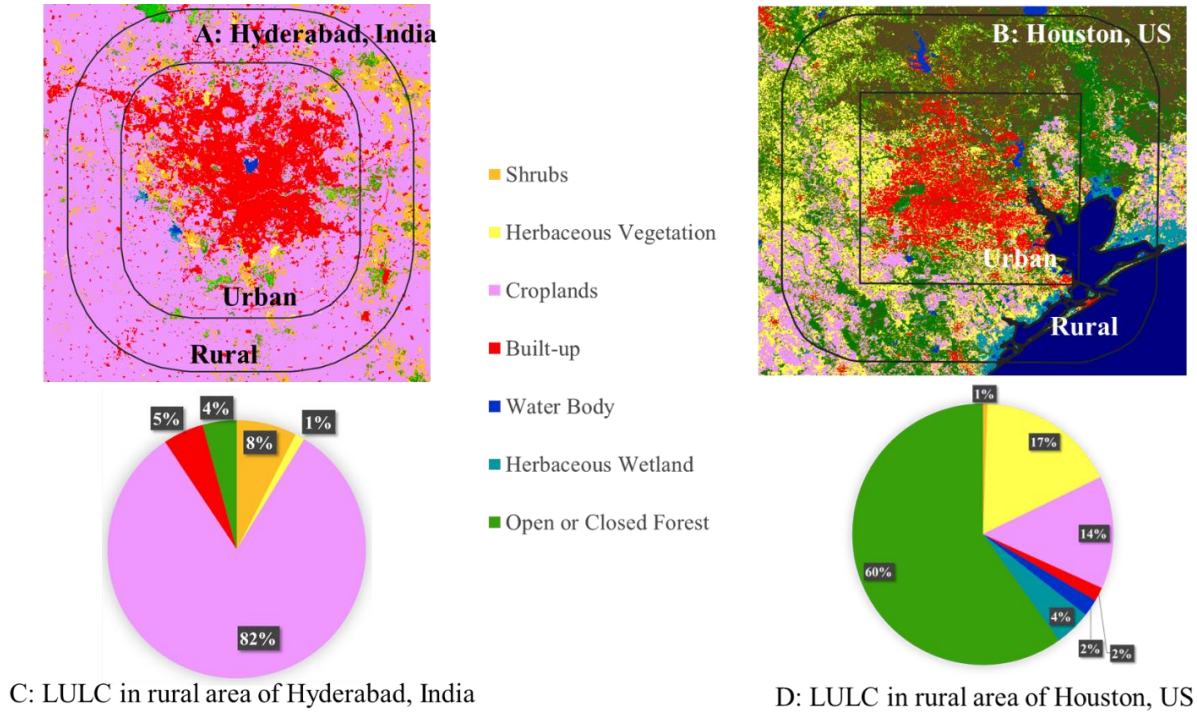

Figure 39: Land Use Land Cover (LULC) within the urban and rural boundaries of A: Hyderabad, India, and B: Houston, US. The LULC stats within the rural boundaries of C: Hyderabad, India, and D: Houston, US, show 82% of rural Hyderabad is cropland and 60% of rural Houston is forested.

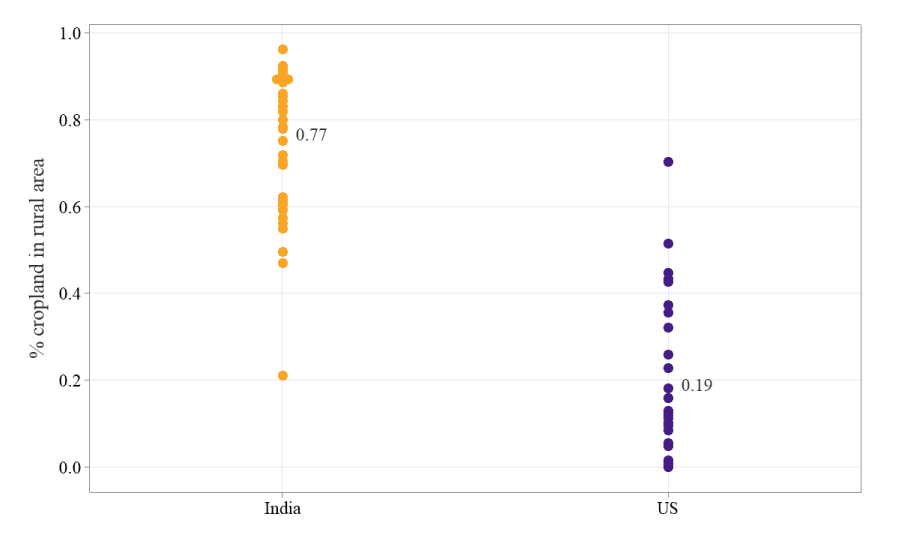

Figure 40: The percentage of cropland land use type in the rural areas of cities in India and the US. The % cropland in rural areas averages 77% and 19% in India and the US, respectively.

As discussed in Chapter 4, the croplands in India are seasonal and irrigation dependent. The soil type varies, and saturation level could be low, especially during summers and winters, the non-monsoon seasons across most of the country. Table 19 lists and compares the thermal characteristics of the standard surface material types in the urban and rural areas of India and the US and the variation in their performance with the time of the day (refer to Appendix B for the thermal properties of the conventional LULC material types). As discussed in Section 4.5.2.3 of Chapter 4, rural India tends to gain heat quickly with sunrise and lose heat quickly with sunset; however, the green vegetation in the rural US stays at a relatively constant temperature throughout the day. With all the tree canopy, the heat loss from rural US happens slower than in rural Indian areas and could lead to lower nighttime ΔT compared to India. These variations in the thermal performance of different LULCs lead to differences in ΔT between India and the US, as shown in Table 19. A correlation analysis further showed if and how the LULC type links to ΔT.

Table 19: Standard materials that constitute Indian and US urban and rural areas, and the variation in their thermal performance with the time of the day

	India		US	
	Urban	**Rural**	**Urban**	**Rural**
Material type	Concrete, glass, asphalt, brick	Peat, clay, or sandy soils – unsaturated during summers and winters	Concrete, glass, asphalt, brick, wood	Saturated soils, swamps, wooded forests
Thermal characteristics	Thermal admittance is greater than rural	Lowest thermal admittance across all other material compared here	Thermal admittance is lower than in rural	Highest thermal admittance
Heat transfer	**DAY:** Heat gain at a lower rate compared to rural **NIGHT:** Heat loss at a lower rate compared to the rural	**DAY:** Heat gain happens quickly with radiation **NIGHT:** Tends to lose heat immediately after sunset	**DAY:** Heat gain at a higher rate compared to rural **NIGHT:** Heat loss at a faster rate compared to the rural	Heat gain is prolonged, and so surfaces are lower temperatures compared to urban areas
Variation across the day	High variation in surface thermal performance with the time of the day		Low variation in surface thermal performance with the time of the day in rural areas	
Temperatures	**DAY:** Urban LST < Rural LST **NIGHT:** Urban LST > Rural LST		**DAY:** Urban LST > Rural LST **NIGHT:** Urban LST > Rural LST	
Urban-Rural Temperature Differences (ΔT)	**DAY: -ΔT** **NIGHT: +ΔT**		**DAY: +ΔT** **NIGHT: +ΔT**	

5.6.3 Rural and Urban LULC, and ΔT: A correlation analysis for India

A Spearman's correlation between the percentage of croplands in rural areas of India and the ΔT showed that the amount of cropland in rural areas does not impact the daytime ΔT. However, during nighttime, there is a statistically significant (p-value<0.05) correlation between the percentage of cropland and ΔT, as seen in Figure 41. The Spearman's correlation shows a moderately positive correlation between % cropland and nighttime ΔT in summers(r_s= 0.44) and winters (r_s= 0.33) in India. As the % of cropland land use increases in rural areas, the nighttime ΔT increase. These results support the theory discussed in Section 5.6.2. Rural areas in India lose heat faster and reach lower LSTs in the nighttime, increasing the difference between urban and rural LSTs (higher nighttime ΔT). Daytime, a statistically significant (p-value<0.05) correlation exists between the 'greenness' of the rural areas and ΔT, as seen in Figure 42. This correlation is stronger than those observed between ΔNDVI and ΔT (refer to Section 4.4) or NDVI and LST (Section 4.3.1). Based on these correlations, in India, daytime and nighttime ΔT has a stronger correlation with the 'greenness' of rural areas and not the greenness in urban areas.

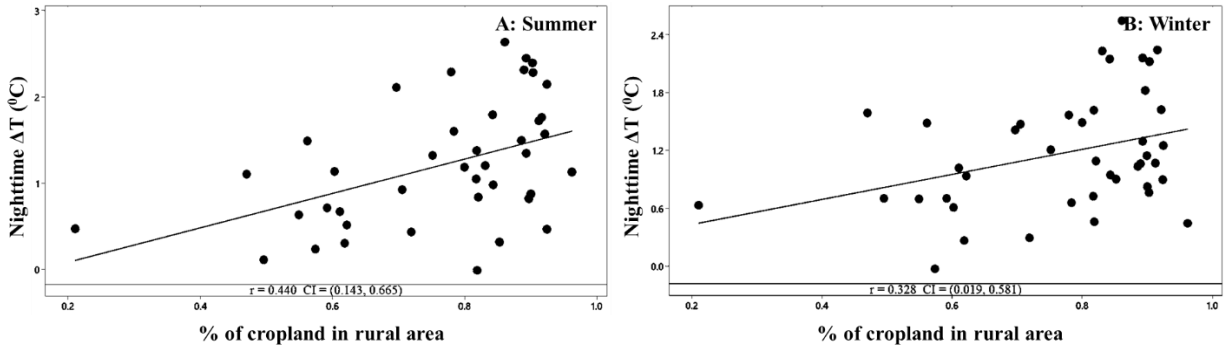

Figure 41: Spearman's correlation between % cropland in a rural area and nighttime ΔT (^{0}C) in India during A: Summers and B: Winters

Figure 42 shows Spearman's correlation between NDVI (the higher the value, the greener the vegetation) of the rural areas and ΔT. As seen in Figure 42, during the daytime, a moderate to

strong positive correlation exists between rural NDVI and ΔT in both summers (r_s = 0.63) and winters (r_s = 0.4). Therefore, when rural area greenness increases, the actual impact of urban areas on ΔT appears. Higher LSTs in urban areas are apparent compared to green rural areas, increasing the daytime ΔT. Lack of greenness in rural areas in India, therefore, masks the impact of urban areas on ΔT, deceptively showing them cooler. During the nighttime, although a statistically significant correlation (p-value <0.05) exists, the strength of the correlation decreases both during summers (r_s = -0.35) and winters (r_s = -0.39) and is negative. So, when the rural area greenness increases, these rural areas are warmer than non-green rural areas, decreasing the difference between urban-rural LST (nighttime ΔT). These correlations from India can also explain the observed ΔT trends in the US. Since rural areas are greener in the US, the daytime difference between urban-rural LST is higher (high ΔT), and the nighttime difference between urban-rural LST is low (lower ΔT).

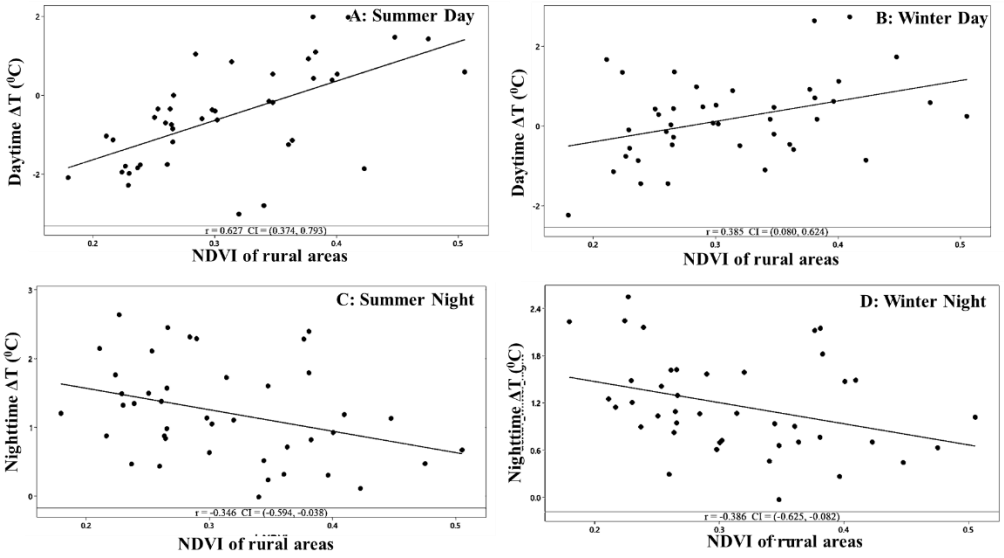

Figure 42: Spearman's correlation between NDVI in rural areas and ΔT during A: Summer days, B: Winter days, C: Summer nights, and D: Winter nights. When NDVI in rural areas increases at night, the ΔT decreases since green rural areas lose heat slower and stay at a higher LST than non-green rural areas. During the daytime, as NDVI increases in rural areas, ΔT increases, showing the actual impact of urban built-up areas of ΔT.

However, all these show how a 'rural' area impacts ΔT and don't provide insight into how the urban built-environment impacts ΔT. Furthermore, it shows the need for a standardized definition of rural areas to estimate ΔT across multiple cities and develop suitable regional and national policies to mitigate UHI. Despite the importance of 'rural' in ΔT trends, urban built-up areas significantly impact ΔT. Figure 43 shows Spearman's correlation between the percentage of built-up land use within an urban area and ΔT. There is a statistically significant (p-value <0.05) correlation between % of built-up areas within the urban areas and ΔT, and it is always positive. As the amount of built-up land use increased, the ΔT increased. In the daytime, these correlations are weak to moderate in summers (r_s= 0.3) and winters (r_s= 0.34). During the nighttime, the correlation strength increased compared to the day in both summers (r_s= 0.38) and winters (r_s= 0.46). Unlike the built-up indices used in Chapter 4 that come with limitations in representing built-up areas, these correlations show that as built-up areas increase, the ΔT increase.

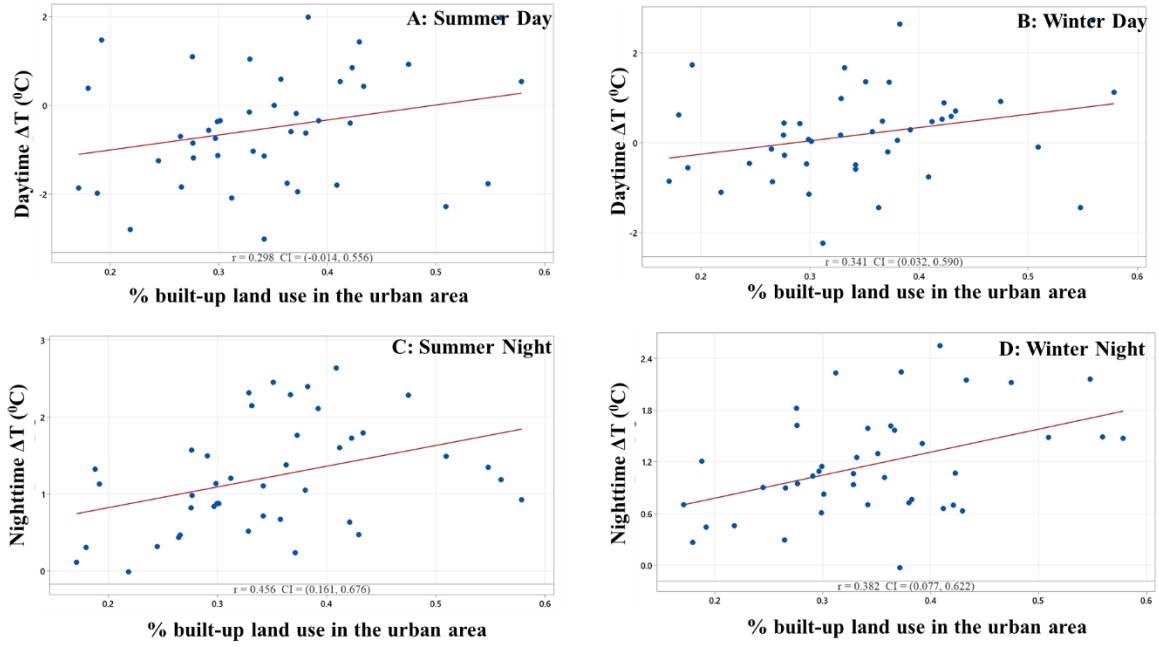

Figure 43: Spearman's correlation between the percentage of built-up land use type within the urban area and ΔT in A: Summer days, B: Winter Days, C: Summer Nights, D: Winter Nights. ΔT increased as the percentage of the built-up area within the urban area increased.

5.7 CONCLUSION

Some key observations from this analysis are 1.)The nighttime ΔT is positive in India and the US, resulting in SUHI, unlike during daytime when SUCI exists across most cities in India. 2.)The magnitude of nighttime SUHI is higher in India compared to the US, and there is a statistically significant difference in ΔT means of India and the US during all seasons and day and night. 3.) Diurnal variation in ΔT is predominant in India across all the seasons and only observed during summers in the US. Peak summers in the US, when the urban built-up areas are heated and hold on to heat compared to the rural green areas, could result in summer ΔT variations. During other seasons in the US, the snow cover, leaf cover, and non-green rural areas could all impact ΔT. 4.)While there was a statistically significant difference in daytime ΔT means across seasons in India and the US, the nighttime ΔT means were not statistically different across seasons. The urban-rural LULC differences between India and the US impact the ΔT and its variation.

The diurnal variation in ΔT is associated with the non-green croplands and the urban built-up land use in India. A larger cropland area in a rural and a larger built-up area in an urban both mean higher nighttime ΔT in a city. However, while the cropland area relates with the nighttime ΔT, it does not significantly impact daytime ΔT. Daytime ΔT correlates with the NDVI in the rural areas and the % of the built-up area within the urban. As the NDVI of rural areas increases, the variation in rural LST between day and night decreases, resulting in lower ΔT during nighttime, as seen in the US. Therefore, this analysis indicates that the lack of green rural areas in India, compared to the US, impacts ΔT diurnal variation. However, the % urban built-up land use explains at least 30% of the variation in ΔT in India during summers and winters' day and night.

6 TEMPORAL CHANGE IN SURFACE URBAN HEAT ISLAND MAGNITUDE

6.1 OVERVIEW

While the diurnal analysis in Chapters 4 and 5 of this study showed the variation in LST and SUHI/SUCI, a temporal analysis of ΔT could show the change in ΔT with the increase in built-up land use (urbanization) over time. Today, more than 50% of the world's population lives in urban areas. An increase in urbanization also means an increase in built-up areas. Section 4.6.3 of Chapter 4 shows that the built-up area land use positively correlates with ΔT. This chapter discusses the increase in built-up land use over 15 years quantified using the GAIA dataset and its correlation with SUHI. Section 3.7.3 of Chapter 3 describes the Global Artificial Impervious Area (GAIA) dataset (Gong et al., 2020) used in this study. The change in ΔT over 15 years is statistically analyzed and correlated with the %ISA within an urban area. With the relatively recent availability of remote sensing data with high spatial and temporal resolution (refer to Section 2.4.2 of Chapter 2), the knowledge of historical and inter-annual variability of SUHI is scant(D. Zhou et al., 2018). However, global temporal studies using remote sensing data have recently gained prominence(T. Chakraborty & Lee, 2019; Z. Liu et al., 2022). This chapter presents the impact of urbanization on SUHI over the recent years and how comparable it is in a rapidly urbanizing country India and a more developed nation, the US. SUHI is quantified using MYD11A2 data and the urban and rural delineation and ΔT calculation method detailed in Section 3.5 of Chapter 3.

This study compared the ΔT (Mean Urban LST – Mean Rural LST) from two different periods instead of the LSTs to control the impact that climate change and weather would have on

temperatures over the years. Further, to minimize the effect of weather anomalies on ΔT, a 5-year average LST of 2003-2007 and 2018-2022 was used to calculate ΔT in the 15-year interval. Throughout this chapter, the average ΔT of 2003-2007 is ΔT_{2003}, and the average of 2018-2022 is ΔT_{2018}. Summer and winter ΔT for two different periods 15 years apart explain the seasonal inter-annual change in ΔT. Summers are average April and May for India and July and August for the US (refer to Section 3.2.2.1 of Chapter 3 for seasons). Winter represents the average LST from January and February for both India and the US.

6.2 CHANGE IN IMPERVIOUS SURFACE AREA (ISA) OVER 15 YEARS

As the name suggests, unlike vegetation or most natural soils, the impervious surface area represents surfaces that do not let water penetrate. The impervious surface areas, therefore, primarily represent the built-up areas. Hence, the %ISA has been one of the most widely used variables to understand the impact of built-up areas on SUHI (Imhoff et al., 2010; Mathew et al., 2019; D. Zhou et al., 2018). In this study, the impervious surface areas within the cities in India and the US were quantified using the annual GAIA dataset (refer to Section 3.7.3 of Chapter 3) available for 30 years (1985-2018) (Gong et al., 2020). Figure 44 shows the percentage increase in ISA within the urban boundaries (as discussed in Section 3.5 of Chapter 3) from 2003 to 2018 across cities in India and the US. This plot in Figure 44 shows that the increase in %ISA within the urban areas is higher in India compared to the US. The maximum increase in ISA is 150%(Pune, India) in India compared to 60% (Jacksonville, US) in the US over 15 years. The minimum increase in ISA is 22% (Amritsar, India) in India compared to 4% (Los Angeles, US) in the US. On average, the increase in ISA over the 15 years is 68% in India and 29% in the US. Therefore, understanding how ΔT changed over the 15 years and correlating it with the %ISA could provide insight into how urbanization impacts ΔT.

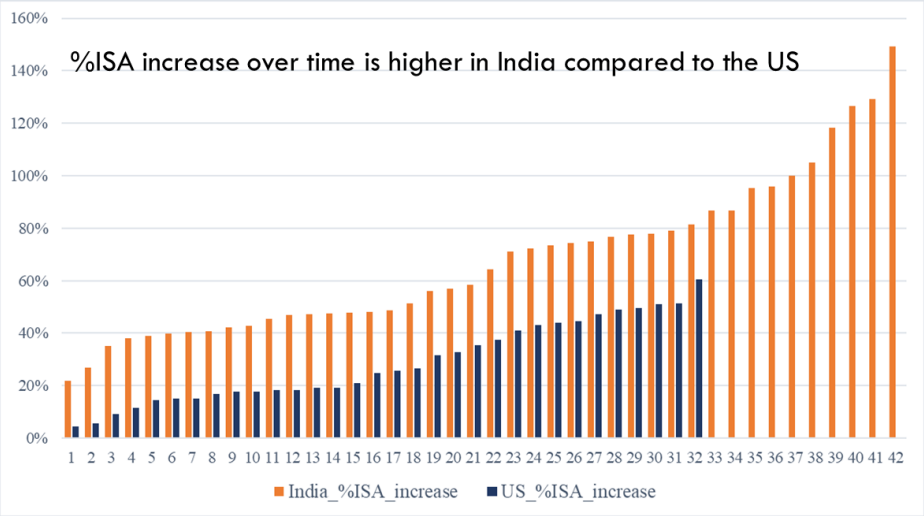

Figure 44: The percentage increase in ISA from 2003 to 2018 across India and the US cities. The average increase in ISA across Indian cities is 68% compared to 29% in the US.

One way to visualize the urbanization trends in India and the US is to see the ISA maps of example cities from India and the US. Figure 45 shows the ISA maps of one big city each from India (Hyderabad, India, with > 10 million population) and the US (Chicago, US, with > 9 million population). In Hyderabad, India, there is a 58% increase in the ISA over 15 years compared to 33% in Chicago. Figure 45 visually explains the urban expansion pattern and intensity across these cities. As seen in Figure 45, while Hyderabad city is expanding outwards, in Chicago, there seems to be a change in land use also within the urban region. This difference in ISA increase patterns provides an insight into each city's existing landscapes and built-up densities. Densely built-up cities in India with no scope to build within the city boundaries start to expand outwards. However, like many other US cities, non-ISA spaces within the urban region could be converted into built-up areas, as seen in Chicago. Section 7.2.5 of Chapter 7 discusses more on these urbanization patterns and how they might impact LSTs.

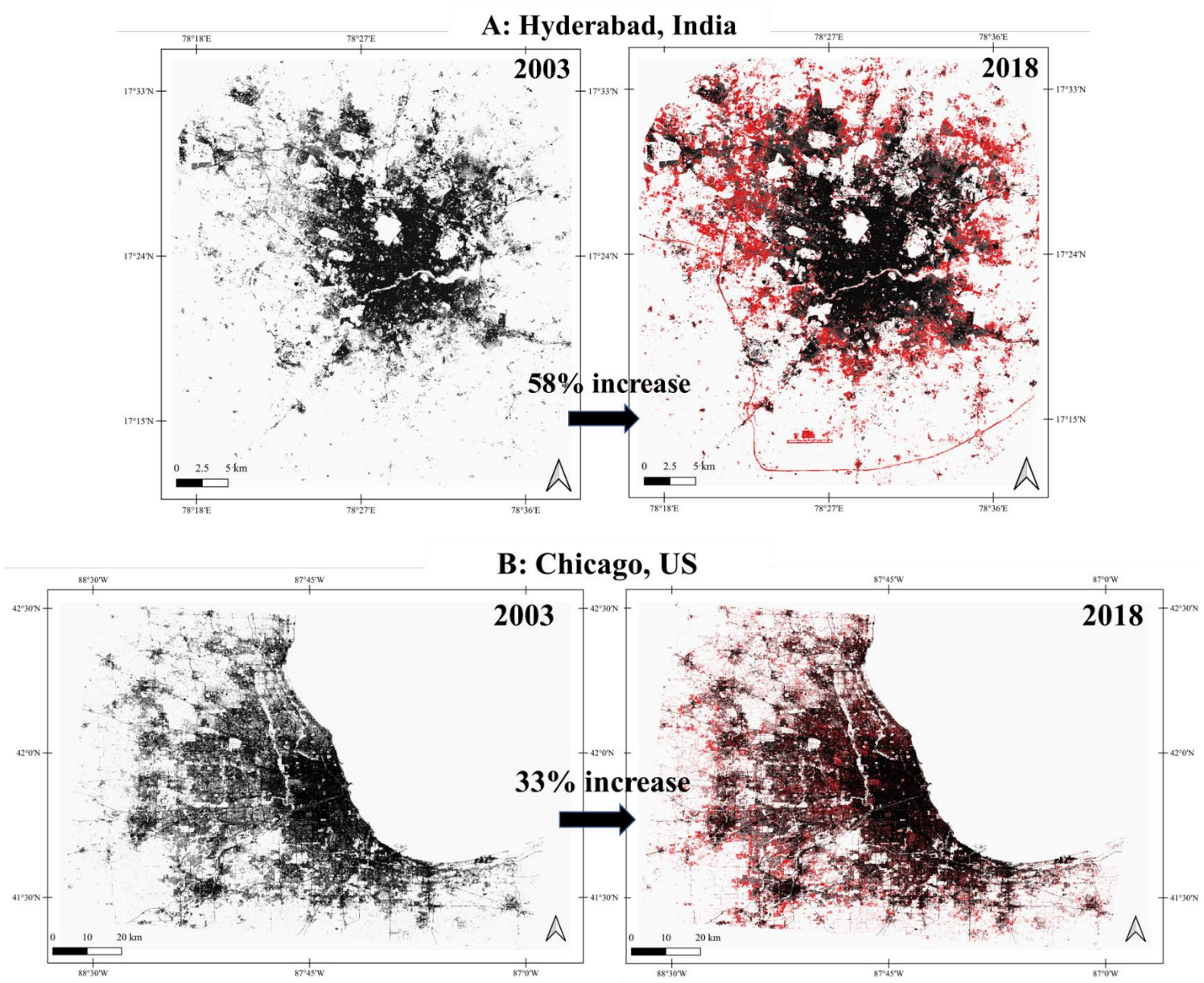

Figure 45: Impervious surface area in A: Hyderabad, India, and B: Chicago, US, 2003 and 2018 (new impervious surface areas after 2003 shown in red). The ISA increased by 58% in Hyderabad, India, and 33% in Chicago, US, over the 15-year

6.3 CHANGE IN ΔT OVER 15 YEARS

The surface urban heat island magnitude (ΔT) for 2003 and 2018 was calculated for all cities in India and the US using the 5 years average LST mentioned in Section 6.1. Figure 46 shows the ΔT difference (ΔT_{2018}- ΔT_{2003}) in summers and winters during daytime and nighttime across India and the US cities. As seen in the figure, the difference in ΔT is positive across most cities during all time, indicating higher ΔT in 2018 than in 2003. During the daytime, though a few cities (12/42 in India and 7/32 in the US) showed higher ΔT in 2003, mean ΔT shows an increase in ΔT over the 15 years. During the nighttime in India, the increase in ΔT over the 15 years is more pronounced, as seen in Figure 46B. Overall, the average ΔT change over the 15 years shows an increase in ΔT in India and the US.

6.3.1 Change in ΔT in India.

The ΔT from 2003 is statistically compared with ΔT from 2018 using paired t-test. Table 20 presents the results from the paired t-test for India. The paired t-test results show a statistically significant (p-value < 0.05) difference between the mean ΔT of 2018 and 2003 in the nighttime of summers and daytime and nighttime of winters. Therefore, except during summer daytime, the null hypothesis (μ_difference = 0, where μ_difference = mean(ΔT_{2018}- ΔT_{2003})) can be rejected with 95% confidence, indicating ΔT changed over time. As seen in Table 20, the mean ΔT values show an increase in ΔT over time in India. This ΔT increase during summer nighttime is 0.30 ± 0.19^0C (mean ± one standard deviation) and is highest compared to winter daytime (0.23 ± 0.44^0C) and winter nighttime (0.27 ± 0.17^0C).

These results align with observations from a recent study(Mohammad & Goswami, 2021) from India. The study showed that ΔT increased in a few cities in the daytime while decreasing in others;

however, in the nighttime, ΔT increased across most of the 150 cities studied. However, this study focused on the annual trend of ΔT over time and did not quantify the change in ΔT. Another global temporal study(Z. Liu et al., 2022) that quantified the decadal increase in LST showed that urban core LSTs increased at 0.50 ± 0.20 K·per decade and showed the background climate change to be the most significant contributor. Although, 5% of the studied locations, mainly from China and India, showed a 0.23 K per decade increase in urban core LST due to urban expansion. This study also showed a global mean SUHI increase of 0.16 ± 0.093 K per decade during the day and 0.060 ± 0.033 K per decade at night and noted a decrease in ΔT in some north Asian locations. However, it is essential to note that though the mentioned study uses the same MYD11A2 LST data as used in this study, the ΔT change mentioned is a global average (for 2000 urban clusters) and was quantified differently than in this study. The key observation from this study mentioned is that the urban core areas are warming more than the rural surroundings, and global SUHI is increasing with time. Studies like these show the need to understand how urban built-up areas impact temperatures and how urban built environment needs to be modified to mitigate the UHI phenomenon.

Table 20: Results from paired t-test show a statistically significant difference between ΔT mean of 2018 and 2003 in India, except during summer daytime.

	T value	P value	Mean $\Delta T_{(2018)}$	Mean $\Delta T_{(2003)}$
DAYTIME				
Summer	Not significant		-0.36	-0.44
Winter	3.36	0.002	0.41	0.18
NIGHTTIME				
Summer	9.8	0	1.09	0.80
Winter	10.43	0	1.24	0.96

6.3.2 Change in ΔT in the US

Paired t-tests show the statistical significance of the ΔT change over the years. Table 21 shows the results from the paired t-test for the US. The difference in mean ΔT between 2018 and 2003 is statistically significant (p-value <0.05), except during winter nighttimes. Therefore, except for the winter nighttime, the null hypothesis (μ_difference = 0, where μ_difference = mean(ΔT_{2018}-ΔT_{2003}) can be rejected with 95% confidence. As seen in Table 21, there is an increase in the ΔT means from 2003 to 2018. The ΔT increase during summer daytime is 0.14 ± 0.28 ^{0}C, during the summer nighttime is 0.06 ± 0.15^{0}C, and in the winter daytime is 0.15 ± 0.29^{0}C. This daytime higher increase in ΔT observed in this study across the US is similar to the temporal change in ΔT observed in prior literature(T. Chakraborty & Lee, 2019; Z. Liu et al., 2022). However, these studies mentioned above are global studies with different sample sizes and ΔT calculation methods compared to this study. Therefore, though the overall trends in temporal changes in ΔT align, the absolute values cannot be compared. One of these studies (T. Chakraborty & Lee, 2019) used urban extent data that did not match the LST and SUHI analysis year. Such differences could underestimate the ΔT and the impact of built-up areas, especially in locations with recent rapid development, like India. More literature on this is in Section 2.5.1 of Chapter 2.

Table 21: Results from paired t-test show a statistically significant difference between ΔT mean of 2018 and 2003 in the US, except during winter nighttime.

	T value	P value	Mean $\Delta T_{(2018)}$	Mean $\Delta T_{(2003)}$
DAYTIME				
Summer	2.75	0.01	1.73	1.59
Winter	2.87	0.007	1.20	1.06
NIGHTTIME				
Summer	2.07	0.047	0.87	0.81
Winter	Not significant		0.56	0.49

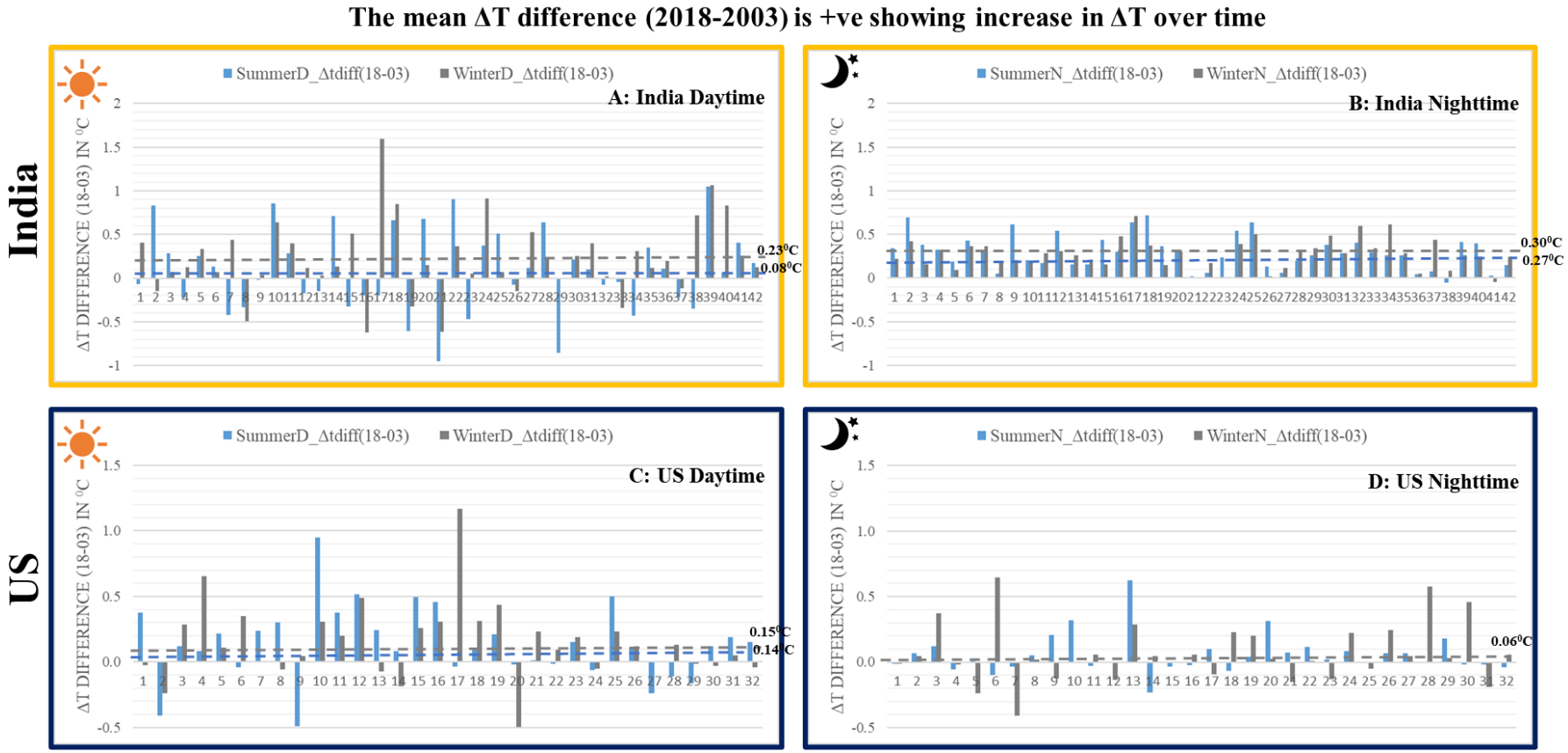

Figure 46: The ΔT difference (ΔT 2018 - ΔT 2003) in summers and winters during daytime and nighttime across India and the US cities. In all the cases – Summer daytime, winter daytime, summer nighttime, and winter nighttime, there is an increase in ΔT over the 15 years in India and the US. The increase in ΔT is more consistent across cities in India during the nighttime than daytime or the nighttime in the US.

6.3.3 Comparison of India and the US: Change in ΔT in 15 years

Table 20 and Table 21 show that the change ΔT from 2003 to 2018 is higher in India than in the US. The nighttime and the winter daytime increase in ΔT in India seem higher than in the US. However, only the nighttime ΔT difference between India and the US was statistically significant. The average nighttime ΔT increase is higher in India than in the US by ≈ 0.2^0C. A two-sample t-test comparing this increase in ΔT in India and the US showed a statistically significant (p-value <0.05) difference between the ΔT increases in India and the US during the nighttime. During the daytime, this difference is statistically insignificant. As shown in Table 22, with 95% confidence, the null hypothesis (μ1-μ2=0; where μ1= ΔT change in India and μ2 = ΔT change in the US)can be rejected.

Table 22: Two-sample t-test results show statistically significant differences between India and the US in the nighttime ΔT change.

		T value	P value	Mean ΔT Change in India over 15 years (2018-2003)	Mean ΔT Change in the US over 15 years (2018-2003)
Summer	Day	Statistically insignificant		0.08	0.14
	Night	5.96	0.000	0.296	0.055
Winter	Day	Statistically insignificant		0.23	0.14
	Night	4.35	0.000	0.274	0.065

6.4 CORRELATION BETWEEN %ISA AND ΔT

An increase in city size increases SUHI (Imhoff et al., 2010). The built-up area land use positively correlates with ΔT in India (see Figure 43). Similarly, a statistically significant (p-value <0.05) positive correlation exists between %ISA and nighttime ΔT in India and the US (only in summer) in both 2018 and 2003. The correlation strength was higher in India compared to the US, and the %ISA explains ≈ 60% of the nighttime ΔT in India.

6.4.1 Correlation between %ISA and ΔT in India

Figure 47 shows Spearman's rank correlation between %ISA within the urban areas and ΔT in 2018 and 2003 in India during summers and winters. In India, the correlation between %ISA and nighttime ΔT is stronger in summers (r_s= 0.63 in 2018, r_s = 0.65 in 2003) than in winters (r_s= 0.55 in 2018, r_s = 0.56 in 2003), as seen in Figure 47. A prior study(Mathew et al., 2016) from Chandigarh, India, showed an increased LST with an increased %ISA. As the %ISA increased, LST increase also in a hot desert climate like Abu Dhabi, where the LST difference between ISA and sand decreased as the %ISA increased(Lazzarini, Marpu, & Ghedira, 2013). This study's impervious surface areas represent the built-up areas and their anthropogenic effects. ISA metric overcomes the limitations with spectral indices - vegetation index NDVI that is season dependent (Yuan & Bauer, 2007) and quantity of vegetation dependent and built-up indices that aren't appropriately differentiating Indian LULC (Tetali et al., 2022). Therefore, as urbanization increases, the impervious surface areas increase (see Figure 45), increasing SUHI. A Spearman's rank correlation also showed that in India, the increase in %ISA from 2003-2018 correlates (p-value <0.05) with the increase in ΔT over the 15 years, as seen in Figure 48. Thus, in India, a moderate to strong positive correlation exists between %ISA and ΔT.

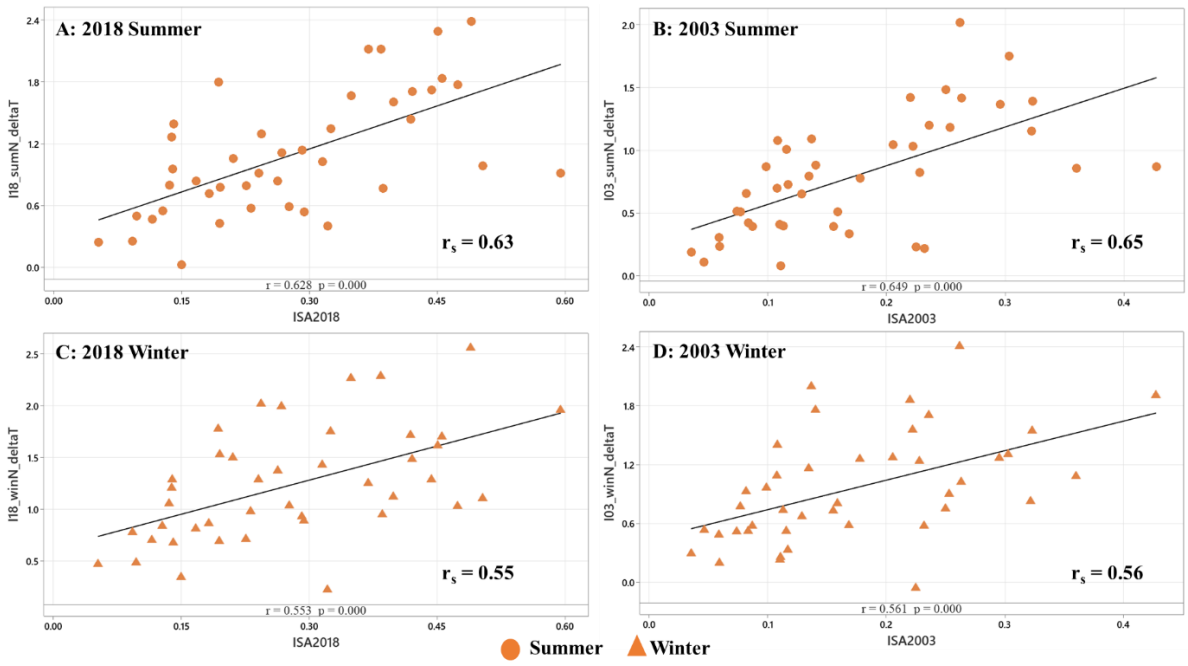

Figure 47: The Spearman's rank correlation between %ISA within an urban area and nighttime ΔT in India during A.) 2018 Summer, B.) 2003 Summer, C.) 2018 Winter, and D.) 2003 Winter.

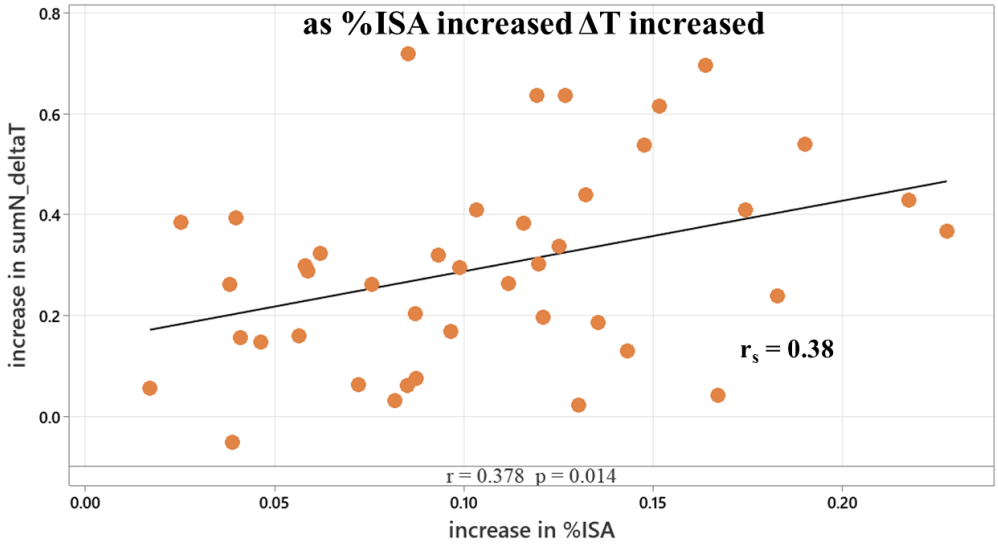

Figure 48: The Spearman's rank correlation between the increase in %ISA and the increase in nighttime ΔT in summers of India over the 15 years.

6.4.2 Correlation between %ISA and ΔT in the US

Figure 49 shows Spearman's rank correlation between % ISA within the urban areas and nighttime ΔT in 2018 and 2003 in the US during summers. In the US, during summers, the correlation between %ISA in urban areas and ΔT is moderate (r_s= 0.58 in 2018, r_s = 0.43 in 2003), as shown in Figure 49. There was no statistically significant correlation between %ISA and ΔT during daytime and winter nighttime. Therefore, the %ISA increase explains up to 58% of the increase in summer nighttime ΔT. Prior literature from the US showed that an increase in urban size increased SUHI(X. Li et al., 2017). However, only a few US studies analyzed the correlation between ISA and SUHI (ΔT). The observations from a study from Pheonix (C. Wang et al., 2016) align with the results presented here.

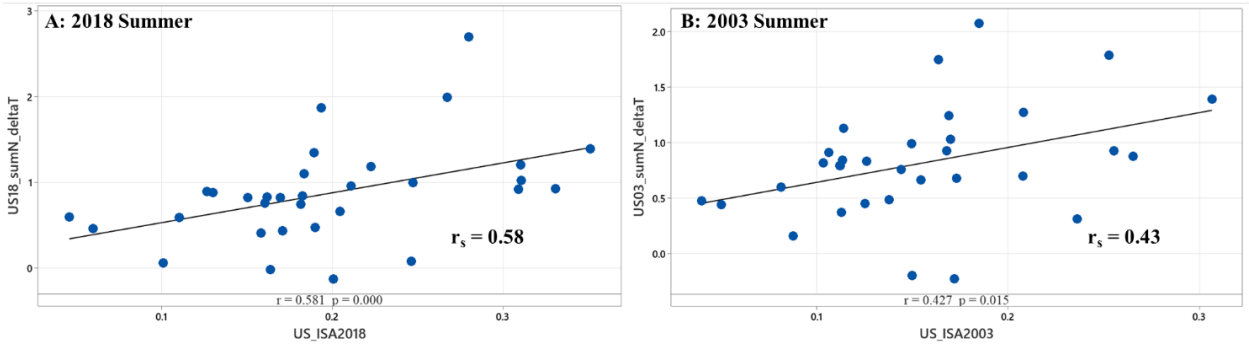

Figure 49: The Spearman's rank correlation between %ISA within an urban area and nighttime ΔT in the US during A.) 2018 Summer and B.) 2003 Summer.

Most prior literature correlated %ISA with LST, not ΔT like in this study, probably due to the differences and non-standardized methodologies of ΔT calculations that could impact the results. However, quantifying ΔT instead of LST and correlating it with %ISA for temporal comparative studies like this could help limit the background climatic disturbances on the observed trend. Such ΔT calculation methodology could also impact this study's daytime correlations between %ISA

and ΔT. As discussed in Chapter 4 and Chapter 5 of this dissertation, the impact of non-built-up LULC types on ΔT seems to be higher during the daytime. This impact of LULC on ΔT could change with the ΔT calculation methodology and the urban/rural definition.

Overall, stronger correlations exist between ISA and ΔT during nighttime in India than in the US. Chapter 5 of this dissertation showed a stronger correlation between daytime ΔT and rural vegetation than the % of built-up areas. Similarly, in this analysis, the contribution of urban built-up areas on nighttime ΔT is significant and seems higher compared to the daytime, especially in India. However, as the city increases (or increasing %ISA), the quantity of vegetation decreases, and hence the benefits of vegetation decrease, as seen in Section 4.3.1 and Section 4.5.1 of Chapter 4. A recent global study(Liu et al., 2022) also noted a similar observation on LST change.

6.5 CONCLUSION

Some key observations in this temporal analysis of ΔT are 1.) There is a statistically significant increase in SUHI over 15 years, except during summer daytime in India and winter nighttime in the US. 2.) The nighttime SUHI increase over 15 years is higher in India by 0.2^0C than in the US. 3.) The correlation between %ISA and nighttime ΔT is stronger in India compared to the US. In India, %ISA explains up to 60% of the nighttime SUHI. Also, the nighttime SUHI increase over the 15 years positively correlates to the increase in %ISA in India.

The impact of non-built-up area land use, such as croplands or snow-covered surfaces, could be more substantial during the daytime summers in India and the nighttime winter in the US, respectively. The dominant thermal performance of such land use (as discussed in Section 4.5.2 of Chapter 4) could result in a statistically insignificant change in the ΔT in summer daytime in India and winter nighttime in the US. Therefore, different LULC types other than urban built-up impact

ΔT. To more precisely estimate the impact of urban built-up areas on SUHI, the conventional way of SUHI quantification (urban-rural) is unsuitable for India.

Prior studies showed increased LST with urbanization/increase in impervious surface area. However, studies showing the temporal changes in ΔT are limited. This study shows the increase in ΔT in India compared to well-researched locations in the US. The impact of increasing ISA is higher in India than in the US. The higher increase in nighttime ΔT and the stronger correlations with %ISA in India can all be due to the higher rate of urbanization in India compared to the US. This urbanization trend is also clear from the increase in the %ISA seen over the 15 years (see Figure 44) in India compared to the US.

Table 22 shows that the average nighttime ΔT increase is higher in India than in the US by $\approx 0.2^0$C. This increase in ΔT ($0.1\text{-}0.2^0$C) in both India and US is comparable to the 0.18^0C increase per decade in global surface temperatures since 1981(LINDSEY & DAHLMAN, 2023), leading to climate change. Though 0.2^0C appears low, this temperature increase can increase extreme weather events such as flooding and heat waves (Wuebbles et al., 2017). The impact of such weather events can be higher across megacities with a population> 10 million. India hosts 6/44 megacities of this world compared to 3 in the US. Hence, such weather events affect a more significant number of people when happening in India.

This impact of urbanization on ΔT shows an immediate need to develop and implement UHI mitigation strategies in India and the US. However, with the rate at which ISA is increasing in India, and with the existing limited vegetation in India (as discussed in Chapter 4 and Chapter 5), it is essential to evaluate if standard measures such as increasing urban vegetation (irrigated and maintained green) are practically possible. Instead, it might be vital for the urban buildings and communities to become 'greener' to mitigate the UHI.

7 VARIATION IN DAYTIME URBAN BUILT-UP AREA LAND SURFACE TEMPERATURES WITH THE CONSTRUCTION PERIOD AND LAND USE OF SPATIAL NEIGHBOR

7.1 OVERVIEW

Chapter 6 of this dissertation discussed the increase in built-up areas in India and the US and the increase in ΔT. Adding to that analysis of built-up area impact on ΔT, this chapter discusses the daytime summer LST of urban built-up areas in different scenarios. Summer daytimes are critical regarding high urban LSTs(Z. Liu et al., 2022) and SUHI magnitude(Imhoff et al., 2010; Peng et al., 2012; D. Zhou et al., 2014), and extreme heat events. This chapter, therefore, focuses on summer daytime when temperatures and their impact are maximum and when the conventional ΔT calculation showed cooler urban areas compared to rural surroundings in India. This chapter primarily consists of two parts. The first showed how the daytime summer LST of the built-up area varied with its construction period. The second part of the chapter discusses the variation in daytime summer LST of built-up areas with the land use of its spatial neighbor. In the first part, the LSTs in two categories – old (constructed before 2007) and new (constructed between 2007-2016) show how the city's expanding 'new' built-up areas compare to the 'old' in terms of their thermal performance – LSTs in this case. The second part of this chapter discusses the variation in urban built-up area LSTs with the change in the spatial neighboring land use, mainly vegetation. Depending on the spatial neighbor's land use type, the built-up area LSTs in four scenarios showed how 'green' vegetation could alter surrounding built-up area LSTs. All 42 cities from India and 32 from the US were analyzed using the summer daytime LST data from 2016.

The annual GAIA (Gong et al., 2020) data represents the built-up land use for this analysis. The old and new areas were identified using the annual GAIA data available at 30m spatial resolution. LST from 2016 uses Landsat 8 data with 30m resolution. Landsat 8 data is more relevant in this analysis than MODIS 1km resolution data since higher spatial resolution can help quantify LSTs based on LULC more accurately. Landsat 8 data are only available for daytime, and this chapter presents the daytime summer urban built-up area LSTs – also when ΔT was negative in India. Therefore, this analysis of built-up area LST during summer daytime provides insight into the thermal performance of India and the US urban areas, which wasn't evident from the ΔT analysis for India.

7.2 LST Comparison of Newer and Old Urban Built-up Areas

7.2.1 Overview

The main objective of this analysis is to understand if the newer areas of cities are any better than the older areas in terms of their thermal performance - LSTs. The average LSTs of newer and older urban built-up areas were calculated and compared. Figure 44 of Chapter 6 shows the increase in artificial impervious areas within India and the US urban boundaries. As the cities grew, there has been an ongoing improvement in the building construction codes worldwide. Several initiatives began worldwide to reduce the impact of the urban built environment on the ecosystem. Some of such attempts are improving the building construction codes and standards – in terms of materials, construction technology, and energy efficiency, and the green building rating systems for buildings and urban communities.

In 2007, India launched the Energy Conservation Building Code (ECBC), its first energy code for commercial buildings, as the residential (IECC 2006) and commercial building (ASRAE 90.1)

energy codes in the US also gained prominence. The start of green building rating systems dates back to the 1990s (the first in Europe). However, a surge in their adoption occurred only in the 2000s and relatively later in India compared to the US(Shan & Hwang, 2018). Though the first LEED-rated green building in India was in 2003, from 2003-2007, there were only 20 LEED projects, with 10 registered in 2007(GBIG, 2023). Around this time, India saw a rapid increase in the adaption of green buildings and other energy efficiency standards. Therefore, in this study, the built-up areas before 2007 are considered 'old,' and those built-over 10 years between 2007-2016 are considered 'new' built-up areas. Though 2007 does not have similar significance in the US as in India, for ease of comparison, built-up areas across the cities in the US were also divided based on the same construction period. New is 2007-2016, and old is before 2007. Figure 50 shows the new-to-old built-up land use ratio in India and the US. As seen in Figure 50, in India, the average new built-up area is 45% of the old built-up area, while in the US, the average new built-up area is 22% of the old. As expected, the increase in built-up areas is higher in India compared to the US.

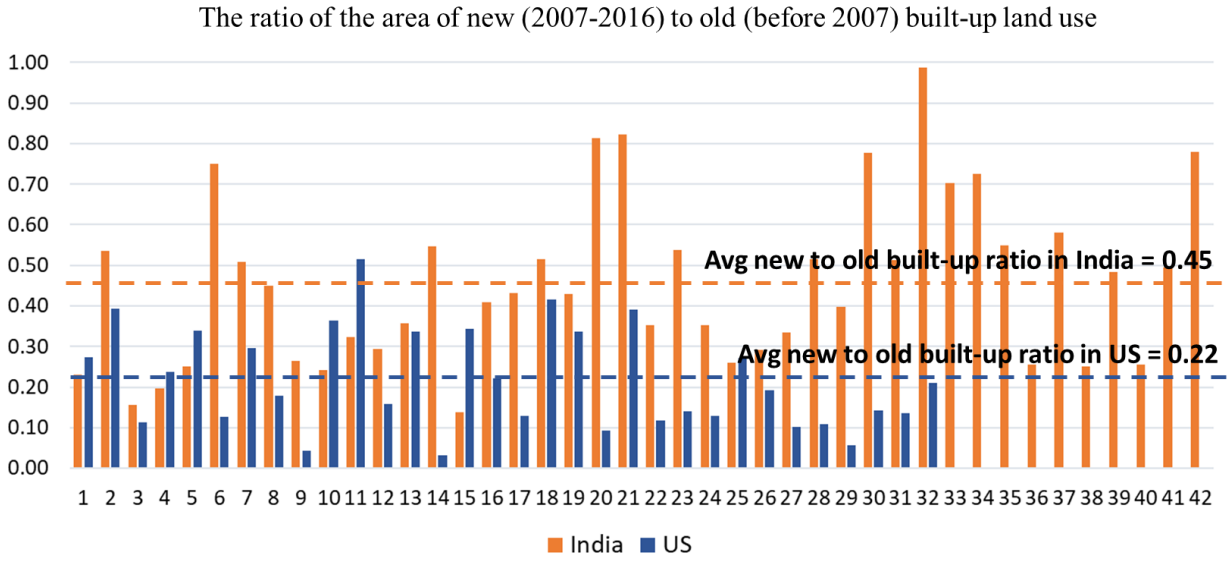

Figure 50: The ratio of the area of new to old built-up land use in India and the US

This section compares summer daytime LSTs from 2016 of old and new built-up areas across 42 cities in India and 32 cities in the US. Prior literature that studied the impact of greener buildings on urban temperatures is minimal (Donghwan, Yong, & Hyoungsub, 2015; Shin, Kim, Gu, & Kim, 2017) and none from India. Therefore, it is most relevant for a country like India to understand if the newer built-up areas would have a lower thermal impact on the outside environment than the older ones.

7.2.2 Built-up area clustering for calculating average LST

For this analysis, the average LST of built-up land use is calculated from the Landsat 8 2016 summertime LST calculated using the methodology detailed in Section 3.5 of Chapter 3. The list of cities in India and the US and the data date are in Appendix A. Using the GAIA data, the built-up areas of each city are clustered based on the construction period. All the ISA from before 2007 were considered the old built-up areas, and the ISA between 2007-2016 was the newly built-up area.

The GAIA data (Gong et al., 2020) at 30m spatial resolution shows all the small and big land parcels of impervious surface areas. As seen in Figure 45 of Chapter 6, it is not uncommon for several small parcels of newer ISA to exist away from the city core across Indian cities and a few US cities (e.g., Houston). New construction also happened in small land parcels within the urban city core, as seen in Chicago, US (see Figure 45 of Chapter 6). To limit the heterogeneity in built-up areas that come with the year of construction and the impact of neighboring pixel land use, in this analysis, the built-up area clusters that are less than 90m x 90m are excluded from the average LST calculations.

Figure 51 shows the two alternatives used to calculate the average LST of the built-up areas. The figure shows that the alternative 8N considers all the built-up area pixels, which have at least 8

neighbors from the same construction period (old /new), forming a total built-up area of 90 m x 90m. The second alternative, 24N, considers all the built-up areas with at least 24 built-up area neighbors from the same construction period (old/new), forming an area of 150m x 150m. The average LST of old and new built-up areas was calculated for the alternative, 8N, and 24N. The difference in LST ($\Delta LST = Avg\ LST_{new} - Avg\ LST_{old}$) using both alternatives was compared to understand if the area of the built-up cluster considered makes any difference in the average LST of the total built-up area.

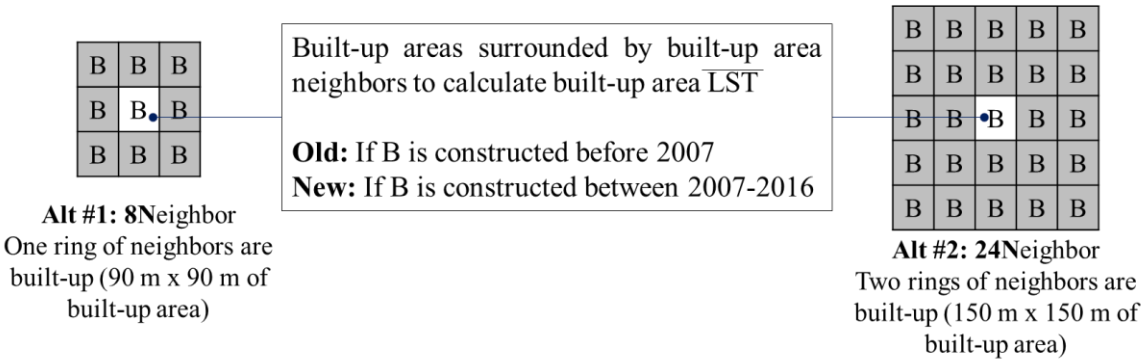

Figure 51: Visual representation of the built-up area parcels (from GAIA data) in two different alternatives, 8N, and 24N, used to calculate the average LST of old and new built-up areas

7.2.3 Comparing LSTs from two different built-up area cluster sizes

First, the LST difference (ΔLST = average LST of new– average LST of old built-up areas of each city) calculated using 8N and 24N are independently tested for statistical significance- to check if the ΔLST is non-zero. Then the ΔLST using the 8N and 24N alternatives is compared. For both alternatives, 8N and 24N, one sample t-test showed that with 95% confidence, the null hypothesis ($\mu = 0$, where μ is the mean ΔLST) could be rejected in India and the US. Table 23 shows results from one sample t-test for alternatives 8N and 24 for India and the US. These results show that the mean ΔLST from alternatives 8N and 24N is non-zero across both countries.

Table 23: One sample t-test results showing that the mean ΔLST (^{0}C) values from alternative 8N and 24N are statistically significant

	Alternative 8N		Alternative 24N	
	T-value	**P-value**	**T-value**	**P-value**
India	4.79	0.000	3.82	0.000
US	3.97	0.000	2.37	0.024

Figure 52 shows the LST difference (ΔLST = average LST of new– average LST of old built-up areas of each city) between new and old built-up areas calculated using alternative 8N and 24 for each of 42 cities in India and 32 in the US. Figure 52 shows that the variation in ΔLST calculated using 8N and 24N is minimal in the case of India. This variation is higher in the case of the US than in India. However, the difference between mean ΔLST is statistically insignificant for both India and the US. A two-sample t-test comparing the mean ΔLST of 8N and 24N showed that with 95% confidence, the null hypothesis ($\mu1-\mu2 = 0$, where $\mu1$ = mean ΔLST using 8N, and $\mu2$= mean ΔLST using 24N) could be accepted. Figure 52 shows the results from the t-test comparing 8N and 24 in India and the US. As seen in Table 24, a p-value >0.05 indicates acceptance of the null hypothesis and shows that the difference between ΔLST means of 8N and 24N is statistically insignificant. This ΔLST comparison indicates that the size of the built-up area cluster considered (8N or 24N) makes no difference in the overall mean LST of the built-up area. Further analysis in this section presents alternative 8N results and discussion.

Table 24:The t-value and p-value from a two-sample t-test comparing mean ΔLST from alternative 8N and 24N show no statistically significant difference.

	T value	P value	8N: μ1 (Mean ΔLST in ^{0}C)	24N: μ2 (Mean ΔLST in ^{0}C)
India	0.09	0.925	0.73	0.76
US	1.05	0.296	-0.76	-0.47

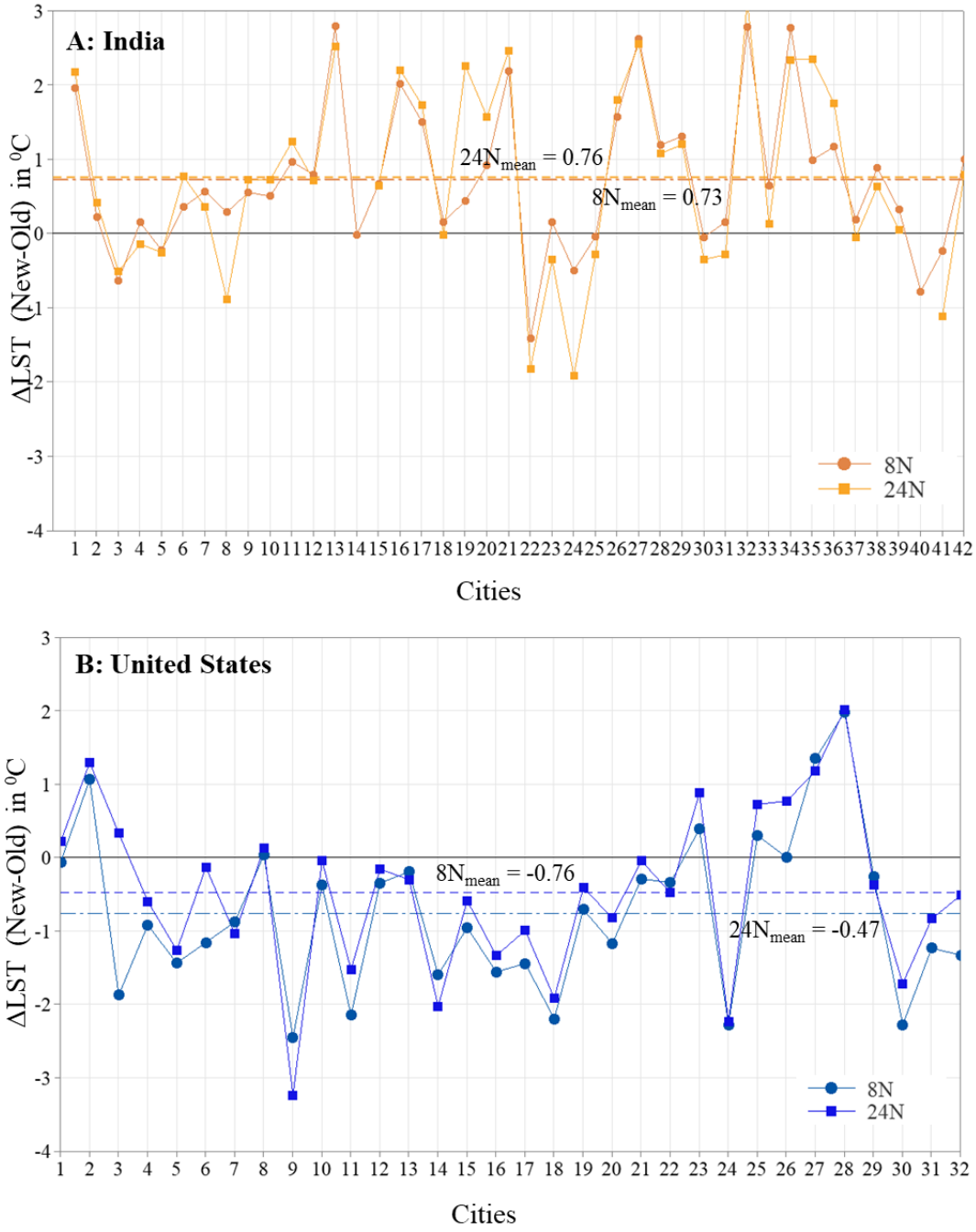

Figure 52: Comparison of the ΔLST (new built-up area LST – old built-up area LST) calculated using 8N and 24N alternatives of built-up area parcels in A: India and B: US. The data show low to no difference in ΔLST calculated using 8N and 24N.

7.2.4 Comparing LST of New and Old built-up areas

Since the difference between the LST means calculated using each of these alternatives is not statistically significant, LST results from alternative 8N for India and the US are shown in Figure 53 and Figure 54, respectively. In India, as seen in Figure 53, the summer daytime LST is higher in the newly built-up areas across most cities (33/42), with an average ΔLST (new-old) of 1.1^0C. In 9/42 cities, the new built-up areas were cooler than the old ones, with an average LST difference (new-old) of -0.4^0C. However, in 25/32 cities of the US, the newly built-up areas have lower LST than the old, with an average ΔLST of -1.2^0C. In 7/32 cities of the US, the LST of newly built-up areas was higher than the old, with an average ΔLST of 0.73^0C. There isn't any obvious pattern related to the city size, population, or climate across the two categories –cities with warmer new built-up areas and cities with cooler new built-up areas. Overall, in India, the mean LST across the newly built-up areas (45.70 ± 6.1^0C) was higher than the old ones (45.97 ± 6.0^0C). The LST range was similar for the new and old built-up areas, with a maximum LST of 64^0C and a minimum of 28^0C. The built-up area LSTs in the US are lower than in India, as noted in Chapter 4. In the US, the mean LST across the newly built-up areas (40.44 ± 6.5^0C) was lower than the old ones(41.20 ± 6.2^0C). For both new and old areas, LSTs ranged between 55^0C and 29^0C. Across all the cities, the average LST difference between the newly built-up areas and the old ones was 0.73 ± 0.99^0C in India and -0.76 ± 1.09^0C in the US. Figure 54 shows the LST difference between the newly built-up areas and the old across all 42 cities of India and 32 cities in the US.

As discussed in Section 7.2.3, these ΔLSTs (new-old) are statistically significant (p-value <0.05). These mean ΔLST values, therefore, show that the newly built-up areas in India are warmer than the old ones, but in the US, it is the inverse. In the US, newly built-up areas are cooler than the old

ones. This variation in the ΔLST could be due to several factors influencing LSTs. A discussion of the plausible factors influencing these results is in Section 7.2.5.

7.2.5 Built-up LST variation in the US with the construction period

Unlike in the case of India, 2007 does not have a specific significance in the US, yet it demarcates this study's new and old areas also in the US. To assess whether 2007 impacted observed trends of LST in the US- average LSTs of built-up areas segregated based on construction periods were quantified, as shown in Figure 55. As seen in Figure 55, the average LST of built-up areas that existed before 1986 is 41.54^0C, compared to 40.94^0C of built-up areas that came into existence between 1986-2006, and 40.44^0C compared to built-up areas that came into existence between 2007-2016. This trend indicates that the built-up areas from different construction periods progressively have lower LSTs. So, though 2007-2016 need not necessarily indicate 'new' built-up areas in the US, it can be supported by the overall trend of newer built-up areas having lower LSTs than the older ones in the US. Therefore, these findings support the results from Section 7.2.4 and show that the newer built-up areas in the US are better regarding their LSTs. However, the difference between average LSTs of 1986-2006 built-up areas and 2007-2016 built-up areas is lower compared to the built-up areas before 1986, and this reduction in LST with construction time could also plateau at some point. Further analysis of LST variation with the construction period is needed to provide more insight into if and when this trend could change or plateau, which is a future work scenario.

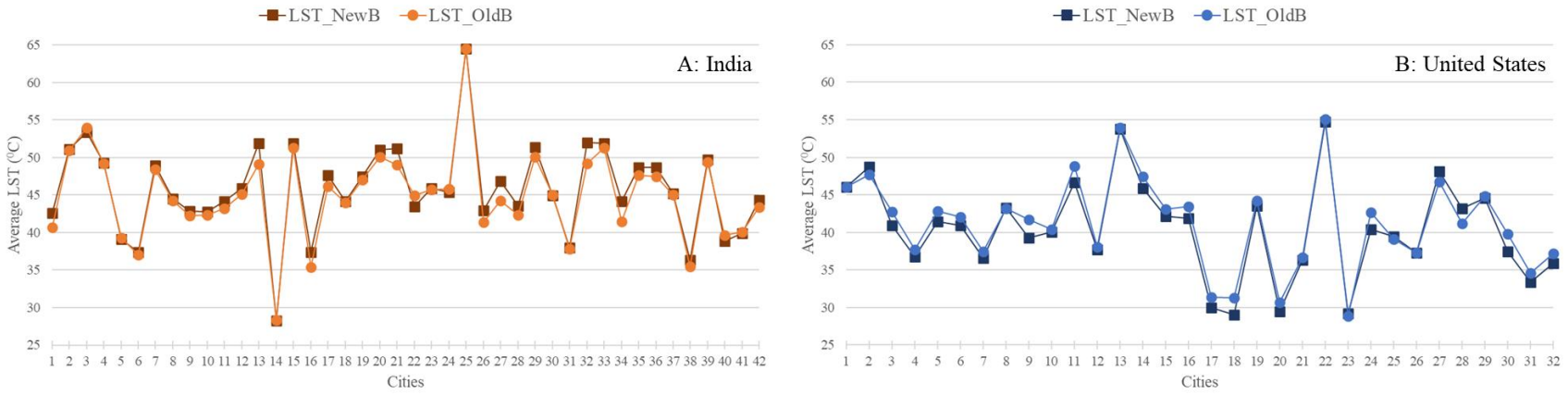

Figure 53: The average LST in the new and old built-up areas of A: India and B: United States. In India, the newly built-up areas are warmer than the old ones; however, in the US, the newly built-up areas are cooler than the old ones.

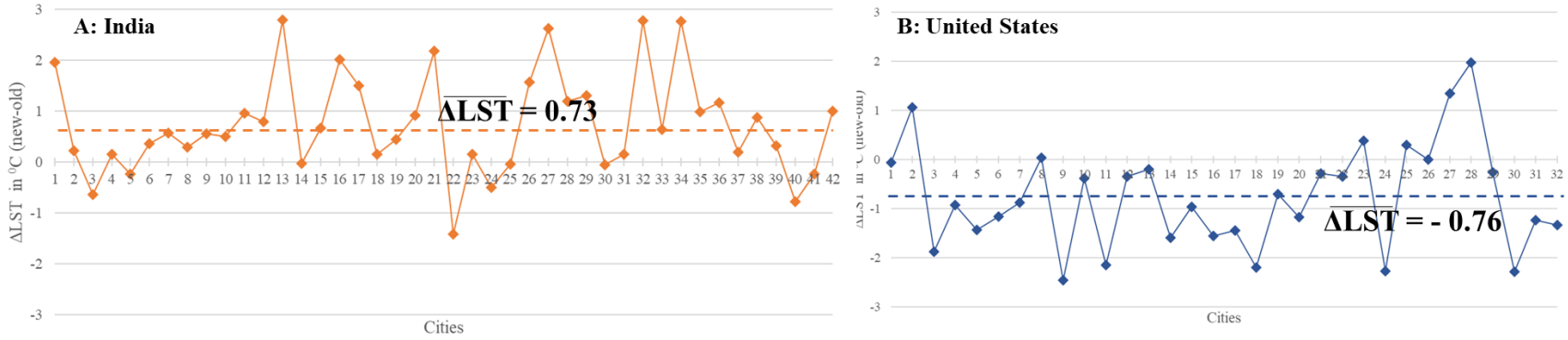

Figure 54: The difference between new and old built-up area LSTs in A: India and B: US.

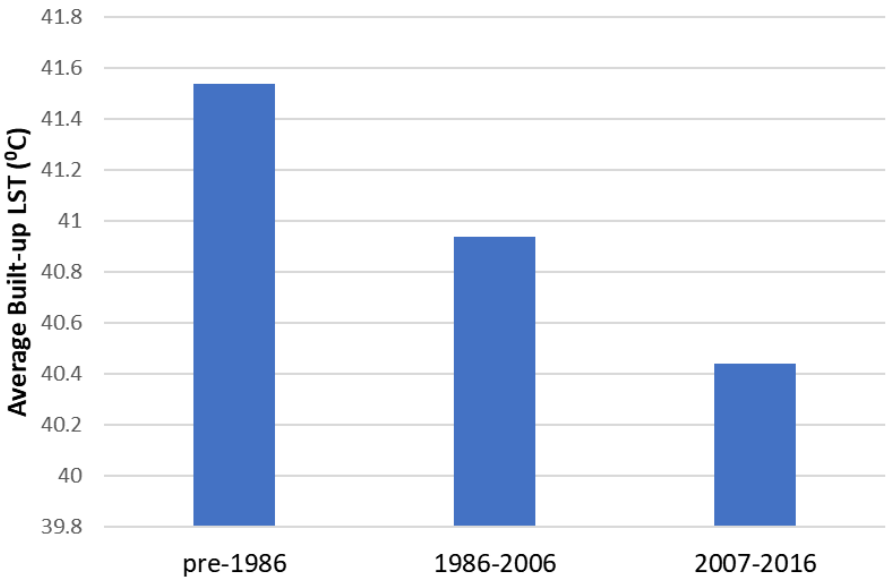

Figure 55: Average LST of built-up areas across the 32 cities in the US, segregated based on the construction period.

7.2.6 A qualitative discussion of the results

When the satellite and the LST calculation method are the same, the factors impacting LST at a given time include the location's climatic, biophysical, and social characteristics. In this case, while the land use (built-up) and background climate remain constant for a city, the micro and neighborhood scales' urban building design differences can change the built-up area LSTs. Urban building design alters the micro-climate(Bueno, 2012) and can impact the LSTs(L. Zhao et al., 2014). The differences in the urban development type and surroundings, the building design, the energy codes, their adoption, and other relevant green building ratings between the new and old built-up areas can alter the LSTs. Buildings can alter the LSTs. The urban development type could also impact the LSTs. While various other factors could impact the built-up LSTs, this discussion focuses on the urban development type, building design, building codes, and rating systems, which could directly or indirectly impact the built-up area LSTs. Differences in all such factors between India and the US could lead to differences observed in built-up area LSTs in this study.

7.2.6.1 Urban development and densities

Rapid urbanization in India is causing an explosive increase in built-up areas across the country's cities. Recent studies (S. Chakraborty, Maity, Dadashpoor, Novotnỳ, & Banerji, 2022; Güneralp, Reba, Hales, Wentz, & Seto, 2020) showed that urban densities are reducing as the cities grow outward across several global south locations of the world, like India. Infill urban development is less common in India than in the US. Such differences in urban expansion patterns – infill vs. extension vs. leapfrog could impact LSTs(Tran et al., 2017). A prior study(Güneralp et al., 2020) also highlighted the inefficiencies in urban expansion across India, with agricultural land converted into urban areas. The study indicated that the conversion of bare soils to urban areas in India also exists across the country's arid and semi-arid lands. As seen in Chapters 4 and 5 of this study, the croplands and bare soils in India could reach higher LSTs than the vegetated areas of the US. Therefore, LSTs of the newly built-up areas in less green regions could be higher than LSTs of the newly built-up areas within the vegetated suburban surroundings in the US. Figure 56 highlights the location of the newly built-up areas in a city from India and the US overlayed on the existing LULC. Figure 56 presents examples of cities in India and the US that are rapidly urbanizing. As seen in Figure 56, differences exist in the surrounding LULC of the new built-up areas, which could impact built-up area LSTs.

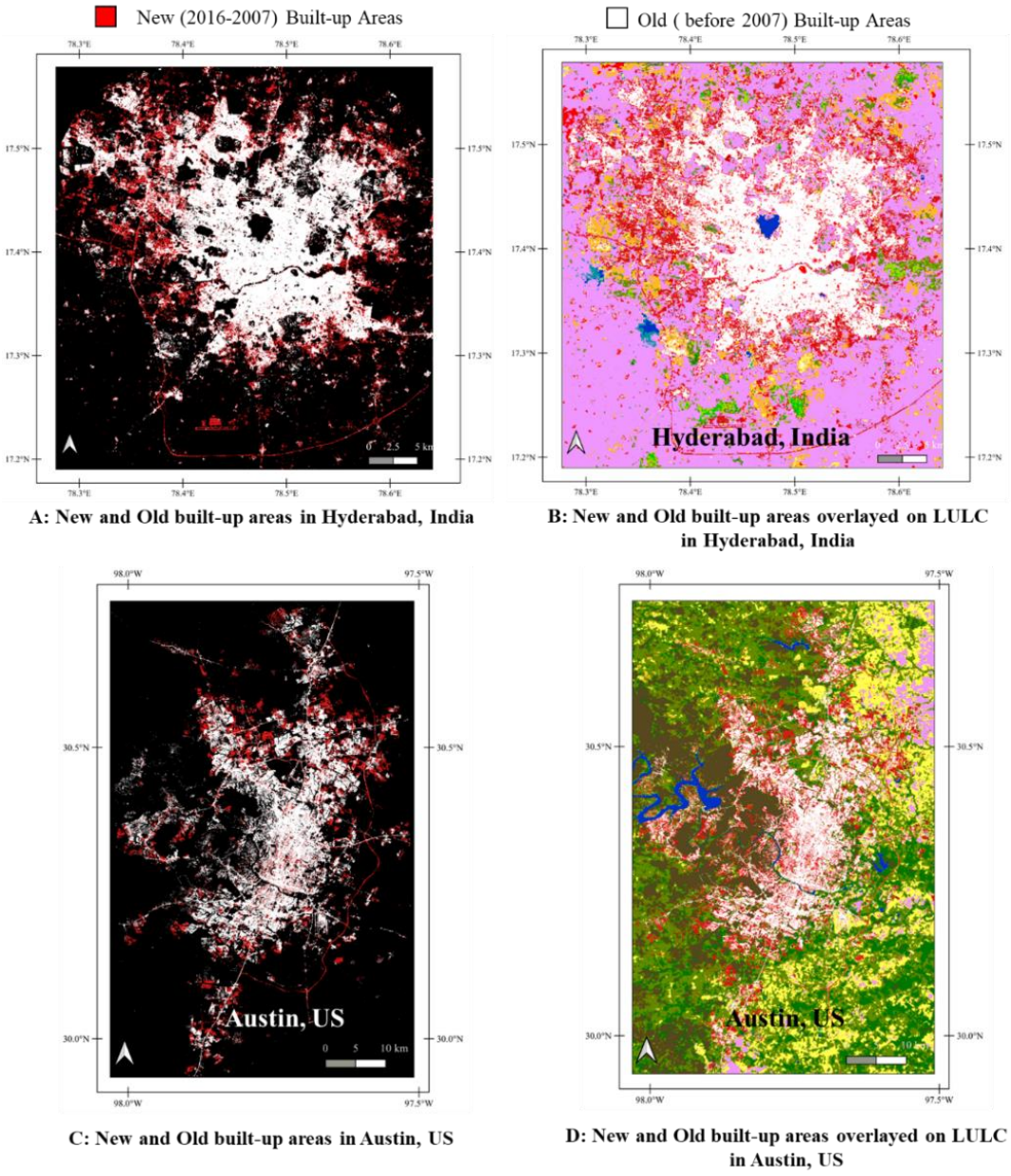

Figure 56: The new (in red) and old (in white) built-up areas in Hyderabad, India, and Austin, US showing surrounding croplands in India and forested areas and shrublands in the US.

Even so, the current urban densities in India are still higher than in the US(Güneralp et al., 2020). Increasing building density increases SUHI and LST (L. Shi et al., 2021; Y. Shi et al., 2019; Zheng et al., 2019). Higher urban built-up and population densities in India (as seen in the example in Figure 57) could also mean increased anthropogenic heat in the urban environment, increasing the overall urban LSTs compared to those in the US (most cities) with lower densities, population, and human and vehicular traffic. Section 3.2.1 of Chapter 3 provides a comparative discussion of the population densities in India and the US.

Figure 57: A representative image of built-up areas in India (Dimitry, n.d.)

7.2.6.2 Urban building design

Buildings in India were traditionally low to mid-rise. However, newer buildings across the megacities are high rises (see Figure 58). Traditional single-story courtyard homes and low/mid-rise commercial buildings with no to low glass use changed to skyscrapers like in the West (Ciara, 2022). The need for more urban floor area within less time could be one reason for the conventional low-rise, thick-wall buildings to change to high-rise, lighter-weight construction. A few studies from China discussed the LST variation with building height. A Beijing study (Zheng et al., 2019) showed that LSTs are sensitive to building height, density, and vegetation cover.

The authors showed that the LSTs decreased as the residential building height increased. In another study(J. Li et al., 2011) from Shanghai, China, higher LSTs were noted in low-mid-rise residential areas compared to high-rise buildings. However, it is essential to understand how many of India's newly built-up areas are high-rise buildings before drawing conclusions based on this literature. High-rise buildings (>10 floors) are mostly seen only across mega-cites and are still not common in most cities. Segregation of urban buildings based on design elements might be necessary to understand the impact of building design on LSTs. Further, buildings in India (mainly residential) changed from more naturally ventilated to air-conditioning-dependent buildings. Anthropogenic heat release from building air conditioning systems also increases outdoor temperatures(Salamanca, Georgescu, Mahalov, Moustaoui, & Wang, 2014) and could impact LSTs. All such changes in building design that happened with time can impact the built-up area LSTs in India noted in this study. The newer built-up areas in India were warmer than the older ones, so the newer building design seems less suitable for reducing LSTs. Such a massive shift in building design is not typical in the US. However, there could be building improvements that could have happened with changes in construction technology, material, and the adaptation of building energy codes and standards.

Figure 58: Highrises amidst traditional low to medium-rise buildings in India (Photo by Vaishnav Chogale on Unsplash)

7.2.6.3 Building energy codes

In India, a national-level energy efficiency code was first launched in 2007 for commercial buildings, while a residential energy building code was launched in 2021. However, in India, the urban residential floor space growth is projected to be higher than the commercial floor area growth(Yu et al., 2017). In the US, residential buildings comply primarily with the International Energy Conservation Code (IECC), and commercial buildings adhere to the ASHRAE 90.1 standard. These IECC and ASHRAE 90.1 codes are revised every three years, making them more stringent to achieve higher energy efficiency in buildings(Energy.Gov, 2022). However, in India, after ECBC's launch in 2007, the code was updated only in 2017. Further, in the US, the building energy codes also apply to building renovations, which isn't the case in India – though building renovations in India are less common than in the US.

Along with building energy codes, in the US, several other national-level standards (e.g., ASHRAE's AEDG, Zero Energy Guide) and local policies (e.g., CALgreen, NYStretch-2020) focus on reducing building energy consumption and are moving towards net zero energy possibility. Also, the US building envelope material testing, rating, and labeling systems could improve building envelope performance (including surface finishes). However, such building materials rating and labeling system is non-existent in India (Evans, Roshchanka, & Graham, 2017).

While developing building codes is essential, a lack of adoption of such codes wouldn't help achieve the energy efficiency goals. In India, compliance with the commercial building code, ECBC, was voluntary and left to the local governments for enforcement. Only 2 states mandate the code, and a little more than 50% of the states (18/28) notified the code at the state level, leaving its enforcement to local municipalities(BEE NITI, 2017; Kwatra, Madan, & Korsh, 2021). In

comparison, in the US, 41/50+1 states adopted IECC 2009 or above for residential buildings, and only two states do not have any statewide commercial code. In the US, 49/(50+1) states either have state-specific commercial codes (8/50) or can comply with either ASHRAE 90.1 (41/50) or IECC (32/50)(Energy.Gov, 2022). Code implementation and comprehensive policies addressing energy and environmental aspects are still limited in developing countries like India, compared to the US(Chandel, Sharma, & Marwaha, 2016; Nejat, Jomehzadeh, Taheri, Gohari, & Muhd, 2015). Lack of penalties/incentives to comply with codes, lack of tools, and lack of training for stakeholders can all impact the implementation of the codes. A 2017 global study(Evans et al., 2017) showed that while several countries – including the US- have such penalties, incentives, tools, and training opportunities to improve code compliance, none exist in India. Further, it also highlighted the lack of building checks in India during the design and construction phase that could ensure code compliance.

Though all this is relevant, it is essential to understand that such building energy codes have more indirect impacts on LSTs. Previous studies showed the interdependence between building energy efficiency on canopy-level air temperatures(Bueno, 2012)and LSTs(Faroughi et al., 2020; L. Zhao et al., 2014). At the same time, most of these codes suggest building surface treatments – increasing surface reflectance (e.g., cool roofs), which reduces LSTs(Hashem Akbari & Kolokotsa, 2016; Santamouris et al., 2017; T. Xu et al., 2012). Therefore, lesser market penetration of building energy codes in India, compared to the US, could impact the LSTs – higher LSTs in newer built-up areas than old ones in India and lower LSTs in newer built-up areas than the old ones in the US.

7.2.6.4 Green rating systems

The green building rating systems (e.g., LEED US, LEED India, IGBC India, GRIHA India) focus on improving a building or community's environmental (indoor and outdoor) and energy performance. Like the building energy codes, the green rating system could also, directly and indirectly, impact the LSTs. Some popular UHI mitigation measures from such rating systems include cool roofs, green roofs, green walls, adding vegetation within site, using cover parking, vegetated pavers, and cool pavements, all of which can impact LSTs. Surface treatments like cool roofs (T. Xu et al., 2012), cool pavements, green walls, and green roofs (H Akbari et al., 2001; Hashem Akbari & Kolokotsa, 2016) are all shown to reduce surface temperatures. Urban built-up areas implementing these surface UHI mitigation measures could result in lower LSTs. The existing research on the outdoor environmental performance of green buildings – their impact on outdoor temperatures, is minimal. Out of the existing few studies, two showed a reduction in outdoor temperatures (Fahmy, Ibrahim, Hanafi, & Barakat, 2018; Shin et al., 2017) surrounding green buildings, and another(Donghwan et al., 2015) concluded that there isn't any significant impact of green buildings on the outdoor temperatures.

Despite the possible benefits, these green rating systems in India and the US are voluntary. Hence, the number of new buildings that comply with such rating systems is still meager compared to the number of new buildings, which is even lower in India(Yu et al., 2017). For example, at the end of 2016, there were 42,623 LEED-certified projects in the US compared to 397 in India. Therefore, differences in the number of new buildings complying with such rating systems and standards could also lead to differences in the observed LSTs across the two countries.

All these factors could be associated with the differences in ΔLST between India and the US. However, future studies should further investigate the characteristics of buildings and the

surrounding built environments to quantify their impact on LSTs. The results from this section show that the built-up area LST range from India is different from the US. The newly (between 2007-2016) built-up areas in India have higher LSTs than old built-up areas (before 2007), but vise-a-versa in the US. In the US, the newer built-up areas seem cooler than the old ones. Therefore, there is a potential and need to improve the thermal performance of the urban built environment in India.

7.3 CHANGE IN BUILT-UP LSTS WITH ITS SPATIAL NEIGHBORS' LAND USE

When built-up areas in each city of India and the US were categorized as new and old based on the construction period, their LSTs varied, and ΔLST was different in India than in the US, as shown in Section 7.2. This section analyzes the LST of built-up clusters by categorizing them based on their spatial neighbors' land use. The primary objective of this analysis is to identify if and how neighboring land use – built-up vs. non-built-up vs. vegetation changes the surrounding built-up land use LSTs. Such information could assist urban designers, planners, and policymakers identify design alternatives to improve the outdoor thermal performance of the urban built environment. As in Section 7.2, Landsat 8 spatial resolution is more appropriate for this LULC-based spatial neighbor analysis. This analysis is, therefore, for daytime, during summers when urban surface LSTs peak, and for the time of the day when conventional ΔT analysis did not show the impact of urban areas on LSTs in India.

7.3.1 Spatial neighbor-based clustering of built-up areas

There are three datasets used for this custom clustering approach – 1.) Landsat 8 daytime summer LSTs of urban areas, 2.) Landsat 8 calculated NDVI within the urban areas, and 3.) The global artificial impervious area (GAIA) data. As in the previous sections of this dissertation, the GAIA

data represents the built-up areas. All eight spatial neighbors of each built-up area pixel (30m x 30m) were checked for the land use type – built-up, non-built-up, or vegetation. The NDVI value of ≥ 0.3 represents green vegetation. The built-up land use was segregated into four scenarios based on its spatial neighbor's land use, as shown in Figure 59. The surrounding 8 spatial neighbors are checked for land use in each scenario. Figure 59 shows the four scenarios where built-up area LSTs are calculated– 1.) **B**uilt-up**_w**ith**_B**uilt-up**:** all built-up (B) areas with all 8 immediate neighbors also of built-up land use, 2.) **B**uilt-up**_w**ith**_N**on**B**uilt-up: all built-up area pixels with at least one (of 8) immediate neighbors as non-built-up (NB) land use, 3.) **B**uilt-up**_w**ith**_G**reen: all the built-up area pixels with at least one immediate neighbor of green vegetation (G) of NDVI ≥ 0.3, and 4.) **B**uilt-up**_w**ith**_N**on**G**reen: all the built-up area pixels with at least one immediate non-green neighbor (NG) (NDVI < 0.3). The first scenario identifies all the built-up clusters using the GAIA data. Using the same GAIA data, the non-impervious areas were considered non-built-up areas in the second case. In the third and fourth scenarios, the GAIA data was used in conjunction with Landsat 8 NDVI data to identify built-up areas with green and non-green neighbors. While the land use type in scenarios B_w_B and B_w_G are built-up and green vegetation, respectively, in the other two scenarios, it can be anything other than built-up and green vegetation. In the B_w_NB scenario, at least one spatial neighbor to the built-up pixel can be any non-built-up land use type such as cropland, forest, grassland, barren, fallow, or water bodies. In the fourth scenario, B_w_NG, at least one spatial neighbor could be any non-green land use with NDVI < 0.3, including built-up land use. The average LSTs of all the built-up clusters are calculated in all four scenarios and compared.

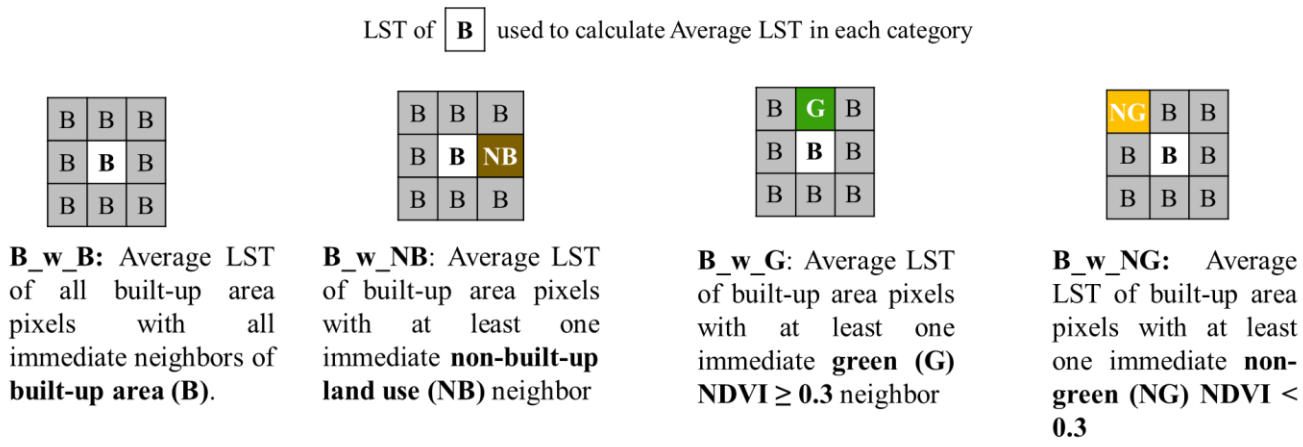

Figure 59: Built-up land use clusters in four scenarios based on the land use of the spatial neighbor

7.3.2 Change in built-up area LSTs with change in land use of its spatial neighbor

For this analysis, the average LST of all built-up land use clusters with all built-up area neighbors (B_w_B) represents a baseline urban scenario. The change in LST with the neighboring pixel is quantified using the LST difference between each scenario and the baseline (B_w_B). The LST difference (ΔLST) between the average LST from each scenario and the baseline scenario(B_w_B) is calculated for 42 cities in India and 32 cities in the US, as shown in Figure 60. The one sample t-tests showed that all these LST differences are statistically significant (p-value <0.05). Figure 60 shows that the ΔLST trends differ for India and the US, except for built-up with green neighbors. Cities across both countries show that having a green neighbor can reduce the LSTs of built-up areas, as seen in Figure 60. The built-up areas with green neighbors are 1.3^0C and 2.4^0C cooler than those with all built-up neighbors in India and the US, respectively.

For the other two scenarios, in India, the ΔLST is positive (an increase compared to baseline) in some cities and negative (a decrease compared to baseline) in others. On average, both the scenarios – B_w_NB neighbor and B_w_NG neighbor are warmer than the baseline by 0.5^0C and 0.3^0C, respectively. In the US, however, the B_w_NG neighbors are warmer (average ΔLST = 1.0^0C), and B_w_NB neighbors are cooler (average ΔLST = -2.6^0C) than the baseline in all cities.

There is a clear difference between India and the US in the ΔLST trends for built-up areas with non-built-up neighbors. Such difference could be because non-built-up neighbors can be any land use, including vegetation. Based on the LULC of the US (see Figure 17 of Chapter 3), the chance of this non-built-up neighbor being green is higher than in India. These (maybe) green neighbors could reduce the overall built-up area LST compared to the baseline. In the case of non-green neighbors, the neighboring pixel is any non-green land use, including barren land or built-up. Therefore, non-green neighbors are increasing the built-up area LSTs in both countries and higher in the US. In India, the B_W_NB neighbor has the highest LST, indicating that the chances of green vegetation are low in India, and having a neighboring built-up area is better than any other non-built-up non-green land use. All these scenarios highlight the benefit of green spatial neighbors within built-up land-use clusters.

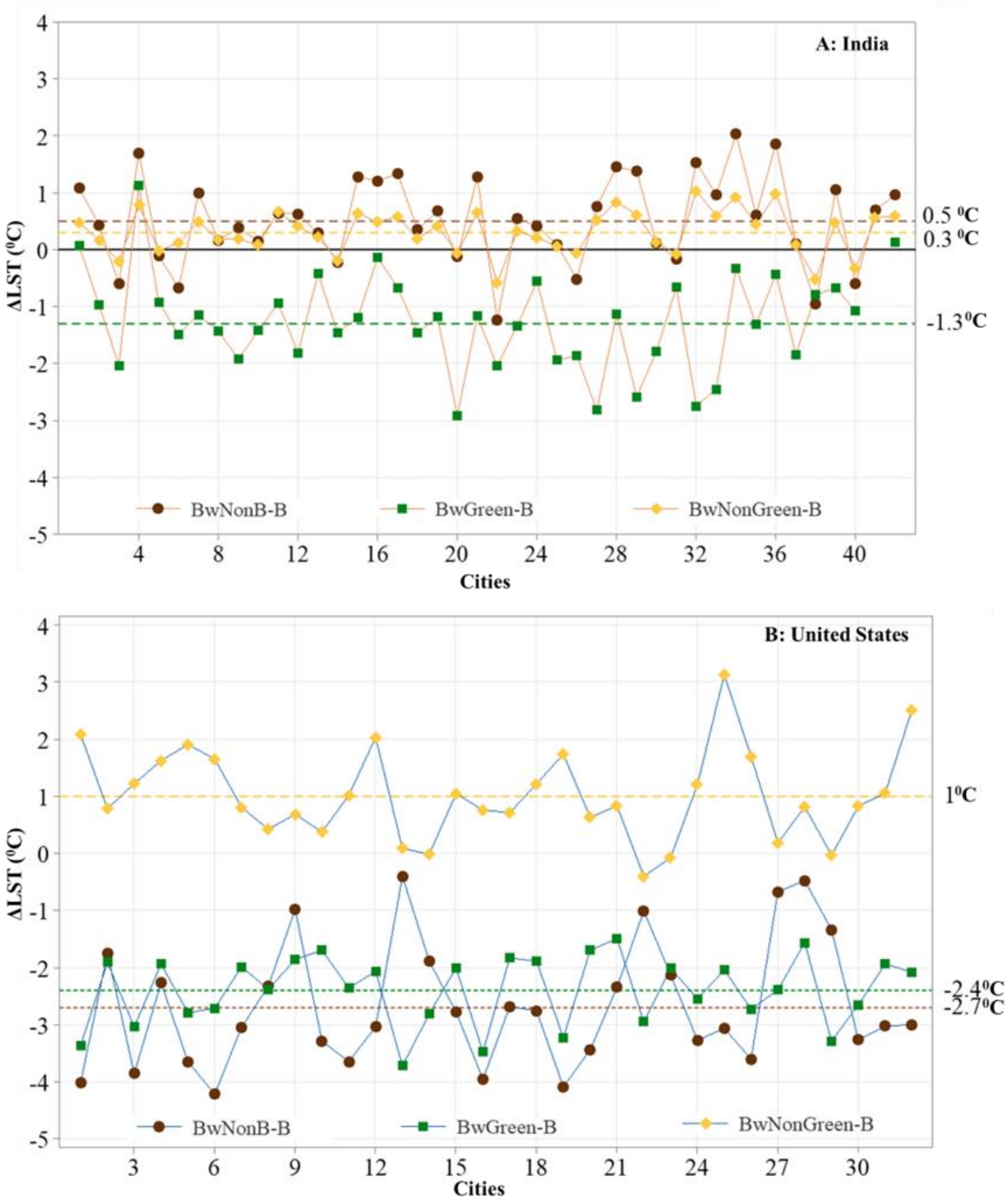

Figure 60: The variation in urban built-up area LST in A: India and B: United States, with three different neighbors (B_w_NB, B_w_G, and B_w_NG) compared to the urban built-up areas with a built-up neighbor(B_w_B).

7.3.3 Impact of vegetation on LSTs

Figure 61 shows the built-up area LSTs in two scenarios – built-up with built-up neighbors and green neighbors in India and the US. In both countries, built-up areas with green neighbors have lower LSTs than those with built-up neighbors. In India, the mean LST in B_w_G is 44.0± 5.9^{0}C compared to 45.3± 6.1^{0}C in the case of B_w_B. In the US, the mean LST in B_w_G is 38.6± 5.9^{0}C compared to 41.0± 6.3^{0}C in the case of B_w_B. The reduction in built-up area LST due to green vegetation is higher in the US (2.4^{0}C) than in India (1.3^{0}C), possibly due to better quantities of greener vegetation. However, the mean LSTs are higher in India compared to the US. A two-sample t-test also showed that the mean ΔLST ($LST_{(B\_w\_G)} - LST_{(B\_w\_B)}$) difference between India and the US is statistically significant (t-value = 6.54, p-value = 0.000). The reduction in built-up area LST due to green neighbors is 1.1^{0}C higher in the US than in India.

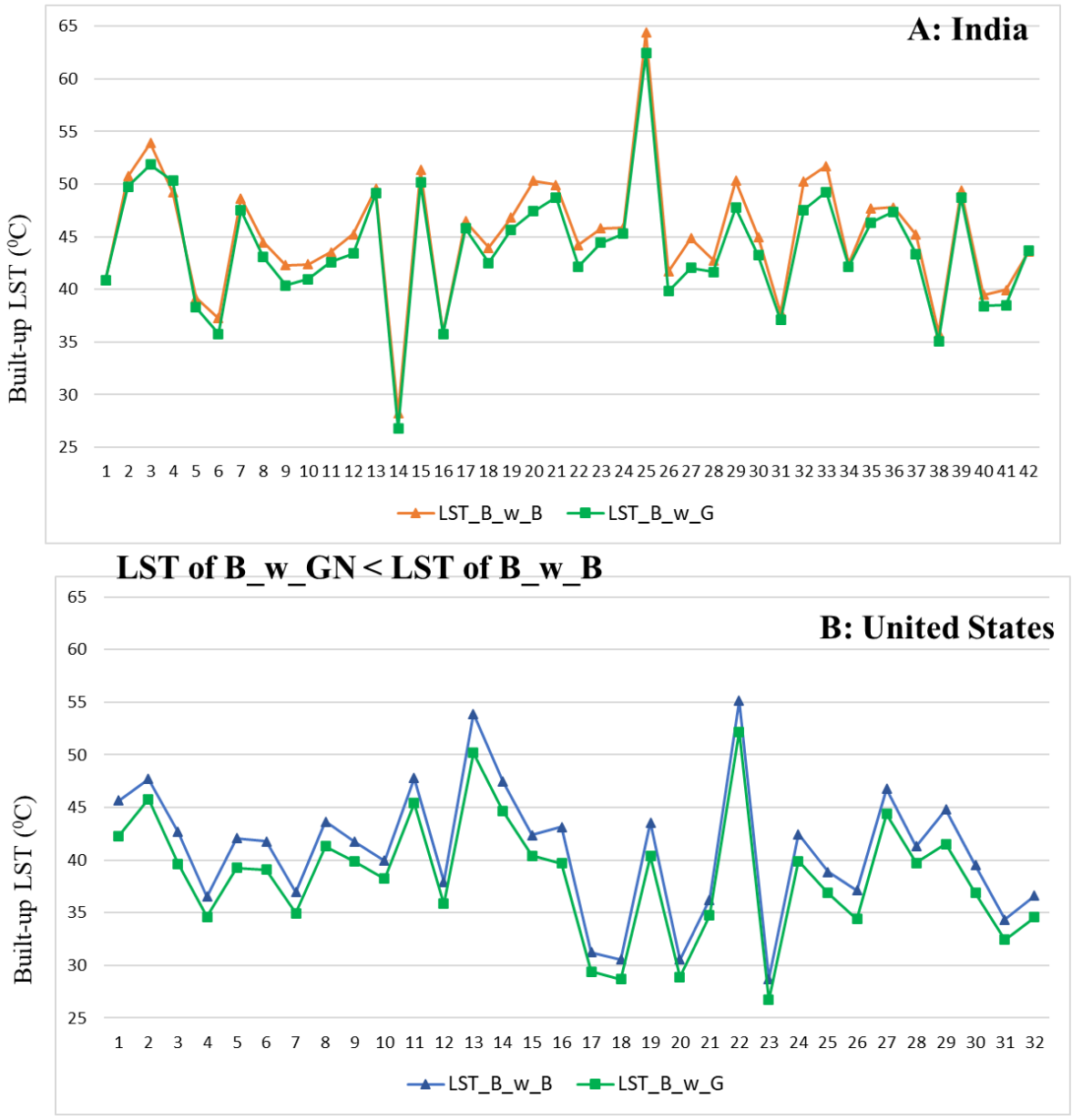

Figure 61: Comparison of built-up area LST in two scenarios, built-up with a built-up neighbor and a green neighbor, in A: India and B: United States. In both countries, built-up areas with green neighbors have lower LST than built-up neighbors.

Figure 62 shows higher LSTs in three scenarios: built-up with built-up (B_w_B), non-built(B_w_NB), and non-green(B_w_NG) neighbors compared to the built-up with the green (B_w_G) neighbor in India. The built-up areas with a built-up neighbor, non-built-up neighbor, and non-green neighbor are 1.3^0C, 1.8^0C, and 1.6^0C warmer than those with at least one green neighbor, respectively. In the US, as discussed in Section 7.3.2, though the built-up areas with a

built-up neighbor and non-green neighbor are warmer than built-up with a green neighbor, it is not the same in the case of built-up with a non-built-up neighbor as seen in Figure 62. Figure 62 shows that the LST of built-up with a non-built-up neighbor is higher than those with green neighbors in only 7/32 cities. In the rest of the 25 cities, LSTs of built-up areas with a non-green neighbor are cooler than those with a green neighbor.

Interestingly, the 7/32 cities (e.g., Phoenix, Las Vegas, Denver, Salt Lake City, San Diego) in which LST of B_w_NB > B_w_G predominantly have herbaceous vegetation or scrublands in and around the urban built-up areas (see the US LULC map in Figure 17 of Chapter 3). These non-forest, non-cropland LULC in these 7 cities could mean that in the rest of the 25 cities, the non-built-up neighbor could most likely be vegetation or water land use resulting in lower LST than built-up areas with green neighbors. Therefore, Figure 60 - Figure 62 together shows that green vegetation can reduce the neighboring built-up area LSTs in India and the US. In India, having a built-up neighbor is better for LSTs than having a non-built-up non-green neighbor.

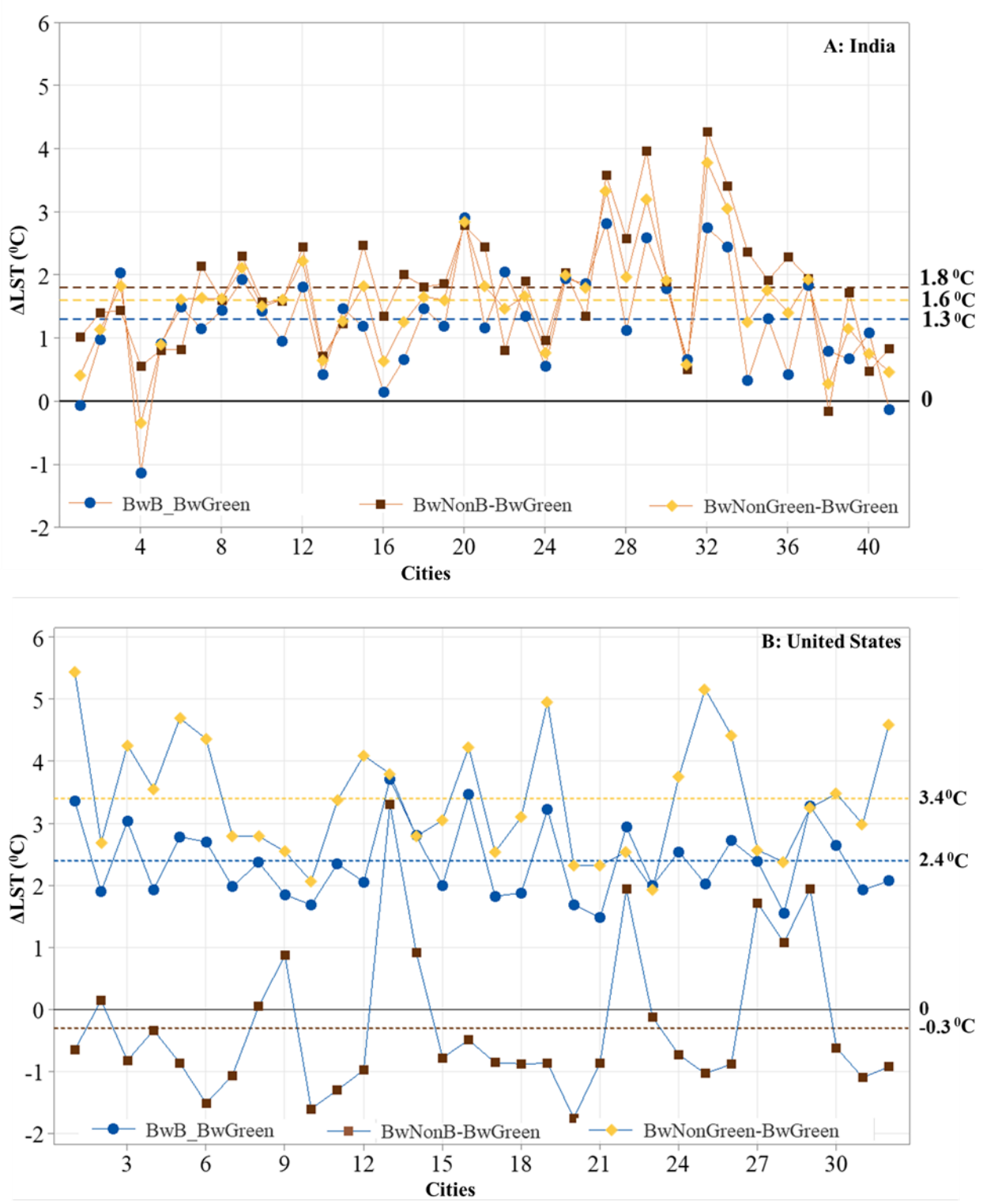

Figure 62: The variation in urban built-up area LST in A: India and B: United States, with three different neighbors (B_w_B, B_w_NB, and B_w_NG) compared to the urban built-up areas with a built-up green neighbor (B_w_G).

7.3.4 Discussion

The impact of urban trees and vegetative surfaces on temperatures is well documented in the literature and is discussed in Section 2.5.2.2 of Chapter 2. Prior literature showed the impact of urban parks (Bowler, Buyung-Ali, Knight, & Pullin, 2010) and green roofs(H. Chen, Ooka, Huang, & Tsuchiya, 2009) on surrounding air temperatures. However, studies on the impact of vegetation on surrounding land surface temperatures are scant, especially in India. Vegetation can decrease ambient air and surface temperatures due to evapotranspiration (ET). The higher the evapotranspiration, the lower the temperatures, and this ET is higher for denser vegetation than bare soil(Moreo, Laczniak, & Stannard, 2007). In this study, the observed reduction in built-up area LSTs with a green neighbor could be due to this evapotranspiration of vegetation creating an oasis effect(H Taha, 1997) and reducing neighboring LSTs. It could also be due to the shading of trees in urban areas. In a field study(Rosenfeld et al., 1995) conducted in Sacramento, trees reduced the cooling energy use by 30-35% when placed on the south and south-west facade of the building. In Athens(Papadakis, Tsamis, & Kyritsis, 2001), on a vertical wall, shading decreased the surface temperature by 8.5^0C compared to a surface directly exposed to solar radiation, and the ambient air temperature is 0.5^0C -3.0^0C cooler in the presence of trees. Future studies should focus on analyzing the type and quantity of vegetation in each of these urban areas to predict the vegetation characteristics reducing the surrounding built-up area LSTs more accurately.

7.4 CONCLUSION

Some of the key findings from this chapter are 1.) The newly (2007-2016) built-up areas in India are warmer (by 0.73^0C) compared to the old (before 2007); however, in the US, the more recent built-up areas are cooler (by 0.76^0C) than the old ones. 2.)At least one 30 m x 30m green vegetative (defined as NDVI $\geq$ 0.3) spatial neighbor within a 90 m x 90m built-up cluster can reduce the LST

of the built-up land use. The urban built-up areas with green neighbors are 1.3^0C and 2.4^0C cooler than those with built-up neighbors in India and the US, respectively. This study's findings show the opportunities to improve urban building and neighborhood design and development, focusing on their impact on the LSTs.

With the advent of various green building/community rating systems and energy and environmental standards for new construction, the newer built-up areas are expected to be 'greener.' They might result in lower LSTs than the old built-up areas. However, this wasn't the case in India. The country is going through rapid urbanization and changes in construction type. High-rise buildings (with greater than 10 floors) are replacing traditional low-rise residential buildings and mid-rise commercial buildings. High-rise commercial spaces with high window wall ratio and increased need for air-conditioning became common. Such changes might adversely impact LSTs. There are several measures that new construction and possibly the old building should also adopt to limit the increase in LSTs. Some of such measures include the addition of cool roofs, green roofs, green walls, and green spaces in urban areas. Building energy codes from both countries focus on such measures. However, based on these results, the adaption or the benefits of such building codes seem limited in India, leaving a potential for future improvements.

The second part of this study showed that having at least 30 m x 30m green areas with NDVI $\geq$ 0.3 within a 90m x 90m built-up area land parcel could reduce the LSTs of built-up areas. The study showed that while green vegetation reduces built-up area LSTs, it is not the same for non-green vegetation (NDVI < 0.3). Non-green and non-built-up neighbors result in higher LSTs than built-up or green neighbors in India. This finding, therefore, is essential, especially in the Indian context where maintenance of the 'greenness' of vegetation can be challenging with the existing high temperatures, pollution, and water scarcity. The evapotranspiration from green vegetative

surfaces impacts the micro-level air temperatures and could impact the LSTs of surrounding built-up surfaces. In coordination with the results from the first part of this chapter, such findings could mean that changing construction trends, which could also be reducing the vegetated areas with an individual's parcel of land, might be increasing urban built-up area LSTs in India. Due to all the existing limitations associated with establishing and maintaining green vegetation in urban areas of India, building surface treatments might provide greater returns. However, having 'green' vegetation closers to built-up areas could be less challenging in the US with the greater availability of land area, greener vegetation, and water resources compared to India. Therefore, policies and initiatives focusing on urban built-up surface greening/treatments in India could be more effective than proposals on increasing and maintaining urban greenery.

8 CONCLUSIONS

The primary goal of this research was to understand the differences, if any, in SUHI and its association with the urban built environment across highly populated cities in India compared to the US. Analysis of the possible similarities or differences in SUHI between these countries is expected to show the relevance and applicability of SUHI research methods and mitigation measures from well-researched locations of the world in the Indian context. This dissertation, therefore, presents a qualitative and quantitative multi-city comparative analysis of land surface temperatures (LST) and the urban-rural LST difference (ΔT). This chapter discusses this study's main findings and contributions and explains the limitations and future work scope.

8.1 RESEARCH CONTRIBUTION

This dissertation has four main research contributions.

1. This research determined the lack of relevance of the global conventional SUHI quantification method and definition in the Indian context.

In Indian SUHI studies that aim to assess the impact of urbanization, geographically delineating urban and rural areas cannot show the impact of urban built-up areas on daytime temperatures; instead shifts the focus toward rural greenery. The conventional SUHI quantification method showed daytime Surface Urban Cool Islands –cooler urban areas compared to rural surroundings in India. However, during the nighttime, SUHI was observed. Since the rural areas in India differ from those of North America or Europe from where UHI research originated, the conventional definition of UHI with an implicit assumption that rural areas are cooler than urban areas needs reevaluation in the Indian context**.**

2. This study showed that the conventional spectral indices do not differentiate built-up land use from other land covers, such as NPV, dry soil, and barren lands, that are dominant in India.

The popular built-up indices such as NDBI and IBI showed similar values across croplands, barren lands, and built-up land use in India, impacting the correlations in this study. The similar values across land use types such as concrete, NPV, and soil could be due to the similar spectral reflectance characteristics of these LULC types in the wavelengths used by conventional built-up indices to identify built-up land use. Therefore, such inadequate differentiation between LULC could also occur across similar locations with low vegetation or drought conditions experienced due to rapid urbanization or climate change. Further, the NDVI values across most of India's urban and rural areas are low (NDVI < 0.3), indicating non-green or no vegetation. Low NDVI values resulted in a weaker correlation between NDVI and LST. Such findings could miscommunicate the association between vegetation and LST or ΔT. Therefore, the conventional spectral indices have limitations in appropriately identifying the Indian LULC types.

3. Due to the existing limitations with conventional SUHI research metrics in the Indian context, this research set up an alternative approach to analyzing the spatial and temporal variation in urban built-up land use LSTs and their variation with land use of spatial neighbors.

This study analyzed the urban built-up LST in various scenarios based on the construction period and the land use of a spatial neighbor. In the first part, this study segregated each city's built-up land use into new (2007-2016) and old (before 2007) clusters and compared the average LST across these clusters. Such comparisons of urban built-up LSTs showed the outdoor thermal performance (LST in this case) of newly built-up areas compared to old ones.

Further, this research categorized built-up land use clusters based on the spatial neighbor land use and NDVI value. The study compared the average LSTs of built-up land use, built-up land use with at least one non-built-up neighbor, built-up land use with at least one green (NDVI $\geq$ 0.3) neighbor, and built-up with at least one non-green (NDVI $\geq$ 0.3) neighbor. This analysis primarily showed the benefit of having a green vegetative spatial neighbor on built-up area LST reduction.

4. This study presented a first-of-its-kind comparative analysis of LST and ΔT between a rapidly urbanizing country, India, and a developed nation, the US.

This study's comparative analysis showed that the LST and SUHI/SUCI trends differ between India and the US—prominent differences in existing LULC are associated with the LST and SUHI/SUCI trends. However, a temporal analysis of ΔT showed an increase in SUHI in India and the US over 15 years. This ΔT increase during the nighttime is higher in India than in the US. Differences in the urban built-up areas between India and the US could contribute to such higher nighttime ΔT increase in India compared to the US.

8.2 SUMMARY OF FINDINGS

This study's comparative analysis of SUHI showed that the findings from India and the US differ. While the US has been a well-researched location with several studies on UHI formation and mitigation measures for at least the last three decades, UHI research in India started gaining prominence only in the last decade. Therefore, this study attempts to address the existing knowledge gaps of UHI studies in India and the US and puts the findings from India in a global perspective through comparison with the US. Some of the key findings from this study are:

8.2.1 LST and ΔT in India and the US

During the daytime, most of the cities in India exhibit SUCI – urban areas are cooler compared to rural surroundings. However, in the US, the conventional SUHI – urban areas warmer than rural surroundings was observed. During the nighttime, SUHI exists across cities in India and the US, and this SUHI is higher in India. The differences in land use in rural areas between India and the US seem to impact the SUHI/SUCI trends. The prevalence of dry, barren, fallow, or non-photosynthetic vegetation land cover in rural areas of India is linked to higher rural LSTs in India during the daytime. Across India, the urban area LSTs are 10-12^{0}C higher than the US ones. Despite this, with the ΔT patterns, the urban areas seem cooler than the rural areas during the daytime, masking the impact of urban areas on urban temperatures.

8.2.2 LST and SUHI variation with vegetation (quantified using NDVI)

The correlation between NDVI and LST is stronger in the US during summer daytime than in India. Low or non-green vegetation, characterized by NDVI < 0.3, dominates urban and rural areas in India during summers and winters, weakening the correlations. For example, in India, the correlation between NDVI and LST strengthens in locations with at least 20% area as vegetation with NDVI ≥ 0.3. A correlation also existed between the NDVI of rural areas and ΔT. During the daytime, this correlation is negative, and at night, it is positive.

While analysis of different urban landscape layouts and green areas is of interest in landscape architecture, this study is one of the first studies that quantified the impact of vegetation on neighboring built-up area LSTs. The results showed that having at least one moderately green vegetative area of 30m x 30m with NDVI ≥ 0.3 within a 90m x 90m cluster of built-up area land use could reduce the LST of built-up land use. However, non-green vegetation (NDVI < 0.3) does not provide the same benefits. Further, this reduction in built-up area LSTs due to neighboring

vegetation land use is higher in the US than in India. Such higher LST reduction in the US could be because there is greener vegetation in the US compared to India, as the average NDVI in US cities is higher than in Indian cities.

8.2.3 Urban built-up land use- LST and ΔT

This study showed a positive correlation between the area of built-up land use and ΔT, which is stronger during nighttime than daytime and in India than in the US. The LST of urban built-up land use showed that in India, the newly (2007-2016) built-up urban areas are warmer than the older (< 2007) ones. In the US, however, it is the inverse. Though further analysis is needed to understand the reason for such observations, these results from India indicate scope for improvement of urban built-up areas to reduce LSTs. The LST of urban built-up land use also changed with the land use of the spatial neighbor. In India and the US, the average urban built-up land use LST of all the existing 90m x 90m clusters is lower than that of 90m x 90m built-up clusters with at least one non-green (quantified as NDVI < 0.3) land use within the cluster. Therefore, these results indicate that having densely built-up land use is better (lower LSTs) than having non-green land use between built-up areas.

8.2.4 Temporal change in SUHI

Research on the temporal trends of SUHI is nascent in India and the US due to a relatively recent (the early 2000s) availability of satellite data with high temporal resolution (day and night, every day). This research, therefore, adds to the existing limited literature on how SUHI changes over time. The temporal analysis from this study showed that ΔT increased over 15 years in both countries. This increase in ΔT over 15 years is statistically significant except for summer daytime in India and winter nighttime in the US. The nighttime increase in SUHI over 15 years is higher in India than in the US and is statistically significant. This higher nighttime increase in ΔT in India

could be due to higher built-up densities, higher population densities, and already higher temperatures than in the US.

8.3 IMPLICATIONS

Some of the implications of this study at a broader level are:

1. This research showed the need to develop more localized SUHI research methods and algorithms suitable for analyzing the impact of the urban built environment across LULC types like India. Increasing temperatures and drought conditions across several global locations (Carrão, Naumann, & Barbosa, 2016; Savelli, Rusca, Cloke, & Baldassarre, 2022)make this even more relevant and improve the applicability of such methods and algorithms across multiple locations.
2. While green vegetation reduced LSTs in both India and the US, the prevalence of green vegetation (NDVI > 0.3) itself seems questionable in India. This research showed that most of the locations in India have non-green or low-green vegetation (NDVI <0.3) in both urban and rural areas during summers and winters. Such observations, coupled with the already-known water scarcity (Mekonnen & Hoekstra, 2016) and air pollution effects(Chaudhary & Rathore, 2018; Pandey & Agrawal, 1994), show that maintenance of urban greenery could cause additional pressure on the water budget of urban India like shown in Adelaide, Australia(Nouri, Chavoshi Borujeni, & Hoekstra, 2019). Therefore, urban greening might not be as practical as in the US in reducing urban temperatures in India, especially during the non-monsoon seasons and drought years. In a country like India, to reduce ambient air and surface temperatures, developing vegetated lands and maintaining them could be more

challenging and less efficient than treating built-up surfaces and reducing anthropogenic rejections from buildings.

3. Increasing ΔT over time in both countries and the higher urban built-up LSTs in the newly built-up areas in India show the need and scope for improvement of the urban built environment and the UHI mitigation policies. Policymakers must reevaluate the UHI mitigation measures suggested in existing codes and standards and their adoption measures. This study also indicates a need for the design community to develop urban buildings and communities that address the increasing outdoor temperatures. Similar to buildings' indoor and energy performance, the outdoor thermal performance of buildings should be evaluated to create ‘micro-climate neutral’ or ‘zero UHI impact’ buildings. Coupling urban micro-climatic models with building whole-building simulations should become a new norm.
4. The findings of this study indicate that the surrounding land use could increase or decrease the urban built-up LSTs. Such a finding could affect the urban planning and design of the new urban communities.
5. Addressing the whole building performance through a systems integration approach could also be relevant in addressing the issues observed through this research. This study showed that vegetation decreases LSTs. However, urban greenery is scant in India. Since maintaining urban greenery in India could lead to water stress, improving and maintaining greenery at an individual building level or urban community scale could be more feasible through systems integration. Reusing greywater and rainwater collection are a few examples of reusing water from the site for irrigation. Therefore, designing buildings and communities integrating various systems could improve indoor and outdoor thermal

performance. Examples of systems integration in buildings include but are not limited to the Robert L Preger Intelligent Workplace (Hartkopf et al., 2017), the Phipps Conservatory, Pittsburgh, PA, and One PNC Plaza, Pittsburgh, PA.

8.4 LIMITATIONS AND FUTURE WORK

Canopy air temperatures (measured at 2m from ground level) directly impact the energy consumption of buildings (Santamouris, 2014b) and outdoor thermal comfort(Jamei, Rajagopalan, Seyedmahmoudian, & Jamei, 2016). The scope of this research is confined to studying land surface temperatures. However, to understand the interaction between the built environment and UHI, extending this SUHI analysis to a micro-scale analysis of canopy urban heat islands is essential. As of 2022, there aren't any SUHI and CUHI coupling studies for India. Integrating LSTs into urban micro-climate modeling (Bueno, 2012; Zhao et al., 2014)would be the next step toward analyzing UHI in India. Also, due to the existing heterogeneity across urban areas, urban parametrization is crucial for studying what type of built-up neighborhoods impact temperatures in what ways. This urban parametrization(Pigeon, Zibouche, Bueno, Le Bras, & Masson, 2014) is a parallel task with building and urban scale simulations. Such integration could help assess the local scale impacts of buildings and not limit them to a single canopy level UHI.

This research quantifies SUHI by customizing the conventional SUHI quantification method that geographically delineates urban and rural areas using concurrent LULC data. Replicating this study using other urban-rural definitions and more recent concepts, such as the Local Climate Zone (LCZ) classification system, might help understand the role of urban built-environment on the temperatures in India compared with the US.

Further, in this research, the approach presented to estimate the variation in urban built-up land use is applied only to daytime. Though daytime is when the conventional ΔT calculation methods showed no SUHI effect in India, it is still relevant to understand the urban built-up area LST during the night and other seasons. Since Landsat 8 high spatial resolution data are only available for daytime, this analysis is limited to daytime in this dissertation. Other local high-resolution satellite data should be explored to extend this analysis to nighttime. Conducting the whole building energy simulations coupled with urban-scale climatic models is another way to address this limitation. It is also essential for future researchers to understand why and how the newly built-up areas in India are warmer than old ones and vice versa in the US. Quantifying the built-up area characteristics, such as albedo, might provide insights into this. However, a neighborhood-level analysis might be needed to identify the built-up area characteristics that influence LSTs precisely.

Lastly, it could be beneficial to establish a correlation between LST and the air temperatures at the canopy level and compare them with the meteorological weather station data. Such analysis would help interpret how the meteorological air temperatures - used across building energy modeling (most times) and perceived by the public to comprehend weather- are similar or different from the actual urban area temperatures.

REFERENCES

Akbari, H, Pomerantz, M., & Taha, H. (2001). Cool surfaces and shade trees to reduce energy use and improve air quality in urban areas. *Solar Energy*, *70*(3), 295–310. https://doi.org/10.1016/S0038-092X(00)00089-X

Akbari, Hashem, & Kolokotsa, D. (2016). Three decades of urban heat islands and mitigation technologies research. *Energy and Buildings*, *133*, 834–842. https://doi.org/10.1016/j.enbuild.2016.09.067

Ali, J. M., Marsh, S. H., & Smith, M. J. (2017). A comparison between London and Baghdad surface urban heat islands and possible engineering mitigation solutions. *Sustainable Cities and Society*, *29*, 159–168. https://doi.org/10.1016/J.SCS.2016.12.010

Alves, E. (2016). Seasonal and Spatial Variation of Surface Urban Heat Island Intensity in a Small Urban Agglomerate in Brazil. *Climate*, *4*(4), 61. https://doi.org/10.3390/cli4040061

AppEEARS Team. (2023). Application for Extracting and Exploring Analysis Ready Samples (AppEEARS) Ver 3.21. Retrieved from NASA EOSDIS Land Processes Distributed Active Archive Center (LP DAAC), USGS/Earth Resources Observation and Science (EROS) Center,Sioux Falls, South Dakota, USA website: https://appeears.earthdatacloud.nasa.gov

Arias, P.A., N. Bellouin, E. Coppola, R.G. Jones, G. Krinner, J. Marotzke, V. Naik, M.D. Palmer, G.-K. Plattner, J. R., M. Rojas, J. Sillmann, T. Storelvmo, P.W. Thorne, B. Trewin, K. Achuta Rao, B. Adhikary, R.P. Allan, K. Armour, G. B., R. Barimalala, S. Berger, J.G. Canadell, C. Cassou, A. Cherchi, W. Collins, W.D. Collins, S.L. Connors, S. Corti, F. C., F.J. Dentener, C. Dereczynski, A. Di Luca, A. Diongue Niang, F.J. Doblas-Reyes, A. Dosio, H. Douville, F. E., V. Eyring, E. Fischer, P. Forster, B. Fox-Kemper, J.S. Fuglestvedt, J.C. Fyfe, N.P. Gillett, L. Goldfarb, I. G., J.M. Gutierrez, R. Hamdi, E. Hawkins, H.T. Hewitt, P. Hope, A.S. Islam, C. Jones, D.S. Kaufman, R.E. Kopp, Y. K., … K. von Schuckmann, S. Zaehle, X. Zhang, and K. Z. (2021). Technical Summary. In Climate Change 2021: The Physical Science Basis. Contribution of Working Group I to the Sixth Assessment Report of the Intergovernmental Panel on Climate Change [Masson-Delmotte, V., P. Zhai, A. Pirani, S.L. Connors, C. Péan, S. Berg. In *Climate Change and Land: an IPCC special report on climate change, desertification, land degradation, sustainable land management, food security, and greenhouse gas fluxes in terrestrial ecosystems*. Cambridge, United Kingdom and New York, NY, USA: Cambridge University Press.

As-syakur, A. R., Adnyana, I. W. S., Arthana, I. W., & Nuarsa, I. W. (2012). Enhanced Built-Up and Bareness Index (EBBI) for Mapping Built-Up and Bare Land in an Urban Area. *Remote Sensing*, *4*(10), 2957–2970. https://doi.org/10.3390/rs4102957

ASHRAE. (2020). *ASHRAE Standard 169-2020. Climatic Data for Building Design Standards*.

Attri, S. D., & Tyagi, A. (2010). Climate profile of India. *Environment Meteorology, India Meteorological Department*, 1–122.

Baldridge, A. M., Hook, S. J., Grove, C. I., & Rivera, G. (2009). The ASTER spectral library

version 2.0. *Remote Sensing of Environment*, *113*(4), 711–715. https://doi.org/10.1016/j.rse.2008.11.007

Barsi, J. A., Schott, J. R., Palluconi, F. D., & Hook, S. J. (2005). Validation of a web-based atmospheric correction tool for single thermal band instruments. In J. J. Butler (Ed.), *Earth Observing Systems X* (Vol. 5882, pp. 136–142). https://doi.org/10.1117/12.619990

Bechtel, B., Alexander, P. J., Böhner, J., Ching, J., Conrad, O., Feddema, J., … Stewart, I. (2015). Geo-Information Mapping Local Climate Zones for a Worldwide Database of the Form and Function of Cities. *ISPRS Int. J. Geo-Inf*, *4*, 199–219. https://doi.org/10.3390/ijgi4010199

Bechtel, B., Demuzere, M., Mills, G., Zhan, W., Sismanidis, P., Small, C., & Voogt, J. (2019). SUHI analysis using Local Climate Zones—A comparison of 50 cities. *Urban Climate*, *28*, 100451. https://doi.org/10.1016/j.uclim.2019.01.005

Bechtel, B., Zakšek, K., Oßenbrügge, J., Kaveckis, G., & Böhner, J. (2017). Towards a satellite based monitoring of urban air temperatures. *Sustainable Cities and Society*, *34*(April), 22–31. https://doi.org/10.1016/j.scs.2017.05.018

BEE NITI. (2017). Roadmap To Fast Track Adoption and Implementation of Energy Conservation Building Code (ECBC) At the Urban and Local Level. *Alliance for an Energy Efficient Economy (AEEE)*, 1–40. Retrieved from http://indiaenergy.gov.in/roadmap-to-fastrack-adoption-and-implementation-of-ecbc-at-the-urban-and-local-level/

Besir, A. B., & Cuce, E. (2018). Green roofs and facades: A comprehensive review. *Renewable and Sustainable Energy Reviews*, *82*, 915–939. https://doi.org/10.1016/J.RSER.2017.09.106

Bhatnagar, M., Mathur, J., & Garg, V. (2018). Determining base temperature for heating and cooling degree-days for India. *Journal of Building Engineering*, *18*, 270–280. https://doi.org/10.1016/J.JOBE.2018.03.020

Bhuvan/ISRO. (n.d.). OGC Web Service Bhuvan-Thematic Services LULC250K_1617. Retrieved May 5, 2019, from https://bhuvan-ras2.nrsc.gov.in/cgi-bin/LULC250K.exe

Borbora, J., Das, A. K., Sah, R. K., & Hazarika, N. (2018). Assessment of Urban Heat Island Effect in Guwahati—A Remote Sensing Based Study. In S. Sarma, AK and Singh, VP and Bhattacharjya, RK and Kartha (Ed.), *URBAN ECOLOGY, WATER QUALITY AND CLIMATE CHANGE* (pp. 149–156). https://doi.org/10.1007/978-3-319-74494-0_11

Bowler, D. E., Buyung-Ali, L., Knight, T. M., & Pullin, A. S. (2010). Urban greening to cool towns and cities: A systematic review of the empirical evidence. *Landscape and Urban Planning*, *97*(3), 147–155. https://doi.org/10.1016/J.LANDURBPLAN.2010.05.006

Buchhorn, M., Lesiv, M., Tsendbazar, N.-E., Herold, M., Bertels, L., & Smets, B. (2020). Copernicus Global Land Cover Layers—Collection 2. *Remote Sensing*, *12*(6), 1044. https://doi.org/10.3390/rs12061044

Budhiraja, B., Pathak, P., & Agrawal, G. (2017). *Spatio-temporal variability of urban heat islands in local climate zones of Delhi-NCR*. *1043110*(October 2017), 37. https://doi.org/10.1117/12.2280253

Bueno, B. (2012). Study and prediction of the energy interactions between buildings and the urban

climate. *PhD Thesis*.

Cai, M., Ren, C., Xu, Y., Lau, K. K. L., & Wang, R. (2018). Investigating the relationship between local climate zone and land surface temperature using an improved WUDAPT methodology – A case study of Yangtze River Delta, China. *Urban Climate*, *24*, 485–502. https://doi.org/10.1016/J.UCLIM.2017.05.010

Cai, Y., Zhang, H., Zheng, P., & Pan, W. (2016). Quantifying the Impact of Land use/Land Cover Changes on the Urban Heat Island: A Case Study of the Natural Wetlands Distribution Area of Fuzhou City, China. *Wetlands*, *36*(2), 285–298. https://doi.org/10.1007/s13157-016-0738-7

Carrão, H., Naumann, G., & Barbosa, P. (2016). Mapping global patterns of drought risk: An empirical framework based on sub-national estimates of hazard, exposure and vulnerability. *Global Environmental Change*, *39*, 108–124. https://doi.org/10.1016/J.GLOENVCHA.2016.04.012

Chakraborty, S., Maity, I., Dadashpoor, H., Novotnỳ, J., & Banerji, S. (2022). Building in or out? Examining urban expansion patterns and land use efficiency across the global sample of 466 cities with million+ inhabitants. *Habitat International*, *120*, 102503. https://doi.org/10.1016/J.HABITATINT.2021.102503

Chakraborty, T., & Lee, X. (2019). A simplified urban-extent algorithm to characterize surface urban heat islands on a global scale and examine vegetation control on their spatiotemporal variability. *International Journal of Applied Earth Observation and Geoinformation*, *74*(September 2018), 269–280. https://doi.org/10.1016/j.jag.2018.09.015

Chandel, S. S., Sharma, A., & Marwaha, B. M. (2016). Review of energy efficiency initiatives and regulations for residential buildings in India. *Renewable and Sustainable Energy Reviews*, *54*, 1443–1458. https://doi.org/10.1016/J.RSER.2015.10.060

Chen, H., Ooka, R., Huang, H., & Tsuchiya, T. (2009). Study on mitigation measures for outdoor thermal environment on present urban blocks in Tokyo using coupled simulation. *Building and Environment*, *44*(11), 2290–2299. https://doi.org/10.1016/J.BUILDENV.2009.03.012

Chen, L., Jiang, R., & Xiang, W.-N. (2016). Surface Heat Island in Shanghai and Its Relationship with Urban Development from 1989 to 2013. *Advances in Meteorology*, *2016*, 9782686. https://doi.org/10.1155/2016/9782686

Chen, W., Zhang, Y., Pengwang, C., & Gao, W. (2017). Evaluation of Urbanization Dynamics and its Impacts on Surface Heat Islands: A Case Study of Beijing, China. *Remote Sensing*, *9*(5), 453. https://doi.org/10.3390/rs9050453

Chen, X.-L., Zhao, H.-M., Li, P.-X., & Yin, Z.-Y. (2006). Remote sensing image-based analysis of the relationship between urban heat island and land use/cover changes. *Remote Sensing of Environment*, *104*(2), 133–146. https://doi.org/10.1016/J.RSE.2005.11.016

Cheval, S., & Dumitrescu, A. (2015). The summer surface urban heat island of Bucharest (Romania) retrieved from MODIS images. *Theoretical and Applied Climatology*, *121*(3), 631–640. https://doi.org/10.1007/s00704-014-1250-8

Choi, Y.-Y., Suh, M.-S., & Park, K.-H. (2014). Assessment of Surface Urban Heat Islands over

Three Megacities in East Asia Using Land Surface Temperature Data Retrieved from COMS. *Remote Sensing*, *6*(6), 5852–5867. https://doi.org/10.3390/rs6065852

Chun, B., & Guldmann, J. M. (2018). Impact of greening on the urban heat island: Seasonal variations and mitigation strategies. *Computers, Environment and Urban Systems*, *71*, 165–176. https://doi.org/10.1016/J.COMPENVURBSYS.2018.05.006

Ciara, N. (2022). Western Architecture is Making India's Heatwaves Worse. Retrieved from TIME website: https://time.com/6176998/india-heatwaves-western-architecture/

Clinton, N., & Gong, P. (2013). MODIS detected surface urban heat islands and sinks: Global locations and controls. *Remote Sensing of Environment*, *134*, 294–304. https://doi.org/10.1016/j.rse.2013.03.008

Copernicus. (2018). Product User Manual. *Copernicus Global Land Operations "Vegetation and Energy" "CGLOPS-1,"* 1–51. Retrieved from https://land.copernicus.eu/global/sites/cgls.vito.be/files/products/CGLOPS1_PUM_SWIV3-SWI10-SWI-TS_I2.60.pdf

Copernicus Global Land Service. (2018). Soil Water Indiex. Retrieved from Soil Water Index website: https://land.copernicus.eu/global/products/swi

Cui, Y., Xu, X., Dong, J., & Qin, Y. (2016). Influence of Urbanization Factors on Surface Urban Heat Island Intensity: A Comparison of Countries at Different Developmental Phases. *Sustainability*, *8*(8), 706. https://doi.org/10.3390/su8080706

Das, M., & Das, A. (2020). Assessing the relationship between local climatic zones (LCZs) and land surface temperature (LST) – A case study of Sriniketan-Santiniketan Planning Area (SSPA), West Bengal, India. *Urban Climate*, *32*, 100591. https://doi.org/10.1016/J.UCLIM.2020.100591

de Jong, R., de Bruin, S., de Wit, A., Schaepman, M. E., & Dent, D. L. (2011). Analysis of monotonic greening and browning trends from global NDVI time-series. *Remote Sensing of Environment*, *115*(2), 692–702. https://doi.org/10.1016/J.RSE.2010.10.011

Deilami, K., Kamruzzaman, M., & Liu, Y. (2018). Urban heat island effect: A systematic review of spatio-temporal factors, data, methods, and mitigation measures. *International Journal of Applied Earth Observation and Geoinformation*, *67*, 30–42. https://doi.org/10.1016/J.JAG.2017.12.009

Demographia. (2016). *Demographia World Urban Areas*. Retrieved from http://demographia.com/db-worldua-intro.pdf

Dhawan, V. (2017). Water and Agriculture in India. *Background Paper for the South Asia Expert Panel during the Global Forum for Food and Agriculture*, 28. Retrieved from https://www.oav.de/fileadmin/user_upload/5_Publikationen/5_Studien/170118_Study_Water_Agriculture_India.pdf

Dian, C., Pongrácz, R., Dezső, Z., & Bartholy, J. (2020). Annual and monthly analysis of surface urban heat island intensity with respect to the local climate zones in Budapest. *Urban Climate*, *31*, 100573. https://doi.org/10.1016/J.UCLIM.2019.100573

References

Dimitry, B. (n.d.). *"Urban Sprawl, Jaipur, India" by Dimitry B is licensed under CC BY 2.0.* Retrieved from https://openverse.org/image/8e39d562-f8e9-4794-ae5e-ae176551644c?q=urban India

Dobrovolný, P. (2013). The surface urban heat island in the city of Brno (Czech Republic) derived from land surface temperatures and selected reasons for its spatial variability. *Theoretical and Applied Climatology*, *112*(1), 89–98. https://doi.org/10.1007/s00704-012-0717-8

Donghwan, G., Yong, K. H., & Hyoungsub, K. (2015). LEED, its efficacy in regional context: Finding a relationship between regional measurements and urban temperature. *Energy and Buildings*, *86*, 687–691. https://doi.org/10.1016/j.enbuild.2014.10.066

Eldesoky, A. H. M., Gil, J., & Pont, M. B. (2021). The suitability of the urban local climate zone classification scheme for surface temperature studies in distinct macroclimate regions. *Urban Climate*, *37*, 100823. https://doi.org/10.1016/J.UCLIM.2021.100823

Energy.Gov. (2022). Building Energy Codes Program. Retrieved from Office of Energy Efficiency and Renewable Energy website: https://www.energycodes.gov/state-portal

Evans, M., Roshchanka, V., & Graham, P. (2017). An international survey of building energy codes and their implementation. *Journal of Cleaner Production*, *158*, 382–389. https://doi.org/10.1016/J.JCLEPRO.2017.01.007

Fahmy, M., Ibrahim, Y., Hanafi, E., & Barakat, M. (2018). Would LEED-UHI greenery and high albedo strategies mitigate climate change at neighborhood scale in Cairo, Egypt? *Building Simulation*, *11*(6), 1273–1288. https://doi.org/10.1007/s12273-018-0463-7

Fan, C., Myint, S. W., Kaplan, S., Middel, A., Zheng, B., Rahman, A., … Blumberg, D. G. (2017). Understanding the impact of urbanization on surface urban heat Islands-A longitudinal analysis of the oasis effect in subtropical desert cities. *Remote Sensing*, *9*(7). https://doi.org/10.3390/rs9070672

Faqe Ibrahim, G. (2017). Urban Land Use Land Cover Changes and Their Effect on Land Surface Temperature: Case Study Using Dohuk City in the Kurdistan Region of Iraq. *Climate*, *5*(1), 13. https://doi.org/10.3390/cli5010013

Faroughi, M., Karimimoshaver, M., Aram, F., Solgi, E., Mosavi, A., Nabipour, N., & Chau, K. W. (2020). Computational modeling of land surface temperature using remote sensing data to investigate the spatial arrangement of buildings and energy consumption relationship. *Engineering Applications of Computational Fluid Mechanics*, *14*(1), 254–270. https://doi.org/10.1080/19942060.2019.1707711

Fu, P., & Weng, Q. (2018). Variability in annual temperature cycle in the urban areas of the United States as revealed by MODIS imagery. *ISPRS Journal of Photogrammetry and Remote Sensing*, *146*, 65–73. https://doi.org/10.1016/J.ISPRSJPRS.2018.09.003

GBIG. (2023). The Green Building Information Gateway. Retrieved September 2, 2023, from https://www.gbig.org/search/advanced

Geletič, J., Lehnert, M., & Dobrovolný, P. (2016). Land Surface Temperature Differences within Local Climate Zones, Based on Two Central European Cities. *Remote Sensing*, *8*(10), 788. https://doi.org/10.3390/rs8100788

References

Giridharan, R., & Emmanuel, R. (2018). The impact of urban compactness, comfort strategies and energy consumption on tropical urban heat island intensity: A review. *Sustainable Cities and Society*, *40*, 677–687. https://doi.org/10.1016/j.scs.2018.01.024

Gong, P., Li, X., Wang, J., Bai, Y., Chen, B., Hu, T., … Zhou, Y. (2020). Annual maps of global artificial impervious area (GAIA) between 1985 and 2018. *Remote Sensing of Environment*, *236*(August 2019), 111510. https://doi.org/10.1016/j.rse.2019.111510

Good, E. J., Ghent, D. J., Bulgin, C. E., & Remedios, J. J. (2017). A spatiotemporal analysis of the relationship between near-surface air temperature and satellite land surface temperatures using 17 years of data from the ATSR series. *Journal of Geophysical Research: Atmospheres*, *122*(17), 9185–9210. https://doi.org/10.1002/2017JD026880

Grover, A., & Singh, R. (2015). Analysis of Urban Heat Island (UHI) in Relation to Normalized Difference Vegetation Index (NDVI): A Comparative Study of Delhi and Mumbai. *Environments*, *2*(4), 125–138. https://doi.org/10.3390/environments2020125

Güneralp, B., Reba, M., Hales, B. U., Wentz, E. A., & Seto, K. C. (2020). Trends in urban land expansion, density, and land transitions from 1970 to 2010: A global synthesis. *Environmental Research Letters*, *15*(4). https://doi.org/10.1088/1748-9326/ab6669

Gupta, N., Mathew, A., & Khandelwal, S. (2019). Analysis of cooling effect of water bodies on land surface temperature in nearby region: A case study of Ahmedabad and Chandigarh cities in India. *The Egyptian Journal of Remote Sensing and Space Science*, *22*(1), 81–93. https://doi.org/10.1016/J.EJRS.2018.03.007

Haashemi, S., Weng, Q., Darvishi, A., & Alavipanah, S. K. (2016). Seasonal variations of the surface urban heat Island in a semi-arid city. *Remote Sensing*, *8*(4). https://doi.org/10.3390/rs8040352

Hari, V., Dharmasthala, S., Koppa, A., Karmakar, S., & Kumar, R. (2021). Climate hazards are threatening vulnerable migrants in Indian megacities. *Nature Climate Change*, *11*(8), 636–638. https://doi.org/10.1038/s41558-021-01105-7

Hartkopf, V., Loftness, V., Aziz, A., Lam, K. P., Lee, S., Cochran, E., & Lasternas, B. (2017). The Robert L. Preger Intelligent WorkplaceTM. The Living Laboratory at Carnegie Mellon University. In *Creating the Productive Workplace* (p. 30).

Heinl, M., Hammerle, A., Tappeiner, U., & Leitinger, G. (2015). Determinants of urban–rural land surface temperature differences – A landscape scale perspective. *Landscape and Urban Planning*, *134*, 33–42. https://doi.org/10.1016/J.LANDURBPLAN.2014.10.003

Hooker, J., Duveiller, G., & Cescatti, A. (2018). Data descriptor: A global dataset of air temperature derived from satellite remote sensing and weather stations. *Scientific Data*, *5*, 1–11. https://doi.org/10.1038/sdata.2018.246

Howard, L. (2012). *The Climate of London*. https://doi.org/10.1017/CBO9781139226905

Imhoff, M. L., Zhang, P., Wolfe, R. E., & Bounoua, L. (2010). Remote sensing of the urban heat island effect across biomes in the continental USA. *Remote Sensing of Environment*, *114*(3), 504–513. https://doi.org/10.1016/j.rse.2009.10.008

References

Indian Meteorological Department. (2019). *Weather Forecasting - Glossary*. 1–13. Retrieved from http://www.imdpune.gov.in/Weather/reports.html

Jiang, Y., Fu, P., & Weng, Q. (2015). Assessing the impacts of urbanization-associated land use/cover change on land surface temperature and surface moisture: A case study in the midwestern united states. *Remote Sensing*, *7*(4), 4880–4898. https://doi.org/10.3390/rs70404880

Kaimaris, D., & Patias, P. (2016). Identification and Area Measurement of the Built-up Area with the Built-up Index (BUI). *International Journal of Advanced Remote Sensing and GIS*, *5*(1), 1844–1858. https://doi.org/10.23953/cloud.ijarsg.64

Kashyap, R., Pandey, A. C., & Kuttippurath, J. (2022). Photosynthetic trends in India derived from remote sensing measurements during 2000–2019: vegetation dynamics and key climate drivers. *Geocarto International*, *37*(26), 11813–11829. https://doi.org/10.1080/10106049.2022.2060325

Kawamura, M., Jyamanna, S., & Tsujiko, Y. (1996). Relation between Social and Environmental Conditions in Colombo, Srilanka and the Urban Index estimated By Satellite Remote Sensing Data. *International Archives of the Photogrammetry and Remote Sensing*, *31*(Part B7), 321–326. https://doi.org/10.1007/978-981-13-3068-1_7

Kikon, N., Singh, P., Singh, S. K., & Vyas, A. (2016). Assessment of urban heat islands (UHI) of Noida City, India using multi-temporal satellite data. *Sustainable Cities and Society*, *22*, 19–28. https://doi.org/10.1016/J.SCS.2016.01.005

Kottek, M., Grieser, J., Beck, C., Rudolf, B., & Rubel, F. (2006). World map of the Köppen-Geiger climate classification updated. *Meteorologische Zeitschrift*, *15*(3), 259–263. https://doi.org/10.1127/0941-2948/2006/0130

Kumar, R., Mishra, V., Buzan, J., Kumar, R., Shindell, D., & Huber, M. (2017). Doinamnt control of agriculture and irrigation on urban heat island in India. *Scientific Reports*, *7*(1), 14054. https://doi.org/10.1038/s41598-017-14213-2

Kwatra, S., Madan, P., & Korsh, J. (2021). Constructing Change with Building Energy Codes in India. Retrieved September 2, 2023, from NRDC.ORG website: https://www.nrdc.org/experts/sameer-kwatra/constructing-change-building-energy-codes-india

Lall, B. A., Talwar, S., Shetty, S., & Singh, M. (2014). *Scoping study for policy initiatives to minimise urban heat island effect for low carbon urban growth*. 1–79. Retrieved from https://shaktifoundation.in/wp-content/uploads/2017/06/Scoping-Study-for-Policy-Initiatives-to-Minimize-Urban-Heat-Island-effect1.pdf

Lazzarini, M., Marpu, P. R., & Ghedira, H. (2013). Temperature-land cover interactions: The inversion of urban heat island phenomenon in desert city areas. *Remote Sensing of Environment*, *130*, 136–152. https://doi.org/10.1016/j.rse.2012.11.007

Lee, J. A., Lee, S. S., & Chi, K. H. (2010). Development of an urban classification method using a built-up index. *International Conference on Electric Power Systems, High Voltages, Electric Machines, International Conference on Remote Sensing - Proceedings*, 39–43.

References

Lehnert, M., Savić, S., Milošević, D., Dunjić, J., & Geletič, J. (2021). Mapping Local Climate Zones and Their Applications in European Urban Environments: A Systematic Literature Review and Future Development Trends. *ISPRS International Journal of Geo-Information*, *10*(4), 260. https://doi.org/10.3390/ijgi10040260

Li, J., Song, C., Cao, L., Zhu, F., Meng, X., & Wu, J. (2011). Impacts of landscape structure on surface urban heat islands: A case study of Shanghai, China. *Remote Sensing of Environment*, *115*(12), 3249–3263. https://doi.org/10.1016/J.RSE.2011.07.008

Li, N., Yang, J., Qiao, Z., Wang, Y., Miao, S., Nichol, J., & Wang, Q. (2021). *remote sensing Urban Thermal Characteristics of Local Climate Zones and Their Mitigation Measures across Cities in Different Climate Zones of China*. https://doi.org/10.3390/rs13081468

Li, W., Migliavacca, M., Forkel, M., Denissen, J. M. C., Reichstein, M., Yang, H., … Orth, R. (2022). Widespread increasing vegetation sensitivity to soil moisture. *Nature Communications*, *13*(1), 1–9. https://doi.org/10.1038/s41467-022-31667-9

Li, X., Zhou, Y., Asrar, G. R., Imhoff, M., & Li, X. (2017). The surface urban heat island response to urban expansion: A panel analysis for the conterminous United States. *Science of The Total Environment*, *605–606*, 426–435. https://doi.org/10.1016/J.SCITOTENV.2017.06.229

Li, Z. L., Tang, B. H., Wu, H., Ren, H., Yan, G., Wan, Z., … Sobrino, J. A. (2013). Satellite-derived land surface temperature: Current status and perspectives. *Remote Sensing of Environment*, *131*, 14–37. https://doi.org/10.1016/j.rse.2012.12.008

LINDSEY, R., & DAHLMAN, L. (2023). Climate Change: Global Temperatures. Retrieved April 2, 2023, from NOAA Climate.gov website: https://www.climate.gov/news-features/understanding-climate/climate-change-global-temperature

Liu, K., Su, H., Zhang, L., Yang, H., Zhang, R., & Li, X. (2015). Analysis of the Urban Heat Island Effect in Shijiazhuang, China Using Satellite and Airborne Data. *Remote Sensing*, *7*(4), 4804–4833. https://doi.org/10.3390/rs70404804

Liu, L., & Zhang, Y. (2011). Urban Heat Island Analysis Using the Landsat TM Data and ASTER Data: A Case Study in Hong Kong. *Remote Sensing*, *3*(7), 1535–1552. https://doi.org/10.3390/rs3071535

Liu, Z., Zhan, W., Bechtel, B., Voogt, J., Lai, J., Chakraborty, T., … Lee, X. (2022). Surface warming in global cities is substantially more rapid than in rural background areas. *Communications Earth & Environment*, *3*(1), 219. https://doi.org/10.1038/s43247-022-00539-x

Ma, Y., Kuang, Y., & Huang, N. (2010). Coupling urbanization analyses for studying urban thermal environment and its interplay with biophysical parameters based on TM/ETM+ imagery. *International Journal of Applied Earth Observation and Geoinformation*, *12*(2), 110–118. https://doi.org/10.1016/J.JAG.2009.12.002

Martins, J. P., Trigo, I., & Freitas, S. C. e. (2020). Copernicus Global Land Operations "Vegetation and Energy" "CGLOPS-1." *Copernicus Global Land Operations*, 1–93. https://doi.org/10.5281/zenodo.3938963.PU

Mathew, A., Khandelwal, S., & Kaul, N. (2016). Spatial and temporal variations of urban heat

island effect and the effect of percentage impervious surface area and elevation on land surface temperature: Study of Chandigarh city, India. *Sustainable Cities and Society*, *26*, 264–277. https://doi.org/10.1016/J.SCS.2016.06.018

Mathew, A., Khandelwal, S., & Kaul, N. (2017). Investigating spatial and seasonal variations of urban heat island effect over Jaipur city and its relationship with vegetation, urbanization and elevation parameters. *Sustainable Cities and Society*, *35*, 157–177. https://doi.org/10.1016/J.SCS.2017.07.013

Mathew, A., Khandelwal, S., & Kaul, N. (2018). Analysis of diurnal surface temperature variations for the assessment of surface urban heat island effect over Indian cities. *Energy and Buildings*, *159*, 271–295. https://doi.org/10.1016/J.ENBUILD.2017.10.062

Mathew, A., Sreekumar, S., Khandelwal, S., & Kumar, R. (2019). Prediction of land surface temperatures for surface urban heat island assessment over Chandigarh city using support vector regression model. *Solar Energy*, *186*, 404–415. https://doi.org/10.1016/J.SOLENER.2019.04.001

Meerdink, S. K., Hook, S. J., Roberts, D. A., & Abbott, E. A. (2019). The ECOSTRESS spectral library version 1.0. *Remote Sensing of Environment*, *230*(October 2018), 111196. https://doi.org/10.1016/j.rse.2019.05.015

Mishra, A., & Liu, S. C. (2014). Changes in precipitation pattern and risk of drought over India in the context of global warming. *Journal of Geophysical Research: Atmospheres*, *119*(13), 7833–7841. https://doi.org/10.1002/2014JD021471

MODIS. (n.d.). MODIS. Retrieved from MODIS Land Surface Temperature and Emissivity (MOD11) website: https://modis.gsfc.nasa.gov/data/dataprod/mod11.php

Mohammad, P., & Goswami, A. (2021). Quantifying diurnal and seasonal variation of surface urban heat island intensity and its associated determinants across different climatic zones over Indian cities. *GIScience \& Remote Sensing*, *0*(0), 1–27. https://doi.org/10.1080/15481603.2021.1940739

Mohanta, K., & Sharma, L. K. (2017). Assessing the impacts of urbanization on the thermal environment of Ranchi City (India) using geospatial technology. *Remote Sensing Applications: Society and Environment*, *8*(August 2016), 54–63. https://doi.org/10.1016/j.rsase.2017.07.008

Moreo, M. T., Laczniak, R. J., & Stannard, D. I. (2007). Evapotranspiration Rate Measurements of Vegetation Typical of Ground-Water Discharge Areas in the Basin and Range Carbonate-Rock Aquifer System , White Pine County , Nevada and Adjacent Areas in Nevada and Utah , September 2005 – August 2006. *U.S. Geological Survey Scientific Investigations Report 2007-5078*, (August 2006), 36.

NASA. (2019). Atmospheric Correction Parameter Calculator. Retrieved from https://atmcorr.gsfc.nasa.gov/

NASA Landsat Science. (2020). Landsat 8. Retrieved April 3, 2023, from Landsat 8 website: https://landsat.gsfc.nasa.gov/satellites/landsat-8/

NASA LDAS. (2022). GLDAS Soil Land Surface. Retrieved from NASA Land Data Assimilation

System website: https://ldas.gsfc.nasa.gov/gldas/soils

Nejat, P., Jomehzadeh, F., Taheri, M. M., Gohari, M., & Muhd, M. Z. (2015). A global review of energy consumption, CO2 emissions and policy in the residential sector (with an overview of the top ten CO2 emitting countries). *Renewable and Sustainable Energy Reviews*, *43*, 843–862. https://doi.org/10.1016/J.RSER.2014.11.066

NOAA. (2016). National Weather Service, Climate Prediction Center, Degree Day Statistics. Retrieved February 10, 2020, from https://www.cpc.ncep.noaa.gov/products/analysis_monitoring/cdus/degree_days/

NOAA. (2021). Meteorological Versus Astronomical Seasons. Retrieved from National Centers for Environmental Information website: https://www.ncei.noaa.gov/news/meteorological-versus-astronomical-seasons#pagetop

Nouri, H., Chavoshi Borujeni, S., & Hoekstra, A. Y. (2019). The blue water footprint of urban green spaces: An example for Adelaide, Australia. *Landscape and Urban Planning*, *190*, 103613. https://doi.org/10.1016/J.LANDURBPLAN.2019.103613

Oke, T. R. (1987). Boundary Layer Climates. In *Boundary Layer Climates* (2nd ed.). https://doi.org/10.4324/9780203407219

Oke, T. R. (1988). The urban energy balance. *Prog. Phys. Geog.*, *12*(4), 471.

Pangaluru, K., Velicogna, I., Geruo, A., Mohajerani, Y., Ciracì, E., Charakola, S., … Rao, S. V. B. (2019). Soil moisture variability in India: Relationship of land surface-atmosphere fields using maximum covariance analysis. *Remote Sensing*, *11*(3). https://doi.org/10.3390/rs11030335

Papadakis, G., Tsamis, P., & Kyritsis, S. (2001). An experimental investigation of the effect of shading with plants for solar control of buildings. *Energy and Buildings*, *33*(8), 831–836. https://doi.org/10.1016/S0378-7788(01)00066-4

Peng, S., Piao, S., Ciais, P., Friedlingstein, P., Ottle, C., Bréon, F.-M., … Myneni, R. B. (2012). Surface Urban Heat Island Across 419 Global Big Cities. *Environmental Science & Technology*, *46*(2), 696–703. https://doi.org/10.1021/es2030438

Peres, L. de F., Lucena, A. J. de, Rotunno Filho, O. C., & França, J. R. de A. (2018). The urban heat island in Rio de Janeiro, Brazil, in the last 30 years using remote sensing data. *International Journal of Applied Earth Observation and Geoinformation*, *64*, 104–116. https://doi.org/10.1016/J.JAG.2017.08.012

Pigeon, G., Zibouche, K., Bueno, B., Le Bras, J., & Masson, V. (2014). Improving the capabilities of the Town Energy Balance model with up-to-date building energy simulation algorithms: an application to a set of representative buildings in Paris. *Energy and Buildings*, *76*, 1–14. https://doi.org/10.1016/J.ENBUILD.2013.10.038

Raj, S., Paul, S. K., Chakraborty, A., & Kuttippurath, J. (2020). Anthropogenic forcing exacerbating the urban heat islands in India. *Journal of Environmental Management*, *257*(October 2019), 110006. https://doi.org/10.1016/j.jenvman.2019.110006

Rasul, A., Balzter, H., & Smith, C. (2015). Spatial variation of the daytime Surface Urban Cool

Island during the dry season in Erbil, Iraqi Kurdistan, from Landsat 8. *Urban Climate*, *14*, 176–186. https://doi.org/10.1016/J.UCLIM.2015.09.001

Rasul, A., Balzter, H., & Smith, C. (2016). Diurnal and seasonal variation of surface Urban Cool and Heat Islands in the semi-arid city of Erbil, Iraq. *Climate*, *4*(3). https://doi.org/10.3390/cli4030042

Revadekar, J. V., Tiwari, Y. K., & Kumar, K. R. (2012). Impact of climate variability on NDVI over the Indian region during 1981-2010. *International Journal of Remote Sensing*, *33*(22), 7132–7150. https://doi.org/10.1080/01431161.2012.697642

Rosenfeld, A. H., Akbari, H., Bretz, S., Fishman, B. L., Kurn, D. M., Sailor, D., & Taha, H. (1995). Mitigation of urban heat islands: materials, utility programs, updates. *Energy and Buildings*, *22*(3), 255–265. https://doi.org/10.1016/0378-7788(95)00927-P

Salamanca, F., Georgescu, M., Mahalov, A., Moustaoui, M., & Wang, M. (2014). Journal of geophysical research. *Nature*, *175*(4449), 238. https://doi.org/10.1038/175238c0

Sandholt, I., Rasmussen, K., & Andersen, J. (2002). A simple interpretation of the surface temperature/vegetation index space for assessment of surface moisture status. *Remote Sensing of Environment*, *79*(2–3), 213–224. https://doi.org/10.1016/S0034-4257(01)00274-7

Santamouris, M. (2014a). Cooling the cities – A review of reflective and green roof mitigation technologies to fight heat island and improve comfort in urban environments. *Solar Energy*, *103*, 682–703. https://doi.org/10.1016/J.SOLENER.2012.07.003

Santamouris, M. (2014b). On the energy impact of urban heat island and global warming on buildings. *Energy and Buildings*, *82*, 100–113. https://doi.org/10.1016/J.ENBUILD.2014.07.022

Santamouris, M., Cartalis, C., Synnefa, A., & Kolokotsa, D. (2015). On the impact of urban heat island and global warming on the power demand and electricity consumption of buildings—A review. *Energy and Buildings*, *98*, 119–124. https://doi.org/10.1016/J.ENBUILD.2014.09.052

Santamouris, M., Ding, L., Fiorito, F., Oldfield, P., Osmond, P., Paolini, R., … Synnefa, A. (2017). Passive and active cooling for the outdoor built environment – Analysis and assessment of the cooling potential of mitigation technologies using performance data from 220 large scale projects. *Solar Energy*, *154*, 14–33. https://doi.org/10.1016/J.SOLENER.2016.12.006

Savelli, E., Rusca, M., Cloke, H., & Baldassarre, G. Di. (2022). *Drought and society : Scientific progress , blind spots , and future prospects*. (September 2021), 1–25. https://doi.org/10.1002/wcc.761

Schwarz, N., Lautenbach, S., & Seppelt, R. (2011). Exploring indicators for quantifying surface urban heat islands of European cities with MODIS land surface temperatures. *Remote Sensing of Environment*, *115*(12), 3175–3186. https://doi.org/10.1016/J.RSE.2011.07.003

Sebastian, D. E., Murtugudde, R., & Ghosh, S. (2023). Soil–vegetation moisture capacitor maintains dry season vegetation productivity over India. *Scientific Reports*, *13*(1), 1–10. https://doi.org/10.1038/s41598-022-27277-6

Shan, M., & Hwang, B. gang. (2018). Green building rating systems: Global reviews of practices and research efforts. *Sustainable Cities and Society*, *39*, 172–180. https://doi.org/10.1016/J.SCS.2018.02.034

Sharma, R., Chakraborty, A., & Joshi, P. K. (2014). Geospatial quantification and analysis of environmental changes in urbanizing city of Kolkata (India). *Environmental Monitoring and Assessment*, *187*(1), 4206. https://doi.org/10.1007/s10661-014-4206-7

Sharma, R., & Joshi, P. K. (2014). Identifying seasonal heat islands in urban settings of Delhi (India) using remotely sensed data – An anomaly based approach. *Urban Climate*, *9*, 19–34. https://doi.org/https://doi.org/10.1016/j.uclim.2014.05.003

Shastri, H., Barik, B., Ghosh, S., Venkataraman, C., & Sadavarte, P. (2017). Flip flop of Day-night and Summer-Winter Surface Urban Heat Island Intensity in India. *Scientific Reports*, *7*(1), 40178. https://doi.org/10.1038/srep40178

Shi, Y., Xiang, Y., & Zhang, Y. (2019). Urban Design Factors Influencing Surface Urban Heat Island in the High-Density City of Guangzhou Based on the Local Climate Zone. *Sensors*, *19*(16), 3459. https://doi.org/10.3390/s19163459

Shin, M. H., Kim, H. Y., Gu, D., & Kim, H. (2017). LEED, its efficacy and fallacy in a regional context-An Urban heat island case in California. *Sustainability (Switzerland)*, *9*(9). https://doi.org/10.3390/su9091674

Singh, P., Kikon, N., & Verma, P. (2017). Impact of land use change and urbanization on urban heat island in Lucknow city, Central India. A remote sensing based estimate. *Sustainable Cities and Society*, *32*, 100–114. https://doi.org/10.1016/J.SCS.2017.02.018

Sussman, H. S., Raghavendra, A., & Zhou, L. (2019). Impacts of increased urbanization on surface temperature, vegetation, and aerosols over Bengaluru, India. *Remote Sensing Applications: Society and Environment*, *16*, 100261. https://doi.org/10.1016/J.RSASE.2019.100261

Taha, H. (1997). Urban climates and heat islands: Albedo, evapotranspiration, and anthropogenic heat. *Energy Build.*, *25*(2), 99.

Taha, Haider. (1997). Urban climates and heat islands: albedo, evapotranspiration, and anthropogenic heat. *Energy and Buildings*, *25*(2), 99–103. https://doi.org/10.1016/S0378-7788(96)00999-1

Taheri Shahraiyni, H., Sodoudi, S., El-Zafarany, A., Abou El Seoud, T., Ashraf, H., & Krone, K. (2016). A Comprehensive Statistical Study on Daytime Surface Urban Heat Island during Summer in Urban Areas, Case Study: Cairo and Its New Towns. *Remote Sensing*, *8*(8), 643. https://doi.org/10.3390/rs8080643

Tetali, S., Baird, N., & Klima, K. (2019). MAPPING AND QUANTIFYING SURFACE URBAN HEAT ISLANDS IN INDIA ' S MOST DENSE CITIES. *Prometheus: Buildings, Cities, and Performance 1.*, *3*, 22–29.

Tetali, S., Baird, N., & Klima, K. (2022). A multicity analysis of daytime Surface Urban Heat Islands in India and the US. *Sustainable Cities and Society*, *77*, 103568. https://doi.org/10.1016/j.scs.2021.103568

References

The Earth Observatory, N. (2000). Measuring Vegetation (NDVI & EVI). Retrieved April 8, 2020, from https://earthobservatory.nasa.gov/features/MeasuringVegetation/measuring_vegetation_2.php

Theeuwes, N. E., Steeneveld, G. J., Ronda, R. J., Rotach, M. W., & Holtslag, A. A. M. (2015). Cool city mornings by urban heat. *Environmental Research Letters*, *10*(11). https://doi.org/10.1088/1748-9326/10/11/114022

Tran, D. X., Pla, F., Latorre-Carmona, P., Myint, S. W., Caetano, M., & Kieu, H. V. (2017). Characterizing the relationship between land use land cover change and land surface temperature. *ISPRS Journal of Photogrammetry and Remote Sensing*, *124*, 119–132. https://doi.org/10.1016/J.ISPRSJPRS.2017.01.001

U.S. Geological Survey. (2019). Landsat 8 Data Users Handbook. *Nasa*, *8*(November), 114. Retrieved from https://landsat.usgs.gov/documents/Landsat8DataUsersHandbook.pdf

United Nations, Department of Economic and Social Affairs, P. D. (2019). *World Urbanization Prospects: The 2018 Revision (ST/ESA/SER.A/420)*. New York.

United Nations. (2018). World Urbanization Prospects 2018. Retrieved April 3, 2023, from World Urbanization Prospects 2018 website: https://population.un.org/wup/Country-Profiles/

US Census Bureau. (2019). TIGER/Line Shapefiles. Retrieved February 10, 2020, from https://www.census.gov/cgi-bin/geo/shapefiles/index.php

USGS. (2019). Earth Explorer. Retrieved August 12, 2018, from https://earthexplorer.usgs.gov/

Valor, E., & Caselles, V. (1996). Mapping land surface emissivity from NDVI: Application to European, African, and South American areas. *Remote Sensing of Environment*, *57*(3), 167–184. https://doi.org/10.1016/0034-4257(96)00039-9

Voogt, J. A., & Oke, T. R. (2003). Thermal remote sensing of urban climates. *Remote Sens. Environ.*, *86*(3), 370.

Wan, Z., Hook, S., & Hulley, G. (2015). MYD11A2 MODIS/Aqua Land Surface Temperature/Emissivity 8-Day L3 Global 1km SIN Grid V0006 [Data set]. https://doi.org/https://doi.org/10.5067/MODIS/MYD11A2.006

Wang, C., Middel, A., Myint, S. W., Kaplan, S., Brazel, A. J., & Lukasczyk, J. (2018). Assessing local climate zones in arid cities: The case of Phoenix, Arizona and Las Vegas, Nevada. *ISPRS Journal of Photogrammetry and Remote Sensing*, *141*, 59–71. https://doi.org/10.1016/j.isprsjprs.2018.04.009

Wang, C., Myint, S., Wang, Z., & Song, J. (2016). Spatio-Temporal Modeling of the Urban Heat Island in the Phoenix Metropolitan Area: Land Use Change Implications. *Remote Sensing*, *8*(3), 185. https://doi.org/10.3390/rs8030185

Wang, H., Zhang, Y., Tsou, J., & Li, Y. (2017). Surface Urban Heat Island Analysis of Shanghai (China) Based on the Change of Land Use and Land Cover. *Sustainability*, *9*(9), 1538. https://doi.org/10.3390/su9091538

Wang, J., Huang, B., Fu, D., & Atkinson, P. (2015). Spatiotemporal Variation in Surface Urban Heat Island Intensity and Associated Determinants across Major Chinese Cities. *Remote Sensing*, *7*(4), 3670–3689. https://doi.org/10.3390/rs70403670

Wang, R., Cai, M., Ren, C., Bechtel, B., Xu, Y., & Ng, E. (2019). Detecting multi-temporal land cover change and land surface temperature in Pearl River Delta by adopting local climate zone. *Urban Climate*, *28*, 100455. https://doi.org/10.1016/J.UCLIM.2019.100455

Wang, S., Ma, Q., Ding, H., & Liang, H. (2018). Detection of urban expansion and land surface temperature change using multi-temporal landsat images. *Resources, Conservation and Recycling*, *128*, 526–534. https://doi.org/10.1016/J.RESCONREC.2016.05.011

Wei, T., Wu, J., & Chen, S. (2021). Keeping Track of Greenhouse Gas Emission Reduction Progress and Targets in 167 Cities Worldwide. *Frontiers in Sustainable Cities*, *3*(July), 1–13. https://doi.org/10.3389/frsc.2021.696381

Weng, Q. (2009). Thermal infrared remote sensing for urban climate and environmental studies: Methods, applications, and trends. *ISPRS Journal of Photogrammetry and Remote Sensing*. https://doi.org/10.1016/j.isprsjprs.2009.03.007

Weng, Q., Lu, D., & Schubring, J. (2004). Estimation of land surface temperature-vegetation abundance relationship for urban heat island studies. *Remote Sensing of Environment*, *89*(4), 467–483. https://doi.org/10.1016/j.rse.2003.11.005

Wuebbles, D. J., Easterling, D. R., Hayhoe, K., Knutson, T., Kopp, R. E., Kossin, J. P., … Wehner, M. . (2017). Our Globally Changing Climate - Climate Science Special Report. *Climate Science Special Report: Fourth National Climate Assessment*, *Volume 1*, 35–72. https://doi.org/10.7930/J08S4N35.1.1

Xia, H., Chen, Y., Song, C., Li, J., Quan, J., & Zhou, G. (2022). Analysis of surface urban heat islands based on local climate zones via spatiotemporally enhanced land surface temperature. *Remote Sensing of Environment*, *273*, 112972. https://doi.org/10.1016/J.RSE.2022.112972

Xu, H. (2008). A new index for delineating built-up land features in satellite imagery. *International Journal of Remote Sensing*, *29*(14), 4269–4276. https://doi.org/10.1080/01431160802039957

Xu, T., Sathaye, J., Akbari, H., Garg, V., & Tetali, S. (2012). Quantifying the direct benefits of cool roofs in an urban setting: Reduced cooling energy use and lowered greenhouse gas emissions. *Building and Environment*, *48*(1). https://doi.org/10.1016/j.buildenv.2011.08.011

Xue, J., You, R., Liu, W., Chen, C., & Lai, D. (2020). *Applications of Local Climate Zone Classification Scheme to Improve Urban Sustainability : A Bibliometric Review*.

Yang, C., He, X., Yan, F., Yu, L., Bu, K., Yang, J., … Zhang, S. (2017). Mapping the Influence of Land Use/Land Cover Changes on the Urban Heat Island Effect—A Case Study of Changchun, China. *Sustainability*, *9*(2), 312. https://doi.org/10.3390/su9020312

Yang, J., Zhan, Y., Xiao, X., Xia, J. C., Sun, W., & Li, X. (2020). Investigating the diversity of land surface temperature characteristics in different scale cities based on local climate zones. *Urban Climate*, *34*, 100700. https://doi.org/10.1016/j.uclim.2020.100700

Yang, Q., Huang, X., & Li, J. (2017). Assessing the relationship between surface urban heat islands

and landscape patterns across climatic zones in China. *Scientific Reports*, *7*(1), 1–11. https://doi.org/10.1038/s41598-017-09628-w

Yang, X., Li, Y., Luo, Z., & Chan, P. W. (2017). The urban cool island phenomenon in a high-rise high-density city and its mechanisms. *International Journal of Climatology*, *37*(2), 890–904. https://doi.org/10.1002/joc.4747

Yu, S., Tan, Q., Evans, M., Kyle, P., Vu, L., & Patel, P. L. (2017). Improving building energy efficiency in India: State-level analysis of building energy efficiency policies. *Energy Policy*, *110*, 331–341. https://doi.org/10.1016/J.ENPOL.2017.07.013

Yuan, F., & Bauer, M. E. (2007). Comparison of impervious surface area and normalized difference vegetation index as indicators of surface urban heat island effects in Landsat imagery. *Remote Sensing of Environment*, *106*(3), 375–386. https://doi.org/10.1016/J.RSE.2006.09.003

Zareie, S., Khosravi, H., Nasiri, A., & Dastorani, M. (2016). Using Landsat Thematic Mapper (TM) sensor to detect change in land surface temperature in relation to land use change in Yazd, Iran. *Solid Earth*, *7*(6), 1551–1564. https://doi.org/10.5194/se-7-1551-2016

Zha, Y., Gao, J., & Ni, S. (2003). Use of normalized difference built-up index in automatically mapping urban areas from TM imagery. *International Journal of Remote Sensing*, *24*(3), 583–594. https://doi.org/10.1080/01431160304987

Zhang, Y., Odeh, I. O. A., & Han, C. (2009). Bi-temporal characterization of land surface temperature in relation to impervious surface area, NDVI and NDBI, using a sub-pixel image analysis. *International Journal of Applied Earth Observation and Geoinformation*, *11*(4), 256–264. https://doi.org/10.1016/J.JAG.2009.03.001

Zhao, C., Jensen, J. L. R., Weng, Q., Currit, N., & Weaver, R. (2020). *Use of Local Climate Zones to investigate surface urban heat islands in Texas*. https://doi.org/10.1080/15481603.2020.1843869

Zhao, L., Lee, X., Smith, R. B., Oleson, K., Zhang, H., Qi, Z., … Chen, M. (2014). Strong contributions of local background climate to urban heat islands. *Nature*, *511*(7508), 216–219. https://doi.org/10.1038/nature13462

Zhao, S., Zhou, D., & Liu, S. (2016). Data concurrency is required for estimating urban heat island intensity. *Environmental Pollution*, *208*, 118–124. https://doi.org/10.1016/j.envpol.2015.07.037

Zhao, Z., Sharifi, A., Dong, X., Shen, L., & He, B.-J. (2021). Spatial Variability and Temporal Heterogeneity of Surface Urban Heat Island Patterns and the Suitability of Local Climate Zones for Land Surface Temperature Characterization. *Remote Sensing*, *13*(21), 4338. https://doi.org/10.3390/rs13214338

Zhou, B., Rybski, D., & Kropp, J. P. (2013). On the statistics of urban heat island intensity. *Geophysical Research Letters*, *40*(20), 5486–5491. https://doi.org/10.1002/2013GL057320

Zhou, D., Xiao, J., Bonafoni, S., Berger, C., Deilami, K., Zhou, Y., … Sobrino, J. (2018). Satellite Remote Sensing of Surface Urban Heat Islands: Progress, Challenges, and Perspectives. *Remote Sensing*, *11*(1), 48. https://doi.org/10.3390/rs11010048

References

Zhou, D., Zhang, L., Hao, L., Sun, G., Liu, Y., & Zhu, C. (2016). Spatiotemporal trends of urban heat island effect along the urban development intensity gradient in China. *Science of The Total Environment*, *544*, 617–626. https://doi.org/10.1016/J.SCITOTENV.2015.11.168

Zhou, D., Zhao, S., Liu, S., Zhang, L., & Zhu, C. (2014). Surface urban heat island in China's 32 major cities: Spatial patterns and drivers. *Remote Sensing of Environment*, *152*, 51–61. https://doi.org/10.1016/J.RSE.2014.05.017

Zhou, D., Zhao, S., Zhang, L., Sun, G., & Liu, Y. (2015). The footprint of urban heat island effect in China. *Scientific Reports*, *5*, 2–12. https://doi.org/10.1038/srep11160

A: LIST OF STUDY LOCATIONS

This section lists study locations from India and the US, along with their latitude, longitude, and date of acquisition of the Landsat 8 data.

INDIA

No.	City	Summer Data Date	Winter Data Date	Latitude (N)	Longitude (E)
1	Agra	5/21/2016	12/15/2016	27.1767	78.0081
2	Ahmedabad	5/19/2016	12/29/2016	23.0225	72.5714
3	Amritsar	4/6/2016	1/12/2016	31.634	74.8723
4	Aurangabad	4/19/2016	1/30/2016	19.8762	75.3433
5	Bareilly	5/14/2016	12/24/2016	28.367	79.4304
6	Bengaluru	5/23/2016	1/16/2016	12.9716	77.5946
7	Bhopal	5/14/2016	12/23/2016	23.2599	77.4126
8	Bhubaneswar	4/9/2016	12/21/2016	20.2961	85.8245
9	Chandigarh	5/28/2016	1/5/2016	30.7333	76.7794
10	Chennai	4/23/2016	-	13.0827	80.2707
11	Coimbatore	5/23/2016	1/16/2016	11.0168	76.9558
12	Delhi	5/21/2016	1/30/2016	28.7041	77.1025
13	Dhanbad	4/25/2016	1/4/2016	23.7957	86.4304
14	Guwahati	3/3/2016	12/16/2016	26.1445	91.7362
15	Gwalior	5/14/2016	12/24/2016	26.2183	78.1828
16	Hyderabad	5/23/2016	12/17/2016	17.385	78.4867
17	Indore	5/21/2016	1/30/2016	22.7196	75.8577
18	Jabalpur	5/23/2016	12/17/2016	23.1815	79.9864
19	Jaipur	5/12/2016	1/5/2016	26.9124	75.7873
20	Jamshedpur	4/25/2016	1/4/2016	22.8046	86.2029
21	Jodhpur	5/10/2016	1/19/2016	26.2389	73.0243
22	Kolkata	4/11/2016	1/6/2016	22.5726	88.3639
23	Kota	5/12/2016	1/5/2016	25.2138	75.8648
24	Lucknow	4/21/2016	10/14/2016	26.8467	80.9462
25	Ludhiana	6/14/2016	1/12/2016	30.901	75.8573
26	Madurai	4/14/2016	11/24/2016	9.9252	78.1198

27	Mumbai	4/17/2016	12/29/2016	19.076	72.8777
28	Mysore	3/20/2016	1/16/2016	12.2958	76.6394
29	Nagpur	4/21/2016	12/17/2016	21.1458	79.0882
30	Nashik	5/12/2016	12/22/2016	19.9975	73.7898
31	Patna	4/16/2016	2/12/2016	25.5941	85.1376
32	Pune	4/26/2016	12/22/2016	18.5204	73.8567
33	Raipur	4/23/2016	1/2/2016	21.2514	81.6296
34	Rajkot	5/17/2016	1/10/2016	22.3039	70.8022
35	Ranchi	4/25/2016	1/4/2016	23.3441	85.3096
36	Solapur	5/5/2016	1/30/2016	17.6599	75.9064
37	Surat	4/17/2016	12/29/2016	21.1702	72.8311
38	Tiruchirappalli	4/14/2016	12/26/2016	10.7905	78.7047
39	Vadodara	5/3/2016	1/12/2016	22.3072	73.1812
40	Varanasi	5/9/2016	2/3/2016	25.3176	82.9739
41	Vijayawada	4/23/2016	2/19/2016	16.5062	80.648
42	Visakhapatnam	5/2/2016	11/26/2016	17.6868	83.2185

UNITED STATES

No.	**City**	**Summer Data Date**	**Winter Data Date**	**Latitude (N)**	**Longitude (W)**
1	Atlanta	7/14/2016	2/4/2016	33.749	-84.388
2	Austin	7/22/2016	1/12/2016	30.2672	-97.7431
3	Boston	7/13/2016	11/18/2016	42.3601	-71.0589
4	Chicago	9/12/2016	10/14/2016	41.8781	-87.6298
5	Cincinnati	7/21/2016	2/28/2016	39.1031	-84.512
6	Cleveland	6/21/2016	2/5/2016	41.4993	-81.6944
7	Columbus	6/12/2016	2/5/2016	39.9612	-82.9988
8	Dallas	7/7/2016	1/28/2016	32.7767	-96.797
9	Denver	8/17/2016	3/10/2016	39.7392	-104.9903
10	Houston	5/5/2016	10/28/2016	29.7604	-95.3698
11	Jacksonville	7/9/2016	11/21/2011	30.3322	-81.6557
12	Kansas City	8/16/2016	12/29/2016	39.0119	-98.4842
13	Las Vegas	6/24/2016	12/17/2016	36.1699	-115.1398
14	Los Angeles	9/26/2016	2/15/2016	34.0522	-118.2437
15	Louisville	9/7/2016	12/28/2016	38.2527	-85.7585

16	Memphis	6/8/2016	12/1/2016	35.1495	-90.049
17	Milwaukee	9/12/2016	10/14/2016	43.0389	-87.9065
18	Minneapolis	9/8/2016	11/11/2016	44.9778	-93.265
19	Nashville	6/10/2016	2/19/2016	36.1627	-86.7816
20	New York City	6/9/2016	2/18/2016	40.7673	-73.97
21	Orlando	5/6/2016	12/16/2016	28.5383	-81.3792
22	Phoenix	7/12/2016	2/3/2016	33.4484	-112.074
23	Pittsburgh	9/25/2016	11/5/2016	40.4406	-79.9959
24	Portland	8/12/2016	9/13/2016	45.5122	-122.6587
25	Raleigh	7/18/2016	11/23/2016	35.7796	-78.6382
26	Richmond	7/2/2016	11/23/2016	37.5407	-77.436
27	Sacramento	7/29/2016	11/18/2016	38.5816	-121.4944
28	Salt Lake City	8/20/2016	11/8/2016	40.7608	-111.891
29	San Diego	8/2/2016	2/8/2016	32.7157	-117.1611
30	Seattle	8/12/2016	1/1/2016	47.6062	-122.3321
31	St Louis	9/19/2016	11/6/2016	38.627	-90.1994
32	Washington DC	7/2/2016	12/23/2016	38.9072	-77.0369

B: THERMAL PROPERTIES OF CONVENTIONAL BUILDING AND NATURAL MATERIALS

The thermal admittance (m, ability of the surface to accept or release heat), thermal diffusivity (K, ability of the material to diffuse heat), and heat capacity (C, amount of heat required to change temp. by 1 K) are some of the vital thermal properties of any surface that explain the heat transfer to and from a surface. Table 25 in this section lists these thermal properties of the conventional building and natural material types seen across urban and rural areas of India and the US.

Table 25: Thermal properties of the conventional building and natural materials found across the urban and rural areas of India and the US. (Oke, 1987)

Material	Type	ρ Density ($kg\ m^{-3} \times 10^3$)	c Specific heat ($J\ kg^{-1}\ K^{-1} \times 10^3$)	C Heat Capacity ($J\ m^{-3}\ K^{-1} \times 10^6$)	k Thermal conductivity ($W\ m^{-1}\ K^{-1}$)	K Thermal diffusivity ($m^2\ s^{-1} \times 10^{-6}$)	μ_s Thermal admittance ($J\ m^{-2}\ s^{-1/2}\ K^{-1}$)
Natural Materials							
Clay Soil (40% pore space)	Dry	1.60	0.89	1.42	0.25	0.18	600
	Saturated	2.00	1.48	2.96	2.20	0.74	2550
Dry Peat soil (80% pore space)	Dry	0.30	1.92	0.58	0.06	0.10	190
	Saturated	2.00	1.55	3.10	1.58	0.51	2210
Sandy soil (40% pore space)	Dry	1.60	0.80	1.28	0.30	0.24	620
	Saturated	2.00	1.48	2.96	2.20	0.74	2550
Snow-fresh		0.10	2.09	0.21	0.08	0.10	130
Snow-old		0.48	2.09	0.84	0.42	0.40	595
Urban Construction Materials							
Asphalt		2.11	0.92	1.94	0.75	0.38	1205
Concrete	Dense	2.40	0.88	2.11	1.51	0.72	1785
	Aerated	0.32	0.88	0.28	0.08	0.29	150
Brick		1.83	0.75	1.37	0.83	0.61	1065
Clay tiles		1.92	0.92	1.77	0.84	0.47	1220
Wood	Light	0.32	1.42	0.45	0.09	0.20	200
	Dense	0.81	1.88	1.52	0.19	0.13	535
Insulation-Polystyrene		0.02	0.88	0.02	0.03	1.50	25
Steel		7.85	0.50	3.93	53.3	13.6	14475
Glass		2.48	0.67	1.66	0.74	0.44	1110
Gypsum board		1.42	1.05	1.49	0.27	0.18	635